EFFECTS OF NEUROTOXIC CONTAMINANTS ON LARVAL FISH, FROM GENES AND
BEHAVIOR TO POPULATIONS

By

Janice Linda Albers

A DISSERTATION

Submitted to
Michigan State University
in partial fulfillment of the requirements
for the degree of

Fisheries and Wildlife – Environmental Toxicology – Doctor of Philosophy

2022

ABSTRACT

After decades of pollution regulation in the United States, many pollutants exist in the environment below levels that cause mortality; even so, sublethal levels of environmental pollutants can still result in indirect mortality and reduced abundance of organisms. Understanding the consequences of pollution at chronic sublethal levels is one of the main goals in toxicology and in environmental risk assessment. This dissertation focuses on understanding the impacts on multiple fish species from environmentally relevant sublethal levels of two developmental neurotoxicants that commonly occur in aquatic environments, methylmercury (MeHg) and 3,3',4,4',5-pentachlorobiphenyl (PCB126). The first chapter provides a background of fish behavior assays used in toxicology; gives background information on a commonly used fish species in toxicology, the Atlantic killifish (KF; *Fundulus heteroclitus*); and summarizes a relatively new technique to compare biological responses to chemical exposure, the Adverse Outcome Pathway (AOP). The second chapter summarizes the impact of MeHg on fish larvae behaviors by conducting an analysis that combines recent research results into feeding, swimming and startle response behavior affects after exposure. Mercury has long been known to cause neurological deficiencies especially during neurological development which can cause temporary and/or permanent impairments to brain function. One way to assess these impacts is by examination of behavior after exposure. This chapter analyzes fish larval behavior effects and constructs predictive models that could be used in future mercury risk assessments. The third chapter focuses on assessing changes in larval fish behavior after exposure to neurotoxicants using a new analytical approach. Typically in toxicological behavior assays, fish behavior is summarized as an average response over the length of the assay. However, average responses could miss more sensitive behavior changes brought on by chemical exposure. New behavior

models such as hidden Markov chain models (HMMs) could potentially detect more behavior alterations and allow for increased accuracy in chemical exposure assessments. This chapter analyzes impacts detected from both traditional and HMM behavior endpoints in yellow perch larvae (YP; *Perca flavescens*) and how they are altered by MeHg and PCB126 embryonic exposure. The fourth chapter of this dissertation applies the new and traditional analytical techniques described in chapter 3 to the specific case of KF after embryonic exposure to MeHg and PCB126. This species of killifish is unique because some populations have naturally evolved tolerance to industrial pollutants which could highlight the biological mechanisms behind this evolution through comparisons between non-adapted and adapted populations. In this chapter, these comparisons are made using the AOP framework, allowing for visualization of molecular, organismal and population level effects from chemical exposure. The fifth chapter in this dissertation investigates different aspects of the AOP framework, specifically whether different biological responses can be shared over three different fish species after exposure to MeHg and PCB126. The AOP framework has been used to assess impacts across different species and chemicals by assuming common biological responses in organisms that share similar molecular, cellular and organ functions. This chapter investigates the use of AOPs in assessing the similarity of biological responses in gene expression, larval behavior and predicted cohort survival and growth. This work advances our knowledge of the sub-lethal impacts of two common neurotoxicants in aquatic ecosystems and their impacts on multiple levels of biological organization in fish larvae.

colleague. Thanks to all the MSU support staff for their assistance. Finally, thanks to my family

and loved ones for their support.

TABLE OF CONTENTS

CHAPTER 1: INTRODUCTION

Abstract

Chronic exposure to low levels of industrial pollutants commonly occurs in aquatic ecosystems, even after decades of regulation, and this exposure can be more harmful when the pollutant is a developmental neurotoxicant. This can create an environment where fish embryos are exposed to neurotoxicants both through parental transfer and direct aquatic exposure after fertilization. Understanding the sublethal effects on fish larva after embryonic exposure would allow us to better understand the risk imposed on these populations by human pollution. Methylmercury (MeHg) and 3,3',4,4',5-pentachlorobiphenyl (PCB126) are two common aquatic industrial pollutants that are also developmental neurotoxicants. By altering neurologic development, molecular and cellular functions can be periodically or permanently altered. These include gene expression and behavior, which could in turn affect fish survival and growth. This dissertation investigates the sublethal effects of fish embryonic exposure to MeHg and PCB126 by collecting information at multiple levels of biological organization. The first chapter explains a new analytical approach to assess yellow perch *Perca flavescens* larval behavior impacts from exposure. Then, a case study is presented using Atlantic killifish *Fundulus heteroclitus* where embryos were exposed to MeHg or PCB126 and biological impacts are assessed in larvae starting at brain gene expression, the resulting behavior, and finally modeled growth and survival. Finally, a summary analysis is presented that examines the similarities between the previously mentioned biological responses from three fish species and both chemicals, to determine whether certain biological endpoints could be used as a measure of fish exposure to these pollutants and the utility of the adverse outcome pathway to extrapolate across contaminants and species.

Introduction

Methylmercury (MeHg) and 3,3',4,4',5-pentachlorobiphenyl (PCB126) are two common

aquatic industrial pollutants that are also developmental neurotoxicants. Low levels of MeHg can

impact a wide range of biological functions in both humans and animals, from widespread brain

damage to subtle impairments in motor and sensory functions (Nogara et al. 2019; Pereira et al.

2019; Yang et al. 2020). Methylmercury exposure results in altered calcium signaling, impaired

mitochondrial function, and accumulation of oxidative stress, all of which can damage neurons

(Caudle and Miller 2015). Methylmercury directly impacts neurotransmitter levels by altering

acetylcholinesterase, sulfhydryl (thiol)-group protein binding, methylation (epigenetics) and

neurogenesis (Sastry and Sharma 1980; Johansson et al. 2007; Bradbury et al. 2008; Farina et al.

2011; Weber et al. 2012; Costa and Giordano 2012; Helmcke and Aschner 2012; Amara et al.

2012; Bose et al. 2012; Ho et al. 2013; Kalueff et al. 2016). PCB126 is an aryl hydrocarbon

receptor agonist and disrupts energy metabolism (Bandiera et al. 1982; Okey 2007; Zhang et al.

2012; Gadupudi et al. 2016). PCB126 alters multiple pathways in mammals that result in

neurological changes including multiple behavioral endpoints in rats (Rice and Hayward 1998,

1999; Rice 1999; Vitalone et al. 2010; Cauli et al. 2013) and fish (Couillard et al. 2011; Rigaud

et al. 2013; Liu et al. 2015; Xu et al. 2015; Glazer et al. 2016). These two chemicals also alter

calcium homeostasis, which is critical in neuron function (Piedrafita et al. 2008b; Costa and

Giordano 2012).

After decades of regulation, levels of MeHg and PCB126 rarely exist at lethal levels in

the aquatic environment, but still persist at concentrations that affect sublethal processes

(Murphy et al. 2012). Although less severe, chronic exposure to sublethal levels of pollutants

can still contribute to fish population declines, e.g. through delayed mortality, physical

deformities, cancer and impairments to feeding, reproduction, swimming, etc. (Sandheinrich and Atchison 1990; Baldwin et al. 2009; Hamilton et al. 2016; Morán et al. 2018). Because MeHg and PCB126 both impact brain function at molecular levels that could ultimately lead to population declines, a toxicological framework known as Adverse Outcome Pathway (AOP) may be a useful tool to assess the impact pathway from molecular to population level impacts of these two neurotoxicants.

The concept of AOPs in toxicology was first introduced by Ankley et al. (2010) which set up a structured pathway concept using mechanistic data at multiple levels of biological organization to translate chemical impacts from molecular to population level adverse outcomes. Each pathway connection between the different levels of biological organization are modular and can be applied across chemicals and species (Villeneuve et al. 2014a, 2014b). Adverse Outcome Pathway modularity allows for cross species and cross chemical applications of the same relationships linking different key events. However, the application across species or chemicals should not be done without confirmation that those relationships apply to either species or chemical. The goal of this project is to illuminate areas where AOPs meet the assumptions that permit application for cross species and chemical extrapolations by examining three different fish species after exposure to sublethal environmentally relevant levels of MeHg and PCB126.

Larval Fish Swimming Behavior Changes and Detection after Sublethal Exposure to Neurotoxicants

The use of animal behavior to determine impacts of neurotoxicant exposure has been studied for more than 100 years (see review in Medved et al. 1964). It typically involves many hours of collecting detailed observational data sometimes on behavior endpoints that were specific to laboratory conditions that rarely translated into real world environments [e.g.

electroshock conditioning in goldfish (Weir and Hine 1970)]. With the advent of new animal

tracking devices and software technologies, a new class of animal behavior studies has allowed

scientists to study animals in situ, including new types of data analyses that are more precise at

determining differing animal behavior states and how they relate to environmental variables

(Hooten et al. 2017). These advancements in in-situ behavior analyses can also be applied to

laboratory behavior experiments (Chon et al. 2010; Li et al. 2013), and by adapting these in-situ

techniques, advances in high throughput toxicity testing can potentially increase precision for

detecting behavior alterations from chemical exposure (Ågerstrand et al. 2020). In addition,

collecting and analyzing behavior data in the laboratory that directly apply to real world

situations (i.e. eating prey, locomotion and responses to startle stimuli) can then be used to

translate individual impacts from chemical exposure to whole populations using individual based

modeling (Murphy et al. 2008; Armstrong et al. 2020).

Chapter 3 of this dissertation applies a modern in-situ behavior analysis model to study

the impacts on laboratory derived larval yellow perch *Perca flavescens* (YP) movement after

exposure to environmental relevant sublethal levels of two neurotoxicants, PCB126 and MeHg.

It also compares the estimates from these new models to more traditional behavior analysis

estimates to determine if the new models are more sensitive to behavior impacts from exposure.

Atlantic Killifish Alterations from Sublethal Exposure to Neurotoxicants: Connecting

Different Levels of Biological Organization

In toxicology, an AOP framework is a structured outline used to connect the chain of

events from toxic exposure to molecular initiating event/s; then to key events in cellular, organ

and organ systems; and finally to whole organism and/or population level impacts (Ankley et al.

2010). By structuring an environmental exposure event using the AOP framework, connections

and relationships can be made both chemically and biologically that could eventually lead to population level impacts. In addition, both chemical and biological impacts that are common across animals could be shared between AOPs in a modular form (https://aopwiki.org/). Adverse Outcome Pathway modularity allows for information sharing as a way to increase our knowledge to more than just the limited number of directly tested organisms.

Atlantic killifish *Fundulus heteroclitus* (KF) have a long history in scientific research as toxicological test subjects and were even the first fish in space (von Baumgarten et al. 1975; Hoffman et al. 1977, 1978). Easy to maintain in captivity, they are commonly found along the east and southeast coast of the U.S. in estuary habitat. The evolution of KF in the highly variable estuarine habitats has resulted in the most genetically diverse species of fish yet studied and is in the 98th percentile of genetic diversity among vertebrates (Reid et al. 2017). In the U.S., KF also have a long history of living in heavily polluted coastal cities and industrial areas. The pollution pressure combined with the high level of genetic diversity may have contributed to the observations that some populations of KF have an evolved tolerance to our pollution (Nacci et al. 2016; Reid et al. 2017), particularly as it pertains to industrial pollutants that activate the aryl hydrocarbon receptor (AhR) such as dioxins and polychlorinated biphenyls (PCBs). Certain KF populations have an evolved tolerance through resistance to reactive oxygen species and cardiac teratogenesis (Arzuaga and Elskus 2010; Clark et al. 2010) mainly by skipping different components in the complex stress response network, which involves AhR and cytochrome P450 gene expression (Nacci et al. 2016).

Using the AOP framework, chapter 4 of this dissertation examines the multiple biological levels of KF response to environmental relevant sublethal levels of two neurotoxicants, PCB126 and MeHg, including brain gene expression, larval behavior and modeled population metrics.

Two distinct populations of KF were examined, one with no history of pollution exposure and one known to have evolved resistance to pollution impacts. This project investigated the connections between biological responses to these two neurotoxicants, explored commonalities between tolerant and intolerant KF populations, and identified possible connections between gene expression and fish behavior.

Adverse Outcome Pathways: Application across Fish Species and Neurotoxicants

The use of AOPs in toxicology has greatly increased our knowledge of how chemicals are impacting biological functions, especially as it pertains to the modular sharing aspect of the AOP framework (https://aopwiki.org/). Many basic molecular and cellular functions and processes are common among different species, which is a main premise in the field of structural biology. In theory, sharing biological information between similar organisms has a long history of practice in science and is commonly referred to as surrogacy. At a molecular and cellular level, surrogacy has become common practice in toxicology being fundamental to risk assessment, biomarkers, alternative animal testing methods and the use of model organisms such as zebrafish *Danio rerio* (ZF; Leonelli and Ankeny 2013; Bambino and Chu 2017; Gupta 2019). In conservation biology, organismal level surrogacy has a history of coming in and out of favor, currently being held to many restrictions [see review by (Murphy et al. 2011) for individual species surrogacy and (Beier and de Albuquerque 2015; Stewart et al. 2018) for biodiversity level surrogacy]. Restrictions with organismal level surrogacy is based on research that rarely finds similarity in responses between limited use laboratory animals (e.g. endangered or threatened species) and commonly used surrogates (e.g. species that are easily kept in captivity) (Jorgenson et al. 2015; Paula et al. 2016). Use of the AOP framework may resolve this contradiction of surrogacy at different biological scales.

Chapter 5 of this dissertation examines the same set of sublethal biological endpoints discussed in the previous chapters in three different fish species after exposure to environmental relevant sublethal levels of two neurotoxicants, PCB126 and MeHg. This chapter assesses the assumptions inherent in the AOP framework, mainly the assumption of agnostic species and chemicals, by summarizing the trends between ZF, a common surrogate, and two native species, YP and KF, and their responses to environmental relevant sublethal levels of two neurotoxicants, PCB126 and MeHg.

Conclusion

This work makes significant progress towards understanding responses of native fish species and laboratory surrogate fish species from exposure to environmentally relevant sublethal levels of two common neurotoxicants, PCB126 and MeHg. Trends of these biological responses to increasing chemical doses broadens our understanding of how individual fish species are impaired by chronic sublethal neurotoxicant pollution, as well as commonalities in response between species. Additionally, this project begins to make connections between brain gene expression and organismal behaviors under chemical perturbation, which expands our knowledge about the links between gene expression and behavior, and how they can be impacted by the environment.

CHAPTER 2: MERCURY EFFECTS ON EARLY LIFE STAGE FISH BEHAVIOR

Abstract

Mercury is ubiquitous in the environment and can induce neurological disturbances in many life forms at very low doses, especially if exposure occurs during early development. Prior research suggests that early life stage fish (ELSF) behavior has been impacted at methylmercury levels starting at 0.0002 ppm. Here, we conducted a literature review, summarizing all available research results about ELSF behavior impacts from MeHg exposure and found different impacts on behavior types. Feeding behaviors that were suppressed by MeHg exposure and swimming behaviors were affected by 26 and 17%, respectively, whereas feeding behaviors that were elevated after MeHg exposure and stimulus behaviors had a positive significant relationship with MeHg dose. These results provide more information about the impacts on ELSF from mercury contamination and how different types of ELSF behaviors are impacted by MeHg exposure.
.

Introduction

Mercury contamination as a result of human activities continues to contribute to global contaminant loadings despite being identified as a serious problem over one hundred years ago. Two major reasons for concerns surrounding mercury contamination is the ability of mercury to bioaccumulate and biomagnify in the food web (Bank 2012; Wentz et al. 2014) and mercury's high neurotoxicity properties (Nabi 2014; Bradley et al. 2017; Yang et al. 2020). Aquatic ecosystems are especially vulnerable since certain aquatic bacteria can change inorganic mercury into methylmercury (MeHg) under anaerobic conditions, which is a form that is highly toxic to biological organisms (Green and Planchart 2018; Yang et al. 2020). Fish, because of their position in the aquatic food web, are mainly exposed to MeHg through food ($\geq 90\%$ of total update) and through the aqueous form as it is absorbed through the gills (Sandheinrich and Wiener 2011). Developmental timing of MeHg exposure is important in understanding toxicological effects on fish, where exposure at even very low levels during embryonic development can alter neural network function, sensorimotor and learning in fish (Weber et al. 2012). Adult fish can tolerate higher exposures of MeHg, but will expose their offspring through maternal transfer in gonadal tissue (Mora-Zamorano et al. 2016a; Liu et al. 2016; Carvan et al. 2017). Consequently, understanding MeHg exposure to early life stage fish (ELSF) is critical to our understanding the risk of mercury contamination in aquatic systems.

Early life stage fish (embryo and larva) are more sensitive to MeHg exposure than juvenile and adult stages. Dillon et al. (2010) summarized the effects of mercury (Hg) on hatch success, morphological abnormalities, growth and survival of adult and ELSF. They found 0.406 ppm of Hg in fish tissues represent 10.9% injury in adult fish but 50% injury in ELSF using lethality-equivalent endpoints. Furthermore, sublethal endpoints such as behavior are typically

more sensitive than lethality-equivalent (Scott and Sloman 2004; Dutra Costa et al. 2020) and when altered from developmental exposure, the effects can last for years (Fjeld et al. 1998). Because of the increased sensitivity of ELSF to neurotoxicants, ELSF behavior endpoints have become a popular way to examine chemical toxicity (Ågerstrand et al. 2020; Dutra Costa et al. 2020).

Early life stage fish behavior can be the most sensitive life stage and response endpoint at the organismal level, therefore the goal of this project was to conduct a literature review and summarize ELSF behavioral impacts from MeHg exposure. We expanded on the lethality-equivalent dose response MeHg relationships produced by Dillon et al. (2010) and conducted a similar analysis on the sublethal ELSF behavior injury over varying levels of MeHg exposure. The objectives of this study were to develop MeHg dose response relationship with larval behavior endpoint effects and determine whether these relationships change depending on the type of behavior.

Methods

Literature search and data collection

A literature search was conducted using the search engine Web of Science© (Copyright Clarivate 2022) and the following terms: mercury, larv*, and/or behav*. We also reviewed online toxicology databases such as ECOTOX (https://cfpub.epa.gov/ecotox/) for relevant studies. We accepted that the quality of the study was sufficient so long as it was published in a peer reviewed scientific journal and had reference control treatments. We only included results from studies that exposed fish embryos to MeHg (i.e. MeHg or MeHg-chloride) since the inorganic forms of mercury can be less toxic than the organic forms (Korbas et al. 2012; Pereira et al. 2019). All relevant research studies used in the analysis included a larval behavior

assessment that determined impacts on various behavior endpoints such as swimming, feeding, or a behavior response from a stimulus. However, these types of research studies have methodologies that could impact result comparisons between studies such as exposure timing, evolved tolerance, etc. Consequently, the following additional restrictions were used to limit the type of study included in the analysis to ensure the data from these studies are comparable.

Life stage at the time of MeHg exposure can alter MeHg toxicity, with developmental exposures being the most toxic (Samson et al. 2001; Dillon et al. 2010). This study focused on the most sensitive life stage, embryonic developmental exposure. The included laboratory studies were restricted to only studies where exposure started at or within 24 hours after fertilization and exposure ended before hatching. Since fish embryos *in situ* are exposed to Hg via pre-fertilization gamete deposition (Alvarez et al. 2006; Mora-Zamorano et al. 2016a; Bridges et al. 2016a, 2016b; Carvan et al. 2017), laboratory studies that exposed parents and then tested F1 progeny for behavior effects were also included in the analysis. Not included in the analysis were studies that exposed previously known isolated tolerant fish populations with a long-term history of *in situ* exposure [e.g. Atlantic killifish *Fundulus heteroclitus* collected from New Bedford Harbor, MA or Piles Creek, NJ (Ososkov and Weis 1996; Zhou and Weis 1998; Whitehead et al. 2012; Nacci et al. 2016)].

Fish larval behavior can be altered after chemical exposure as a consequence of visible gross physical deformities (e.g., spinal curvature) as well as nonvisible internal physiological changes (e.g., neuronal connections between brain and muscles). Gross deformities are typically diagnosed using gross morphology assessments (e.g. Clark et al. 2010; Whitehead et al. 2010), and toxicological studies typically assess fish behavior using fish that do not have any obvious

11

gross physical malformations. Consequently, studies that only assessed behavior on larvae without gross physical deformities were used in the analysis.

Many different types of behavior endpoints can be determined using numerous types of behavior assays (Weis and Candelmo 2012; Ågerstrand et al. 2020; Dutra Costa et al. 2020). Our analyses only included the three most general behavior response types: feeding, response to a stimulus (referred to from now on as just stimulus), and swimming. Feeding behaviors are used to assess effects of MeHg on the consumption of food, including but not limited to consumption rates, prey handling time or prey miss rates. Stimulus type behaviors involved an external stimulus that triggers a measurable behavior response such as response time or response magnitude in visual motor response assays. Swimming type responses include a multitude of different ways to characterize fish swimming such as speed, time spent swimming, or frequency of swimming bouts. From each included research study, the behavior response was recorded from the control and treatment level behavior endpoint mean and the number of larvae that generated the mean. If the mean had been transformed for statistical analysis, then the transformed mean was used to calculate the percent effect. If the means were reported in a table than they were used as reported. However, if the means were reported in a figure, than the values were collected from the figure using WebPlotDigitizer tool (Rohatgi 2019). Studies that included changes in swimming turning angles were not included in the analysis since turning angles are usually measured in radian units and percent effect is not logical with this endpoint.

Embryo tissue Hg concentration was not always reported in the included study documentation (6 out of 13 included studies), so the effect response was determined using MeHg dose levels. When exposure occurred via parental transfer (Murphy et al. 2008; Mora-Zamorano et al. 2017; Ye and Fisher 2020; Albers et al. 2022a), then the parental wet weight tissue

concentration of mercury was used as the embryonic dose exposure level. If exposure occurred via parental transfer and the parental tissue concentrations were not reported, then the wet weight embryo or egg tissue concentrations were used as the dose exposure level. If wet to dry weight conversions were needed, we assumed 87% moisture content in fish egg or larva (Kneib 1993; Albers et al. 2022a, 2022d).

As in Dillon et al. (2010), mean effect sizes were calculated relative to the controls. Percent control-normalized response (PCR) was defined as (treatment response ÷ control response) × 100. Similar to Dillon et al. (2010), we treated each PCR as an independent response measure, so each PCR was an independent observation in the dose response relationship. Dillon et al. (2010) limited their assessment to binomial responses such as the presence or absence of death or malformations which always occur in a negative dose dependent manor. Since behavior endpoints are a continuous sublethal response variable that can be higher or lower than the control after exposure, we deviated from Dillon et al. (2010) in the following ways. 1) Higher and lower trending PCRs were grouped separately. The trend grouping was maintained throughout the analysis and was included as a factor in the models to test for trend grouping differences between behavior responses. If the original PCR was calculated from non-transformed values than the original lower or higher trend grouping was used. However, if the original PCR was calculated from transformed values, then the back transformed lower or higher trend grouping was used. By handling transformed values this way, the original trend relative to the control was maintained even though the effect magnitude was determined from the transformed values. 2) Any PCR that was more than 100 was kept as is, and not changed to 100, as was done in Dillon et al. (2010). 3) If more than one endpoint in the same behavior type was reported from the same group of fish in a study, we averaged the PCR using the following

13

hierarchy. First, for any behavior endpoints that were repeatedly measured using the same parameter over time in the same study, the PCRs were averaged. Second, if multiple kinds of behavior endpoints were measured that occurred within the same behavior type (i.e. stimulus, feeding, or swimming) then those PCRs were averaged. The number of fish in each of these groupings were averaged in the same way. Dillon et al. (2010) also averaged multiple endpoints within a study, but because they were using all lethality-equivalent endpoints the no hierarchical averaging structure was not required.

The relationship between increasing MeHg dose and PCR were examined using a fully parameterized linear models (LM) that included the explanatory variables of MeHg dose, trend type factor (lower or higher relative to the control), and behavior type factor (feeding, stimulus, or swimming) as main effects and all two-way and three-way interactions. Models examining the trends of MeHg effects within each behavior type were also constructed using LMs that included dose and trend as main effects and the two-way interactions. To meet the normality of the residual assumption for LMs, the PCR was transformed using boxcox transformation (Mass R package) and dose was Log_{10} transformed. In addition, each model contained a weighting factor consisting of the average number of fish that were used to determine each PCR value. Alpha ≤ 0.05 was considered significant and alpha ≤ 0.10 was marginally significant. Benchmark dose (BMD) at 10% effect and effective dose at 50% were determined using the predicted means from the linear models. The linear regression equations used to calculate BMDs are also reported so that any percent effect could be calculated

Results

The literature review resulted in 13 previously reported studies examining the impacts of MeHg on the ELSF behavior with multiple studies coming from the seven separate laboratories.

These studies examined MeHg impacts on five separate fish species: Atlantic killifish *Fundulus heteroclitus*, yellow perch *Perca flavescens*, Atlantic croaker *Micropogonias undulates*, sheepshead minnow *Cyprinodon variegatus*, and zebrafish *Danio rerio* (Table S2.1). From these studies, 432 separate PCRs were measured from MeHg-Control comparisons. After hierarchical averaging, 109 observations were used in the statistical modeling. The PCR distribution containing 109 observations was highly right skewed, so a boxcox transformation was used to normalize the residuals (lambda = 0.1121). Length of exposure in the included studies varied from 24 hours to 21 days post fertilization, with the longest exposures occurring during the entire 21-day embryonic development period for Atlantic killifish. Between all the included studies, the dose of MeHg ranged from 0.0002 – 14.73 ppm MeHg, and when reported, these dose levels resulted in embryo or larval tissue concentrations between 0.00039 and 3.14 µg tHg/g wet weight (n = 18 different wet weight tissue samples, 7 of which were estimated from dry weight samples).

The full model results indicate the dose response trend of PCR is different depending on the type of behavior examined, where all the two-way interactions were marginally significant: trend type and behavior type interaction ($F_{(2,97)}$ = 2.74, P-value = 0.0692), trend type and dose ($F_{(2,97)}$ = 3.74, P-value = 0.0560), and behavior type and dose ($F_{(2,97)}$ = 2.50, P-value = 0.0877). Consequently, a separate model predicting PCR was constructed for each type of behavior.

Two thirds of the feeding behavior observations had a lower trend PCR after exposure to MeHg (n = 23 out of 34). Both higher and lower trend groups of feeding behaviors were examined with a feeding only model, where PCR had a significant dose response interaction with feeding trend type ($F_{(1,30)}$ = 9.84, P-value = 0.0038). Indicating the feeding PCRs had a different relationship with MeHg depending on the trend type, consequently we constructed a separate

model for each feeding trend type. After running separate models for each feeding trend type, the higher trend feeding PCRs had a significant positive linear relationship with increasing MeHg dose (P-value = 0.0016, n = 11, adjusted R-squared = 0.65; Figure 2.1A). Using the 95% predicted confidence intervals from the model, the estimated BMD_{10} for higher trend feeding behavior is 0.0047, and ED50 is 0.67 ppm MeHg (Figure 2.1A). Whereas the lower trend feeding PCRs did not change with increasing MeHg dose (P-value = 0.7614, n = 23, adjusted R-squared = -0.04, Figure 2.1B). Consequently, feeding behaviors that are decreased by MeHg are on average affected 26.4% (back transformed mean of 3.95) relative to the control.

The PCR of stimulus behaviors were evenly distributed between higher and lower trend groups (n = 13, 6 higher and 7 lower) after exposure to MeHg. The stimulus-only behavior model indicated stimulus behaviors have a significant positive relationship with MeHg exposure ($F_{(1,9)}$ = 11.46, P-value = 0.0081). The relationship was the same whether the stimulus behavior had a higher or lower trend group PCR [i.e. non-significant dose-trend interaction ($F_{(1,1)}$ = 2.76, P-value = 0.1309) and non-significant trend group main effect ($F_{(1,1)}$ = 2.61, P-value = 0.1410)]. Consequently, the two trend group PCR types were combined and a model containing all stimulus PCRs was constructed (Figure2. 2). Using the 95% predicted confidence intervals from the model, the estimated $BMDL_{10}$ of the stimulus behavior type is 0.0201 and BMD_{10} is 0.3936 ppm of MeHg (Figure 2.2).

Sixty percent of the swimming behavior observations had a lower trend PCR after exposure to MeHg (n = 37 out of 62). Both higher and lower trend groups of swimming behaviors were examined with a swimming only model, where PCR had no significant patterns with dose or trend type (overall model $F_{(3,58)}$ = 0.75, P-value = 0.5271). Consequently,

swimming behaviors whether increased or decreased after MeHg exposure are on average

affected 17.39% (back transformed mean of 3.37) relative to the control.
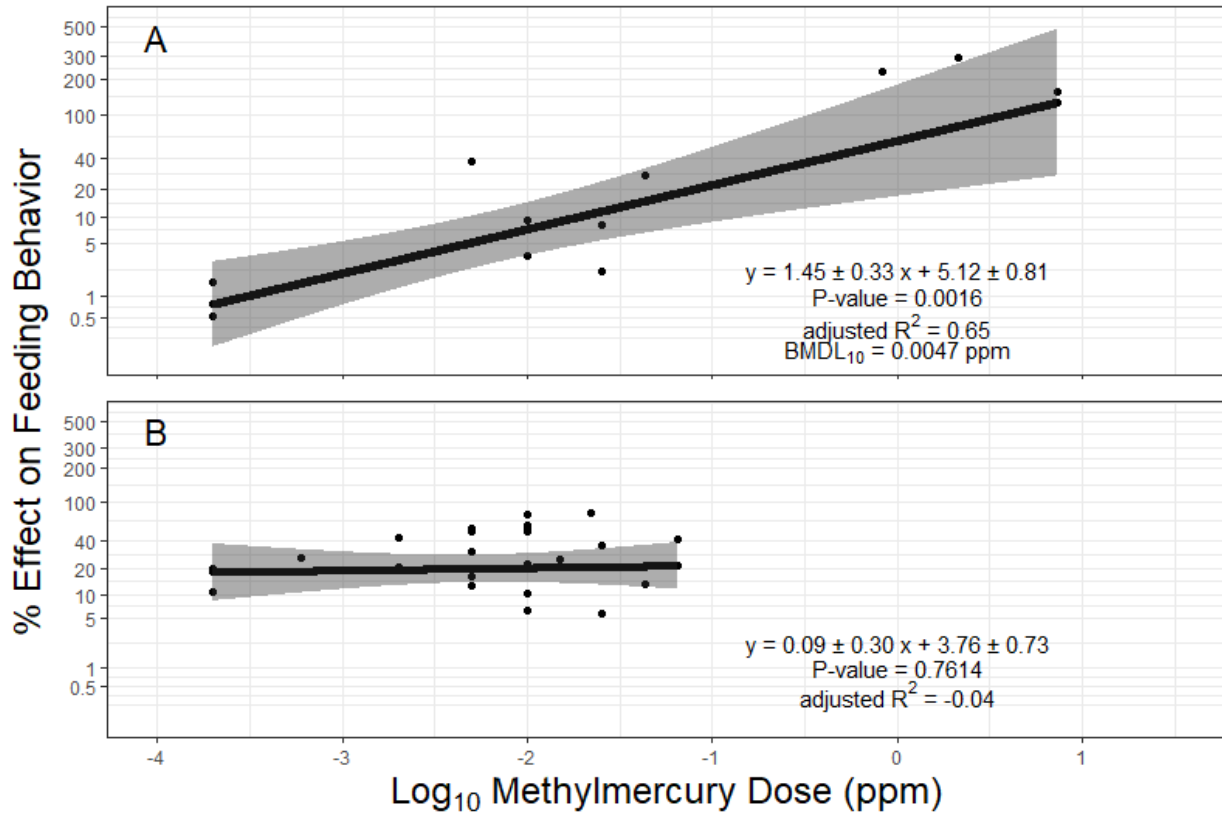
Figure 2.1. Linear relationship between the percent effect on early life stage fish feeding behaviors and methylmercury dose. Panel A are feeding behaviors that were higher relative to the control and panel B are feeding behaviors that were lower. Grey shaded area is the predicted 95% confidence interval. Parameter variance reported in model equation is standard error.
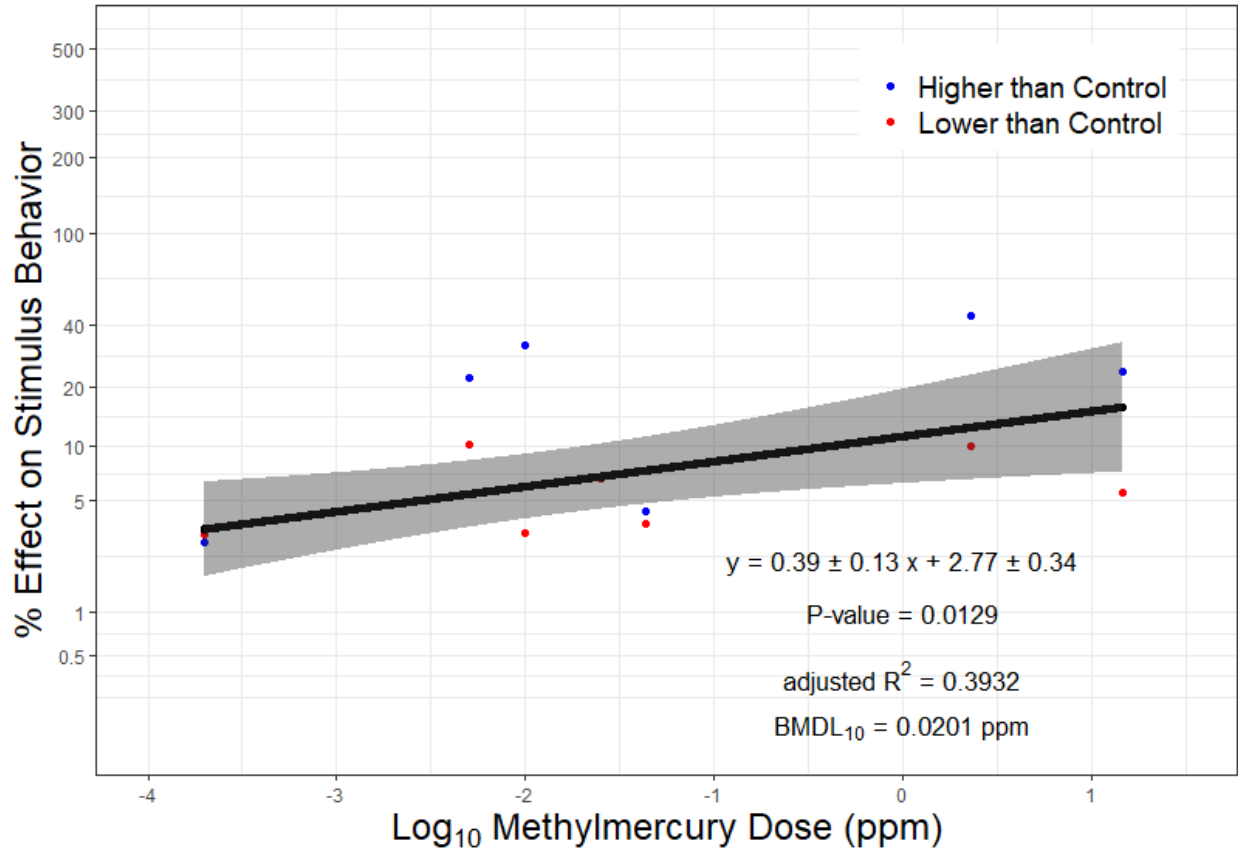
Figure 2.2. Linear relationship between the percent effect on early life stage fish stimulus behaviors and methylmercury dose. Parameter variance is standard error.

Discussion

The numerous recent studies examining MeHg exposure impacts on ELSF behavior has allowed for a more diverse examination of environmental risk using sublethal behavior impacts. By understanding these individual level behavior changes, appropriate levels of risk can be applied to impacts from low levels of contaminants, and through population modeling, could be used to understand impacts on larger populations of fish (e.g. Murphy et al. 2008; Armstrong et al. 2020; Albers et al. 2022a). This study surveyed the scientific literature and summarized MeHg effects on three general fish behavior types: feeding, stimulus and swimming behaviors. The effects summarized occurred on five different species of fish larva, at MeHg doses relevant to current aquatic ecosystems across the United States [0.0001 – 10 ppm; (Wentz et al. 2014)].

Not all behavior types examined exhibited a dose dependent relationship with increasing levels of MeHg dose, swimming and lowered feeding behaviors had a constant 17 and 26% effect across all doses of MeHg. While the effect on these behaviors did not respond to increasing levels of MeHg, the change in behaviors is still relevant since PCR is calculated using an unexposed control group of fish within each study. The PCR of stimulus and higher feeding behaviors of ELSF did have a positive dose dependent relationship with MeHg dose, with higher feeding behavior effects increasing almost four times faster than stimulus behaviors over the same level of MeHg increase. As multiple studies in this review have demonstrated, increases in stimulus and feeding behaviors after MeHg exposure are not uncommon and may be due to multiple reasons. First, depending on the behavior measured, an increase in response is not unexpected. For example, some of the increases in feeding behaviors included prey handling time, larva reaction distance to prey, time to react to environmental startle, etc. Second, since the responses examined in these studies are sublethal effects, multiple biological compensatory mechanisms could result in a behavior response contrary to expectations, such as increases in activity requiring more energy, thus increases in prey capture probability. Because mercury has multiple modes of action occurring in these complex organisms, reasons into why some behavior responses increase after exposure may never be determined. But it is clear by this review that behavior endpoints are more complex and more difficult to summarize than the constant negative impact of lethality.

The differences found in the study between the three behavior types (feeding, stimulus and swimming) and how they responded to MeHg may be contributed to the different parts of the brain used in the performance of each behavior and how mercury discriminately disrupts those areas. Recent zebrafish (ZF) brain imaging techniques have shown that when ZF perform

different types of behaviors, different areas of the brain are stimulated. During swimming bouts, ZF use a medial stripe of glycinergic neurons (Dunn et al. 2016; Severi et al. 2018). In contrast, there is a localized area in the cerebellum whose activity correlates with a visual stimulus (Severi et al. 2018). Feeding behavior is more complex, integrating four parts of the brain (Cong et al. 2017); where an area near the contralateral optical tectum is first activated during eye orientation on prey, the three addition groups of neurons in the hypothalamus, midbrain and hindbrain were activated as the fish orientated the head to prey, closed the distance to the prey, attempts to capture prey, and finally captures prey. Mercury also differentially affects brain areas and cell types, with the cerebellum and visual cortex being primary targets, specifically granule cells in the cerebellum are very sensitive to MeHg induced neurotoxicity (Kaur et al. 2012). The combination of selective toxicity and behavior use of different parts of the fish brain could make different behavior endpoints more or less effected by MeHg exposure.

The results from this study reiterate the sensitivity of ELSF behavioral endpoints to MeHg as compared to lethality-equivalent endpoints. Dillon et al. (2010) found that growth and survival of ELSF was affected by MeHg starting at 0.02-0.05 ppm, whereas MeHg effects on ELSF behavior starting as low as 0.0002 ppm (Weis and Weis 1995b). Very low levels of mercury are ubiquitous across the landscape, creating a background of low level contamination (Amirbahman and Fernandez 2012). Indeed, we found the controls in the included studies had an average of 0.0076 ppm Hg (n=6) typically from laboratory feed contaminated fish food. Dillion et al. (2010) found that ELSF with 0% injury to lethality-equivalent endpoints had a median Hg tissue concentration of 0.05 mg/kg (n=7). Using the relationships constructed in this study, a level of 0.05 ppm is predicted to alter increased feeding behaviors by 16%, 21% effects on decreased feeding behaviors, 7.5% effect on stimulus behaviors, and 12.8% on swimming

behaviors. But most wild populations of fish across the U.S. are exposed to low levels of MeHg from the pervasive Hg pollution stored in the soil that is continually deposited from air pollution (Amirbahman and Fernandez 2012; Bank 2012; Pacyna et al. 2016; Blukacz-Richards et al. 2017). While the scale of mercury pollution is global, research suggests Hg levels can be lowered in aquatic environments if regulations and limitations are enacted (Pacyna et al. 2016; Blukacz-Richards et al. 2017; Blanchfield et al. 2022; Zolkos et al. 2022).

Since sublethal endpoints are inherently more sensitive than lethal endpoints, we expected to find lower MeHg dose effect concentrations using sublethal ELSF behavior. However, impacts on ELSF behaviors in this study were found to be within the confidence intervals predicted for ELSF lethal-equivalent predictions (Dillon et al. 2010). Using the reported tissue-dose levels, a tissue level of 0.1 ppm Hg wet weight is equivalent to ~0.004 ppm dose of MeHg (Mora-Zamorano et al. 2016a; Albers et al. 2022c, 2022d). Using the relationships constructed in this study, a dose of 0.004 ppm MeHg resulted in 20% injury to decreased feeding behaviors, 4.5% injury to increased feeding behaviors, 5.3% stimulus behaviors, and 12% on swimming behaviors. These fall with the 95% confidence intervals of predicted effect using the ELSF lethality-equivalent model by Dillon et al. (2010), where a tissue concentration of 0.1 ppm Hg would result in an increase of 19.8 (0.07-35.5) percent increase for ELSF. In addition, the one ED50 calculated in this study for increasing feeding behaviors was also within the predicted confidence interval of the EC50 ELSF lethality-equivalent model by Dillon et al. (2010), suggesting ELSF may have a similar PCR sensitivity between lethal and sublethal endpoints. The overlap of lethal and sublethal sensitivity may be from the higher variability of behavior expression relative to lethal endpoints which results in high variability in PCR predictions. In addition, some behaviors had a constant effect regardless of the MeHg dose,

indicating that some behaviors are affected even at the lowest doses of MeHg. Those behaviors that are constantly affected also add variability to any overall dose dependent relationship.

One major limitation with the results of this study is from the use of MeHg dose to predict effects as compared to actual mercury concentration in the tissue of ELSF. This study limitation was from the lack of reporting the tissue concentrations in 46% of the included studies. As evident by the three studies that reported tissue concentrations after ~5-32 hours post fertilization (hpf) embryonic exposure (Mora-Zamorano et al. 2016a; Albers et al. 2022c, 2022d), tissue concentrations in larva are at least two orders of magnitude higher than the dose concentration. Elevated MeHg tissue concentrations are caused by many factors including: bioaccumulation of MeHg; contaminated laboratory space from the prevalence of Hg in the air, soil and water; and/or contaminated commercially available foods (Weiss et al. 2005; Dorea 2006; Alexander et al. 2008). Because of the uncertainty with Hg dose and tissue concentrations, reporting tissue Hg concentrations from each treatment in every study is required to use and understand study results and implications. We once again reiterate the importance that all toxicologists measure resulting tissue concentrations after any chemical dosing experiment (McCarty et al. 2011).

Mercury is prevalent in the environment and can have neurological impacts at very low doses, especially if exposure occurs during development. Exposure to ELSF is no exception, where results from this study show that some ELSF behaviors are altered at any level of MeHg embryonic exposure, while other behaviors have $BMDL_{10}$ starting at 0.0049 ppm MeHg have been found to be more susceptible than adult or juvenile fish and ELSF behavior impacts has been impacted at MeHg levels starting at 0.0002 ppm. We summarized all available research about ELSF behavior impacts from MeHg exposure and found differential impacts on behavior

types. Swimming and feeding behaviors that were lowered by MeHg exposure had constant

effects no matter the MeHg dose. Whereas, stimulus behaviors and feeding behaviors that were

increased after MeHg exposure had a positive relationship with dose. Lastly, ELSF behavior

effects after MeHg were within the same predicted range of ELSF lethality-equivalent effects.

Because behavior is so crucial to ELSF survival (feeding, evading predators), perturbations can

have significant population implications. Knowing how different types of behaviors are

impacted and which critical ones are impacted the most will give risk assessors the tools needed

to better assess the impacts from mercury contamination to individuals and populations.

CHAPTER 3: ALTERED LARVAL YELLOW PERCH SWIMMING BEHAVIOR DUE TO METHYLMERCURY AND PCB126 DETECTED USING HIDDEN MARKOV CHAIN MODELS

Abstract

Fish swimming behavior is a commonly measured response in aquatic ecotoxicology because behavior is considered a whole organism level effect that integrates many sensory systems. Recent advancements in animal behavior models, such as Hidden Markov Chain models, suggest an improved analytical approach for toxicology. Using both new and traditional approaches, we examined the sublethal effects of PCB126 and methylmercury on yellow perch larvae (*Perca flavescens*) using three doses. Both approaches indicate larvae increase activity after exposure to either chemical. The middle methylmercury-dosed larvae showed multiple altered behavior patterns. 1) Larvae had a general increase in activity, typically performing more behavior states, more time swimming and more swimming bouts per second. 2) When larvae were in a slow or medium swimming state, these larvae tended to switch between these states more often. 3) Larvae swam slower during the swimming bouts. The upper PCB126-dosed larvae exhibited a higher proportion exhibited a fast swimming state, but the total time spent swimming fast decreased. The middle PCB126-dosed larvae transitioned from fast to slow swimming states less often than the control larvae. These results indicate developmental exposure to very low doses of these neurotoxicants alter yellow perch larvae overall swimming behaviors, suggesting neurodevelopment alteration.

Introduction

Toxicologists use behavioral endpoints because they measure whole organism level effects of chemicals by integrating many sensory systems and generate a measurable physical manifestation that represents the health of an organism (Handy et al. 1999; Clotfelter et al. 2004; Campbell et al. 2005). Although exhibited behaviors can be caused by many factors (i.e. physiological deformities, learned experiences, environment), they are critical in understanding impacts from exposure to neurotoxic chemicals. Often the behavioral endpoints evaluated in a toxicological study are calculated using an overall generalized summary statistic over the entire assay. For example, to determine mercury or PCB effects on fish larvae, studies have used behavior endpoints such as average swimming speed, total distanced traveled or total number of turns during the time period of the assay (Weis and Weis 1995b; Couillard et al. 2011; Péan et al. 2013; Mora-Zamorano et al. 2016a, 2017; Bridges et al. 2016a). While these endpoints are appropriate in determining general trends in activity, they may not detect subtle chemical alterations that affect how the larvae are swimming. Fine scale behavioral discrimination is required because we are increasingly able to determine physiological mechanisms underlying behavior. Recent zebrafish studies have made direct connections between functioning putative cholinergic efferent neurons, motor neurons and detailed swimming behavior [i.e. glide phase of burst and glide locomotion (Lunsford et al. 2019)] and that maturation of swimming occurs within the first few days of life (Roussel et al. 2020), suggesting embryonic exposure can be critical to measured effects on swimming endpoints.

With advancements in behavior analyses, researchers can now more easily study animal movement strategies and transitions between behavior states (Egnor and Branson 2016; Edelhoff et al. 2016). Discrete state-space models have become a common way to analyze animal

25

movement data that has consistent observation rates [see review by (Jonsen et al. 2013;

McClintock et al. 2014)]. Hidden Markov chain models (HMM) are state space models that

include components to determine direct and indirect behavioral influences (Zucchini et al. 2017).

Hidden Markov Chain models have been used to find how different types of behavior (i.e.

behavior states) performed by animals relate to such things as neural activity and habitat use [e.g.

(McKellar et al. 2015; Dunn et al. 2016; Marques et al. 2020)]. Hidden Markov Chain models

are often used in the analysis of human behavior including investigating changes due to chemical

exposure [e.g. (Patzelt et al. 2014)] but only a few researchers have used HMMs to assess the

effects of chemical exposure on fish behavior. In the early 2010s before the recent proliferation

of HMM computational tools were available, researchers confirmed applicability of HMMs in

toxicology by comparing them with self-organizing maps and determined permutation entropy

and fractal dimension of zebrafish (*Danio rerio*) decreased after exposure to formaldehyde (Liu

et al. 2011; Li et al. 2013). They also applied HMMs to data collected after exposure of

zebrafish and *Daphnia magna* to Diazinon [O, O-diethyl-O-(2-isopropyl-6-methyl-pyrimidine-4-

yl) phosphorothioate], where zebrafish turned right more often but *Daphnia magna* movement

was not altered (Chon et al. 2010; Nguyen et al. 2011). To our knowledge, no recent studies

have applied the new suite of HMM analytical tools to behavioral toxicology, which are a

promising development, particularly given the recent focus of using behavioral endpoints in the

regulation of chemicals and emphasis on population level relevant behaviors (Ågerstrand et al.

2020).

Methylmercury (MeHg) and PCB126 (3,3',4,4',5-pentachlorobiphenyl) are two common

aquatic industrial pollutants that are also known developmental neurotoxicants. Methylmercury

exposure can lead to a range of adverse effects from widespread brain damage to subtle

impairments in motor and sensory functions in both humans and animal models including zebrafish (Nogara et al. 2019; Pereira et al. 2019; Yang et al. 2020). Methylmercury tends to disrupt multiple cellular sites resulting in altered calcium signaling, impaired mitochondrial function, and accumulation of oxidative stress, all of which can damage neurons (Caudle and Miller 2015). In addition to being an aryl hydrocarbon receptor agonist, PCB126 has demonstrated effects on multiple behavioral endpoints in rats (Rice and Hayward 1998, 1999; Rice 1999; Vitalone et al. 2010; Cauli et al. 2013) and fish (Couillard et al. 2011; Rigaud et al. 2013; Liu et al. 2015; Xu et al. 2015; Glazer et al. 2016). Similar to MeHg, PCB126 alters multiple pathways in mammals that result in neurological changes (Kodavanti et al. 1993; Seegal et al. 2005; Coccini et al. 2007; Piedrafita et al. 2008b; Ndountse and Chan 2009). Fish embryonic exposure to PCB126 does not always lead to larval behavior changes, but can result delayed adult behavior changes (Glazer et al. 2016; Aluru et al. 2017).

The goal of this study is to understand the neurotoxic effects on the expression of both overall behavior characteristics and of different behavioral states in yellow perch (YP; *Perca flavescens*) after exposure to low levels of MeHg and PCB126. Our objective is to determine how neurotoxicant pollutants altered spontaneous swimming of larval fish by examining endpoints that summarize swimming characteristics over the entire behavioral assay and also those that examine swimming patterns that represent different behavior states within an assay such as different types of swimming. These behavior observations could be used in future work to model impacts of pollution on the growth and survival of larval fish (e.g., (Murphy et al. 2008; Armstrong et al. 2020)).

Methods

Fish dosimetry and husbandry

Yellow perch embryo procurement, exposure and husbandry protocols from Mora-Zamorano et al. (2017) were followed. A general description and noted exceptions follow. All methods were approved by the University of Wisconsin at Milwaukee Institutional Animal Care and Use Committee (IACUC, #18-19#04). All fish were spawned under controlled laboratory conditions. For each years' spawning, five pairs of fish were spawned and one egg ribbon per pair was obtained and maintained as biological replicates. To minimize handling time, a subset of eggs were extracted from the egg ribbons (experimental replication) using a sterilized leather hole punch (Sona Enterprises #791LP; 6 egg masses per pair in 2016 and 10 egg masses per pair in 2017, totaling 240 egg masses). These circular egg masses were plated in metal-free, plastic culture petri dishes (100 mm diameter × 25 mm depth) containing an average of 0.62 ml of media per egg [5/8" hole punch in 2016 (~81 eggs) and 3/4" hole punch in 2017 (~115 eggs)].

This study chose exposure levels and timing that either mimicked parental transfer of MeHg or water transfer for PCB126 (Westerlund et al. 2000; Alvarez et al. 2006; Mora-Zamorano et al. 2016a; Bridges et al. 2016a, 2016b; Carvan et al. 2017). Due to the behavioral focus of this study, we used dose levels of these chemicals that did not create any observable physical deformities [e.g. Early Life-Stage Toxicity score (Heiden et al. 2005)] which would alter behavioral endpoints like swimming or eating. To that end, a preliminary dosimetry/sensitivity study was used in addition to previous research results (e.g. (Mora-Zamorano et al. 2017)) to determine dosing levels that met these criteria and all larvae exhibiting deformities or died with 24 hr after assay were removed from analysis. Embryos in this study were exposed for 20 hours after plating [~7-27 hpf, starting at 2-4 cell stage] with either 0,

0.00021 and 0.02156 ppm MeHg (based on 0, 0.001 and 0.1 µM of MeHg; MeHgCl in a 100%

ethanol solvent), or 0, 0.01 and 1ppm PCB126 (PCB126 in a 100% DMSO) [each 0

concentration treatment (i.e. control) contained water and the appropriate solvent resulting in all

treatments containing either 33.33ppm ethanol or 500ppm DMSO]. Yellow perch fertilized and

dosed egg masses were rinsed 4 times with clean embryo medium to stop chemical exposure. See

Supplemental section for more husbandry details.

Directly after exposure in 2016, three fertilized egg masses were randomly chosen from

the 30 egg masses in each dose and were removed from their petri dish and stored at -80°C until

chemical analysis in either Eppendorf tubes for MeHg treatments or glass vials with Teflon

coated tops for PCB126 treatments. PCB126 treated samples were analyzed with GC/ECD using

EPA method 8082 with a minimum detection limit of 0.5 pg of PCB126 in the 0.5 mL sample.

MeHg treated samples were freeze-dried prior to acid digestion. Total dry weight of mercury

was detected using a MERX-T automated mercury system (Brooks Rand Instruments, Seattle,

WA) with Mercury Guru™ software (version 4.7.6) via the manufacturer's protocol in

accordance with EPA Method 1631(Carvan et al. 2017) (n=3, Table S3.1). The precision of this

instrument had a relative standard deviation of 2%, the Limit of Blank (LoB) was 2.19 pg.

Swimming assay

Typically, YP larvae initiate swimming at 17 dpf (Mora-Zamorano et al. 2017) at which

point they were presented with food. We wanted to assess behavior at the point where larvae

were independent and actively swimming and feeding. Consequently, the locomotion assay was

conducted when YP larvae were 27 dpf, where 10 larvae were placed in a square slanted side

petri-dish (outside dimensions of 72.5 x 72.5 mm, swimming area dimensions of 56 x 56 mm) with 25 ml of water (~8 mm water depth; see Table S3.2 for the number of assays and fish). Since previous locomotion assays indicated MeHg impacted YP larvae only during light periods (Mora-Zamorano et al. 2017), light levels were held constant during the entire locomotion assay and set to 69 lx (MacPhail et al. 2009). Similar to previous studies(Mora-Zamorano et al. 2017), light was generated using an LCD computer monitor placed below the petri dish and set to illuminate the dish using pure white light (Red:255, Green:255, Blue:255). Since LCD screens do no generate much heat, temperature in the petri dish was assumed to be similar to the room and water temperature (19-21 $^{\circ}$C). Assays were conducted during the afternoon between 1200 and 1730 hr to minimize within day variability (MacPhail et al. 2009). The swimming assay was performed within a testing chamber that isolated the 10 larvae in the petri dish from light and sound, has been described in three previous studies (Mora-Zamorano et al. 2016b, 2016a, 2017), and provided adequate light and video surveillance to view all individual movement. Similar to previous studies(Mora-Zamorano et al. 2016b, 2016a, 2017; Carvan et al. 2017), the larvae were allowed to acclimate for 5 min, then spontaneous larval movement was constantly recorded at a rate of 30 frames per sec for 5 more minutes (8987 total frames after processing), resolution of 650 x 650 pixels/mm with a final mean visual resolution of 7.77 pixels/mm (SD = 0.41, n=122). Spontaneous movement (movement not initiated by some external stimuli but by the fish's inner impulse or inclination) was used in this assay in contrast to other common toxicological assays that use external stimuli to instigate fish movement. Videos were saved as avi format using a Logitech C920 camera and MATLAB Image Acquisition Toolbox (R2012b).

Data collection

Spontaneous movement of larvae was tracked using Ctrax software (version 0.5.18 (Branson et al. 2009)). Tracking errors were corrected using the Ctrax Fixerrors GUI (version 0.2.24). Manual correction was also required at locations where the fish ceased movement but the track did not (this occurred due to the mismatch between the precise tracking software and the pixelated video of small larvae and it presents as a type of sudden movement between two separate parts of the fish's body, i.e. the track "jitters" rapidly back and forth). Any track deviation greater than 1 pixel or 0.15 mm, was corrected to accurately represent the middle point of each larvae. We used the Behavioral Microarray MATLAB Toolbox, compute_perframe_stats script (Branson et al. 2009; MATLAB 2017) to compute speed (i.e. velocity magnitude of fish center, not center of rotation) per frame for each individual fish from the corrected Ctrax trajectories. Similar to Ingebretson and Masino (2013), the centroid location defined the individual larvae location and activity at each frame, where swimming was defined as movement that was at least 1 mm/sec or 0.03333 mm per frame (i.e. magnitude of velocity at larvae center) and lasted longer than 5 frames (0.166 sec). Whereas the resting behavior occurred during frames where movement was less than 1 mm/sec or if greater than 1 mm/sec, lasted less than 5 frames. Where resting behavior occurred, speed and distance for those frames were changed to zero. In addition, starting at frame three, we recalculated the turning angle using the same method as Ctrax, as the difference between the four-quadrant inverse tangent of the two trajectories where the first trajectory was constructed from the first two locations in the sequence, and the second trajectory from the second two locations in the sequence. This results in a turning angle that ranges from -3.14 to 3.14, where zero is straight ahead movement, a

negative value indicates a right turn and a positive value indicates a left turn. Larval orientation was assumed to be in the direction of movement.

Behavior endpoints

Twelve average behavioral endpoints were assessed from the swimming assay to determine effects from exposure (Table S3.3): number of swimming and extreme swimming bouts; swimming bout duration, speed and turning angle; total distance traveled and time swimming; number of fish lengths swam during entire assay; overall average step length and variability, turning angle and variability. Extremely fast swimming bouts were used to indicate times of intense swimming behavior where fish were swimming almost half the length of the petri dish in one second (i.e. 30mm/s). Even though fish were of similar size (average size of 7 mm $\pm$ 1.15 SD, n= 1220), fish length was also measured and incorporated into the Fish Lengths endpoint (Table S3.3). A pictorial diagram of the analytical steps taken in this study can be found in Figure S3.3.

Hidden Markov model fitting

In addition to the more general overall endpoints that summarize the entire assay, a state space model (HMM) was constructed for each larvae's swimming track to determine whether there were multiple swimming behavior states occurring within each assay and the characteristics of the behavior states (Figure S3.3) For each best fit HMM, the output parameters from that model were used to describe the different behavioral states and were used as additional behavior endpoints in our subsequent statistical analyses to determine how these states change after chemical exposure. An HMM was not constructed for any individual larvae and excluded from

32

the subsequent analyses if the larvae did not have at least one swimming bout (10 larvae in MeHg treatments and 3 larvae in the PCB126 treatments were removed; Table S3.2). Because the data collected in this study were precise locations taken at constant intervals, the R package moveHMM (Michelot et al. 2016; R Core Team 2019) was used to construct the HMMs that uses frequentist inferential tools to determine parameter estimates. The HMMs were constructed using the same modified step lengths and turning angles calculated for the averaged endpoints as described in Table S3.3 (i.e. used the prepData function in moveHMM R package for object formatting only). In addition, all HMMs did not contain any covariates since all fish were maintained in constant laboratory conditions and the main goal of this analysis was to test between exposure treatments.

The HMM model fitting procedure consisted of testing a range of swimming states that contained a range of initial values, resulting in multiple fitted models to select the one best fit model from. This procedure was conducted so that the resulting best fit model accurately represented the type of behavior each fish exhibited. The range of potential models consisted of three different behavior states: slow, medium and fast swimming states where s1 HMMs contained only one behavior state, s2 HMMs contained any two behavior states, and s3 HMMs contained all three behavior states. Using a potential of three behavior states, we constructed a list of 10 possible HMMs to test and from which to select the best fit model (Table S3.4). These 10 potential models differed in the number of behavior states and initial starting values for each state so as to encompass the range of behaviors exhibited by the individual larva.

The initial values were either set as a constant or calculated from each larva's swimming track (Table S3.4). The slowest swimming state in the s1_slow, s2 and s3 HMMs had constant initial values which were based on the tracking location accuracy in this study (≤ 0.15 mm).

33

Initial values in these models for slow swimming mean step length was 0.1 mm, slow swimming step length standard deviation was 0.01, and the slow swimming turning angle mean was 0. Medium and fast swimming states in all HMMs had 0.01 for the percentage of zeros (i.e. distance moved equal to zero). The rest of the initial values were determined from the individual larvae's tracking data. The percentage of zeros inputs were determined by the percentage step lengths ≤ 0.15 mm. The initial parameter values for the s2 and s3 HMMs were calculated only when the larva was moving (i.e. step length > 0.15 mm) including mean step length, mean angle, standard deviation (i.e. Kappa) of the step length or angle, respectively. For any behavior state other than slow swimming, a range of initial mean values were tested (25th, 50th, or 75th percentiles) and again based on time steps where step lengths were > 0.15 mm.

Best fit hidden Markov model selection

Once all 10 of the possible HMMs were fit for each larvae, a hierarchical selection for the best fitting model was conducted. First, an HMM was rejected if it did not converge or parameter estimates from the HMM were unrealistic (i.e. infinite step variance or AIC, step length mean for any state > 50 mm, or a defined state never occurred; 56 out of 1207 larvae; see Table S3.2 for distribution across treatments). Second, since HMMs contain different numbers of parameters corresponding to the number of behavior states, comparison between models was a two-step process. First, the best fit model within each group of HMMs that have the same number of states (e.g. s1_slow, vs s1_25 vs s1_50 vs s1_75) was selected. The model with the lowest AIC was used to select the best one, two and three state HMM for each larva. Second, to select the best overall model for each larvae, we compared the AIC between the differing state

34

HMMs and choose the lowest AIC, so long as it was at least 10% lower than the next highest AIC (e.g. s1 vs. s2 vs. s3).

<u>Best fit hidden Markov model behavior state standardization</u>

To compare between individual larva, the HMM behavior states were standardized by reordering and renaming. The HMM state initial values were set up in increasing step length means (slow, medium, fast), but the resulting best fit HMM output behavior states for each individual larvae did not always have increasing step length. This is because the final HMM behavior state is defined by not only the step length but also turning angle characteristics and/or the behavior state that was performed first in the time series was what was used to label the state. The best fit HMM behavior states were subsequently standardized and reordered in two steps. First, for each larva's best fit HMM, the states were reordered using the mean step length to describe them as slow, medium and faster swimming behavior states (i.e. changed the state label). Second, we confirmed the behavior states reported from the s1 and s2 HMMs were correctly classified and labeled as slow, medium or fast. To do this, the states in the s1 and s2 HMMs were compared to the slow, medium and fast states produced by the s3 HMMs by constructing 12 Linear Discriminant Models (LDA), one base model for predicting s1 and s2 within each of the 12 year/chemical dose combinations (Table S3.5). The 12 LDA base predicting models were constructed using the lda function in the MASS package (Venables and Ripley 2002) and only using larvae with an s3 HMM. The base predicting LDA models were constructed using the four HMM behavior descriptive parameters to predict the slow, medium and fast swimming behavior states (model equation: slow, medium and fast swimming = turning angle concentration + turning angle mean + step length mean + step length standard deviation).

The number of observations in the base predicting LDA models was the number of larvae times three (i.e. three behavior states) thus treating all within and between fish behavior states as independent of one another (Table S3.5). The 2016 MeHg middle dose treatment only had one larva where a s3 model was selected; therefore, there was no renaming of s1 or s2 states in this year/chemical dose group (i.e. 15 larvae; Table S3.5). Linear Discriminant Models prediction accuracy for base predictive models was measured using cross validation where a random draw of 80% of the data was used to construct a model and then calculated prediction accuracy of the remaining 20% of the data. This was done 50 times for each of the 11 groups of data to determine total accuracy over all predicted behavior states (59 ± 0.06 %) and within behavior state accuracy (slow state = 56 ± 0.15 %, medium state = 52 ± 0.24 %, and fast state = 69 ± 0.09 %; Table S3.5). Sometimes the LDA predicted the same state to occur more than once for a larva. If that occurred, step length was used to reorder them. For example, if two slow states or two medium speed states were predicted for the larva than the lower mean step length was assigned the slow state and the higher one a medium state (Table S3.5; MeHg: 111 out of 380 larvae; PCB126: 108 out of 321 larvae). If two fast states were predicted than the lower mean step length state was renamed to medium (Table S3.5; MeHg: 12 out of 380 larvae; PCB126: 5 out of 321 larvae).

After standardizing the behavior states using this LDA procedure, all larvae had states ordered using the mean step length to describe them as slow, medium and faster swimming behavior states. In addition, all larvae with a s1 and s2 HMM had behavior states that were labeled relative to those exhibited by larvae in s3 HMMs. This standardization allowed for HMM results to be comparable between larvae and treatments. For example, when examining effects of exposure levels on fast swimming states, this comparison only used fish that performed

the standardized fast swimming behavior making the number of larvae for each comparison

unique (see Treatment Testing section below; Table S3.5).

Treatment testing

All behavioral endpoints were examined for chemical dose treatment differences using

Bayesian statistical methods (see supplemental for additional details). We choose to analyze

each behavior endpoint independently in order to allow for comparisons of multiple individual

behavior endpoints between analytical methods and determination of endpoint sensitivity to

chemical exposure. Since the multiple endpoints are from the same fish and collinearity may

occur between them, we considered using a Multivariate model that combined all 12 behaviors

and tested for treatment differences, however the currently available Bayesian software cannot

handle such complexity and would likely not converge. In addition, multiple individual behavior

endpoints produced in this study are to be used as inputs for an Individual Based Model of young

of year growth and survival. All Bayesian models consisted of two main effects (treatment and

year), main effect interaction, and a random batch effect since assays were ran in batches of 10

larvae. Due to high variability between years, a model containing a non-constant variance

parameter was constructed that estimated each year variance separately. Response variables and

residuals were examined for normality using density distributions and Box Cox transformation

were applied where needed in all non-negative response variables using the boxcox function in

the MASS package (Table S3.6; Venables and Ripley 2002). All responses that were normally

distributed either with or without a transformation were predicted using a normal distribution

model, whereas those that were severely right skewed were predicted using a t distribution model

where degrees of freedom (df) was estimated with uniform distribution [dunif (3,30); Table S3.7

and S3.8, respectively]. Priors were set to be non-informative and all models were run with three chains (see supplemental material for detailed methods). To facilitate future use of parameter estimates, both population and individual level parameter estimates were generated. Lastly, a Chi-Square test from the R stats package (R Core Team 2019) was used to determine whether the proportion of s1, s2 and s3 HMMs selected were different between treatments. Alpha level was set at 0.05.

Results

The amount of mercury found in larvae from the 0, 0.00021 and 0.02156 ppm dosed treatments were 0.39 ± 0.08, 3.34 ± 0.64 and 420.62 ± 88.02 ppb wet weight, respectively (Table S3.1; average accuracy of $98.06 \pm 11.57\%$, n = 14 base standard samples). Neither the PCB126 control nor the 0.01 ppm PCB126 dosed larvae had any detectable levels of PCB126 in the whole embryo samples, but the 1 ppm dose had 0.006 ± 0.005 ppm PCB126 wet weight (Table S3.1, average detection limit of 0.000316 ± 0.000063 ppm, n = 9, maximum of 0.000478 ppm; average accuracy at 1μg/L of $110 \pm 0.099\%$, n=2).

On average 94.7 ± 0.06 % of larvae within each chemical/year/treatment group were successfully fitted with an HMM (Table S3.2). The number of larvae that consisted of one, two, or three behavior states exhibited a consistent pattern within each treatment, where a s1 model was found the least, followed by a s3 model, and most larvae exhibiting a s2 model (i.e. two behavior states; Figure 3.1; Table S3.5). The proportion of each HMM type changed as chemical levels changed, with the upper MeHg dose having significantly more s2s relative to s3s as compared to the middle MeHg dose (Chi-squared = 20.095, P-value = 0.0002; Figure 3.1). In PCB126, the proportion of three behavior HMMs increased in the upper dose until the proportion

of s2 and s3 HMMs were almost even (control vs upper: Chi-squared = 12.82, P-value = 0.0036; middle vs upper: Chi-squared = 11.525, P-value = 0.0088; Figure 3.1).
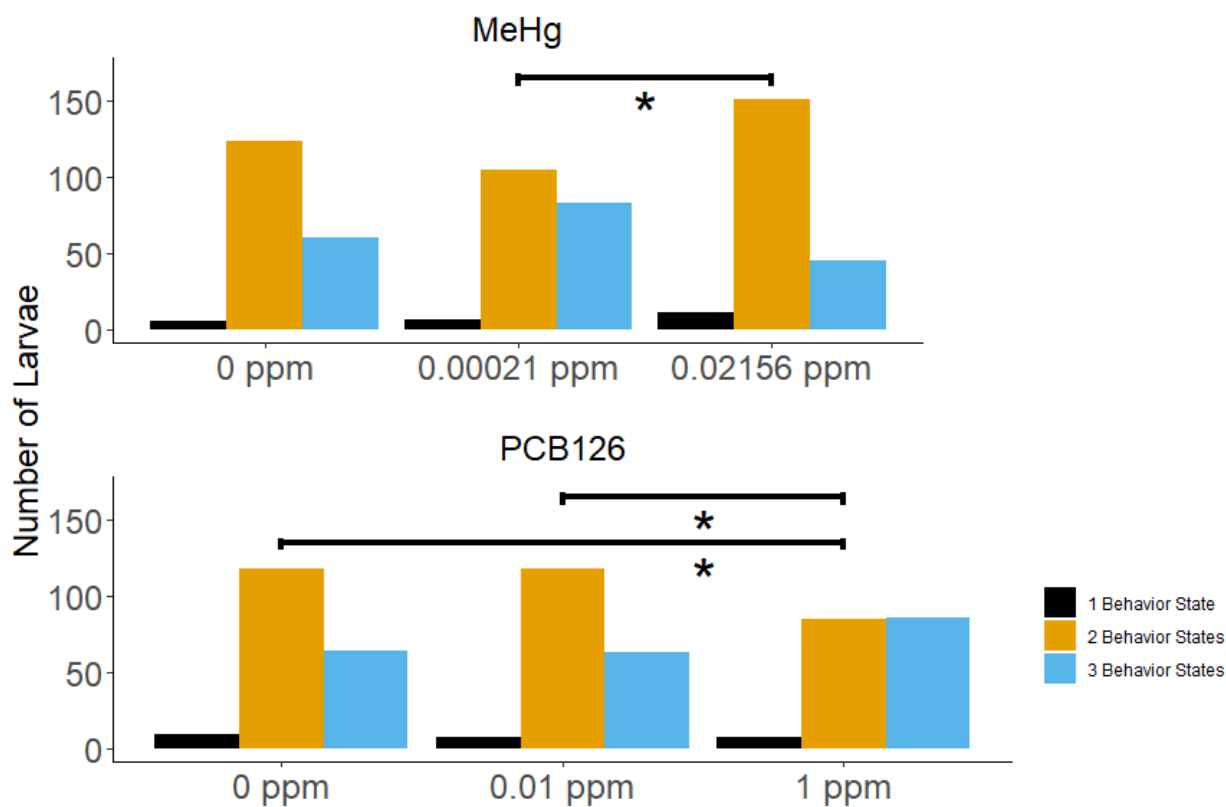
Figure 3.1. Number of best fit hidden Markov models for yellow perch larvae that contained one, two, or three different behavior states and were exposed to sublethal levels of methylmercury (MeHg) and PCB126. * indicates significance at ≤ 0.05

Of the 72 different behavior endpoints examined (36 for each chemical), 17 differed between the treatments (Table 3.1); four in the PCB126 tests and 13 in the MeHg tests. By random chance, the number of tests that could be significant is ~4 (0.05 alpha level × 72 tests = 3.6). None of the behavior endpoints tested had similar trends between chemicals. However, the slow state step length exhibited the opposite trend between chemicals, with the MeHg middle

dose having the lowest step length variation in the slow state and the PCB126 middle dose

having the highest.

Table 3.1. Significant results of the treatment effects on yellow perch larvae behavior after exposure to sublethal levels of methylmercury and PCB126. Presented for each behavior endpoint and treatment is the mean (original or back-transformed), transformed mean, P-value in parentheses, and pattern of significant trends. Trends are based on original mean trends. P-values and trends are reported in the following order: first level is the trend between control and middle treatment, second is middle verses upper treatment and third is control vs upper treatment (neg = significant negative trend, pos = significant positive trend, — = no significant trend).

Parameter	Control Treatment	Middle Treatment	Upper Treatment	Significant Trends
Methylmercury				
Swimming Bouts (per sec)	0.105	0.174	0.119	Pos Neg —
	63.71	48.51	60.33	
	(0.0020)	(0.0174)	(0.4148)	
Swimming Bout Speed (mm/s)	5.59	3.77	4.77	Neg — —
	38.96	45.77	41.63	
	(0.0198)	(0.1538)	(0.2258)	
Swimming Bout Turning Angle	1.013	1.279	0.850	— Neg —
	169	185.5	158.6	
	(0.0780)	(0.0061)	(0.1626)	
Total Time Swimming (sec)	61.14	139.6	101	Pos Neg
	(0.0002)	(0.0016)	(0.0388)	Pos
Overall Turning Angle Variation	1.293	1.477	1.117	— Neg —
	25.54	27.87	23.34	
	(0.2368)	(0.0280)	(0.1811)	
HMM Model Parameters				
Slow State				
Step Length Variation	0.084	0.060	0.112	— Pos —
	76.71	82.46	70.52	
	(0.1406)	(0.0039)	(0.0708)	
Medium State				
Step Length (mm)	0.206	0.219	0.163	— Neg —
	5.18	5.00	5.9	
	(0.6356)	(0.0348)	(0.0660)	
Step Length Variation	0.172	0.172	0.127	— Neg Neg
	5.56	5.56	6.44	
	(0.9968)	(0.0388)	(0.0192)	

Table 3.1 (cont'd)

Count	1292	1539	2063	— — Pos
	292.9	300.7	314.2	
	(0.5372)	(0.2966)	(0.0058)	
Fast State				
Step Length (mm)	0.634	0.578	0.493	— — Neg
	4.34	4.61	5.06	
	(0.8378)	(0.7254)	(0.0266)	
Turning Angle	-0.172	0.075	0.153	— — Pos
	(0.6788)	(0.890)	(0.0286)	
State Transition Probabilities				
Medium -> Slow	0.034	0.046	0.030	Pos Neg —
	59.31	49.58	63.1	
	(0.0414)	(0.0074)	(0.3476)	
Slow -> Medium	0.0099	0.0146	0.0119	Pos — —
	71.07	60.61	66.5	
	(0.0351)	(0.2664)	(0.3916)	
PCB126				
Total Time Swimming (sec)	68.23	87	50.02	— Neg —
	(0.3182)	(0.0278)	(0.2894)	
HMM Model Parameters				
Slow State				
Step Length Variation	0.079	0.113	0.064	— Neg —
	82.78	76.53	85.66	
	(0.1118)	(0.0336)	(0.5016)	
Fast State				
Count	1807	1753	806	— Neg Neg
	332	330	292	
	(0.8988)	(0.0124)	(0.0057)	
State Transition Probabilities				
Fast -> Slow	0.016	0.009	0.015	Neg Pos —
	58.0	74.2	58.7	
	(0.0242)	(0.0412)	(0.9214)	

When comparing the middle MeHg treatment to the control, YP larvae had more swimming bouts but swam slower, spent more total time swimming, and had a higher probability

switching between the medium to slow and slow to medium states (Table 3.1). In comparison

with the upper MeHg treatment, the middle MeHg treatment larvae had more swimming bouts

with higher turning angle and variability, spent more total time swimming, had lower slow state

step length variation, higher medium state step length and variation, and had a higher probability

switching between the medium to slow and slow to medium states. The YP larvae in the MeHg

upper treatment (verses the control treatment) had lower medium state step length variation,

more time performing the medium state, smaller fast state step lengths, and more left turns

during the fast state. Both MeHg treatments spent more time swimming than the control

treatment, but the middle treatment was the highest.

When comparing the middle PCB126 treatment to the control, YP larvae had a lower

probability of switching from fast to slow state (Table 3.1). In comparison with the upper

PCB126 treatment, the middle PCB126 larvae spent more total time swimming, had a higher

slow state step length variation, and a lower probability of switching from fast to slow state.

Additionally, the upper PCB126 treatment spent less time in the fast state as compared to either

the control or middle dose.

The effect of year was significant in 44 out of 72 behavioral endpoint models, where 9

out of the 44 had higher values in 2017 than 2016 (Table S3.9). For this study, the effect of

treatment was the only interest, consequently all other effects in the model were used to remove

variation in the treatment effect estimate. Batch variability ranged 1 – 69% of the total random

variation for 2016 and 1-86% for 2017 with the higher levels associated with the overall

behavior metrics (i.e. overall turning angle variation, swimming bout turning angle, total time

swimming, etc.) versus the HMM swimming parameters (Table S3.9). Consequently, depending

on the response variable the impact of the random batch variable can be low to high, indicating

that accurate representation of data collection with a hierarchical model is essential in determining differences between treatments for some behavioral endpoints.

Discussion

This study investigated sublethal impacts to YP larval swimming behavior after developmental exposure to environmentally relevant neurotoxicants MeHg and PCB126. After examining both traditional and new analytical techniques, more behavior endpoints were altered after MeHg exposure than PCB126. In addition, the new HMM analytical techniques found more altered swimming characteristics than the traditional methods for both chemicals. Many behavior endpoints did not exhibit a threshold response but a non-linear response (Lushchak 2014) which may be an indication of a compensatory mechanism that fish are known to have (e.g. neurogenesis (Calabrese 2008, 2016; Bhatia et al. 2019)).

Using a well-known neurotoxicant MeHg, YP larvae behavior was altered by very low but environmentally relevant exposures during embryo development. YP larvae that were exposed to MeHg during the first 24 hr of development had an increase in activity at 27 dpf but mainly in the middle dose, suggesting a nonlinear response. YP larvae exposed to the middle dose spent more time swimming, performed more behavior states, more swimming bouts per second and switched between slow and medium swim states more often. However, they swam slower during the swimming bouts and did not travel any more distance than the control larvae (measured either as total distance traveled or in fish lengths). Most of these differences were not present when larvae are exposed to the higher dose with only an increase in total time swimming. Higher dosed larvae have decreased variability in the medium step length, perform the medium state more, the fast state less, and turn more often to the left during the fast state. Additionally,

43

higher dosed YP larvae also increased activity more than control larvae but not to the same extent as middle dosed larvae with some aspects of locomotion performed at lower levels than the controls. These changes indicate the middle dosed YP larvae are more active and have a more diverse set of swimming states than unexposed larvae but these effects can be somewhat reversed at higher doses.

The MeHg nonlinear responses observed in this study could be permanent or just representing one later point in time of the recovery process (i.e. temporary response after 26 days of recovery). Evidence to suggest the MeHg nonlinear responses are part of a threshold response in YP was observed by Mora-Zamorano et al. (2017), who found YP total distance traveled in a lighted environment decreased at 0.21 µg/g Hg in tissue (tested up to 3.29 µg/g), but no changes in activity or distance travel in a dark environment. The 0.21 µg/g of Hg concentration in tissue was the highest level tested in our study, but we also included a dose at 0.02 µg/g Hg. Combining the results from this study and Mora-Zamorano et al. (2017) indicates that total distance traveled may be affected at a tissue concentration as low as 0.21 µg/g Hg, but swimming bout abundance and speed may be affected at tissue concentrations as low as 0.02 µg/g Hg. Conversely, there is evidence from Atlantic killifish (*Fundulus heteroclitus*) that suggest these results could be part of a recovery process. Research on temporary alterations in fish behavior after embryonic mercury exposure has been observed with multiple studies on killifish that show recovery of some behaviors such as prey capture ability, predation and collisions [see review by (Weis 2014)]. Indeed, killifish have shown decreased sensitivity of individuals from sites with a history of mercury and PCB126 contamination (Zhou and Weis 1998; Zhou, R. Scali, J. S. Weis 2001; Nacci et al. 2010), suggesting killifish have compensatory mechanisms for pollution (Oleksiak et al. 2011; Foster 2012). However, examination of grayling

(*Thymallus thymallus*), zebrafish and Atlantic croaker (*Micropogonias undulatus*) show permanent impairments after embryonic mercury exposure [see review by (Weis 2014)], indicating dramatic differences in the ability of a fish species to recover from mercury exposure. Additional research is needed with YP that includes assessment at more time points before it is known whether the effects observed in this study are permanent. Regardless, even if the effects are temporary, they still may impact larval survival, because these impairments are occurring in critical life stage (Vélez-Espino et al. 2006).

Compared to MeHg, PCB126 neurotoxic effects are not as well studied in fish; even so, PCB126 did alter YP larvae locomotion behavior after embryonic exposure. Yellow perch larvae that were exposed to very low concentrations of PCB126 during the first 24 hr of development had altered behavior, but to a lesser extent than those exposed to MeHg in this study. At the upper PCB126 dose, a higher proportion of fish exhibited a fast state, but the total time spent in the fast state decreased. In addition, the larvae exposed to the middle dose transitioned from fast to slow state less often than the control larvae. This suggests at the high PCB126 dose in this study, PCB126 caused fish to swim in faster states but for a shorter time period, transitioning from fast to slow less often. PCB126 has been found to increase larval activity in some fish species, but not all. Killifish larva swimming speed increased at 0.5 ppm PCB126 (dose level) but not total distance or activity (Couillard et al. 2011). PCB126 increased adult rainbow trout (*Oncorhynchus mykiss*) swimming speed, but recovery time was impaired due to higher metabolic costs during recovery and muscle restoration (Bellehumeur et al. 2016). However, in 5 dpf larval zebrafish with 0.385 ppm of PCB126 exhibited decreased swimming activity (Di Paolo et al. 2015). Since activity trends after PCB126 are mixed, inter-species differences may be a major factor in determining impacts of PCB126 exposure. One caution

should be noted with the results from this study, which is the confounding effect of the dimethyl sulfoxide solvent (DMSO) on fish behavior (Hallare et al. 2006; Huang et al. 2018). However, we feel this confounding effect was minimal because we used freshly purchased 500ppm DMSO, which at this concentration and quality has been shown to have small confounding effects.

Multiple nonlinear dose responses were observed in this study as the chemical level increased, both positive and negative trends (Mattson 2008; Lushchak 2014); where one nonlinear dose response was observed after PCB126 exposure and six after MeHg exposure (Table 3.1; Figure 3.1). This is not unexpected since fish are known to have compensatory mechanisms (e.g. neurogenesis) (Calabrese 2008, 2016; Bhatia et al. 2019). These response endpoints may indicate the subset of behavior endpoints that involve sensory components that include compensatory mechanisms. A linear response over both doses did not occur with any of the behavior endpoints in this study (Table 3.1; Figure 3.1), indicating the dose levels did not encompass the transition where compensatory mechanisms were overwhelmed or the behavior endpoint did not include any compensatory mechanism. However, some behavior endpoints had the upper dose deviate significantly from the control or from the middle dose (Table 3.1). These doses are potentially the lowest effect concentrations for these behavior endpoints.

Until the recent expansion of tools that implement hierarchical modeling (e.g. HMM), behavior endpoints were typically calculated as an average over time. Now with the choice of average endpoints or more specific within assay/behavior endpoints, the ability to detect behavior alterations due to toxicants has expanded. In this study, the HMMs found more significant behavior differences between the control and treatments, more so with PCB126 than MeHg. Taken individually, HMM results indicate MeHg decreased activity in the high dose (higher slow state step length and lower medium state step length), in contrast, the averaged

46

endpoints indicate increased activity in the middle dose (increased number of swimming bouts and total time swimming but lower bout speed; Table 3.1). This may be the result of the nonlinear dose response with each method being sensitive to only one aspect of the dose response curve or due to the limited dose range. PCB126 results were more consistent between the two analytical methods, both indicating decreased activity in the higher dose (total time swimming, less fast state swimming; Table 3.1).

These two different analytical approaches to summarizing behavior endpoints have advantages and disadvantages. Overall behavior endpoints have been a common way of assessing toxicological effects on behavior and thus have previous research using a variety of toxicants and species describing how they are affected by exposure. They are easy to calculate and apply to individual based population models that can simulate population level changes due to behavior [IBMs; e.g. (Rearick et al. 2018)]. However, they may not be sensitive enough to detect more nuanced behaviors or states within, such as with PCB126 in this study. In comparison, HMMs consider, and adjust for, different behavior states and correlation between data points. These properties of HMMs make them well suited for animal movement data (Hooten et al. 2017). In this study, HMMs were used as an assessment tool to find differences between treatments, in addition to determining specific behaviors. Use of HMMs could be expanded to many toxicological behavior assays. For example, HMMs could be used in behavior assays that examine the decision process (i.e. states) during y mazes or feeding assays (e.g. (Marques et al. 2020)), different startle states during VMRs, anxiety-related behavior during swimming or social assays, or feeding strategies during feeding assays (e.g. (Dunn et al. 2016)). However, HMMs can be difficult to construct, especially when you do not have a predefined behavior of interest because it is difficult to determine whether the defined behavior state is the

47

same type over individuals. Data quality may also be an issue if the tracking algorithm is not sensitive to subtle movements or artificially adds movement when the animal is motionless. In addition, HMMs require evenly timed relocations, which in field studies may be difficult, but is easy with laboratory video assays such as those used in this study. Even so, the usefulness of HMMs for analyses of behavior in many different sizes and types of animals, bioinformatics and other time series data has increased their popularity (Escola et al. 2011; Zucchini et al. 2017).

Having more sensitive behavior analytical tools will be important in multiple aspects of toxicology including advancing our understanding of sublethal effects to inform risk assessment, Adverse Outcome Pathway construction, and/or genetic sources of behavior. For example, more sensitive behavior detection could assist with connections to other subtle key physiological events or allow for fine scale connections between gene expression and behavior performance. In addition, new artificial intelligence animal behavior tools continue to be developed that will aid in application of these methods to high throughput applications (Ingebretson and Masino 2013; Reif et al. 2016; Villeneuve et al. 2018). However, the key in applying individual animal behavior endpoints in management actions is making them relevant to the population level such as through growth and/or survival (Ågerstrand et al. 2020). To date, application of individual behavior endpoints to population level impacts has mainly been through use of Individual Based Modeling (Murphy et al. 2008; Armstrong et al. 2020) or Leslie matrix population models (Rearick et al. 2018); which the results from this study will be applied. Consequently, combining random walk models within the Individual Based Modeling framework is needed in order to apply the HMM results from this study to population level impacts.

As computing power increases, more innovative behavior analyses will be possible. These innovations will advance our understanding of how pollutants affect species and our

understanding of pollution risk. As our understanding grows, research results should guide

future regulation recommendations as well as risk assessment.

CHAPTER 4: IMPACTS ON ATLANTIC KILLIFISH FROM NEUROTOXICANTS: GENES, BEHAVIOR AND POPULATIONS

Abstract

To understand the biological risk of pollutants, connections, both correlative and mechanistic, are needed between the exposure event and key events at the molecular, cellular and organismal level. This study examined gene expression, behavior and simulated cohort growth and survival from embryonic exposed fish larvae to neurotoxicants. Atlantic killifish *Fundulus heteroclitus* from both contaminant adapted and non-adapted populations were exposed to sublethal-environmentally relevant levels of methylmercury (MeHg) and PCB126. Non-adapted killifish from Scorton Creek, MA (SCO) exposed to MeHg exhibited brain gene expression changes in the si:ch211-186j3.6, si:dkey-21c1.4, scamp1 and klhl6 genes, which coincided with similar changes in feeding and swimming behaviors. Embryos from SCO were also exposed to PCB126 had lower physical activity levels coinciding with a general upregulation in numerous nucleic and cellular brain gene sets (BGS) and down regulation in numerous signaling, nucleic and cellular BGS. PCB126 exposures were repeated on toxic adapted larvae from New Bedford Harbor, MA (NBH). The NBH had only subtly altered swimming behaviors that coincided with 98% fewer altered BGS than SCO. Ultimately, we predicted decreases in SCO and NBH cohort survival after only PCB126 exposure and only SCO larvae with decreases in growth after PCB126 exposure. Overall, these results suggest connections between killifish larval brain gene expression and behavior, as well as decreases in modeled larval survival after embryonic exposure to PCB126, even for tolerant NBH populations.

.

Introduction

Sublethal levels of neurotoxic chemicals such as polychlorinated biphenyl (specifically 3,3',4,4',5-pentachlorbiphenyl congener, PCB126) and methylmercury (MeHg) commonly exist in an industrial landscape as aquatic pollutants (Murphy et al. 2012). However, there is limited ability to predict sublethal impacts or assess risk from these neurotoxic chemicals on individual fish, multiple species, or their populations. One approach to solving this problem is to examine the neurobehavioral impacts through an Adverse Outcome Pathway (AOP) framework (Garcia-Reyero and Murphy 2018) constructed using standard laboratory fish species along with local species of conservation. Fundamental to the AOP framework is connecting the chain of events from toxic exposure, molecular initiating event/s, to key events in cellular, organ and organ systems; to whole organism and/or population level impacts (Ankley et al. 2010). Adverse Outcome Pathways are constructed to be modular and chemically agnostic, where comparing the results from two different chemicals can illustrate areas of commonality but also differences (https://aopwiki.org/). For example, PCB126 and MeHg potentially interrupt different neurological development pathways (Bradbury et al. 2008; Cambier et al. 2009; Xu et al. 2012; Ho et al. 2013); consequently similarities between these two chemicals at the molecular level may be limited. However, similarities may increase as impacts are scaled up from molecular to the more integrative organism and population level effects.

This study developed an AOP that starts at a neurotoxicant embryonic exposure and measured three types of endpoints or key events: 1) brain gene expression, 2) individual behavior and 3) predicted population impacts. Using an AOP framework, these particular key events allow us to elucidate how environmental contaminants influence genes which in turn influences individual fish behavior (Hunt et al. 2019). This research is approachable because of recent

51

advances in efficient gene expression tools and shows promise in pursuits that connect the environment to animal behavior (Walton et al. 2020), especially toxic environments.

A well-known example of a fish species that demonstrates genetic modifications because of a toxic environment is found in populations of non-migratory small *Fundulus heteroclitus* (Atlantic killifish, KF) that have survived in the wild after long-term exposure to industrial pollution. This model fish species is of interest to toxicologists because some populations have been found to have genetically adapted in the wild to dioxin-like contaminants (DLCs) (Nacci et al. 1999) and other populations continue to persist in mercury polluted environments (Weis et al. 1981; Smith and Weis 1997; Pereira et al. 2019). This study examined this unique species and compared two genetically distinct populations, one known to have chemical tolerance and one without ancestral exposure to pollutants. Response differences between these two populations could lead to insight into the molecular machinery underlying this evolved tolerance. Further, examining similarities between gene expression and behavior endpoints could indicate how brain gene expression drives behavior. Consequently, this study determined differences of brain gene expression, behavior and cohort metrics after sublethal embryonic exposure to two neurotoxicants, MeHg and PCB126, in adapted and non-adapted KF populations.

Methods

Populations

In this study, two populations of KF were used to assess effects of a model DLC, PCB126. These KF populations had been found previously to be relatively PCB-sensitive (Scorton Creek, Barnstable, MA; SCO) or PCB-tolerant (New Bedford Harbor, MA; NBH), respectively (Nacci et al. 2010). Disparities in MeHg sensitivity between these KF populations

have not been previously documented (Pereira et al. 2019); consequently, a subset of the SCO

KF population were used to assess effects of MeHg exposure.

Parental killifish husbandry and methylmercury exposure

Killifish (100 – 200 fish) were collected from the wild using baited traps and maintained

as previously described (e.g., Nacci et al. 2010). In brief, KF were returned to US

Environmental Protection Agency (EPA) Office of Research and Development marine aquarium

facilities (Narragansett, RI), and held in ~250 L tanks supplied with free-flowing uncontaminated

seawater. Relatively uncontaminated KF from SCO (parental generation, P) were held in the lab

for > six months before use as breeding stock in this study. However, highly contaminated NBH

killifish were held for $\geq$ 2 year depuration before producing F1 progeny, which were grown to

maturity (1 – 2 years) then used as breeding stock in this study. All procedures using live

vertebrate animals at the EPA were conducted in accordance with Animal Care and Use

Protocols approved by the University of Wisconsin at Milwaukee Institutional Animal Care and

Use Committee (IACUC, #18-19#04) and EPA ACUP # Eco23-03002 and Eco230-07-001.

Before the onset of the adult KF dietary exposures (24 April 2017), selected KF were

transferred to six ~250 L tanks (2 NBH F1 tanks, 4 SCO P tanks), acclimated up to 23º C

(breeding temperature) and then held for 4 weeks. Each tank held 36 (24 female and 12 male)

size matched KF [~7 g mean wet weight (ww) or 1.75 g mean dry weight (dw)]. KF were fed

constructed diets containing ~30% wild fish (ww/ww) and components such as Tetramin

Tropical Flake, which supported healthy growth and reproduction in KF (unpublished data). The

diets included wild sockeye salmon *Oncorhynchus nerka* fillet (naturally low in MeHg) or wild

tuna steak (naturally high in MeHg), which are believed to be relatively similar nutritionally

(Celia Chen, Dartmouth, personal communication). Therefore, a tuna-based diet was used to produce high MeHg KF breeding stock and a salmon-based diet was used to produce low MeHg or reference (control) KF breeding stock since native SCO whole KF contain a low level of mercury [Hg; 186.10 ± 23.30 ng tHg/g dw KF, standard deviation (SD), n=5, sampled April 27, 2017]. The low MeHg KF breeding stock received a daily estimated dose of ~ 300 ng tHg/g dw KF/day through their salmon-based diet. Adult KF in this treatment had a body concentration of Hg similar to the wild caught fish referenced above at 162.46 ± 20.21 ng tHg/g dw KF (SD, n=8); their larval progeny contained 9.80 ± 2.49 ng tHg/g dw KF at 3 days post fertilization (dpf, SD, n=9). The high MeHg KF breeding stock received a daily estimated dose of ~ 3600 ng tHg/g dw KF/day through their tuna diet. Adult KF in this treatment had a body concentration of 564.09 ± 269.29 ng tHg/g dw KF (SD, n=5); their larval progeny contained 35.09 ± 17.06 ng tHg/g dw KF (SD, n=16) at 2 dpf. Preliminary data (unpublished, Kate Buckman, Dartmouth College) demonstrated that maternal KF achieved tHg concentrations equivalent to their dietary consumption of ~1200 ng Hg/g dw by day 42 and produced embryos containing 35 - 100 ng Hg/g dw.

Treatment groups of embryos from killifish breeding stock

After adult KF dietary exposures ($\geq$ 103 d) were completed, KF were strip spawned and mixed to produce embryos from each of these three KF breeding stocks: SCO Low MeHg diet, SCO High MeHg diet, NBH Low MeHg diet. NBH larva were not tested for higher level MeHg impacts in this experiment because it was outside the scope of the study. Embryos were maintained during early development at the EPA as per KF Embryo Larval Assay (ELA) protocol, as described below. Subsamples of the embryos from SCO Low MeHg diet and NBH

Low MeHg diet KF were exposed directly to PCB126 during development, 1 to 7 dpf. Direct exposures to 40 or 400 ng/L nominal concentrations of PCB126 were selected to produce embryo concentrations equal to 0.1x or 1.0x, respectively, PCB126 measured in wild NBH killifish (189 ng/g dw) (Nacci et al. 1999). However, the higher exposure was completely lethal to SCO embryos and produced some lethality in NBH embryos (Table 4.1), therefore these treatment groups were not assessed for behavior. Since Hg tissue concentrations in the Low MeHg diet (salmon) were similar to wild caught SCO KF (see concentrations stated in previous section), the Low MeHg diet was labeled as the control. Thus, there were five embryo treatment groups analyzed in the behavior sections of this study: 1) Embryos from SCO Low MeHg diet KF without further direct exposures (SCO-Ctrl); 2) Embryos from SCO High MeHg diet KF without further direct exposures (SCO-MeHg); 3) Embryos from SCO Low MeHg diet KF exposed directly to a low level (40 ng/L) of PCB126 (SCO-PCB); 4) Embryos from NBH Low MeHg diet KF without further direct exposures (NBH-Ctrl); 5) Embryos from NBH Low MeHg diet KF directly exposed to a low level (40 ng/L) of PCB126 (NBH-PCB) (Figure 4.1). Of all the possible pairwise comparisons between the five treatments, this study was focused on only three types of comparisons. 1) The comparison that determined only High MeHg impacts, SCO-Ctrl vs SCO-MeHg. 2) The four comparisons between the PCB treatments and KF populations [(a)SCO-Ctrl vs SCO-PCB, (b) SCO-Ctrl vs NBH-Ctrl, (c) SCO-PCB vs NBH-PCB, (d) NBH-Ctrl vs NBH-PCB]. 3) All five of these comparisons combined to determine if there were any responses that were similar between the two chemicals.

Table 4.1. Embryo treatment groups used in larval behavioral assays, where Atlantic killifish larvae originated from adults from Scorton Creek, MA (SCO) or New Bedford Harbor, MA (NBH). Larvae were fed low mercury (i.e. control) or high mercury (Hg) diets and exposed directly to PCB126 at nominal concentrations of 40 ng/L (Low PCB) or 400 ng/L (High PCB). Endpoints reported include hatching, survival, and ratings for phenotypic abnormalities, including those specific to the heart. Lethal treatment groups (PCB126 400 ng/L) were not used in larval behavior studies (DND = did not determine, NA = not applicable).

Parents	Parent or Offspring Treatment	Treatment Number	PCB126 ng/g[a]	Mercury ng/g	% Embryo Survival	% Hatch	% Larval Survival	Phenotypic Abnormalities Mean Score	Heart Abnormalities Mean Score
SCO	Control[b]	1	0	9.8 ± 2.49	100	100	90	0	0
	Hg ~3600 ng tHg/g dw/day	2	NA	35.09 ± 17.06	100	87.5	87.5	0.13	0
	PCB126 40 ng/L[b]	3	19	DND	100	100	87.5	0.25	0.63
	PCB126 400 ng/L[b]	N/A	189	DND	100	0	0	4.6	4
NBH	Control[b]	4	0	DND	100	100	100	0	0
	PCB126 40 ng/L[b]	5	19	DND	85.71	85.71	85.71	0	0
	PCB126 400 ng/L[b]	N/A	189	DND	66.67	66.67	55.56	0.86	0.86

[a] Estimated using previous experiments (Nacci et al 1999)

[b] Also exposed to ~300 ng tHg/g dw/day through salmon-based diet
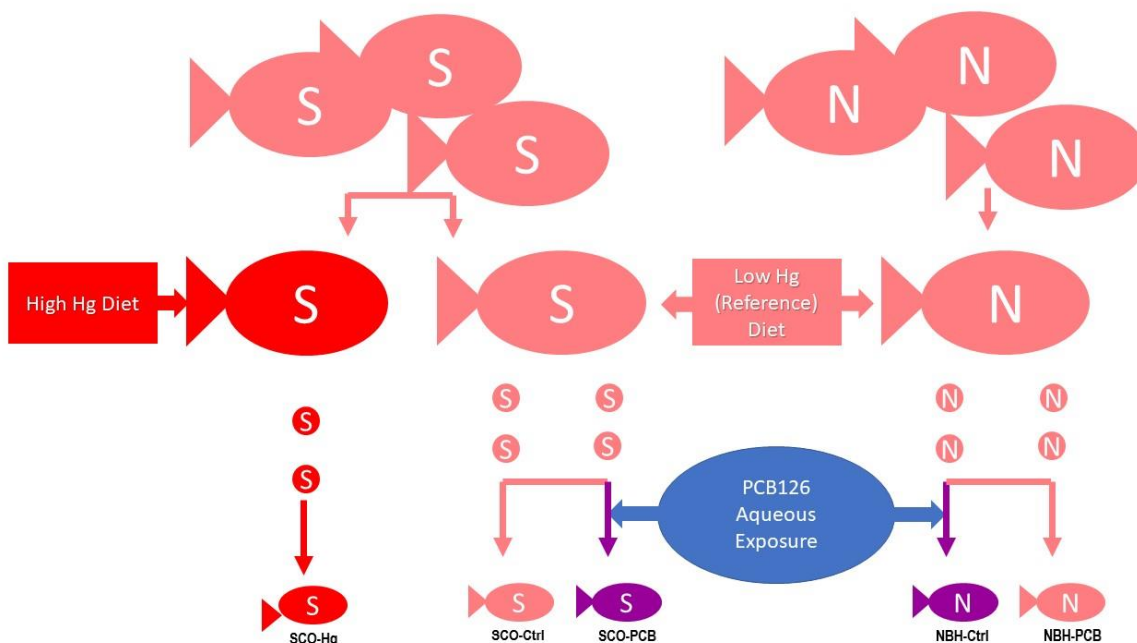
Figure 4.1. Atlantic killifish larval treatment groups (labeled as in text) showing adult populations from Scorton Creek (S) or New Bedford (N) and fed diets low (control) or high in mercury (Hg), producing embryos (circles), subsets of which were exposed during development to PCB126.

Embryo-larval assessments

Routine rearing and monitoring of the early development of KF embryos, ELA methods, were conducted as described in Huang et al. (2019). Briefly, one dpf embryos were transferred into individual vials containing 10 mL sea water, amended with acetone (0.01% acetone, Sigma Chemical, St. Louis, MO, USA) or chemical-acetone stocks of PCB126 (Accustandard, New Haven, CT). At seven dpf, embryos were transferred to a 12-well disposable plate (Thermo Fisher Scientific, Rockville, MD, USA) containing uncontaminated sea water-dampened 20 mm Restek Cellulose filters made for ASE 200 extraction cells (Restek, Bellefonte, PA, USA). A subset of embryos from each treatment group were sent to UWM for Hg or behavioral analyses. The remaining embryos from each treatment group remained at EPA (≥ 20) and incubated at 23° C. At 10 dpf, embryos were phenotyped microscopically for abnormalities in developmental

stage and features were noted (Clark et al. 2010; Whitehead et al. 2010). At 14 dpf, sea water

was added to each well and the plates were rocked gently to initiate hatching. Individual larvae

were maintained in single wells containing 3 mL sea water for all assessments, incubated at 23°

C, fed 24-h hatched *Artemia* ad lib daily, and renewed with sea water on alternate days.

Individuals were assessed daily for survival until seven days post hatching (dph) when the ELA

was terminated (Table 4.1).

To assess the degree of neurological impact, three different larval behavior assays were

conducted: visual motor response assay (VMR), a free swimming locomotion assay, and a

feeding assay (Figure 4.2). From these assays, 83 different larval behaviors were measured, 48,

30 and 5 endpoints, respectively. See supplemental section for behavior assay details.
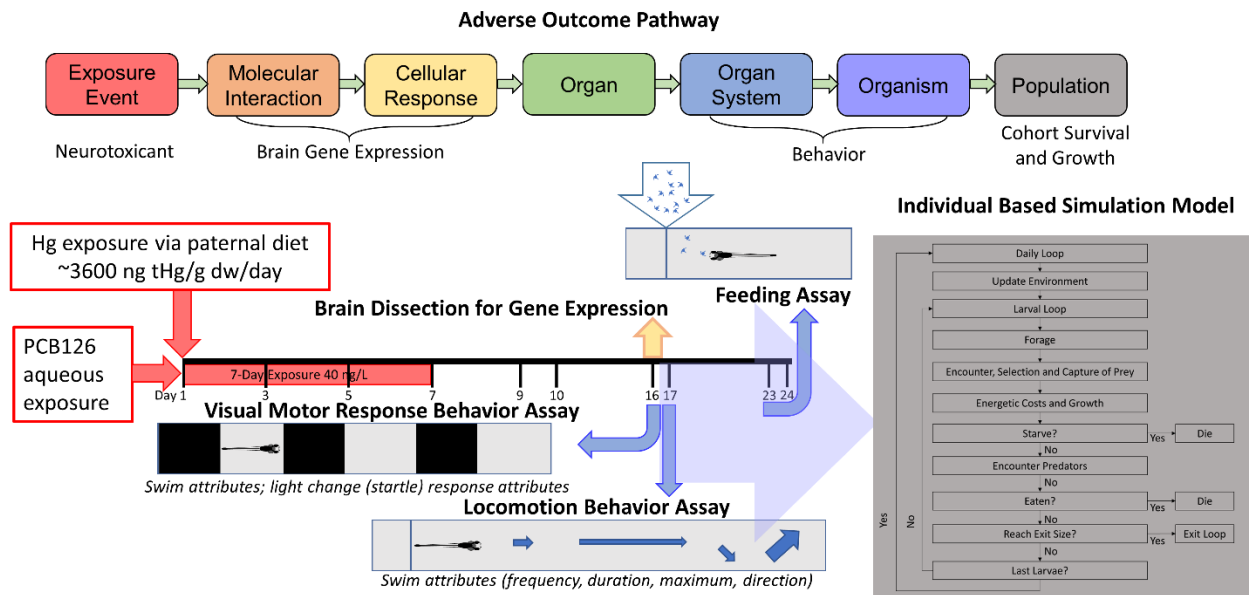
Figure 4.2. Behavior assays used in this study to collect data on Atlantic killifish larvae for
assessment of chemical responses and for inputs into the Individual Based Model.

58

<u>Behavior treatment testing</u>

All behavioral endpoints were examined for treatment differences using Bayesian statistical methods (see Supplemental section for additional details). Bayesian models for locomotion behavior responses consisted of one main effect (treatment with 5 levels), covariate variable (time of test and/or dpf) and a random batch effect since assays were ran in batches of 12-well dishes. Bayesian models for feeding behavior were the same except no random batch was included since each assay was conducted with one larva. Response variables and residuals were examined for normality using density distributions and Box Cox transformation were applied where needed in all non-negative response variables using the boxcox function in the MASS package (Table S4.4; Venables and Ripley 2002). All responses that were normally distributed either with or without a transformation were predicted using a normal distribution model, responses that were severely right skewed were predicted using a t distribution model where degrees of freedom (df) was estimated with dunif (3, 30), and responses that were proportional were fit with a logistic distribution model (Tables S4.5, S4.6, S4.7 and S4.8, S4.9, respectively). Priors were set to be non-informative and all models were ran with three chains (see supplemental material for detailed methods; Table S4.5). To facilitate future use of parameter estimates, this study generated both overall population and individual level parameter estimates (Table S4.11). Lastly, a Chi-Square test from the R stats package (R Core Team 2019) was used to determine whether the proportion of s1, s2 and s3 HMMs selected were different between treatments.

Brain gene expression

Brain collection

Brain collection was performed essentially as described by Vargas et al. (2011) on 17 dpf MeHg and PCB126 exposed larvae. A random subset of larvae were removed after the VMR assay to contribute brain samples for gene expression at 16 dpf (n=69, 36 of whom had been through the VMR assay and 33 had not). Larvae were gently transferred to a 60 mm petri dish and 4°C embryo medium was quickly added to provide anesthesia. Five larvae were transferred to a new petri dish, water was removed, and individuals were immobilized in a drop of 2% low melting point agarose made with artificial cerebral spinal fluid (aCSF; 131 mM NaCl, 2 mM KCl, 1.25 mM KH$_2$PO$_4$, 2 mM MgSO$_4$, 10 mM glucose, 2.5 mM CaCl$_2$, 20 mM NaHCO$_3$). A dissection pin was used to mount the larvae in dorsal/ventral recumbency, just under the surface of the agarose. Artificial cerebral spinal fluid was added and dishes were placed on ice. Intact brains were removed using dissection pins, transferred individually in 5µl aCSF to 1.5 ml microcentrifuge tubes, then frozen in liquid nitrogen prior to storage at -80°C.

Brain gene analysis

Genomic analysis was conducted at Mississippi State University, Institute for Genomics, Biocomputing and Biotechnology. Total RNA was isolated from 6 embryos' brains per treatment from individual 17 dpf embryos using the Qiagen RNeasy® Micro Kit (Germantown, MD, USA) following the Purification of Total RNA from Animal and Human Tissues protocol in the RNeasy® Micro Handbook with slight modifications. The modification included homogenization of brain tissue in 350 µL of RLT buffer using a pellet pestle and elution of Total RNA using 15 µL of RNase-free water. RNA quality was assayed using the Agilent High

Sensitivity RNA ScreenTape System (Waldbronn, Germany) for the Agilent 2200 TapeStation (Palo Alto, CA, USA), and RNA was quantified using the NanoDrop 2000 (ThermoFisher Scientific, Waltham, MA).

The raw reads from 36 KF samples (6 groups with 6 reps) were mapped and quantified using salmon (Patro et al. 2017) (v1.3.0) against the reference transcriptome (see below). tximport (Soneson et al. 2015) (v1.16.1) was used to import transcript-level estimates from salmon summarize this data to the gene level. These genes were filtered such that only genes with an average log Counts per Million > 1 across all samples were retained for differential expression. edgeR (v3.30.3) was used to determine differentially expressed genes (DEGs). OrthoFinder (v2.5.4) was used to find orthologous genes in *D. rerio*. The GAGE R package (Luo et al. 2009) (v2.40.0) was used to perform gene-set enrichment analysis using *D. rerio* GO gene-sets, KEGG gene-sets and the *D. rerio* orthologs of genes that passed the filter. Significant trends were determined using an alpha of 0.05 [false discovery rate (FDR) and q-value].

Behavior/gene expression comparisons

Each endpoint response, either gene or behavior, was summarized over all treatments by first determining whether there was a significant difference found while testing the treatment comparisons. When a significant difference was found, a positive (Pos) or negative (Neg) trend was indicated using the relative amount of the first treatment to the second treatment. For example in the comparison between SCO-Ctrl vs SCO-PCB treatments, if the SCO-PCB treatment had a higher level than the SCO-Ctrl treatment, the summary is positive. If the SCO-PCB treatment had a lower level than the SCO-Ctrl treatment, the summary is negative. The endpoint value used to determine the trend direction were the back-transformed treatment means.

The resulting summary pattern was used to group behavior and gene expression endpoints that responded the same together. This approach is more robust than other data mining methods (e.g. PCA) because it 1) takes into account the treatment design of the experiment and the comparisons and 2) limits comparisons to only those endpoints that were determined to be statistically different from one another, which limits the excessive comparison of all endpoints.

Individual based model

A generalized Individual Based Model (IBM) was developed that incorporated the sublethal effects of MeHg and PCB126 on larval KF from two different populations known to have different exposure histories and responses to toxicants. The model is described in Ivan et al. (unpublished), with brief details provided here. Our IBM was adapted from a generalized larval fish model (Letcher et al. 1996) using bioenergetics equations for the California killifish *F. parvipinnis* (Deslauriers et al. 2017). See Table S4.11 for all model parameter values.

Briefly, the IBM tracked 2500 individual larvae (based on wild densities) from hatch to juvenile transition, defined at 24 mm (Abraham 1985) or after 100 days, whichever occurred first (Figure 4.3). Daily, individuals forage, grow and experience mortality. KF forage on two types of prey. Foraging consists of prey encounters, handling time, capture success and consumption of nauplii and/or copepods. Swimming speed, handling time, larvae reactive distance and capture success all determine how many prey an individual KF larval consumes. KF then grow ($G_{j,d}$ in g/d) as

$$G_{j,d} = C_{j,d} - R_{j,d} - F_{j,d} - U_{j,d} - SDA_{j,d}$$

where $C_{j,d}$ (g/d) is the consumption of prey by larval fish j, $R_{j,d}$ is respiration (g/d), $F_{j,d}$ is egestion (g/d), $U_{j,d}$ is the excretion (g/d) and $SDA_{j,d}$ (g/d) is the specific dynamic action.

Consumption is determined via the foraging but capped at $Cmax_{j,d}$ (g/d) as determined from the Wisconsin Bioenergetic equations (Deslauriers et al. 2017). Finally, KF are monitored for starvation and predation mortality. Predators of KF are adult KF and their predation rates are temperature dependent (Deslauriers et al. 2017). Fish that die are removed from the daily loop, as are fish that reach 24mm. Output variables of interest are 1) the number of survivors (fry that reach the exit length within the 100 days) and 2) the mean growth rate (mm/d) of survivors.

Sublethal effects of MeHg and PCB126 were incorporated into the model via multipliers which are based off of the Bayesian individual level predicted treatment posterior distributions (Table S4.12). The individual level posterior distributions were used to create 10,000 random values from a truncated normal distribution. If the posterior distribution was from a transformed behavior endpoint, than these random values were back transformed. From these random values, the multiplier distributions were generated (S12). Multipliers were placed on larval swimming speed from the locomotion assay; larval capture success of zooplankton, larval handling time of zooplankton, and larval reactive distance to zooplankton from the feeding assay. At the start of each simulation (replication), each model individual j was assigned a multiplier for each of the above four variables. For each simulated KF (j), a swimming speed multiplier (SM_j) was generated as

$$SM_j = TD_j/MD$$

where TD_j is the average speed (mm/s) by fish j and MD is the treatment mean average speed (mm/s). Multipliers for handling time ($HM_j = TH_j/MH$), capture success ($CM_j = TC_j/MC$) and reactive distance ($RM_j = TR_j/MR$) were calculated for each experimental fish j as using the same procedure. Finally, the amount of time a fish was active was determined by the proportion of time fish were active in the locomotion assay. Proportions were derived from

the posterior distributions for each scenario. If necessary, back-transformations were performed

prior to the multiplier calculation. Lastly, the proportion of time a KF was actively searching for

food or encountering a predator was scaled to the percent of time active larvae were in the

locomotion assay by randomly assigning a time scaler to each fish at the beginning of the

simulation (i.e. multiply 12 hours by percent of time active in assay).

The model was calibrated using SCO KF such that growth rates were set to be

approximately 0.3mm/d (unpublished). To determine if differences occurred between which

season the adult fish spawn, we ran simulations for spring and summer runs. For spring runs

beginning on Julian day 110, the first fish reached 24mm around day 53 with several individuals

still growing but under the size of 24mm at the end of the model run (Figure S4.2). For the

summer runs (Julian day 230), the first fish to reach 24mm at the end of the model run was on

day 48 with few fish remaining in the simulation at the end of the model run (Figure S4.2). For

each scenario (population X toxicant effect) the model was run 10 times to account for

stochasticity. All results are reported as means of each simulation within a scenario. In addition

to the scenarios, we also examined the impacts of these toxicants on the two KF populations in

two different simulated seasons.
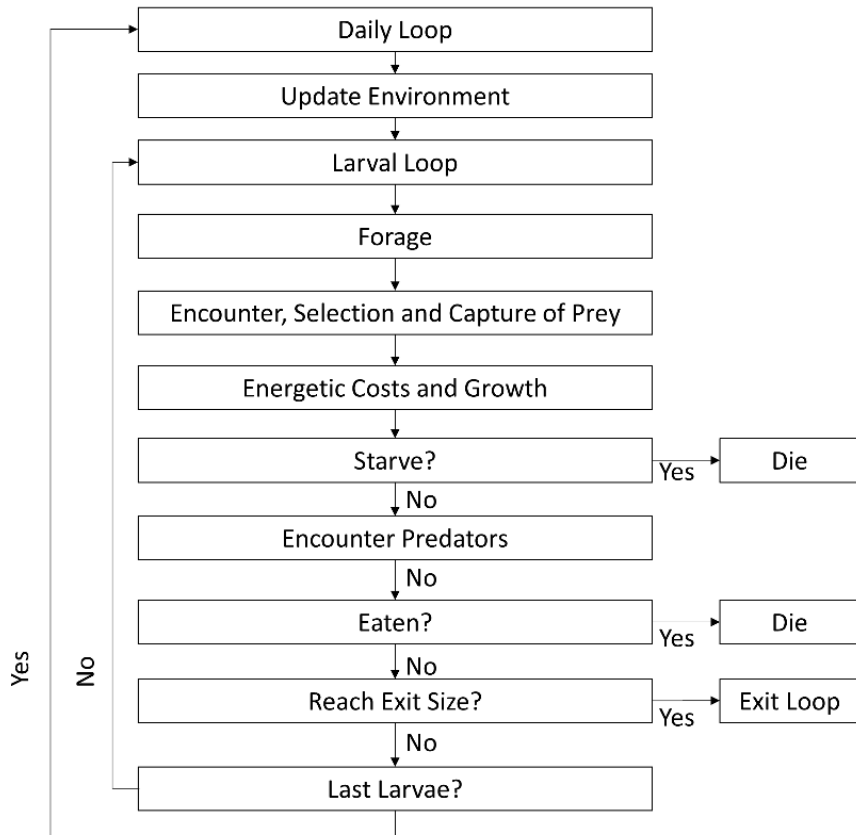
Figure 4.3. Model flow chart showing daily processes included in the generalized individual-based model to assess contaminant effects on Atlantic killifish larval cohorts.

Results

Behavior endpoints

Many larval behaviors were either inherently different between the SCO and NBH populations or affected by MeHg in their parent's diet, and/or exposure to PCB126 during development. Of the 83 behavior endpoints tested, 49 had at least one treatment difference from chemical exposure (Table 4.2-4.4, S4.13 and S4.14). By random chance, the number of significant tests that could be significant is ~4 (0.05 alpha level × 83 tests = 4.15). More significant behavior patterns were found with behavior endpoints that examined swimming

characteristics (30) than were found with stamina/activity type behaviors (24), even though both had similar levels of testing over all assays (33 total swimming characteristics where examined, 31 stamina/activity type behaviors, 2 startle, 5 feeding behavior types). Although both the VMR and locomotion assay were examined for the same suite of 10 swimming endpoints (Table S4.2), the same set of swimming endpoints did not exhibit the same trends across treatments (Table 4.2, 3). The exceptions being 1) the overall swimming bout turning angle from the locomotion assay and the average swimming bout turning angle in light periods 2 and 4 of the VMR assay (Table 4.2, ref 2); and 2) swimming bouts (per sec) and the number of swimming bouts per second in periods 2-5 in the VMR assay (Table 4.2, ref 3). Endpoints such as swimming bout duration, total time swimming and total distance traveled did not consistently report treatment differences during lighted or dark periods in the VMR assay and the locomotion assay.

Thirteen feeding, swimming and startle behavior endpoints were different between the control SCO and NBH populations (Table 4.2, ref 6-11, 15). As compared to NBH, SCO larvae had higher swimming bout duration (Table 4.2, ref 9); total time swimming (Table 4.3, ref 7); transition probabilities from the medium to the fast state (Table 4.2, ref 9), slow to medium or fast states (Table 4.2, ref 11,15); medium state turning angle (Table 4.2, ref 11). As compared to SCO, NBH larvae were higher in larval capture probability, reaction distance (Table 4.2, ref 8) and capture attempts (Table 4.2, ref 6); startle magnitude in period 3 (Table 4.2, ref 8); transition probability from slow to slow, medium to slow, and medium to medium state swimming (Table 4.2, ref 10).

Increased MeHg exposure altered SCO larvae behavior endpoints (Table 4.3). For example, SCO larval capture probability, capture attempt ratio and reaction distance increased when higher MeHg levels were fed to their parents. Mercury also increased the probability of a

SCO larva staying in the fast or medium swimming state. In addition, MeHg exposure decreased

SCO larva total distance traveled, step length and variation in the final VMR period; swimming

bout duration and total time swimming in the VMR period 3; turning angle variation in the

medium behavior state and the transition probability from the medium to fast state (Table 4.3).

Occasionally both MeHg and PCB126 made certain behavior endpoints respond similarly

in the SCO larvae (Table 4.4). For example, both MeHg and PCB126 made SCO larvae

increased the number of capture attempts, with PCB126 increasing it more than MeHg (Table

4.4, ref 2). Additionally, both chemicals decreased the duration of swimming bouts and total

time swimming in VMR period 3 (Table 4.4, ref 1, 3). Lastly, the probability of staying in the

medium state response differed between the chemicals and populations, where MeHg increased

it in the SCO larvae while PCB126 decreased it in the NBH larvae (Table 4.4, ref 4).

Most behavior alterations found in this study were from PCB126 (Table 4.2). For

example, larval handling time of prey increased in every PCB126 treatment (Table 4.2, ref 1).

While other behavior endpoints increased with PCB126 exposure but differed in severity

between populations. For example, PCB126 exposure resulted in SCO larvae proportionally

missing more prey but NBH larvae missed even more (Table 4.2, ref 2). Swimming bouts during

light periods also changed with increases in the turning angle (Table 4.2, ref 2) and decreases in

bout frequency (Table 4.2, ref 3) both in the locomotion and VMR assays; again more severely

in the NBH larvae. Some behavior endpoints were only altered in either the SCO or NBH

population. For the SCO larvae, PCB126 decreased SCO larvae total time swimming (Table 4.2,

ref 7) and total distance traveled in the locomotion assay and swimming bout duration in the

VMR period 1 (Table 4.2, ref 5); total distance traveled, overall step length and variation in

VMR period 3 (Table 4.2, ref 3). PCB126 increased SCO larvae overall mean turning angle in

the VMR period 2 and variation in period 3, with the latter being higher in the NBH larvae but no different than the NBH controls (Table 4.2, ref 3, 4). For only the NBH larvae, PCB126 decreased the probability of staying in the slow or medium state in addition to medium to slow state transition probability (Table 4.2, ref 10); increased medium state turning angle and slow to medium, fast to slow and slow to fast state transition probabilities (Table 4.2, ref 11, 13, 15). Lastly, after PCB126 exposure, NBH larvae had a smaller mean and variation in the medium state step length in the locomotion assay, but the NBH mean medium step length was still higher than the SCO population (Table 4.2, ref 12, 14).

Table 4.2. Summary of PCB126 significant treatment patterns found in Atlantic killifish behavior endpoints. Significant trends are reported using the following comparisons: SCO-Ctrl vs SCO-PCB, SCO-Ctrl vs NBH-Ctrl, SCO-PCB vs NBH-PCB, NBH-Ctrl vs NBH-PCB (Tan = significant negative trend compared to control, Blue = significant positive trend compared to control, Black = no significant trend compared to control, HMM = Hidden Markov Chain model endpoint, TP = Transition Probability).

Reference Number	Significant Treatment Pattern				Behavior Endpoint
	SCO-Ctrl vs SCO-PCB	SCO-Ctrl vs NBH-Ctrl	SCO-PCB vs NBH-PCB	NBH-Ctrl vs NBH-PCB	
1	Blue	Black	Blue	Blue	Prey Handling Time
2	Blue	Black	Blue	Black	Prey Miss Proportion, Overall Turning Angle Variation Period 1, Overall Turning Angle Variation Period 3
3	Tan	Black	Tan	Black	Swimming Bouts (per sec), Swimming Bouts Period 1 (per sec), Swimming Bouts Period 2 (per sec), Swimming Bouts Period 3 (per sec), Swimming Bouts Period 4 (per sec), Swimming Bout Speed Period 1 (mm/s), Total Distance Traveled Period 1 (mm), Total Time Swimming Period 1 (sec), Overall Step Length Period 1 (mm), Overall Step Length Variation Period 1, Total Distance Traveled Period 3 (mm), Overall Step Length Period 3 (mm), Overall Step Length Variation Period 3
4	Blue	Black	Black	Black	Overall Turning Angle Period 2
5	Tan	Black	Black	Black	Total Distance Traveled (mm), Swimming Bout Duration Period 1 (sec), Swimming Bout Duration Period 3 (sec)
6	Blue	Blue	Black	Black	Capture Attempt Ratio
7	Tan	Tan	Black	Black	Total Time Swimming (sec)
8	Black	Blue	Black	Black	Prey Capture Probability, Reaction Distance (mm), Startle Magnitude Period 2
9	Black	Tan	Black	Black	Swimming Bout Duration (sec), HMM Medium -> Fast TP
10	Black	Blue	Black	Tan	HMM Slow -> Slow TP, HMM Medium -> Slow TP, HMM Medium -> Medium TP
11	Black	Tan	Black	Blue	HMM Medium State Turning Angle, HMM Slow -> Medium TP
12	Black	Black	Blue	Tan	HMM Medium State Step Length (mm)
13	Black	Black	Black	Blue	HMM Fast -> Slow TP
14	Black	Black	Black	Tan	HMM Medium State Step Length Variation, Swimming Bout Turning Angle
15	Black	Tan	Blue	Black	HMM Slow -> Fast TP
16	Black	Black	Blue	Black	Swimming Bout Duration Period 2 (sec), Swimming Bout Duration Period 4 (sec)
17	Black	Black	Tan	Black	Startle Magnitude Period 4, Swimming Bout Turning Angle Period 3

Table 4.3. Summary of mercury significant treatment patterns found in Atlantic killifish behavior endpoints, SCO-Ctrl vs SCO-MeHg (Tan = significant negative trend compared to control, Blue = significant positive trend compared to control, Black = no significant trend compared to control, HMM = Hidden Markov Chain model endpoint, TP = Transition Probability).

SCO-Ctrl vs SCO-Hg	Behavior Endpoint
Blue	Capture Attempt Ratio, Prey Capture Probability, Reaction Distance (mm), HMM Fast -> Fast TP, HMM Medium -> Medium TP
Tan	HMM Medium State Turning Angle Variation, HMM Medium -> Fast TP, Swimming Bout Duration Period 3 (sec), Total Time Swimming Period 3 (sec), Overall Step Length Period 4 (mm), Overall Step Length Variation Period 4, Total Distance Traveled Period 4 (mm)

Table 4.4. Summary of mercury and PCB126 significant treatment patterns found in Scorton Creek and PCB126 effects on New Bedford Harbor Atlantic killifish behavior endpoints. Significant trends are reported using the following comparisons: SCO-Ctrl vs SCO-MeHg, SCO-Ctrl vs SCO-PCB, SCO-Ctrl vs NBH-Ctrl, SCO-PCB vs NBH-PCB, NBH-Ctrl vs NBH-PCB (Tan = significant negative trend compared to control, Blue = significant positive trend compared to control, Black = no significant trend compared to control, HMM = Hidden Markov Chain model endpoint, TP = Transition Probability).

	Significant Treatment Pattern					
Reference Number	SCO-Ctrl vs SCO-Hg	SCO-Ctrl vs SCO-PCB	SCO-Ctrl vs NBH-Ctrl	SCO-PCB vs NBH-PCB	NBH-Ctrl vs NBH-PCB	Behavior Endpoint
1	Tan	Tan	Black	Tan	Black	Total Time Swimming Period 3 (sec)
2	Blue	Blue	Blue	Black	Black	Capture Attempt Ratio
3	Tan	Tan	Black	Black	Black	Swimming Bout Duration Period 3 (sec)
4	Blue	Black	Blue	Black	Tan	HMM Medium -> Medium Transition Probabilities

Genetic endpoints

On average, there were 64986960.22 fragments per sample, with a standard deviation of 7013305.57. The average mapping rate to the reference transcriptome was 80.49%. Of the 26771 transcripts quantified, 16017 transcripts were retained after filtering. The comparison of

two groups of fish with the most differentially expressed genes was between the SCO-Ctrl and NBH-Ctrl with 3220 (Table S4.15). However, SCO and NBH larvae have only 210 differences in gene expression when both are exposed to the low dose of PCB126 (SCO-PCB 40 ng/L vs NBH-PCB 40 ng/L). SCO larvae had 383 altered genes as compared to the controls after exposure to the low PCB126 dose, which is 29 times more than the 8 altered genes found in the NBH larvae after low dose PCB126 exposure compared to the control. Even though the NBH larvae had few gene alterations after exposure to the low dose PCB126, the high dose of PCB126 altered the gene expression order of magnitude higher with 830 genes differentially expressed. This indicates that 5% of NBH larvae genes are altered by high levels of PCB126. All differentially expressed genes and pathways found in this study are reported in Tables S4.16 and S4.17. In addition, all patterns that were found to be similar between differentially expressed genes and behaviors can be found in Tables S4.19 and S4.20.

Behavior/gene expression comparison

The SCO KF who were exposed to either MeHg or PCB126 exhibited a change in the number of times the KF larvae attempted to capture prey and the duration of swimming bouts during period 3 of the VMR (Table S4.18). The same reaction to chemical exposure observed in these two behaviors was also observed in four genes including the scamp1 gene which is predicted to be involved in protein transport and degradation of the trans-Golgi network membrane.

By itself, the higher dose of MeHg in the SCO parents created offspring that increased the frequency of multiple feeding behaviors such as capture attempt ratio, capture probability and reaction distance (Figure 4.4 and Table S4.19). These increases coincided with the upregulation of 16 genes including si:ch211-186j3.6 which is thought to be involved with calcium ion binding

activity and homophilic cell adhesion. The down regulation of six genes coincided with decreases in five different sustained swimming behaviors in the last two periods of the VMR as well as decreases in medium to fast swimming transition probability detected in the HMM analyses. These six genes include si:dkey-21c1.4 (integral component of the membrane), scamp1 and klhl6 (B cell receptor signaling pathway and germinal center formation).

The most changes observed after PCB126 exposure occurred in SCO larvae resulting in the most gene expression and behavior similarities in treatment trends (Figure 4.5 and S4.20). Altered brain gene expression mainly occurred with nucleic functions followed by cellular, signaling, neural and metabolic functions. These changes coincided with altered stamina swimming type behaviors such as total distance traveled and total time swimming, as well as capture attempt ratio. PCB126 also affected NBH larvae but with less alterations to gene expression and behaviors. PCB126 down regulated the cmc2 and rab4a genes in NBH larvae resulting in the perturbation of the metabolic KEGG pathway involved in oxidative phosphorylation (KEGG 190; Figure S4.3; Table 4.5). This pathway is important in providing energy and regulating metabolism in the brain, and has been connected with multiple neurodegeneration diseases (Kawamata and Manfredi 2017; Area-Gomez et al. 2019). In addition to these genomic changes, six HMM behaviors were also altered in NBH larvae mainly pertaining to transition probabilities between swimming states. The two populations of KF had numerous differences in gene expression (3088), gene sets and pathways (275) and behavior (11; Tables 4.2, S4.20 and S4.21). Gene expression was most different between the two populations in the nucleic, cellular and signaling genes (Table S4.20), while nucleic, metabolic and cellular gene sets were most different (Table S4.21). These genomic differences coincided with NBH larvae having lower swimming bout duration lengths, higher capture probability and longer reaction distance.

Table 4.5. Significant PCB126 treatment patterns shared by gene expression and behavior endpoints in the New Bedford Harbor (NBH) Atlantic killifish found in this study. Genes with unknown names and functions are only reported in Table S19. Both the original and opposite behavior endpoint trends are listed. Significant trends are reported in the following order: SCO-Ctrl vs SCO-PCB, SCO-Ctrl vs NBH-Ctrl, SCO-PCB vs NBH-PCB, NBH-Ctrl vs NBH-PCB (Tan = significant negative trend compared to control, Blue = significant positive trend compared to control, Black = no significant trend compared to control).

| Significant Treatment Pattern | | | | | Behavior Endpoint | |
SCO-Ctrl vs SCO-PCB	SCO-Ctrl vs NBH-Ctrl	SCO-PCB vs NBH-PCB	NBH-Ctrl vs NBH-PCB	Gene Expression	Original Treatment Pattern	Opposite Treatment Pattern
Black	Black	Black	Tan	**Metabolic:** cmc2, rab4a	HMM Medium State Step Length Variation, Swimming Bout Turning Angle	HMM Fast -> Slow TP
Tan	Black	Black	Black	**Neural:** avp, si:dkey-175g6.2, uba1, gad2, ext2, usp22, spata2 **Nucleic:** polr2a, kdm2ab, rapgef1b, dyrk1b **Signaling:** pi4kab, plcl1, gareml, grin2ab, stx16, c2cd5, slc6a8, slc8a2b, kctd9a, prkab1a, si:ch211-168f7.5, slc30a1a **Metabolic:** arhgap1, mag, selenoi, epn3b, sucla2, plcxd3, elovl6, atp1b2b, arhgap25 **Development:** aldh1a2 **Circulatory:** b4gat1, pam, numb **Cellular:** ache, fam163ba, sec62, slc25a14, clptm1, coro7, bcat2, rusc1 **Protein Binding and Synthesis:** oat, znf598 **Miscellaneous:** abl2, klhl26, b3galt1b	Swimming Bout Duration Period 3 (sec), Total Distance Traveled (mm)	Overall Turning Angle Period 2
Blue	Black	Black	Black	**Neural:** grna, fam53b, psma6a, nusap1, scinla, pmm2, ckma **Nucleic:** nrm, anapc15, olig4, tead3b, msx1a, nsmce2, emx2, heyl, nt5c2l1, foxn4, rad51ap1, her12, pane1, cpsf3, pagr1, spi1b, ascl1b **Signaling:** myl1, adh5, si:dkey-148a17.6, fcer1g, mylz3, pvalb3, hvcn1, sparc **Metabolic:** naga, lcat, gch2, rgs18, rac2 **Development:** acta1b, tnnt3a, vegfd, dla **Sensory:** vps28, lhfpl4b, bco1 Stress: slc25a39, cpn1 **Circulatory:** hcls1, ckmb, mb **Transport:** scamp4, cahz **Cellular:** nmrk1, mlc1, egln3, mibp, hs2st1b, vsir, rdh8a, tmem45a, si:dkey-9i23.16 **Imunity:** ctss2.1, tnfaip8l2b **Protein Binding and Synthesis:** sumf1 **Miscellaneous:** si:dkey-225f5.4, si:ch211-236d3.4, fam89b	Overall Turning Angle Period 2	Swimming Bout Duration Period 3 (sec), Total Distance Traveled (mm)

Table 4.5 (cont'd)

		Neural: atcaya, ubap1, hectd1, rnf41, tulp4a, lrrc4.1, neurl1aa, desi1a, lnx1, sema3ab, zdhhc17, cntnap2a, usp24 **Nucleic:** fam98a, seta, senp3b, bhlhe41, rerea, rc3h1b, rprd2a, grid2ipa, evx2, khdc4, tent4a, kdm3b, arid2, fut9a, znf346, rfx1b, elk4, qkia, foxj3, srfb, zfr2, klf6a, larp4ab, pdik1l, ssbp4 **Signaling:** erbin, spred2a, crk, map3k9, ppp3ccb, nlk1, araf, gramd4a, ndrg3a, zmym2, bmp2k, slit1b, ppp2r5ca, iqsec2b, gpr63, pdpk1b, dusp8a, gnb1b **Metabolic:** tbc1d22b, gal3st3, arfgap1, casd1, atp8a2, cdk17, pitpnab, pdk3a, ralaa, ptdss1a, nudt3b **Development:** tmem65 Stress: rlim, kmt2e **Circulatory:** mybpc2b **Transport:** atp1a3a, ptpn23a, scamp1, slc6a17, ap2b1 **Cellular:** ano8b, zgc:114120, tmem86a, asphd2, si:dkeyp-27e10.3, shank1, enah, ubap2a, kiaa1549la, tm9sf3, syt14a, zdhhc20b, clip3, tspan7b, klc2, ubap2l, dmtn **Digestive:** mtor **Protein Binding and Synthesis:** mcu, nlgn2a, bag6 **Miscellaneous:** ajm1, zgc:158464, scaf8	Total Time Swimming (sec)	Capture Attempt Ratio
		Neural: stmn1b, im:7136398, slc25a1b, exosc8, snapin **Nucleic:** acin1a, znf207b, pithd1, eif2a **Signaling:** rgn, micu2 **Metabolic:** gpx1a, hibadhb, chchd3b, rasd1, ntpcr, ptcd2 **Development:** acvrl1, psenen, fgfbp3 **Circulatory:** acta2 **Transport:** crabp1a, chmp5b, stxbp3 **Cellular:** ccdc90b, ppcs, c18h3orf33, cd63, srr, tha1, srxn1, tspan14, atp6ap1a, tbce, tmem9b, tspan3a **Digestive:** scpep1 **Imunity:** ifi30 **Protein Binding and Synthesis:** alg3	Capture Attempt Ratio	Total Time Swimming (sec)
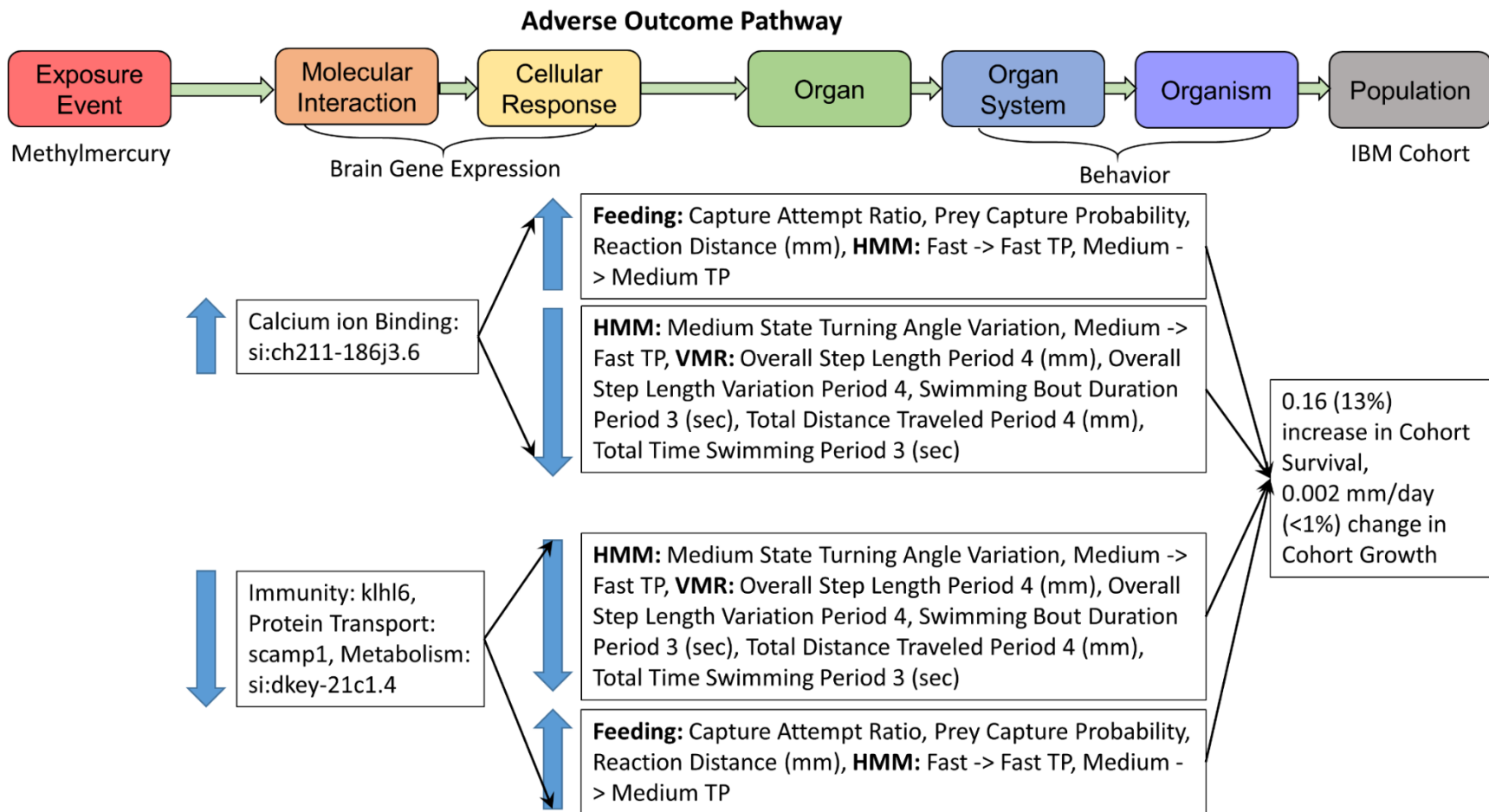
Figure 4.4. Significant mercury response patterns shared by gene expression and behavior endpoints in Scorton Creek (SCO) Atlantic killifish found in this study. Both the original and opposite behavior endpoint trends are listed. (HMM = Hidden Markov Chain model endpoint, TP = Transition Probability).

Adverse Outcome Pathway
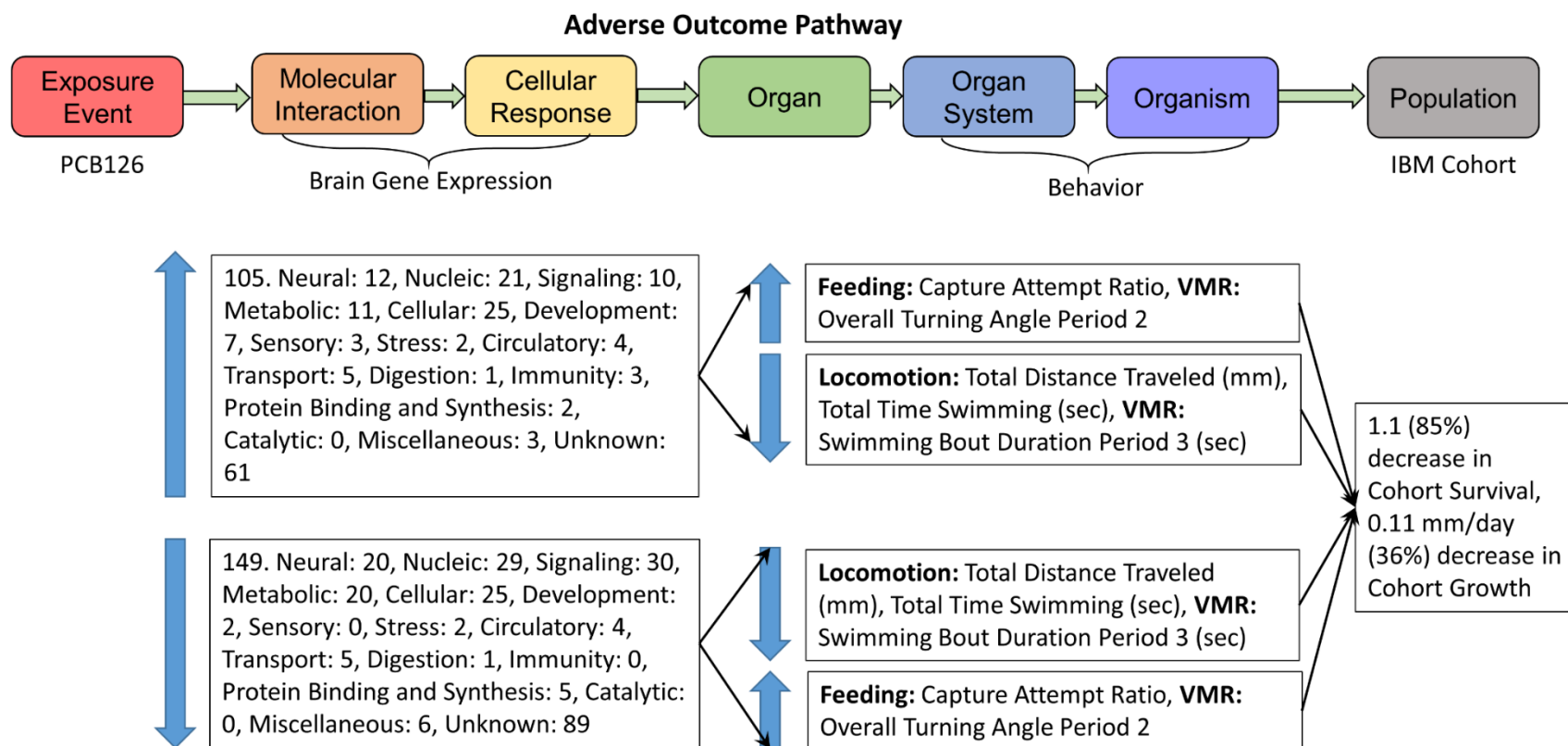
Figure 4.5. Tally of the significant PCB126 response patterns shared by gene expression and behavior endpoints in the Scorton Creek (SCO) Atlantic killifish found in this study. Both the original and opposite behavior endpoint trends are listed (HMM = Hidden Markov Chain model endpoint).

Individual based model

The SCO and NBH simulated population growth and survival were different between toxicant treatments. Control populations for both SCO and NBH experienced similar survival rates (1-2%) with SCO mean survival 28% higher than that of NBH (Figure 4.6; Table S4.22). Likewise, growth rates of SCO control populations were 2.3% higher than those of NBH (~0.3mm/d; Figure 4.6A). The effects of MeHg on the SCO population were minimal, with MeHg treatment resulting in 9% higher survival than that of the control (Figure 4.6). In contrast to MeHg, exposure to PCB126 produced substantial sublethal effects in both SCO and NBH. SCO populations exposed to PCB126 experienced almost no survival in any replicates after 100 days (Figure 4.6). NBH populations exposed to PCB126 had low survival at 0.4% (Figure 4.6), which was 38% lower than the control. Growth rates between control and PCB treatments in NBH fish were the same at 0.29 mm/d (Figure 4.6). Patterns between spring and summer runs were similar in both growth and survival for both populations and treatments. One notable exception was the summer SCO populations that were exposed to PCB126 ended up with 0.29% higher survival after 100 days as compared to spring, but the growth rate remained 85% less than the control (Figure 4.6).
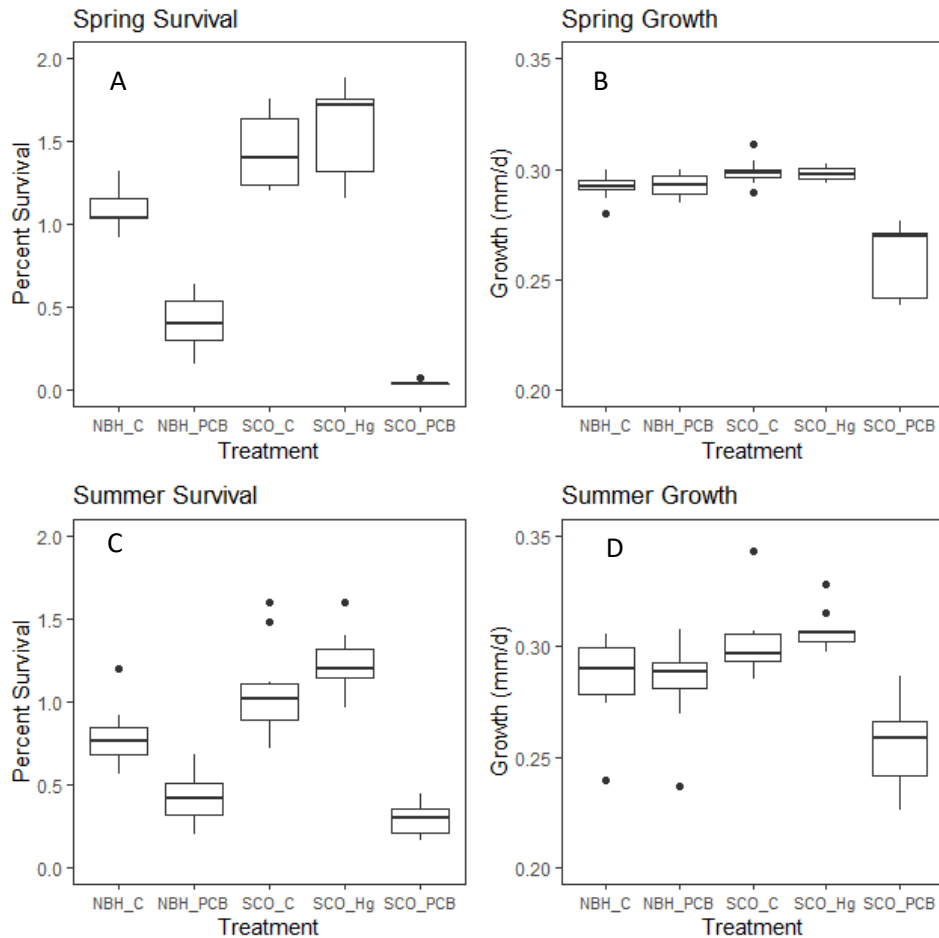
Figure 4.6. Mean percent survival and growth (mm/d) of Atlantic killifish survivors for 10 replicates of each treatment for spring and summer scenarios. SCO=Scorton Creek, NBH=New Bedford Harbor, Hg=methylmercury treatment, PCB = PCB126 treatment, C= control treatment.

Discussion

This study found numerous altered gene expressions and behaviors after exposure to MeHg or PCB126 KF in the embryonic stage. In addition, multiple altered gene expressions and behaviors changed with the same pattern across the treatments, suggesting an association between the altered gene expression and performed behavior. Lastly, these altered behaviors resulted in a reduction of predicted survival of PCB126 exposed KF larvae and reduced growth in SCO KF larvae. The multiple key event alterations found in this study suggest multiple AOPs

after sublethal embryonic exposure of PCB126 or MeHg. In addition, the two different KF

populations responded differently to the same PCB126 exposure suggesting flexibility in KF

population response that depended on ancestor exposure history.

Both MeHg and PCB126 exposure produced down regulation in the scamp1 gene and

decreases in capture attempts (Table S4.18). PCB126 and MeHg are contaminants that

commonly co-occur in polluted aquatic environments. Multiple AOPs have been identified for

each of these neurotoxicants, but it is unclear whether they share any AOPs (Liu et al. 2014;

Calò et al. 2018; Nogara et al. 2019; Yang et al. 2020). Research into each of these

neurotoxicants as individuals and in combination has been a long standing human risk research

question since there is the potential for human embryo exposure to both neurotoxicants after

contaminated parental fish consumption. Whether MeHg, PCB126 or MeHg + PCB126

antagonize or potentiate impacts during embryo development is still an active research question,

generating mixed answers in studies that used rats as test subjects. Results so far indicate that

depending on endpoint examined, age or sex of the rat, the combination of MeHg and PCB126

exposure can be additive, synergistic, or dampening (Vitalone et al. 2008, 2010; Piedrafita et al.

2008; Cauli et al. 2013; and references therein). However, similarities between MeHg and

PCB126 exposure on fish development has only just begun to be assessed, but using fish instead

of rats may lead to the same ambiguous answer. Our previous study that examined similar

behavior endpoints in yellow perch (*Perca flavescens*) found no similarities between embryos

exposed to either MeHg or PCB126 (Albers et al. 2022d), which is contrary to the results from

this study using KF. However, the gene set responses found between the MeHg and PCB126

exposed KF larvae in this study could be important endpoints to study when investigating

whether these two chemicals work in an additive, synergistic or dampening way. Comparisons

between this study and a future study examining gene sets in larvae that are exposed to a mixture of MeHg and PCB126 may lead to direct determination of the type of chemical mixture interactions.

Mercury exposed SCO parents produced offspring with altered gene expression and behaviors (Figure 4.4 and Table S4.19). These changes involved four known genes involved in signaling, immunity, protein transport and metabolism that coincided with feeding behaviors, swimming characteristics and stamina. The klhl6, scamp1, si:ch211-186j3.6 and si:dkey-21c1.4 genes have not be previously reported as mercury sensitive genes. Although behavior effects from these altered genes are likely since swimming is directly linking to fish metabolic and cell signaling processes, this study is the first to report that these genes had a connection to fish behavior endpoints. These behavior endpoints included HMM behaviors (medium swimming state turning angle variation, staying in the fast swimming state, and transitioning from the medium to fast swimming state), fish larva stamina in the last period of the VMR assay (total distance traveled, step length and variation), feeding reaction distance, and the probability of capturing prey. These MeHg effects on fish swimming behaviors were expected because MeHg exposure predominately affects the hippocampus region of the brain (Costa and Giordano 2012), the same region that regulates swimming behavior in fish (Godoy et al. 2015; McPherson et al. 2016; Huang et al. 2016).

The alterations in SCO KF larval gene expression and behaviors after MeHg exposure did not ultimately result in decreases in predicted cohort survival or growth. The IBM in this study predicted MeHg had either no effect to slight increases in cohort survival and growth. The averaged survival of simulated SCO KF in both spring and summer scenarios increased 0.16 or 13% from the control treatment caused by an increase in both capture rates and increases in the

distance at which larvae detected prey; increases in these feeding metrics offset the loss in feeding from slower movement rates. This resulted in a < 1% change in simulated cohort growth. Previous research has shown that MeHg exposure can increase or decrease fish larvae feeding metrics (see review in Albers et al. 2022a). This may occur because feeding behavior is a combination of many different physical attributes such as swimming, perception and sight. Consequently, the IBM was a good tool to summarize changes to multiple behavior endpoints into an overall group level change showing an increase in survival and growth.

Scorton Creek KF embryos exposed to PCB126 also had altered gene expression and behaviors, linking PCB126 embryonic exposure to both molecular and organism level effects as well as associating specific behaviors with certain gene expression (Figure 4.5 and Table S4.20). Scorton Creek KF larvae after exposure had lower physical activity levels that were associated with many altered genes, and showed general upregulation in numerous genes involved in nucleic and cellular brain functions and down regulation in signaling, nucleic and cellular functions. Decreases in the total time swimming and total distance traveled were associated with an upregulation of nerve maintenance, development and neurotransmitters (e.g. genes *lrrc4.1*, *atcaya*, *ext2*, *gad2*), as well as brain ubiquitin processes (e.g. genes *hectd1*, *lnx1*, *neurl1aa*, *rnf41*, *spata2*, *tulp4a*, *uba1*, *ubap1*) and cellular functions. Additionally, the decrease in activity coincided with a down regulation of brain DNA functions such as binding, splicing and transcription (e.g. *elk4*, *fam98a*, *kdm2ab*, *seta*); as well as brain metabolism (e.g. *arfgap1*, *atp8a2*, *elovl6*, *pitpnab*). Previous research has also found links between PCB126 exposure and decreases in tissue energy supplies and impaired adult fish swimming ability (Nault et al. 2012; Bellehumeur et al. 2016). Aluru et al. (2017) found adult zebrafish exposed to PCB126 as embryos to also have enrichment of calcium signaling and MAPK signaling pathways and

downregulation of various metabolic pathways. Other studies found PCB126 embryonic exposure did not alter larval behavior but impaired adult short- and long term habituation to novel environments (Glazer et al. 2016), suggesting that reprogramming gene expression patterns during development could extend impacts into adulthood.

In this study, the SCO KF larvae had the most altered gene expression and behaviors compared to any other group, and this resulted in the highest predicted change in cohort survival and growth. The behavior changes to SCO KF after exposure to PCB126 resulted in simulations with a 1.1 percent decrease in cohort survival (down 85% from control) and 36 percent decrease in growth (0.11 mm/day). These results were from PCB126 having a large impact on SCO swimming and travel time, as well as handling time. These behavior changes resulted in no survival in these scenarios, suggesting substantial decreases in population longevity in KF populations without any evolved tolerance. This would ultimately suggest that all exposure levels of PCB126 in this study is lethal to the survival of young of year fish.

Previous work in zebrafish suggests delayed mortality from embryonic exposure to PCB126 because of developmental effects on swim bladder inflation and cartilaginous tissues (Di Paolo et al. 2015). While Glazer et al. (Glazer et al. 2016) found no effect on zebrafish swimming behaviors, they did find impairment in short- and long-term habituation to a novel environment in adult zebrafish. Multiple molecular alterations have been implicated for these delays including reprograming of brain gene expression patterns resulting in adult brain metabolism and behavior (Aluru et al. 2017). As well as the PCB126 altering liver gluconeogenic enzymes in rats leading to wasting disorders (Gadupudi et al. 2016). These delayed affects are an important aspect in understanding population trends and risks to

population persistence while individuals of the population are being embryonically exposed to sublethal levels of PCB126.

Although NBH larvae were collected from a known PCB tolerant wild population, the F1 offspring in our study were still affected by PCB126. New Bedford Harbor KF larvae had subtle swimming characteristics that were altered after PCB126 exposure (Table 4.6), which coincided with a 98% fewer altered brain gene expressions as compared to SCO larvae (Figure 4.5 and Table S4.21). However, with these fewer changes in behaviors and brain gene expression, this study still predicted NBH KF larva had decreased survival (54% relative to control), although not as extreme as the SCO exposed KF (Figure 4.6). The decrease in NBH survival was from decreased swimming time, resulting in lower encounters with prey relative to the control cohort. Results from this study suggest NBH KF populations are susceptible to low levels of embryonic exposure to PCB126 even with evolved pollution tolerance which contradicts lethality and ethoxyresorufin-O-deethylase (EROD) activity endpoints examined in previous studies (see review Nacci et al. 2010). These results suggest NBH KF may have evolved to withstand exposure levels that are lethal, but are still susceptible to sublethal impacts that alter individuals, but still allow the population to persist. Possible reasons why this study found NBH KF were susceptible to PCB126 exposure include 1) use of behavior and genetic endpoints that are in general more sensitive to chemical exposure in fish than lethality or gross morphology (Little and Finger 1990; Melvin and Wilson 2013; Faimali et al. 2017). 2) Use of sensitive HMM behavior endpoints to detect larvae behavior alterations, as compared to traditional behavior endpoints, where HMM behavior endpoints have been shown to increase the sensitivity of toxicological behavior analyses (Albers et al. 2022d). 3) Examination of all differentially expressed genes in larval brain tissue and not just those genes known to be affected by DLCs.

Each of the two KF population examined in this study responded to PCB126 exposure in unique ways. Killifish offspring from a population with no previously documented exposure to DLCs (SCO) had substantial alterations to their brain gene expression, behavior and predicted survival and growth after PCB126 exposure. While offspring from a KF population with a known tolerance to DLCs (NBH) were still affected but had different and fewer alterations to their behavior and brain gene expression, and not as severe reduction in predicted survival, relative to SCO KF. In comparison to SCO larvae, NBH KF larvae appear to have an evolved oxidative phosphorylation pathway (KEGG 190), being already at a lower state before PCB126 exposure relative to SCO and only altered in NBH after exposure, possibly from their ancestral history with DLCs. These results are not unexpected since previous research suggests KF may be an emerging example of parallel contemporary evolutions driven by human-mediated pollution (Nacci et al. 2016), especially with DLCs (Nacci et al. 2010). The KF ability to adapt seems to be driven by the extremely high genetic variation especially in genes associated with immune function and olfaction (Reid et al. 2017). Indeed, the highest changes of differentially expressed genes were found when comparing the control groups between NBH and SCO at 3220 (Table S4.8). The lowest level of changes were observed between NBH control larvae and PCB126 (40 ng/L) treatments with only 8 DEGs. Previous research indicates that KF genes associated with neurological, development and cytoskeletal have changed the least, indicating they are required for population persistence (Reid et al. 2017). Results indicate embryonic exposure to PCB126 impact these same gene types in both the non-adapted and adapted KF, but to a lesser extent in adapted KF.

Even though NBH fish are known to have a tolerance to chemical pollutants, the mechanism of tolerance is yet to be fully understood. Our results suggest the pollution tolerance

may be associated with a metabolic pathway (Table S4.21), as well as other possible evolved

differences due to population isolation. However, previous research into KF tolerance has

mainly focused on cytochrome P450 (*Cyp*) and aryl hydrocarbon receptor (*AhR*) gene expression

in gill and liver tissues (Arzuaga and Elskus 2010; Nacci et al. 2010, 2016; Clark et al. 2010;

Whitehead et al. 2010; Aluru et al. 2011; Gräns et al. 2015; Celander et al. 2021). NBH KF to

have evolved tolerance through resistance of reactive oxygen species and cardiac teratogenesis

(Arzuaga and Elskus 2010; Clark et al. 2010) mainly through bypassing components in the

complex stress response network which involves *AhR* and *Cyp* gene expression (Nacci et al.

2016). The present study did not examine liver or gill tissue, but brain tissue where *AhR*

regulates the timing of restorative neurogenesis and is crucial for the survival of newborn

neurons (Di Giaimo et al. 2018). Fish brain tissue contains *AhR1* and *AhR2* (Shankar et al. 2020)

which are also the two forms of *AhR* that are suspected in producing KF tolerance (Reitzel et al.

2014). Similar results were found in the NBH larvae in the present study, where *AhR2*

expression occurred in high enough levels in the brain to compare between PCB126 treated NBH

larvae and controls. But *AhR2* expression was only increased in High PCB126 dose of NBH

larva (400 ng/L) and no changes were detected in the SCO brains after exposure to 40 ng/L

PCB126 (Table S4.16). Additionally, Whitehead et al. (2012) found tolerant KF populations

expressed AhR gene battery members in a dose dependent manor with PCB126 including

glutathione S-transferase (*GST*) and forkhead box (*FOX*) Q1 genes. Forkhead box proteins are

transcription factors that regulate the expression of genes in cell growth, proliferation,

differentiation and longevity; and are important to embryonic development (Katoh and Katoh

2004; Hannenhalli and Kaestner 2009). The *GST* gene family encodes genes important to

detoxication and toxification mechanisms by conjugation of reduced glutathione (Nebert and

Vasiliou 2004). We also found NBH control larva had higher baseline expression levels of gstt2 and foxn4; as well as lower baseline expression levels of *foxo6b*, *foxj3*, *foxp1b*, *foxo1a*, *foxp2* and *foxg1a*, relative to SCO control. Interestingly, the present study did not detect *Cyp* genes at a high enough level to test for differences between treatments, which also may be because this study only examined brain tissue.

The AOP framework that was the base of this study, facilitated the organization of biological connections, impacts from neurotoxicant exposure, and comparisons between two separate KF populations and two neurotoxicants. The AOPs constructed here allow us to make connections between diverse biological endpoints such as gene expression, behavior and cohort population metrics. By making these connections, the AOP framework conceptually demonstrates the potential paths of environmental pollutants impacting hierarchical levels of biological organizations that ultimately predict affects to fish populations and fitness. Effects from both MeHg and PCB126 found in the present study will allow for appropriate levels of risk to be assigned to sublethal levels of neurotoxicants in our environment. These results will provide a more diverse and complete understanding of how contaminants affects the response and long-term persistence of fish populations.

CHAPTER 5: HOW FAR CAN ADVERSE OUTCOME PATHWAYS TAKE US? LESSONS LEARNED FROM DEVELOPING A NEUROBEHAVIOR AOP

Abstract

Understanding the risk from sublethal impacts on fish populations from environmentally relevant pollution levels involves interpreting complex biological information collected from suborganismal and organismal levels of biological organization. The Adverse Outcome Pathway framework (AOP) is a way to organize and predict impacts on populations using suborganismal processes. The AOP framework has only been in existence for a decade and has proven useful for certain situations, but the limits of their usefulness are still being explored. Adverse Outcome Pathway assumptions were examined in this study; specifically, whether the differing responses from multiple levels of biological organization were similar between two neurotoxicants [PCB126 and methylmercury (MeHg)], and whether multiple species would have similar responses to these neurotoxicants across the different levels of biological organization. After examining over 120,000 treatment-control biological endpoint tests, only the pyrimidine metabolism pathway (KEGG 2D:00240) was perturbed after exposure to MeHg or PCB126 in both yellow perch *Perca flavescens* (YP) and zebrafish *Danio rerio* (ZF). After PCB126 exposure, ZF and YP exhibited down regulated *cyp1a* gene and the previously mentioned perturbation in the pyrimidine metabolism KEGG 2D 240 pathway). ZF and Atlantic killifish *Fundulus heteroclitus* (KF) also had increases in prey miss proportion and downregulation of the *ndrg3a* gene, the DNA metabolic process (GO:0006259), and in DNA replication (GO:0006260). KF and YP were the least similar, both having a down regulation of the chromosome gene set (GO:0005694). After MeHg exposure, KF and ZF were the most similar with 3 behavior endpoints that responded the same direction. Findings from this study examining sublethal levels of exposure to two neurotoxicants suggest more similarities at lower

levels of AOPs between species and chemicals than at higher AOP levels. Genomic endpoints were found to be the most similar between species and chemicals, consequently, genomics may be a relatively good tool to assess general trends from sublethal pollution. The insights gained from this study increase our understanding of how AOPs can be used in risk assessment, by illuminating areas where species surrogacy and chemical agnostics could occur and where they may be inappropriate.

.

Introduction

Adverse Outcome Pathway framework (AOP) as a framework to organize toxicity pathways using mechanistic data at multiple levels of biological organization (from molecules to populations) was first introduced in 2010 (Ankley et al. 2010). This framework has been proven successful with linking many different types of biological perturbations from chemical stressors to generate a very diverse group of biological pathways (https://aopwiki.org/). One hypothesis in this framework is that each modular biological pathway can be used for any chemical that perturbs the same key events or species that share the same biological structure. This modular pathway approach can assist with network analyses or help determine impacts from several chemicals with multiple modes of action and chemical mixtures (Villeneuve et al. 2014a, 2014b). This modular biological hypothesis has been supported for AOPs key events at molecular, cellular and organ levels (Knapen et al. 2015; Brockmeier et al. 2017; McBride 2018). Tools have also been constructed to extrapolate the impacts observed on individuals to populations which are typically limited to modeling exercises that can be logistically difficult to confirm in situ and to extrapolate across species [see Key Event #360 entitled "Decrease Population Growth Rate" that has 56 AOPs linked to it at aopwiki.org (Villeneuve and Garcia-Reyero 2010)]. Further, recent examples with predicting impacts from dioxin-like compounds across bird and fish species using AOPs is very promising (Doering et al. 2018, 2020).

One of the main goals in toxicology is to assess the environmental and human risk of the millions of manmade chemicals and to simplify this, the AOP the modular interchange of chemical impacts with similar modes of action is especially useful. One example of this AOP flexibility may be demonstrated by the impacts of two well-known developmental neurotoxicants, methylmercury (MeHg) and 3,3',4,4',5-pentachlorobiphenyl (PCB126). Both

have multiple mechanisms of action, some being shared between the two chemicals, while others are not. These two chemicals alter calcium homeostasis which is critical in neuron function (Piedrafita et al. 2008b; Costa and Giordano 2012). In addition, MeHg directly impacts neurotransmitter levels by altering acetylcholinesterase, sulfhydryl (thiol)-group protein binding, methylation (epigenetics) and neurogenesis (Sastry and Sharma 1980; Johansson et al. 2007; Bradbury et al. 2008; Farina et al. 2011; Weber et al. 2012; Costa and Giordano 2012; Helmcke and Aschner 2012; Amara et al. 2012; Bose et al. 2012; Ho et al. 2013; Kalueff et al. 2016). Whereas PCB126 is a aryl hydrocarbon receptor agonist and disrupts energy metabolism (Bandiera et al. 1982; Okey 2007; Zhang et al. 2012; Gadupudi et al. 2016). Since MeHg and PCB126 could be impacting brain function through at least one similar pathway, an AOP framework may be a useful tool to assess the similarity on the biological impacts of these two neurotoxicants.

The use of surrogate fish species in research is common practice especially when considering rare or difficult-to-culture fish species, but should always be done with caution [see review by Murphy et al. (2011)]. Surrogacy has also become common practice when research uses model organisms such as zebrafish *Danio rerio* (ZF; Leonelli and Ankeny 2013; Bambino and Chu 2017). The ease of ZF culture, physical attributes and conscious pain status has allowed ZF to become a popular biological tool to discover many aspects of biology that are transferable to human applications (https://zfin.org/). While ZF are a good tool to study different aspects of human biology, their use as a surrogate species for other native fish species remain uncertain (Van Veld and Nacci 2008; King-Heiden et al. 2012; Whitehead et al. 2012), especially as it relates to higher levels of biological organization such as behavior (Faimali et al. 2017; Dutra Costa et al. 2020).

One of the steps in using ZF as a surrogate is to first test whether the species of interest have similar responses as ZF. Zebrafish surrogacy for two native U.S. fish species was investigated in this study, Atlantic killifish *Fundulus heteroclitus* (KF) and yellow perch *Perca flavescens* (YP). Atlantic killifish have a long history in scientific research as toxicological test subjects. They are commonly found along the east and southeast coast of the U.S. in estuary habitat, habitats that also has a long history of industrial pollution (Reid et al. 2017). This has resulted in some populations of KF evolving tolerance (Nacci et al. 2016; Reid et al. 2017), particularly as it pertains to industrial pollutants that activate the aryl hydrocarbon receptor (AhR) such as PCBs. Yellow perch are common to the Great Lakes region and a popular sport fish. Similar to the east and gulf coast of the U.S., the Great Lakes region also has a long history of industrial pollution resulting in the contamination of Great Lakes YP stocks (Wiener et al. 2012). Great Lakes industrial pollution is one of many possible causes behind fluctuations in Great Lakes YP populations (e.g. Visha et al. 2018).

The AOP framework was used for three recent studies to provide a diverse suite of YP and KF biological responses after sublethal embryonic exposure to MeHg and PCB126 (Albers et al. 2022a, 2022b; Ivan et al. 2022). These studies examined brain gene expression as a molecular/cellular response, larval behavior as an organismal response, and constructed an Individual Based Model (IBM) as a way to predict cohort response metrics. These three previously published studies were developed to support this study's goal of interrogating specific assumptions of the AOP framework. For this study we combined results from three previous studies (Albers et al. 2022a, 2022b; Ivan et al. 2022) with new corresponding results from ZF and additional YP feeding behavior and gene expression results. The objectives of this research are to 1) using an AOP framework, assess the impact of environmentally relevant sublethal

91

levels of two neurotoxicants on multiple fish species through multiple levels of biological organization; 2) determine whether the two neurotoxicants impact a diverse set of biological outcomes in a similar way; and 3) assess the similarities between the responses of three fish species in order to evaluate the surrogate potential of ZF for KF and YP. These objectives will increase our understanding of the potential and limitations of the modular structure AOPs as it is applied across two neurotoxicants and three fish species. Additionally, we will better understand risk from sublethal levels of pollution to fish populations and how and where it is appropriate to use information across chemicals and species.

Methods

Exposure and fish husbandry

Multiple toxicity experiments were conducted on the embryos of three species of fish [ZF, YP and KF from Scorton Creek, MA] and two neurotoxicants (MeHg via MeHgCl and PCB126). Embryonic exposure levels and dose timing focused on the embryo developmental stage and was either the actual or mimicked parental transfer of MeHg through gametes or water transfer of PCB126 by dosing embryos during the first 24 hr (ZF and YP) or actual parental transfer by parental dosing (KF) (Westerlund et al. 2000; Alvarez et al. 2006; Mora-Zamorano et al. 2016a; Bridges et al. 2016a, 2016b; Carvan et al. 2017). Chemical dose levels were set to be very low so that larvae did not show any obvious physical deformities and also represented concentrations found in the waters of the United States, with tissue levels less than 3 µg/g mercury and 0.05 µg/g PCB126 wet weight (Rose et al. 2003; Grimes et al. 2008; Wiener et al. 2012; Oziolor et al. 2018). The YP and KF embryonic dosing and assay methods were described in detail in two previous articles (Albers et al. 2022a, 2022d) and similar methods were used for ZF and further YP behavior assays, which are described in detail in the supplemental section of

this paper. Briefly, embryos were dosed with either MeHg or PCB126 during the first 24 hours of development using sublethal chemical levels. At various points in larval development, different biological endpoints were sampled to represent different levels of biological organization. Larval brain gene expression was collected and represents molecular and cellular responses to exposure, individual larval behavior represents the whole organism level response, and an Individual Based Model was used to estimate cohort survival and growth as KF and YP population level responses.

Each fish species required different levels of external chemical embryonic exposure to obtain similar internal chemical tissue concentrations because individual species have unique sensitivity and biology. Using the goal of no observable morphological deformities in larva as a guide (actual deformities, reduced swim bladder inflation and swim up, etc.), dosing levels for each species were determined using a combination of preliminary dosing test experiments (unpublished) and previous published research (Grimes et al. 2008; Mora-Zamorano et al. 2017). The highest external dose that did not result in any visible physical deformities in each species was used as the highest dose in each experiment, which ensured no overt visible toxicity in this study (Table 5.1). Additionally, to ease comparisons between fish species, we adjusted sampling times of each endpoint to occur at the same larval developmental stage. Embryo tissue collection for chemical concentration determination occurred soon after chemical exposure ended (1 dpf YP and ZF, 3 dpf KF; 3 batches for each treatment that contained multiple embryos). Brain gene expression sample collection occurred the day behavior assays started (25 dpf YP, 17 dpf KF, 6 dpf ZF; 6 larva per treatment). Locomotion and Visual Motor Response (VMR) behavior assays were conducted just after larvae were actively swimming (6 dpf ZF, 16 and 17 dpf KF, 27 dpf

YP). Feeding assays occurred just after larvae started actively feeding (30-38 dpf YP, 23-24 dpf

KF, 16 dpf ZF).

Contaminant response endpoints from the embryonic exposures were collected at varying

levels of biological organization during larval development. Each of these endpoints were

collected on a separate set of fish to maintain independence, with only a few exceptions

occurring with the KF larvae (42% of fish in the locomotion assay had been in the VMR assay,

all fish in the feeding assay had also been in the locomotion assay and 44% had also been

through the VMR assay). Larval brain gene expression was assessed at a developmental time

point before the behavior assays were conducted (again an exception occurred with KF larvae

where 52% of larvae that contributed brains for the gene expression had been through the VMR

assay; see supplemental document for more details). Each species brain transcriptome was

analyzed, which contained genes unique to each species. To compare between species, each

non-ZF species was aligned with ZF orthologous genes and common ZF gene names were used

for comparisons. Gene expression from each species-treatment group were processed using

Gene Ontology (GO) term gene sets and Kyoto Encyclopedia of Genes and Genomes (KEGG)

pathways to determine alterations to gene groups.

Larval behaviors were assessed using three types of behavior assays: feeding, locomotion

and VMR. Yellow perch larva behavior could not be assessed using the VMR because the larva

did not survive in the small individual well plates required for the VMR. Each behavior assay

was conducted using the same methods for each species (see supplemental for details), and the

same set of behavior endpoints were calculated for each species. A subset of behavior endpoints

were used to model KF and YP individual larvae behavior in an Individual Based Model: prey

handling time, prey miss proportion, larva reaction distance to prey, swimming speed and total

swimming time (Albers et al. 2022a; Ivan et al. 2022). A separate IBM run was conducted for each treatment using their treatment altered behaviors until they reached the juvenile stage [KF at 24 mm (Abraham 1985) and YP at 20 mm (Auer 1982)], at which time individual larval growth and survival were estimated. Albers et al. (2022a) estimated both spring and summer KF cohorts, but both resulted in similar treatment patterns, consequently, the summer treatment results were used in this study. An IBM was not constructed for ZF because population impacts were not ecologically relevant.

Analysis

For each biological endpoint measured in each chemical treatment (e.g. KF feeding behavior in the middle MeHg dose), a test was conducted against a set of control larvae to determine if the biological endpoint was statistically increased or decreased after chemical exposure. For the empirically measured endpoints, a statistical test was conducted using a Bayesian model that tested for differences between chemical treatments after removing the variation accounted for by multiple covariates (see Bayesian Model Analysis section in the supplemental material). For the IBM estimated endpoints, treatments were compared with the controls using estimates that include uncertainty and if the 95% confidence intervals did not overlap, they were considered to be either an increase or decrease from the control. All differentially expressed genes (DEGs), gene sets and pathway analyses used the false discover rate of 0.05 to compensate for multiple comparisons. Only the behavior endpoint P-values were not adjusted for multiple comparisons. Of the 424 behavior endpoint comparisons made in this study, 21 could be significant by random chance (0.05 alpha level $\times$ 424 tests = 21.2). Some of the statistical test results used in this study have already been reported in previous articles

(Albers et al. 2022a, 2022d; Ivan et al. 2022). All the ZF test results are presented in the supplemental (Tables S5.1-S5.17) with the YP transcriptomic analyses and feeding assay results (Tables S5.18-S5.23).

Typically, AOP studies use correlations between endpoints to show causation or connections between biological endpoints. Because only two chemical doses were deployed in this study, the biological causation between endpoints as chemical dose increases was limited (i.e. only three data points for each correlation). In addition, the resulting internal chemical concentrations, which were not available until after endpoint data collection occurred, suggested a limited number of treatments have similar internal chemical levels, thereby further decreasing the number of appropriate comparisons. Consequently, we limited our comparisons to only those treatments with similar internal chemical concentrations (see 'Adjusted Treatment' column in Table 5.1). With one control-treatment comparison in each species-chemical combination, comparisons were limited to general increases or decreases in each measured endpoint.

For this study, in the end, there were three main comparisons that remained and were used that measured endpoints and their relative change as compared to the control treatment. 1) Comparison of endpoint changes between chemicals and species. The results from this comparison could suggest possible areas for future research into endpoints that are common across multiple species and neurotoxicants. 2) Comparison of endpoint changes between species within each chemical. This will determine if certain species responded in a similar pattern, suggesting good species surrogates during similar toxicology studies. 3) Comparison of endpoint changes between chemicals within each species. These results would suggest endpoints that are impacted by both neurotoxicants, i.e. shared AOPs between chemicals.

Table 5.1. Summary of mercury from methylmercury (MeHg) treatments and 3,3',4,4',5-pentachlorobiphenyl (PCB126) tissue concentrations found in larvae from this study. Relative lethality measures represented relative species sensitivity (ND = not detected; NA, not applicable; SCO = Scorton Creek killifish, MA). Italicized values are estimated using wet weight or results from previous studies.

Chemical Treatment	Level of Treatment, Dose	Adjusted Treatment	Concentration in Solvent (ppb)	(µM)	Dry Weight Tissue Concentration (n=3) Mean	SD	Wet Weight Tissue Concentration (n=3) Mean	SD	Units for Tissue Concentration	Relative Lethality Measure (LD50 ppb dw; LC50 ppb)	
					Yellow Perch						
MeHg Treatments											
	Control	Control	0	0	5.26	1.16	0.39^{1}	NA	ppb		
	Middle	Middle	0.25	0.001	40.35	5.76	3.34^{1}	NA	ppb		
	High		25.108	0.1	5251.5	1187.30	420.62^{1}	NA	ppb		
PCB126 Treatments										LD50	1000[c]
	Control	Control	0	0	NA	NA	ND	NA	ppb		
	Middle		10	30.63	NA	NA	ND	NA	ppb		
	High	Middle	1000	3063.42	11.82^{1}	NA	6.367	5.333	ppb		
					Zebrafish						
MeHg Treatments										LC50	103.6[f]
	Control	Control	0	0	10.21^{1}	NA	5.5^{g}	1.5^{g}	ppb		
	Middle	Middle	0.25	0.001	36.01^{1}	NA	19.4^{g}	3^{g}	ppb		
	High		25.108	0.1	5232.4^{1}	NA	2819.2^{g}	457.2^{g}	ppb		
PCB126 Treatments										LD50	100[c]
	Control	Control	0	0	NA	NA	ND	NA	ppb		
	Middle		0.1	0.31	NA	NA	ND	NA	ppb		
	High	Middle	10	30.63	NA	NA	ND	NA	ppb		
					Killifish						
MeHg Treatments										LC50	72.7[e]
	SCO - Control daily dose	Control	300	1.194	9.80	2.49	1.70^{1}	NA	ppb		
	SCO - Hg daily dose	Middle	3600	14.34	35.09	17.06	6.46^{1}	NA	ppb		

97

Table 5.1 (cont'd)

PCB126 Treatments									LD50	10[d]
SCO - PCB126 40 ng/L[b]	Middle	0.04	0.12	*19[a]*	NA	*4.1[1]*	NA	ppb		
SCO - PCB126 400 ng/L[b]		0.4	1.23	*189[a]*	NA	*41.2[1]*	NA	ppb		

[a] Estimated using previous experiments (Nacci et al. 1999)
[b] Also exposed to ~300 ng tHg/g dw/day through salmon-based diet
[c] Estimated based on relative TCDD potency (Spitsbergen et al. 1988; Elonen et al. 1998; Toomey et al. 2001)
[d] D. Nacci unpublished data on fish from a relatively uncontaminated site.
[e] (Sharp and Neff 1982)
[f] (Selderslaghs et al. 2012)
[g] (Carvan et al. 2017), n=9
[1] Estimated using percent moisture of 87% (Kneib 1993; Albers et al. 2022a, 2022d)

Results

After aligning all treatment-control tests by the species' internal tissue concentrations, there were 121,324 treatment-control tests performed in this study; 1,313 were found to have either a statistical increase or decrease in the biological endpoint after chemical exposure (Table 5.2 and S5.24). Of the 1,313 statistically significant comparisons found in this study, none of the biological endpoints measured in this study responded in the same direction in all species after both chemical exposures, including no similarity in trends of predicted cohort survival and growth (Table 5.2). However, the pyrimidine metabolism pathway (KEGG 2D:00240) was perturbed after exposure to MeHg and PCB126 in both YP and ZF (Table 5.3). This KEGG 2D pathway was also perturbed in KF but only significantly so after PCB126 exposure. Additionally, KEGG:00240 had significantly reduced activity in PCB126 exposed KF and MeHg exposed ZF (Table S5.24). The most altered genes in this pathway for these species after exposure were *polr2a* and *polr2j* involved in RNA polymerase II activity and transcription; *uck2a* gene which is involved in kinase activity, cytidine 5'-triphosphate and uridine monophosphate salvage and phosphorylation; *cmpk* gene which is involved in nucleoside triphosphate biosynthetic process; and the *nt5e* gene which is predicted to have 5'-nucleotidase activity and involved in the response to copper ion (Bradford et al. 2022).

After exposure to the same chemical, 21 biological endpoints had similar patterns in at least two fish species (Figure 5.1, Table 5.3), of which 14 were genes, gene sets, or gene pathways. Out of the 21 common endpoints, 14 were from MeHg exposure, of which 11 endpoints had the same response in both YP and ZF larvae to MeHg. These 11 endpoints include 3 increased swimming behavior endpoints and 7 down regulated genomic endpoints, and the previously mentioned perturbation in the Pyrimidine metabolism KEGG 2D:00240 pathway.

99

After MeHg exposure, YP and KF were the least similar in their responses with no common

trends among endpoints, whereas KF and ZF had 3 behavior endpoints that responded the same

direction. No biological endpoints responded in a similar direction in all three species after

MeHg exposure.

Out of the 21 common endpoints between multiple species, 7 occurred after PCB126

exposure, none of which occurred in all three fish species (Figure 5.1, Table 5.3). Where ZF and

YP exhibited down regulated *cyp1a* gene and the previously mentioned perturbation in the

pyrimidine metabolism KEGG 2D:00240 pathway). After PCB126 exposure, ZF and KF also

had increases in prey miss proportion and downregulation of the *ndrg3a* gene, the DNA

metabolic process (GO:0006259) and in DNA replication (GO:0006260). Lastly, KF and YP

both had a down regulation of the chromosome gene set (GO:0005694).

Within each fish species, at least one behavior and genomic endpoint were altered by

each neurotoxicant (Table 5.3), and 27 endpoints responded with the same pattern after exposure

to both chemicals indicating possible similarities in adverse outcome pathways (Figure 5.1,

Table 5.3). However, each species exhibited a different proportion of the endpoint types (i.e.

genomic, behavior and population; Figure 5.1). For example, KF responded to either exposure

with decreases in *scamp1* gene expression and two swimming characteristics in the VMR assay,

as well as increases in prey capture attempt ratios and three gene expressions (currently

unidentified genes), whereas YP had three KEGG 2D pathways that were perturbed by both

neurotoxicants: DNA replication, pyrimidine metabolism and cell cycle (Table 5.3). Lastly, ZF

had 17 endpoints that responded in the same direction after exposure to either neurotoxicant, 15

of which were genomic endpoints that involved decreased activity in DNA metabolism and

replication, as well as perturbed KEGG 2D pathways (e.g. PPAR signaling, glutathione

metabolism, metabolism of xenobiotics by cytochrome P450, pyrimidine metabolism and drug metabolism; Table 5.3).

Table 5.2. Summary of the number of biological endpoints examined in this study and the number found to increase or decrease after embryonic exposure to environmentally relevant levels of methylmercury (MeHg) and 3,3',4,4',5-pentachlorobiphenyl (PCB126; KEGG = Kyoto Encyclopedia of Genes and Genomes, GO = Gene Ontology, IBM = individual based model).

Species	Chemical	Endpoints	Number of Biological Endpoints		
			Examined	Increased	Decreased
Yellow Perch *Perca flavescens*	MeHg	Genes	17838	6	2
		KEGG Gene Pathways	123	0	1
		KEGG 2D Gene Pathways[a]	123	3	NA
		GO Term Gene Sets	2643	0	7
		Behaviors	41	4	1
		IBM	2	2	0
	PCB126	Genes	17838	9	2
		KEGG Gene Pathways	123	0	0
		KEGG 2D Gene Pathways[a]	123	4	NA
		GO Term Gene Sets	2643	0	6
		Behaviors	41	0	1
		IBM	2	0	0
Atlantic Killifish *Fundulus heteroclitus*	MeHg	Genes	16017	16	6
		KEGG Gene Pathways	120	0	0
		KEGG 2D Gene Pathways[a]	120	0	NA
		GO Term Gene Sets	2637	0	0
		Behaviors	83	5	7
		IBM	2	0	0
	PCB126	Genes	16017	177	248
		KEGG Gene Pathways	120	12	5
		KEGG 2D Gene Pathways[a]	120	0	NA
		GO Term Gene Sets	2637	37	54
		Behaviors	83	6	18
		IBM	2	0	2
Zebrafish *Danio rerio*	MeHg	Genes	16400	1	2
		KEGG Gene Pathways	151	1	14
		KEGG 2D Gene Pathways[a]	151	15	NA

Table 5.2 (cont'd)

	GO Term Gene Sets	4123	73	177
	Behaviors	87	25	4
	IBM	0	0	0
PCB126	Genes	16400	40	178
	KEGG Gene Pathways	151	2	1
	KEGG 2D Gene Pathways[a]	151	14	NA
	GO Term Gene Sets	4123	73	31
	Behaviors	87	7	14
	IBM	0	0	0

[a] KEGG 2D pathways are perturbed which is a combination of increased and decreased gene expression

Table 5.3. Summary of the biological endpoints that responded in the same direction across species or chemicals in this study (TP = Transition Probabilities, HMM = Hidden Markov Chain Model, sec = second, KF = Atlantic killifish *Fundulus heteroclitus*, YP = yellow perch *Perca flavescens*, ZF = zebrafish *Danio rerio*, MeHg = methylmercury, PCB126 = 3,3',4,4',5-pentachlorobiphenyl, KEGG = Kyoto Encyclopedia of Genes and Genomes, GO = Gene Ontology)

Chemical	Species	Direction of Response after Exposure	Endpoint
			Same Response Between Species
PCB126	KF/YP	Down	**Gene Sets:** Nucleic: chromosome GO:0005694
PCB126	KF/ZF	Down	**Gene:** *ndrg3a* **Gene Sets:** Nucleic: DNA metabolic process GO:0006259, DNA replication GO:0006260
PCB126	KF/ZF	Up	**Behavior:** Prey Miss Proportion
PCB126	YP/ZF	Down	**Gene:** *cyp1a*
PCB126	YP/ZF	Perturbed	**Gene Sets:** Metabolic: Pyrimidine metabolism KEGG 2D:00240
MeHg	KF/ZF	Down	**Behavior:** HMM Medium State Turning Angle Variation
MeHg	KF/ZF	Up	**Behavior:** HMM Medium -> Medium TP, Prey Capture Probability
MeHg	YP/ZF	Down	**Gene Sets:** Nucleic: mitotic cell cycle GO:0000278, DNA metabolic process GO:0006259, DNA replication GO:0006260, DNA-dependent DNA replication GO:0006261, mitotic cell cycle process GO:1903047 Cellular: cell cycle process GO:0022402, Cell cycle KEGG:004110
MeHg	YP/ZF	Perturmed or Up	**Gene Sets:** Metabolic: Pyrimidine metabolism KEGG 2D:00240 **Behavior:** HMM Slow -> Medium TP, Swimming Bouts (per sec), Total Time Swimming (sec)
			Same Response Between MeHg and PCB126
Both	KF	Down	**Gene:** *scamp1* **Behavior:** Swimming Bout Duration Period 3 (sec), Total Time Swimming Period 3 (sec)
Both	KF	Up	**Gene:** loc105917295, loc105924291, loc105934237 **Behavior:** Capture Attempt Ratio
Both	YP	Perturbed	**Gene Sets:** Nucleic: DNA replication KEGG 2D:03030 Metabolic: Pyrimidine metabolism KEGG 2D:00240 Cellular: Cell cycle KEGG 2D:04110
Both	ZF	Down	**Gene Sets:** Nucleic: mitotic cell cycle GO:0000278, DNA metabolic process GO:0006259, DNA replication GO:0006260

Table 5.3 (cont'd)

Both	ZF	Perturbed or Up	**Gene Sets:** Signaling: PPAR signaling pathway KEGG 2D:03320 Metabolic: Glutathione metabolism KEGG 2D:00480, Retinol metabolism KEGG 2D:00830, Metabolism of xenobiotics by cytochrome P450 KEGG 2D:00980, Pyrimidine metabolismKEGG 2D:00240, Drug metabolism - other enzymes KEGG 2D:00983, Drug metabolism - cytochrome P450 KEGG 2D:00982 Cellular: ECM-receptor interaction KEGG 2D:04512 Imunity: Intestinal immune network for IgA production KEGG 2D:04672 Miscellaneous: Steroid biosynthesis KEGG 2D:00100, Steroid hormone biosynthesis KEGG 2D:00140, Phototransduction KEGG 2D:04744 **Behavior:** HMM Medium State Step Length Variation, Overall Step Length Variation

Figure 5.1. Summary of the biological endpoints that responded in the same direction after chemical exposure to methylmercury (MeHg) and 3,3',4,4',5-pentachlorobiphenyl (PCB126).

Discussion

This study investigated multiple assumptions behind the AOP framework using multiple fish species, neurotoxicants and endpoints across three levels of biological organization after environmentally-relevant levels of exposure. This allowed for numerous response comparisons across multiple chemical and biological levels, resulting in none of the endpoints responding in a similar way across all three fish species and two neurotoxicants examined. The highest level of biological organization, the predicted fish cohort survival and growth, did not respond similarly between any of the groups. The next lowest biological level tested, larval behavior, also did not show any similarities between all species and chemicals test; however, there were some behavior endpoints that responded the same between two species. The most commonalities found in this study between species after either neurotoxicant exposure occurred with the lowest level of biological organization tested, the genomic endpoints: individual gene expression, GO gene sets, KEGG and KEGG 2D pathways. The most similar responding genomic endpoints were the KEGG 2D pathways, with GO gene sets, individual genes and KEGG pathways occurring to a lesser extent. The only common endpoint found in this study over multiple species and chemicals was the pyrimidine metabolism pathway (KEGG 2D:00240), which was perturbed after exposure to MeHg and PCB126 in both YP and ZF, as well as KF exposed to PCB126.

Pyrimidine derivatives are the building blocks of DNA and RNA (i.e. cytosine, thymine and uracil), and the pyrimidine metabolism pathway ensures a balanced supply of purines and pyrimidines exists for DNA/RNA synthesis, thus becoming an important component of DNA/RNA repair mechanisms. Both neurotoxicants used in this study directly and/or indirectly damage DNA. PCB126 is an AhR agonist, where AhR activation leads to higher rates of cancer and DNA damage (Wang et al. 2020). Oxidation of pyrimidines by hydroxyl radicals is a

common impact from heavy metals resulting in multiple adducts products in DNA (Jan et al. 2015). Heavy metals are hypothesized to create genome instability at low doses (Langie et al. 2015) and the pyrimidine metabolism pathway in human salivary gland cells has been previously reported to be enriched after MeHg exposure (Nogueira et al. 2021). With the increased prevalence of new omics tools, such as those used in this study, there is increased potential in understanding of how xenobiotics damage DNA using direct and indirect mechanisms [i.e. DNA/RNA damage repair mechanisms, DDRs (Langie et al. 2015; Costa 2022)]. While more research is needed before DDR can be used as biomarker [e.g. too sensitive to many types of pollution, or biased by natural repair pathways as suggested by Palmqvist et al. (2003)], it has the potential for widespread use since DDR applies to many species both eukaryotes and prokaryotes, since individual survival and species evolution requires efficient DNA repair mechanisms (Costa 2022).

An important aspect to this study was the multiple ways in which species and treatments were aligned before comparisons were conducted. First, dosing levels were unique to each species and set to a level that did not exhibit visible signs of physical malformations. Second, endpoints were collected at the same stage of development between species, which was a different day post hatch. Third, whole larvae tissue concentrations were used to align treatments between species. These precautions were taken because previous research has shown that sublethal effects are not as consistent across species as lethal effects. Sublethal effects often present with a non-linear response (Lushchak 2014), making internal chemical concentrations critical to compare the same part of the curve. In addition, sublethal effects are not consistent through time; some impacts are temporary or delayed and only affect a certain life stage (Samson et al. 2001; Vitalone et al. 2008, 2010; Glazer et al. 2016), or are permanent (Fjeld et al. 1998;

Onishchenko et al. 2012; Nabi 2014), while others can only affect a certain group of individuals, such as effects on males and not females (Vitalone et al. 2010). The ability of sublethal effects to be time and group dependent required multiple alignment procedures to make sure species comparisons were accurate. Indeed, all three alignment procedures were required in this study before any similarities were found between all three species during analysis. Consequently, we recommend that any comparisons in future studies between species should at minimum use tissue concentrations and similar developmental periods for endpoint collection as a basis for any species comparisons or when using species surrogates.

After embryonic exposure to the same neurotoxicant, some fish species responded more closely to one another, indicating possible surrogacy, but these similarities were not consistent between the two neurotoxicants. After MeHg exposure, YP and ZF responded in the same response direction with 11 different endpoints (42% of YP significant responses, 3% of ZF), suggesting ZF may be an appropriate MeHg surrogate for YP. With KF MeHg exposure, ZF responded the same direction in three endpoints (3% of all KF significant endpoints and 1% of ZF), suggesting ZF does not respond to MeHg in a similar way as KF. After sublethal embryonic PCB126 exposure, ZF had two and four endpoints that responded in the same direction as YP and KF, respectively (10% and <1% of all altered endpoints), suggesting ZF could be a PCB126 surrogate for YP. Overall, these results suggest that although ZF reacted in a similar pattern for some endpoints, ZF did not on many other endpoints. Depending on the type of endpoint examined, different conclusions, possibly incorrect conclusions, could be made when using ZF as a surrogate for YP and KF after MeHg or PCB126 exposures. These interspecies similarities were concluded using mostly genomic endpoints, but this study found little support of surrogates using behavior endpoints. Even so, the similarities found in this study using

transcriptomics supports the use of omics in determining other types of toxic surrogates and may explain the popularity of AOPs that use lower levels of biological organization (Brockmeier et al. 2017; McBride 2018; Seim et al. 2022). The combination of each species' molecular responses and different chemical modes of action between PCB126 and MeHg in this study, lead to different surrogate choices, and should be taken into consideration when using ZF as a toxic surrogate for any species. Indeed, research on toxic surrogates has suggested that if toxic surrogates are to be effective, specific comparison conditions are needed that compare toxicant level (Banks et al. 2010), chemical mode of action (Jones et al. 1998; Zhang et al. 2010), and biological stage of comparison [e.g. sex or age (Jorgenson et al. 2015)].

While this study did find similarities between chemicals and species, the lack of similarities between all species and chemicals was unexpected. In this study, particular attention was given to conducting all tests using the same methodology across species and chemicals. As well as including relatively large numbers of individual larvae (100s per treatment in behavior assays, 6 individuals for genetic endpoints) and endpoints, which would theoretically increase the number of similarities. However, no similarities between all species and chemicals with this large effort suggests the results from this study are not because of low power, but a real lack of similarity. Additionally, inconsistent responses across species and chemical occurred at the unexpected levels of biological organization. Initially, one idea was that the population AOP level endpoints would integrate suborganismal and organismal levels of biological organization, and therefore would be more consistent over species and chemicals. However, none of the IBM endpoints were consistent across KF or YP or either chemical and only a few behavior endpoints and individual genes were consistent across chemicals. One exception to this was the KEGG pathway analysis, which examines pathways in both a directional and holistic assessment (e.g.

KEGG 2D), and ended up being the most frequently consistent endpoints examined across species and chemicals

The reasons why this study did not find more similarities could be attributable to multiple factors. The limited number of chemical dosages may initially suggest a limited study scope, but more chemical doses would probably increase the number of differences based on current results, thus not increasing the chance of finding more similarities. The fact that this study focused on sublethal endpoints may be one reason for the limited number of similarities. Sublethal endpoints are much more variable than lethal endpoints, consequently, this would limit the ability to find similarities between species and chemicals. Lastly, one possible reason for the limited similarities is that the chemicals and species used in this experiment are not similar enough in their modes of action (i.e. MeHg and PCB126 have too many dissimilar modes of action, or ZF, KF and YP are too genetically distinct species). For example, in general, PCBs predominantly perturb the AhR pathway (Doering et al. 2018, 2020), whereas MeHg has multiple significant pathways including neurotransmitter disruption, calcium homeostasis, thiol modulation and DNA damage (Farina et al. 2011; Costa and Giordano 2012; Weber et al. 2012). The number of response similarities within chemicals and species were alike (383 for species and 275 for chemicals), suggesting the same level of dissimilarity between chemicals and species. Regardless, this study was able to predict fish cohort changes in growth and survival, but since the IBM results were not consistent between YP and KF, thus limiting the ability to predict chemical impacts on across populations.

Modeling of population level responses in AOPs is typically determined through some type of simulation exercise, with IBMs being a preferred technique (e.g. Stinckens et al. 2018; Armstrong et al. 2020). This study used IBMs to predict cohort survival and growth during the

first 100 days for YP and KF, but none of the results from these simulations were similar between YP and KF. If cohort responses for the same chemical are not similar between species, IBMs may not be suitable for this purpose or could be lacking important aspects. For example, in this study only 5 of the 41 (YP) or 83 (KF) measured behaviors were used as inputs for the IBMs (prey handling time, prey miss proportion, prey reaction distance, swimming bout speed and total time swimming). Four of these five behaviors were perturbed in KF, while only total time swimming was altered in YP. These five endpoints may not be sufficient in capturing the breadth of perturbations that occurred in each species, where YP also had 14 more behaviors altered by either chemical and KF had 38. For example, Rearick et al. (2018) used predator escape performance and predation rates to estimate impacts on fish larvae from oestrogen. In addition, incorporation of the HMM behaviors may prove a useful addition to IBMs. However, behavior endpoints alone may not be sufficient in transferring perturbations to the IBM, where more direct connections between the IBM and sub-organismal responses are required. Incorporating bioenergetics components into an IBM could be a very important aspect since dioxins are known to directly impact metabolism (Zhang et al. 2012; Gadupudi et al. 2016) and metabolomics can be a major AOP component (e.g. Davis et al. 2017). Lastly, more diverse modeled endpoints are needed besides cohort survival and growth. Sex ratios would be an important aspect of an AOP IBM, especially if pollutants discriminate between genders [e.g. dioxin-like PCBs, androgenic and oestrogenic substances (Cauli et al. 2013; Hazlerigg et al. 2014; Gadupudi et al. 2016)].

This study investigated multiple assumptions behind the AOP frameworks, namely the ability to apply AOPs to multiple species and chemicals. Many different types of biological endpoints were evaluated for each of three fish species in this study including brain gene

expression, gene functional groups and gene pathways [KF results were reported in (Albers et al. 2022a)]; traditional swimming, feeding and stimulus behaviors and newer state based behavior metrics from hidden Markov chain models (Albers et al. 2022b); and predicted larval growth and survival from IBMs [YP results were reported in (Ivan et al. 2022)]. While the results of this study are narrow in scope because limited number of chemical doses were examined, the results suggest that not all levels of biological organization respond in a similar patterns across ZF, YP and KF, as well as across two developmental neurotoxicants, MeHg and PCB126. Genomic endpoints did show some promise of consistency between species and chemicals, and could be used to indicate a perturbation is occurring, which then can be followed up with more detailed studies on what is affected and scope of the problem. Additionally, multiple critical aspects of conducting similar AOP research were highlighted. 1) Innate species differences need to be considered and compensated for in order to properly compare differences between species. 2) Time points where biological endpoints are collected need to be thoroughly assessed during the design phase, since causality between key events is dependent upon closeness in time and space. 3) More analytical tools are needed for comparing between species and chemicals. These include comparisons between species and chemicals using nonlinear sublethal dose responses or gene functional analyses, disparate biological endpoints that are typically not linked to one another, finer population level metrics that are connected to molecular and cellular functions, and more direct ways to connect molecular functions like gene expression to organismal responses like behavior.

By expanding the analytical tools to connect between different levels of biological organisms we will be able to more accurately predict risk from environmental pollutants using AOPs and protect organisms from detrimental exposures. This study is an attempt to illustrate

all these connections and possible similarities between species and chemicals. This is an important research need considering all the toxic chemicals in the environments, and this study was able to elaborate on lessons learned in this attempt. Without the organizational structure of the AOP framework, it would be difficult to successfully present the study findings, and despite some AOP shortcomings, this study did find some similarities and contributes to the knowledgebase needed for more accurate risk assessments.

The implications of this study suggest focusing on a set of current tools that continue to improve (i.e. genomics) as well as many new aspects of AOPs could be incorporated. Results from the brain gene expression endpoints in this study were able to span species and chemicals, increasing the applicability of these types of endpoints especially in relation DDR. Understanding how DDR impacts brain cell function thus impacting behavior using functional imaging could make both spatial and temporal connections between genes and behavior that were not possible in this study. In addition, this study used two chemicals that did not share many modes of action. Expanding AOPs and AOP IBMs to more easily incorporate multiple modes of action may also increase AOP utility across chemicals. Lastly, AOP IBMs may need to include more parameters with direct connections to molecular and cellular levels (e.g. omics). These direct connections may help in AOP IBM precision and flexibility for application across species and chemicals.

LITERATURE CITED

Abraham, B. J. 1985. Species profiles life histories and environmental requirements of coastal fishes and invertebrates Mid-Atlantic USA mummichog and striped killifish. U S Fish and Wildlife Service Biological Report 8211, 223 p.

Ågerstrand, M., K. Arnold, S. Balshine, T. Brodin, B. W. Brooks, G. Maack, E. S. McCallum, G. Pyle, M. Saaristo, and A. T. Ford. 2020. Emerging investigator series: use of behavioural endpoints in the regulation of chemicals. Environmental Science: Processes & Impacts 22(1):49–65.

Albers, J. L., B. W. Clark, D. E. Nacci, R. H. Klingler, A. Thrash, J. P. Steibel, L. N. Ivan, N. Garcia-Reyero, M. J. Carvan, and C. A. Murphy. 2022a. Impacts on Atlantic killifish from neurotoxicants: genes, behavior and populations. Journal Environmental Science & Technology.

Albers, J. L., M. J. Garcia-Reyero Vinas, Natalia Carvan, K. Chou, and C. A. Murphy. 2022b. Mercury effects on early life stage fish behavior. Journal Environmental Science & Technology.

Albers, J. L., N. Garcia-Reyero, M. J. Carvan, A. Thrash, and C. A. Murphy. 2022c. How far can Adverse Outcome Pathways take us? Journal Environmental Science & Technology.

Albers, J. L., J. P. Steibel, R. H. Klingler, L. N. Ivan, N. Garcia-Reyero, M. J. Carvan, and C. A. Murphy. 2022d. Altered larval yellow perch swimming behavior due to methylmercury and PCB126 detected using hidden Markov chain models. Environmental Science & Technology 56(6):3514–3523.

Alexander, J., G. Auðunsson, D. Benford, A. Cockburn, J. Cravedi, E. Dogliotti, A. Di Domenico, M. Férnandez-Cruz, P. Fürst, J. Fink-Gremmels, C. Galli, P. Grandjean, J. Gzyl, R. van L. Gerhard Heinemeyer, Niklas Johansson, Antonio Mutti, Josef Schlatter, and C. V. P. and P. Verger. 2008. Mercury as undesirable substance in animal feed - Scientific opinion of the Panel on Contaminants in the Food Chain. EFSA Journal 6(4):654.

Aluru, N., S. I. Karchner, and L. Glazer. 2017. Early Life Exposure to Low Levels of AHR Agonist PCB126 (3,3′,4,4′,5-Pentachlorobiphenyl) Reprograms Gene Expression in Adult Brain. Toxicological Sciences 160(2):386–397.

Aluru, N., S. I. Karchner, and M. E. Hahn. 2011. Role of DNA methylation of AHR1 and AHR2 promoters in differential sensitivity to PCBs in Atlantic Killifish, Fundulus heteroclitus. Aquatic Toxicology 101(1):288–294.

Alvarez, M. del C., C. A. Murphy, K. A. Rose, I. D. McCarthy, and L. A. Fuiman. 2006. Maternal body burdens of methylmercury impair survival skills of offspring in Atlantic croaker (Micropogonias undulatus). Aquatic Toxicology 80(4):329–337. Elsevier.

Amara, I. E. A., A. Anwar-Mohamed, G. Abdelhamid, and A. O. S. El-Kadi. 2012. Effect of mercury on aryl hydrocarbon receptor-regulated genes in the extrahepatic tissues of C57BL/6 mice. Food and Chemical Toxicology 50(7):2325–2334.

Amirbahman, A., and I. J. Fernandez. 2012. The Role of Soils in Storage and Cycling of

Mercury. Pages 99–118 Mercury in the environment: Pattern and process. University of California Press, Berkeley, CA.

Ankley, G. T., R. S. Bennett, R. J. Erickson, D. J. Hoff, M. W. Hornung, R. D. Johnson, D. R. Mount, J. W. Nichols, C. L. Russom, P. K. Schmieder, J. A. Serrrano, J. E. Tietge, and D. L. Villeneuve. 2010. Adverse outcome pathways: A conceptual framework to support ecotoxicology research and risk assessment. Environmental Toxicology and Chemistry 29(3):730–741. Wiley-Blackwell.

Area-Gomez, E., C. Guardia-Laguarta, E. A. Schon, and S. Przedborski. 2019. Mitochondria, OxPhos, and neurodegeneration: cells are not just running out of gas. Journal of Clinical Investigation 129(1):34–45.

Armstrong, B. M., F. X. Mora-Zamorano, M. J. Carvan, S. McNaught, N. Basu, J. Head, R. H. Klingler, L. Ivan, and C. A. Murphy. 2020. Exploring the Impacts of Methylmercury-Induced Behavioral Alterations in Larval Yellow Perch in Lake Michigan Using an Individual-Based Model. Transactions of the American Fisheries Society 149(6):664–680.

Arzuaga, X., and A. Elskus. 2010. Polluted-site killifish (Fundulus heteroclitus) embryos are resistant to organic pollutant-mediated induction of CYP1A activity, reactive oxygen species, and heart deformities. Environmental Toxicology and Chemistry 29(3):676–682.

Auer, N. A. (ed. . 1982. Identification of larval fishes of the Great Lakes basin with emphasis on the Lake Michigan drainage. Ann Arbour, MI (USA) Great Lakes Fishery Commission.

Baldwin, D. H., J. A. Spromberg, T. K. Collier, and N. L. Scholz. 2009. A fish of many scales: extrapolating sublethal pesticide exposures to the productivity of wild salmon populations. Ecological Applications 19(8):2004–2015.

Bambino, K., and J. Chu. 2017. Zebrafish in Toxicology and Environmental Health. Pages 331–367.

Bandiera, S., S. Safe, and A. B. Okey. 1982. Binding of polychlorinated biphenyls classified as either phenobarbitone-, 3-methylcholanthrene- or mixed-type inducers to cytosolic Ah receptor. Chemico-Biological Interactions 39(3):259–277.

Bank, M. S. 2012. Mercury in the environment: Pattern and process. University of California Press, Berkeley, CA.

Banks, J. E., A. S. Ackleh, and J. D. Stark. 2010. The Use of Surrogate Species in Risk Assessment: Using Life History Data to Safeguard Against False Negatives. Risk Analysis 30(2):175–182.

von Baumgarten, R. J., R. C. Simmonds, J. F. Boyd, and O. K. Garriott. 1975. Effects of prolonged weightlessness on the swimming pattern of fish aboard Skylab 3. Aviation, space, and environmental medicine 46(7):902–906. United States.

Beier, P., and F. S. de Albuquerque. 2015. Environmental diversity as a surrogate for species representation. Conservation Biology 29(5):1401–1410.

Bellehumeur, K., D. Lapointe, S. J. Cooke, and T. W. Moon. 2016. Exposure to sublethal levels of PCB-126 impacts fuel metabolism and swimming performance in rainbow trout.

Comparative Biochemistry and Physiology Part B: Biochemistry and Molecular Biology 199:97–104.

Bhatia, T. N., D. B. Pant, E. A. Eckhoff, R. N. Gongaware, T. Do, D. F. Hutchison, A. M. Gleixner, and R. K. Leak. 2019. Astrocytes Do Not Forfeit Their Neuroprotective Roles After Surviving Intense Oxidative Stress. Frontiers in Molecular Neuroscience 12:87.

Blanchfield, P. J., J. W. M. Rudd, L. E. Hrenchuk, M. Amyot, C. L. Babiarz, K. G. Beaty, R. A. D. Bodaly, B. A. Branfireun, C. C. Gilmour, J. A. Graydon, B. D. Hall, R. C. Harris, A. Heyes, H. Hintelmann, J. P. Hurley, C. A. Kelly, D. P. Krabbenhoft, S. E. Lindberg, R. P. Mason, M. J. Paterson, C. L. Podemski, K. A. Sandilands, G. R. Southworth, V. L. St Louis, L. S. Tate, and M. T. Tate. 2022. Experimental evidence for recovery of mercury-contaminated fish populations. Nature 601(7891):74–78.

Blukacz-Richards, E. A., A. Visha, M. L. Graham, D. L. McGoldrick, S. R. de Solla, D. J. Moore, and G. B. Arhonditsis. 2017. Mercury levels in herring gulls and fish: 42 years of spatio-temporal trends in the Great Lakes. Chemosphere 172:476–487.

Bose, R., N. Onishchenko, K. Edoff, A. M. Janson Lang, and S. Ceccatelli. 2012. Inherited Effects of Low-Dose Exposure to Methylmercury in Neural Stem Cells. Toxicological Sciences 130(2):383–390.

Bradbury, S. P., R. W. Carlson, T. R. Henry, S. Padilla, and J. Dowden. 2008. Toxic Responses of the Fish Nervous System. Pages 417–455 *in* R. T. Di Giulio and D. E. Hinton, editors. The Toxicology of Fishes. Taylor and Francis, Boca Raton, FL.

Bradford, Y. M., C. E. Van Slyke, L. Ruzicka, A. Singer, A. Eagle, D. Fashena, D. G. Howe, K. Frazer, R. Martin, H. Paddock, C. Pich, S. Ramachandran, and M. Westerfield. 2022. Zebrafish information network, the knowledgebase for Danio rerio research. Genetics 220(4).

Bradley, M., B. Barst, and N. Basu. 2017. A Review of Mercury Bioavailability in Humans and Fish. International Journal of Environmental Research and Public Health 14(2):169.

Branson, K., A. A. Robie, J. Bender, P. Perona, and M. H. Dickinson. 2009. High-throughput ethomics in large groups of Drosophila. Nature Methods 6(6):451–457.

Bridges, K. N., B. K. Soulen, C. L. Overturf, P. E. Drevnick, and A. P. Roberts. 2016a. Embryotoxicity of maternally transferred methylmercury to fathead minnows (Pimephales promelas). Environmental Toxicology and Chemistry 35(6):1436–1441.

Bridges, K., B. Venables, and A. Roberts. 2016b. Effects of dietary methylmercury on the dopaminergic system of adult fathead minnows and their offspring. Environmental Toxicology and Chemistry 36(4):1077–1084. Wiley-Blackwell.

Brockmeier, E. K., G. Hodges, T. H. Hutchinson, E. Butler, M. Hecker, K. E. Tollefsen, N. Garcia-Reyero, P. Kille, D. Becker, K. Chipman, J. Colbourne, T. W. Collette, A. Cossins, M. Cronin, P. Graystock, S. Gutsell, D. Knapen, I. Katsiadaki, A. Lange, S. Marshall, S. F. Owen, E. J. Perkins, S. Plaistow, A. Schroeder, D. Taylor, M. Viant, G. Ankley, and F. Falciani. 2017. The Role of Omics in the Application of Adverse Outcome Pathways for Chemical Risk Assessment. Toxicological Sciences 158(2):252–262.

Calabrese, E. J. 2008. Astrocytes: Adaptive Responses to Low Doses of Neurotoxins. Critical Reviews in Toxicology 38(5):463–471.

Calabrese, E. J. 2016. Preconditioning is hormesis part I: Documentation, dose-response features and mechanistic foundations. Pharmacological Research 110:242–264.

Calò, M., A. Bitto, P. Lo Cascio, F. Giarratana, D. Altavilla, T. Gervasi, L. Campone, N. Cicero, and P. Licata. 2018. PCB-126 effects on aryl hydrocarbon receptor, ubiquitin and p53 expression levels in a fish product (Sparus aurata L.). Natural Product Research 32(10):1136–1144.

Cambier, S., G. Bénard, N. Mesmer-Dudons, P. Gonzalez, R. Rossignol, D. Brèthes, and J.-P. Bourdineaud. 2009. At environmental doses, dietary methylmercury inhibits mitochondrial energy metabolism in skeletal muscles of the zebra fish (Danio rerio). The International Journal of Biochemistry & Cell Biology 41(4):791–799. Pergamon.

Campbell, H. A., R. D. Handy, and D. W. Sims. 2005. Shifts in a Fish's Resource Holding Power during a Contact Paired Interaction: The Influence of a Copper-Contaminated Diet in Rainbow Trout. Physiological and Biochemical Zoology 78(5):706–714. The University of Chicago Press.

Carvan, M. J., T. A. Kalluvila, R. H. Klingler, J. K. Larson, M. Pickens, F. X. Mora-Zamorano, V. P. Connaughton, I. Sadler-Riggleman, D. Beck, and M. K. Skinner. 2017. Mercury-induced epigenetic transgenerational inheritance of abnormal neurobehavior is correlated with sperm epimutations in zebrafish. PLOS ONE 12(5):e0176155.

Caudle, W. M., and G. W. Miller. 2015. Neurotoxicity: toxic effects oN the Nervous system. Pages 157–168 in S. M. Roberts, R. C. James, and L. P. Williams, editors. Principles of Toxicology. John Wiley & Sons, Inc.

Cauli, O., B. Piedrafita, M. Llansola, and V. Felipo. 2013. Gender differential effects of developmental exposure to methyl-mercury, polychlorinated biphenyls 126 or 153, or its combinations on motor activity and coordination. Toxicology 311(1–2):61–68.

Celander, M. C., J. V. Goldstone, N. R. Brun, B. Clark, S. Jayaraman, D. Nacci, and J. J. Stegeman. 2021. Resistance to Cyp3a induction by polychlorinated biphenyls, including non-dioxin-like PCB153, in gills of killifish (Fundulus heteroclitus) from New Bedford Harbor. Environmental Toxicology and Pharmacology 83:103580.

Chon, T.-S., Y. Liu, and S.-H. Lee. 2010. Hidden Markov Model and Self-Organizing Map Applied to Exploration of Movement Behaviors of Daphnia magna (Cladocera: Daphniidae). Journal of the Korean Physical Society 56(3(1)):1003–1010.

Clark, B. W., C. W. Matson, D. Jung, and R. T. Di Giulio. 2010. AHR2 mediates cardiac teratogenesis of polycyclic aromatic hydrocarbons and PCB-126 in Atlantic killifish (Fundulus heteroclitus). Aquatic Toxicology 99(2):232–240.

Clotfelter, E. D., A. M. Bell, and K. R. Levering. 2004. The role of animal behaviour in the study of endocrine-disrupting chemicals. Animal Behaviour 68(4):665–676.

Coccini, T., E. Roda, A. F. Castoldi, M. Goldoni, D. Poli, G. Bernocchi, and L. Manzo. 2007. Perinatal co-exposure to methylmercury and PCB153 or PCB126 in rats alters the cerebral

cholinergic muscarinic receptors at weaning and puberty. Toxicology 238(1):34–48.

Cong, L., Z. Wang, Y. Chai, W. Hang, C. Shang, W. Yang, L. Bai, J. Du, K. Wang, and Q. Wen. 2017. Rapid whole brain imaging of neural activity in freely behaving larval zebrafish (Danio rerio). eLife 6.

Costa, L. G., and G. Giordano. 2012. Methylmercury Neurotoxicity: A Synopsis of In Vitro Effects. Pages 219–227 Methylmercury and Neurotoxicity. Springer US, Boston, MA.

Costa, P. M. 2022. Current aspects of DNA damage and repair in ecotoxicology: a mini-review. Ecotoxicology 31(1):1–11.

Couillard, C. M., B. Légaré, A. Bernier, and Z. Dionne. 2011. Embryonic exposure to environmentally relevant concentrations of PCB126 affect prey capture ability of Fundulus heteroclitus larvae. Marine Environmental Research 71(4):257–265.

Cowan, J. H. J., E. D. Houde, and K. A. Rose. 1996. Size-dependent vulnerability of marine fish larvae to predation: an individual-based numerical experiment. ICES Journal of Marine Science 53:23–37.

Davis, J. M., D. R. Ekman, D. M. Skelton, C. A. LaLone, G. T. Ankley, J. E. Cavallin, D. L. Villeneuve, and T. W. Collette. 2017. Metabolomics for informing adverse outcome pathways: Androgen receptor activation and the pharmaceutical spironolactone. Aquatic Toxicology 184:103–115.

Deslauriers, D., S. R. S. R. Chipps, J. E. J. E. Breck, J. A. J. A. Rice, and C. P. C. P. Madenjian. 2017. Fish Bioenergetics 4.0: An R-based modeling application. Fisheries 42(11):586–596.

Dillon, T., N. Beckvar, and J. Kern. 2010. Residue-based mercury dose-response in fish: An analysis using lethality-equivalent test endpoints. Environmental Toxicology and Chemistry 29(11):2559–2565.

Doering, J. A., J. Dubiel, and S. Wiseman. 2020. Predicting Early Life Stage Mortality in Birds and Fishes from Exposure to Low-Potency Agonists of the Aryl Hydrocarbon Receptor: A Cross-Species Quantitative Adverse Outcome Pathway Approach. Environmental Toxicology and Chemistry 39(10):2055–2064.

Doering, J. A., S. Wiseman, J. P. Giesy, and M. Hecker. 2018. A Cross-species Quantitative Adverse Outcome Pathway for Activation of the Aryl Hydrocarbon Receptor Leading to Early Life Stage Mortality in Birds and Fishes. Environmental Science & Technology 52(13):7524–7533.

Dorea, J. G. 2006. Fish Meal in Animal Feed and Human Exposure to Persistent Bioaccumulative and Toxic Substances. Journal of Food Protection 69(11):2777–2785.

Dunn, T. W., Y. Mu, S. Narayan, O. Randlett, E. A. Naumann, C.-T. Yang, A. F. Schier, J. Freeman, F. Engert, and M. B. Ahrens. 2016. Brain-wide mapping of neural activity controlling zebrafish exploratory locomotion. eLife 5:1–29.

Dutra Costa, B. P., L. Aquino Moura, S. A. Gomes Pinto, M. Lima-Maximino, and C. Maximino. 2020. Zebrafish Models in Neural and Behavioral Toxicology across the Life Stages. Fishes 5(3):23.

Edelhoff, H., J. Signer, and N. Balkenhol. 2016. Path segmentation for beginners: an overview of current methods for detecting changes in animal movement patterns. Movement Ecology 4(1):21.

Egnor, S. E. R., and K. Branson. 2016. Computational Analysis of Behavior. Annual Review of Neuroscience 39(1):217–236.

Elonen, G. E., R. L. Spehar, G. W. Holcombe, R. D. Johnson, J. D. Fernandez, R. J. Erickson, J. E. Tietge, and P. M. Cook. 1998. Comparative toxicity of 2,3,7,8-tetrachlorodibenzo- p - dioxin to seven freshwater fish species during early life-stage development. Environmental Toxicology and Chemistry 17(3):472–483.

Emran, F., J. Rihel, and J. E. Dowling. 2008. A Behavioral Assay to Measure Responsiveness of Zebrafish to Changes in Light Intensities. Journal of Visualized Experiments (20):6.

Escola, S., A. Fontanini, D. Katz, and L. Paninski. 2011. Hidden Markov Models for the Stimulus-Response Relationships of Multistate Neural Systems. Neural Computation 23(5):1071–1132.

Faimali, M., C. Gambardella, E. Costa, V. Piazza, S. Morgana, N. Estévez-Calvar, and F. Garaventa. 2017. Old model organisms and new behavioral end-points: Swimming alteration as an ecotoxicological response. Marine Environmental Research 128:36–45.

Farina, M., J. B. T. Rocha, and M. Aschner. 2011. Mechanisms of methylmercury-induced neurotoxicity: Evidence from experimental studies. Life Sciences 89(15–16):555–563.

Fjeld, E., T. . Haugen, and L. . Vøllestad. 1998. Permanent impairment in the feeding behavior of grayling (Thymallus thymallus) exposed to methylmercury during embryogenesis. Science of The Total Environment 213(1–3):247–254.

Fleeger, J. W., D. S. Johnson, K. A. Galván, and L. A. Deegan. 2008. Top-down and bottom-up control of infauna varies across the saltmarsh landscape. Journal of Experimental Marine Biology and Ecology 357(1):20–34.

Foster, K. S. 2012. Synthesis and evaluation of naturally occuring halogenated bipyrroles in a relevant marine species, Fundulus heteroclitus. Univeristy of Mississippi.

Fulford, R. S., J. A. Rice, T. J. Miller, F. P. Binkowski, J. M. Dettmers, and B. Belonger. 2006. Foraging selectivity by larval yellow perch (Perca flavescens): implications for understanding recruitment in small and large lakes. Canadian Journal of Fisheries and Aquatic Sciences 63(1):28–42.

Gadupudi, G. S., W. D. Klaren, A. K. Olivier, A. J. Klingelhutz, and L. W. Robertson. 2016. PCB126-Induced Disruption in Gluconeogenesis and Fatty Acid Oxidation Precedes Fatty Liver in Male Rats. Toxicological Sciences 149(1):98–110.

Garcia-Reyero, N., and C. A. Murphy, editors. 2018. A Systems Biology Approach to Advancing Adverse Outcome Pathways for Risk Assessment. Springer International Publishing, Cham.

Di Giaimo, R., T. Durovic, P. Barquin, A. Kociaj, T. Lepko, S. Aschenbroich, C. T. Breunig, M. Irmler, F. M. Cernilogar, G. Schotta, J. S. Barbosa, D. Trümbach, E. V. Baumgart, A. M.

Neuner, J. Beckers, W. Wurst, S. H. Stricker, and J. Ninkovic. 2018. The Aryl Hydrocarbon Receptor Pathway Defines the Time Frame for Restorative Neurogenesis. Cell Reports 25(12):3241-3251.e5.

Glazer, L., M. E. Hahn, and N. Aluru. 2016. Delayed effects of developmental exposure to low levels of the aryl hydrocarbon receptor agonist 3,3′,4,4′,5-pentachlorobiphenyl (PCB126) on adult zebrafish behavior. NeuroToxicology 52:134–143.

Godoy, R., S. Noble, K. Yoon, H. Anisman, and M. Ekker. 2015. Chemogenetic ablation of dopaminergic neurons leads to transient locomotor impairments in zebrafish larvae. Journal of Neurochemistry 135(2):249–260.

Gräns, J., B. Wassmur, M. Fernández-Santoscoy, J. Zanette, B. R. Woodin, S. I. Karchner, D. E. Nacci, D. Champlin, S. Jayaraman, M. E. Hahn, J. J. Stegeman, and M. C. Celander. 2015. Regulation of pregnane-X-receptor, CYP3A and P-glycoprotein genes in the PCB-resistant killifish (Fundulus heteroclitus) population from New Bedford Harbor. Aquatic Toxicology 159:198–207.

Green, A. J., and A. Planchart. 2018. The neurological toxicity of heavy metals: A fish perspective. Comparative Biochemistry and Physiology Part C: Toxicology & Pharmacology 208:12–19.

Grimes, A. C., K. N. Erwin, H. A. Stadt, G. L. Hunter, H. A. Gefroh, H.-J. Tsai, and M. L. Kirby. 2008. PCB126 Exposure Disrupts ZebraFish Ventricular and Branchial but Not Early Neural Crest Development. Toxicological Sciences 106(1):193–205.

Gupta, R. C., editor. 2019. Biomarkers in Toxicology. Elsevier.

Hallare, A., K. Nagel, H.-R. Köhler, and R. Triebskorn. 2006. Comparative embryotoxicity and proteotoxicity of three carrier solvents to zebrafish (Danio rerio) embryos. Ecotoxicology and Environmental Safety 63(3):378–388.

Hamilton, P. B., I. G. Cowx, M. F. Oleksiak, A. M. Griffiths, M. Grahn, J. R. Stevens, G. R. Carvalho, E. Nicol, and C. R. Tyler. 2016. Population-level consequences for wild fish exposed to sublethal concentrations of chemicals - a critical review. Fish and Fisheries 17(3):545–566.

Handy, R. ., D. . Sims, A. Giles, H. . Campbell, and M. . Musonda. 1999. Metabolic trade-off between locomotion and detoxification for maintenance of blood chemistry and growth parameters by rainbow trout (Oncorhynchus mykiss) during chronic dietary exposure to copper. Aquatic Toxicology 47(1):23–41.

Hannenhalli, S., and K. H. Kaestner. 2009. The evolution of Fox genes and their role in development and disease. Nature Reviews Genetics 10(4):233–240.

Hartman, K. J., and S. B. Brandt. 1995. Predatory demand and impact of striped bass, bluefish, and weakfish in the Chesapeake Bay: applications of bioenergetics models. Canadian Journal of Fisheries and Aquatic Sciences 52(8):1667–1687.

Hazlerigg, C. R. E., C. Tyler, K. Lorenzen, J. Wheeler, and P. Thorbek. 2014. Population relevance of toxicant mediated changes in sex ratio in fish: An assessment using an individual-based zebrafish (Danio rerio) model. Page Ecological Modelling.

Heiden, T. K., R. J. Hutz, and M. J. Carvan. 2005. Accumulation, Tissue Distribution, and Maternal Transfer of Dietary 2,3,7,8,-Tetrachlorodibenzo-p-Dioxin: Impacts on Reproductive Success of Zebrafish. Toxicological Sciences 87(2):497–507.

Helmcke, K. J., and M. Aschner. 2012. Caenorhabditis elegans as a Predictive Model for Methylmercury-Induced Neurotoxicity. Pages 319–333 Methylmercury and Neurotoxicity. Springer US, Boston, MA.

Ho, N. Y., L. Yang, J. Legradi, O. Armant, M. Takamiya, S. Rastegar, and U. Strähle. 2013. Gene Responses in the Central Nervous System of Zebrafish Embryos Exposed to the Neurotoxicant Methyl Mercury. Environmental Science & Technology 47(7):3316–3325.

Hoffman, R. B., S. J. Boyd, R. J. von Baumgarten, and A. A. Baky. 1978. Effect of prehatching weightlessness on adult fish behavior in dynamic environments. Aviation, space, and environmental medicine 49(4):576–581. United States.

Hoffman, R. B., G. A. Salinas, and A. A. Baky. 1977. Behavioral analyses of killifish exposed to weightlessness in the Apollo-Soyuz test project. Aviation, space, and environmental medicine 48(8):712–717. United States.

Hooten, M., D. Johnson, B. McClintock, and J. Morales. 2017. Animal Movement. CRC Press, Boca Raton, FL.

Houde, E. D. 1969. Sustained Swimming Ability of Larvae of Walleye (Stizostedion vitreum vitreum) and Yellow Perch (Perca flavescens). Journal of the Fisheries Research Board of Canada 26(6):1647–1659.

Huang, S. S. Y., S. Noble, R. Godoy, M. Ekker, and H. M. Chan. 2016. Delayed effects of methylmercury on the mitochondria of dopaminergic neurons and developmental toxicity in zebrafish larvae (Danio rerio). Aquatic Toxicology 175:73–80.

Huang, W., D. C. Bencic, R. L. Flick, D. E. Nacci, B. W. Clark, L. Burkhard, T. Lahren, and A. D. Biales. 2019. Characterization of the Fundulus heteroclitus embryo transcriptional response and development of a gene expression-based fingerprint of exposure for the alternative flame retardant, TBPH (bis (2-ethylhexyl)-tetrabromophthalate). Environmental Pollution 247:696–705.

Huang, Y., R. Cartlidge, M. Walpitagama, J. Kaslin, O. Campana, and D. Wlodkowic. 2018. Unsuitable use of DMSO for assessing behavioral endpoints in aquatic model species. Science of The Total Environment 615:107–114.

Hunt, J., D. J. Hosken, and N. Wedell. 2019. Genes and Behaviour. John Wiley & Sons, Ltd, Chichester, UK.

Ingebretson, J. J., and M. A. Masino. 2013. Quantification of locomotor activity in larval zebrafish: considerations for the design of high-throughput behavioral studies. Frontiers in Neural Circuits 7.

Ivan, L. N., C. A. Murphy, M. J. Jones, M. J. Carvan, J. L. Albers, and N. Garcia-Reyero. 2022. Exploring the sublethal effects of toxicants on larval fish populations in the face of model uncertainty.

Jan, A., M. Azam, K. Siddiqui, A. Ali, I. Choi, and Q. Haq. 2015. Heavy Metals and Human Health: Mechanistic Insight into Toxicity and Counter Defense System of Antioxidants. International Journal of Molecular Sciences 16(12):29592–29630.

Johansson, C., A. F. Castoldi, N. Onishchenko, L. Manzo, M. Vahter, and S. Ceccatelli. 2007. Neurobehavioural and molecular changes induced by methylmercury exposure during development. Neurotoxicity Research 11(3–4):241–260.

Jones, S. ., L. . King, L. . Sappington, F. . Dwyer, M. Ellersieck, and D. . Buckler. 1998. Effects of carbaryl, permethrin, 4-nonylphenol, and copper on muscarinic cholinergic receptors in brain of surrogate and listed fish species. Comparative Biochemistry and Physiology Part C: Pharmacology, Toxicology and Endocrinology 120(3):405–414.

Jonsen, I. D., M. Basson, S. Bestley, M. V. Bravington, T. A. Patterson, M. W. Pedersen, R. Thomson, U. H. Thygesen, and S. J. Wotherspoon. 2013. State-space models for bio-loggers: A methodological road map. Deep Sea Research Part II: Topical Studies in Oceanography 88–89:34–46.

Jorgenson, Z. G., K. Buhl, S. E. Bartell, and H. L. Schoenfuss. 2015. Do Laboratory Species Protect Endangered Species? Interspecies Variation in Responses to 17β-Estradiol, a Model Endocrine Active Compound. Archives of Environmental Contamination and Toxicology 68(1):204–215.

Kalueff, A. V., D. J. Echevarria, S. Homechaudhuri, A. M. Stewart, A. D. Collier, A. A. Kaluyeva, S. Li, Y. Liu, P. Chen, J. Wang, L. Yang, A. Mitra, S. Pal, A. Chaudhuri, A. Roy, M. Biswas, D. Roy, A. Podder, M. K. Poudel, D. P. Katare, R. J. Mani, E. J. Kyzar, S. Gaikwad, M. Nguyen, and C. Song. 2016. Zebrafish neurobehavioral phenomics for aquatic neuropharmacology and toxicology research. Aquatic Toxicology 170:297–309.

Katoh, M., and M. Katoh. 2004. Human FOX gene family (Review). International Journal of Oncology.

Kaur, P., M. Aschner, and T. Syversen. 2012. Methylmercury Neurotoxicity: Why Are some Cells more Vulnerable than Others? Pages 241–258 Methylmercury and Neurotoxicity. Springer US, Boston, MA.

Kawamata, H., and G. Manfredi. 2017. Proteinopathies and OXPHOS dysfunction in neurodegenerative diseases. Journal of Cell Biology 216(12):3917–3929.

King-Heiden, T. C., V. Mehta, K. M. Xiong, K. A. Lanham, D. S. Antkiewicz, A. Ganser, W. Heideman, and R. E. Peterson. 2012. Reproductive and developmental toxicity of dioxin in fish. Molecular and Cellular Endocrinology 354(1):121–138.

Knapen, D., L. Vergauwen, D. L. Villeneuve, and G. T. Ankley. 2015. The potential of AOP networks for reproductive and developmental toxicity assay development. Reproductive Toxicology 56:52–55. Pergamon.

Kneib, R. 1993. Growth and mortality in successive cohorts of fish larvae within an estuarine nursery. Marine Ecology Progress Series 94:115–127.

Kneib, R. T., and J. H. Parker. 1991. Notes: Gross Conversion Efficiencies of Mummichog and Spotfin Killifish Larvae from a Georgia Salt Marsh. Transactions of the American Fisheries

Society 120(6):803–809.

Kodavanti, P. R., D. S. Shin, H. A. Tilson, and G. J. Harry. 1993. Comparative Effects of Two Polychlorinated Biphenyl Congeners on Calcium Homeostasis in Rat Cerebellar Granule Cells. Toxicology and Applied Pharmacology 123(1):97–106.

Korbas, M., T. C. MacDonald, I. J. Pickering, G. N. George, and P. H. Krone. 2012. Chemical Form Matters: Differential Accumulation of Mercury Following Inorganic and Organic Mercury Exposures in Zebrafish Larvae. ACS Chemical Biology 7(2):411–420.

Langie, S. A. S., G. Koppen, D. Desaulniers, F. Al-Mulla, R. Al-Temaimi, A. Amedei, A. Azqueta, W. H. Bisson, D. Brown, G. Brunborg, A. K. Charles, T. Chen, A. Colacci, F. Darroudi, S. Forte, L. Gonzalez, R. A. Hamid, L. E. Knudsen, L. Leyns, A. Lopez de Cerain Salsamendi, L. Memeo, C. Mondello, C. Mothersill, A.-K. Olsen, S. Pavanello, J. Raju, E. Rojas, R. Roy, E. Ryan, P. Ostrosky-Wegman, H. K. Salem, A. I. Scovassi, N. Singh, M. Vaccari, F. J. Van Schooten, M. Valverde, J. Woodrick, L. Zhang, N. van Larebeke, M. Kirsch-Volders, and A. R. Collins. 2015. Causes of genome instability: the effect of low dose chemical exposures in modern society. Carcinogenesis 36(Suppl 1):S61–S88.

Leonelli, S., and R. A. Ankeny. 2013. What makes a model organism? Endeavour 37(4):209–212.

Letcher, B. H., J. A. Rice, L. B. Crowder, and K. A. Rose. 1996. Variability in survival of larval fish: disentangling components with a generalized individual-based model. Canadian Journal of Fisheries and Aquatic Sciences 53(4):787–801.

Li, Y., J.-M. Lee, T.-S. Chon, Y. Liu, H. Kim, M.-J. Bae, and Y.-S. Park. 2013. Analysis of movement behavior of zebrafish (Danio rerio) under chemical stress using hidden Markov model. Modern Physics Letters B 27(02):1350014.

Little, E. E., and S. E. Finger. 1990. Swimming behavior as an indicator of sublethal toxicity in fish. Environmental Toxicology and Chemistry 9(1):13–19.

Liu, H., R. Gooneratne, X. Huang, R. Lai, J. Wei, and W. Wang. 2015. A rapid in vivo zebrafish model to elucidate oxidative stress-mediated PCB126-induced apoptosis and developmental toxicity. Free Radical Biology and Medicine 84:91–102.

Liu, H., F.-H. Nie, H.-Y. Lin, Y. Ma, X.-H. Ju, J.-J. Chen, and R. Gooneratne. 2014. Developmental toxicity, oxidative stress, and related gene expression induced by dioxin-like PCB 126 in zebrafish (Danio rerio). Environmental Toxicology 31(3):295–303. Wiley-Blackwell.

Liu, Q., R. H. Klingler, B. Wimpee, M. Dellinger, T. King-Heiden, J. Grzybowski, S. L. Gerstenberger, D. N. Weber, and M. J. Carvan. 2016. Maternal methylmercury from a wild-caught walleye diet induces developmental abnormalities in zebrafish. Reproductive Toxicology 65:272–282.

Liu, Y., S.-H. Lee, and T.-S. Chon. 2011. Analysis of behavioral changes of zebrafish (Danio rerio) in response to formaldehyde using Self-organizing map and a hidden Markov model. Ecological Modelling 222(14):2191–2201.

Lunn, D., D. Spiegelhalter, A. Thomas, and N. Best. 2009. The BUGS project: Evolution,

critique and future directions. Statistics in Medicine 28(25):3049–3067.

Lunsford, E. T., D. A. Skandalis, and J. C. Liao. 2019. Efferent modulation of spontaneous lateral line activity during and after zebrafish motor commands. Journal of Neurophysiology 122(6):2438–2448.

Luo, W., M. S. Friedman, K. Shedden, K. D. Hankenson, and P. J. Woolf. 2009. GAGE: generally applicable gene set enrichment for pathway analysis. BMC Bioinformatics 10(1):161.

Lushchak, V. I. 2014. Dissection of the Hormetic Curve: Analysis of Components and Mechanisms. Dose-Response 12(3):466–479.

MacPhail, R. C., J. Brooks, D. L. Hunter, B. Padnos, T. D. Irons, and S. Padilla. 2009. Locomotion in larval zebrafish: Influence of time of day, lighting and ethanol. NeuroToxicology 30(1):52–58. Elsevier.

Madon, S. P., G. D. Williams, J. M. West, and J. B. Zedler. 2001. The importance of marsh access to growth of the California killifish, Fundulus parvipinnis, evaluated through bioenergetics modeling. Ecological Modelling 136(2–3):149–165.

Marques, J. C., M. Li, D. Schaak, D. N. Robson, and J. M. Li. 2020. Internal state dynamics shape brainwide activity and foraging behaviour. Nature 577(7789):239–243.

Marteinsdottir, G., and K. W. Able. 1992. Influence of egg size on embryos and larvae of Fundulus Heteroclitus (L.). Journal of Fish Biology 41:883–896.

MATLAB. 2017. MATLAB 2017b version 9.3.0.713579. The MathWorks, Inc., Natick, Massausetts, United States.

Mattson, M. P. 2008. Hormesis defined. Ageing Research Reviews 7(1):1–7.

McBride, M. T. 2018. The Application of Omics Data to the Development of AOPs. Pages 177–198 *in* N. Garcia-Reyero and C. A. Murphy, editors. A Systems Biology Approach to Advancing Adverse Outcome Pathways for Risk Assessment. Springer International Publishing, Cham.

McCarty, L., P. Landrum, S. Luoma, J. Meador, A. Merten, B. Shephard, and A. van Wezel. 2011. Advancing environmental toxicology through chemical dosimetry: External exposures versus tissue residues. Integrated Environmental Assessment and Management 7(1):7–27.

McClintock, B. T., D. S. Johnson, M. B. Hooten, J. M. Ver Hoef, and J. M. Morales. 2014. When to be discrete: The importance of time formulation in understanding animal movement. Movement Ecology 2(1):21.

McKellar, A. E., R. Langrock, J. R. Walters, and D. C. Kesler. 2015. Using mixed hidden Markov models to examine behavioral states in a cooperatively breeding bird. Behavioral Ecology 26(1):148–157.

McPherson, A. D., J. P. Barrios, S. J. Luks-Morgan, J. P. Manfredi, J. L. Bonkowsky, A. D. Douglass, and R. I. Dorsky. 2016. Motor Behavior Mediated by Continuously Generated

Dopaminergic Neurons in the Zebrafish Hypothalamus Recovers after Cell Ablation. Current Biology 26(2):263–269.

Melvin, S. D., and S. P. Wilson. 2013. The utility of behavioral studies for aquatic toxicology testing: A meta-analysis. Chemosphere 93(10):2217–2223.

Michelot, T., R. Langrock, and T. A. Patterson. 2016. moveHMM: an <scp>R</scp> package for the statistical modelling of animal movement data using hidden Markov models. Methods in Ecology and Evolution 7(11):1308–1315.

Mora-Zamorano, F. X., R. Klingler, N. Basu, J. Head, C. A. Murphy, F. P. Binkowski, J. K. Larson, and M. J. Carvan. 2017. Developmental Methylmercury Exposure Affects Swimming Behavior and Foraging Efficiency of Yellow Perch (Perca flavescens) Larvae. ACS Omega 2(8):4870–4877.

Mora-Zamorano, F. X., R. H. Klingler, C. A. Murphy, N. Basu, J. Head, and M. J. Carvan. 2016a. Parental Whole Life Cycle Exposure to Dietary Methylmercury in Zebrafish (Danio rerio) Affects the Behavior of Offspring. Environmental Science & Technology 50(9):4808–4816.

Mora-Zamorano, F. X., K. R. Svoboda, and M. J. Carvan. 2016b. The Nicotine-Evoked Locomotor Response: A Behavioral Paradigm for Toxicity Screening in Zebrafish (Danio rerio) Embryos and Eleutheroembryos Exposed to Methylmercury. PLOS ONE 11(4):e0154570.

Morán, P., L. Cal, A. Cobelo-García, C. Almécija, P. Caballero, and C. Garcia de Leaniz. 2018. Historical legacies of river pollution reconstructed from fish scales. Environmental Pollution 234:253–259.

Murphy, C. A., S. Bhavsar, and N. Gandhi. 2012. Contaminants in Great Lakes Fish: Historic, Current, and Emerging Concerns. Pages 203–258 in W. W. Taylor, editor. Great Lakes Fisheries Policy and Management: A Binational Perspective. Michigan State University Press, Project MUSE, East Lansing.

Murphy, C. A., K. A. Rose, M. del C. Alvarez, and L. A. Fuiman. 2008. Modeling larval fish behavior: Scaling the sublethal effects of methylmercury to population-relevant endpoints. Aquatic Toxicology 86(4):470–484. Elsevier.

Murphy, D. D., P. S. Weiland, and K. W. Cummins. 2011. A Critical Assessment of the Use of Surrogate Species in Conservation Planning in the Sacramento-San Joaquin Delta, California (U.S.A.). Conservation Biology 25(5):873–878.

Nabi, S. 2014. Toxic Effects of Mercury. Springer India, New Delhi.

Nacci, D., L. Coiro, D. Champlin, S. Jayaraman, R. McKinney, T. R. Gleason, W. R. J. Munns, J. L. Specker, and K. R. Cooper. 1999. Adaptations of Wild Populations of the Estuarine Fish Fundulus Heteroclitus to Persistent Environmental Contaminants. Marine Biology 134(1):9–17.

Nacci, D. E., D. Champlin, and S. Jayaraman. 2010. Adaptation of the Estuarine Fish Fundulus heteroclitus (Atlantic Killifish) to Polychlorinated Biphenyls (PCBs). Estuaries and Coasts 33(4):853–864.

Nacci, D., D. Proestou, D. Champlin, J. Martinson, and E. R. Waits. 2016. Genetic basis for rapidly evolved tolerance in the wild: adaptation to toxic pollutants by an estuarine fish species. Molecular Ecology 25(21):5467–5482.

Nault, R., S. Al-Hameedi, and T. W. Moon. 2012. Effects of polychlorinated biphenyls on whole animal energy mobilization and hepatic cellular respiration in rainbow trout, Oncorhynchus mykiss. Chemosphere 87(9):1057–1062.

Ndountse, L. T., and H. M. Chan. 2009. Role of N-methyl-D-aspartate receptors in polychlorinated biphenyl mediated neurotoxicity. Toxicology Letters 184(1):50–55. Elsevier.

Nebert, D. W., and V. Vasiliou. 2004. Analysis of the glutathione S-transferase (GST) gene family. Human Genomics 1(6):460.

Nguyen, T. Van, Y. Liu, I.-H. Jung, T.-S. Chon, and S.-H. Lee. 2011. Unraveling Markov processes in movement patterns of indicator species in response to chemical stressors. Modern Physics Letters B 25(12n13):1143–1149.

Nogara, P. A., C. S. Oliveira, G. L. Schmitz, P. C. Piquini, M. Farina, M. Aschner, and J. B. T. Rocha. 2019. Methylmercury's chemistry: From the environment to the mammalian brain. Biochimica et Biophysica Acta (BBA) - General Subjects 1863(12):129284.

Nogueira, L. S., C. P. Vasconcelos, J. R. Plaça, G. P. Mitre, L. O. Bittencourt, M. S. da S. Kataoka, E. H. C. de Oliveira, and R. R. Lima. 2021. Non-Lethal Concentration of MeHg Causes Marked Responses in the DNA Repair, Integrity, and Replication Pathways in the Exposed Human Salivary Gland Cell Line. Frontiers in Pharmacology 12.

Okey, A. B. 2007. An Aryl Hydrocarbon Receptor Odyssey to the Shores of Toxicology: The Deichmann Lecture, International Congress of Toxicology-XI. Toxicological Sciences 98(1):5–38.

Oleksiak, M. F., S. I. Karchner, M. J. Jenny, D. G. Franks, D. B. Mark Welch, and M. E. Hahn. 2011. Transcriptomic assessment of resistance to effects of an aryl hydrocarbon receptor (AHR) agonist in embryos of Atlantic killifish (Fundulus heteroclitus) from a marine Superfund site. BMC Genomics 12(1):263.

Onishchenko, N., S. Spulber, and S. Ceccatelli. 2012. Behavioural Effects of Exposure to Methylmercury During Early Development.

Ososkov, I., and J. S. Weis. 1996. Development of Social Behavior in Larval Mummichogs after Embryonic Exposure to Methylmercury. Transactions of the American Fisheries Society 125(6):983–987.

Oziolor, E. M., J. N. Apell, Z. C. Winfield, J. A. Back, S. Usenko, and C. W. Matson. 2018. Polychlorinated biphenyl (PCB) contamination in Galveston Bay, Texas: Comparing concentrations and profiles in sediments, passive samplers, and fish. Environmental Pollution 236:609–618.

Pacyna, J. M., O. Travnikov, F. De Simone, I. M. Hedgecock, K. Sundseth, E. G. Pacyna, F. Steenhuisen, N. Pirrone, J. Munthe, and K. Kindbom. 2016. Current and future levels of mercury atmospheric pollution on a global scale. Atmospheric Chemistry and Physics

16(19):12495–12511.

Palmqvist, A., H. Selck, L. J. Rasmussen, and V. E. Forbes. 2003. Biotransformation and genotoxicity of fluoranthene in the deposit feeding polychaete Capitella sp. Environmental Toxicology and Chemistry 22(12):2977.

Di Paolo, C., K. J. Groh, M. Zennegg, E. L. M. Vermeirssen, A. J. Murk, R. I. L. Eggen, H. Hollert, I. Werner, and K. Schirmer. 2015. Early life exposure to PCB126 results in delayed mortality and growth impairment in the zebrafish larvae. Aquatic Toxicology 169:168–178. Elsevier.

Patro, R., G. Duggal, M. I. Love, R. A. Irizarry, and C. Kingsford. 2017. Salmon provides fast and bias-aware quantification of transcript expression. Nature Methods 14(4):417–419.

Patzelt, E. H., Z. Kurth-Nelson, K. O. Lim, and A. W. MacDonald. 2014. Excessive state switching underlies reversal learning deficits in cocaine users. Drug and Alcohol Dependence 134:211–217.

Paula, D. P., D. A. Andow, A. Bellinati, R. V. Timbó, L. M. Souza, C. S. S. Pires, and E. R. Sujii. 2016. Limitations in dose–response and surrogate species methodologies for risk assessment of Cry toxins on arthropod natural enemies. Ecotoxicology 25(3):601–607.

Péan, S., T. Daouk, C. Vignet, L. Lyphout, D. Leguay, V. Loizeau, M.-L. Bégout, and X. Cousin. 2013. Long-term dietary-exposure to non-coplanar PCBs induces behavioral disruptions in adult zebrafish and their offspring. Neurotoxicology and Teratology 39:45–56.

Pereira, P., M. Korbas, V. Pereira, T. Cappello, M. Maisano, J. Canário, A. Almeida, and M. Pacheco. 2019. A multidimensional concept for mercury neuronal and sensory toxicity in fish - From toxicokinetics and biochemistry to morphometry and behavior. Biochimica et Biophysica Acta (BBA) - General Subjects 1863(12):129298.

Piedrafita, B., S. Erceg, O. Cauli, and V. Felipo. 2008a. Developmental exposure to polychlorinated biphenyls or methylmercury, but not to its combination, impairs the glutamate–nitric oxide–cyclic GMP pathway and learning in 3-month-old rats. Neuroscience 154(4):1408–1416.

Piedrafita, B., S. Erceg, O. Cauli, P. Monfort, and V. Felipo. 2008b. Developmental exposure to polychlorinated biphenyls PCB153 or PCB126 impairs learning ability in young but not in adult rats. European Journal of Neuroscience 27(1):177–182.

Plummer, M., N. Best, K. Cowles, and K. Vines. 2005. CODA: Convergence Diagnosis and Output Analysis for MCMC. R News 6:7–11.

R Core Team. 2019. R: A language and environment for statistical computing. R version 4.0.4, x86_64-w64-mingw32/x64 (64-bit), Vienna, Austria.

Rearick, D. C., J. Ward, P. Venturelli, and H. Schoenfuss. 2018. Environmental oestrogens cause predation-induced population decline in a freshwater fish. Royal Society Open Science 5(10):181065.

Reid, N. M., C. E. Jackson, D. Gilbert, P. Minx, M. J. Montague, T. H. Hampton, L. W. Helfrich,

B. L. King, D. E. Nacci, N. Aluru, S. I. Karchner, J. K. Colbourne, M. E. Hahn, J. R. Shaw, M. F. Oleksiak, D. L. Crawford, W. C. Warren, and A. Whitehead. 2017. The Landscape of Extreme Genomic Variation in the Highly Adaptable Atlantic Killifish. Genome Biology and Evolution 9(3):659–676.

Reif, D. M., L. Truong, D. Mandrell, S. Marvel, G. Zhang, and R. L. Tanguay. 2016. High-throughput characterization of chemical-associated embryonic behavioral changes predicts teratogenic outcomes. Archives of Toxicology 90(6):1459–1470.

Reitzel, A. M., S. I. Karchner, D. G. Franks, B. R. Evans, D. Nacci, D. Champlin, V. M. Vieira, and M. E. Hahn. 2014. Genetic variation at aryl hydrocarbon receptor (AHR) loci in populations of Atlantic killifish (Fundulus heteroclitus) inhabiting polluted and reference habitats. BMC Evolutionary Biology 14(1):6.

Rice, D. C. 1999. Effect of Exposure to 3,3′,4,4′,5-Pentachlorobiphenyl (PCB 126) Throughout Gestation and Lactation on Development and Spatial Delayed Alternation Performance in Rats. Neurotoxicology and Teratology 21(1):59–69.

Rice, D. C., and S. Hayward. 1998. Lack of Effect of 3,3′4,4′,5-Pentachlorobiphenyl (PCB 126) Throughout Gestation and Lactation on Multiple Fixed Interval–Fixed Ratio and DRL Performance in Rats. Neurotoxicology and Teratology 20(6):645–650.

Rice, D. C., and S. Hayward. 1999. Effects of Exposure to 3,3′,4,4′,5-Pentachlorobiphenyl (PCB 126) Throughout Gestation and Lactation on Behavior (Concurrent Random Interval–Random Interval and Progressive Ratio Performance) in Rats. Neurotoxicology and Teratology 21(6):679–687.

Rigaud, C., C. M. Couillard, J. Pellerin, B. Légaré, P. Gonzalez, and P. V Hodson. 2013. Relative potency of PCB126 to TCDD for sublethal embryotoxicity in the mummichog (Fundulus heteroclitus). Aquatic toxicology (Amsterdam, Netherlands) 128–129:203–214. Institut des Sciences de la Mer, Université du Québec à Rimouski, Rimouski, Québec, Canada.

Rohatgi, A. 2019. WebPlotDigitizer. https://automeris.io/WebPlotDigitizer.

Rose, K., C. Murphy, S. Diamond, L. A. Fuiman, and P. Thomas. 2003. Using Nested Models and Laboratory Data for Predicting Population Effects of Contaminants on Fish: A Step Toward a Bottom-Up Approach for Establishing Causality in Field Studies. Pages 231–257 Human and Ecological Risk Assessment.

Roussel, Y., M. Paradis, S. F. Gaudreau, B. W. Lindsey, and T. V. Bui. 2020. Spatiotemporal Transition in the Role of Synaptic Inhibition to the Tail Beat Rhythm of Developing Larval Zebrafish. eneuro 7(1):ENEURO.0508-18.2020.

Samson, J. C., R. Goodridge, F. Olobatuyi, and J. S. Weis. 2001. Delayed effects of embryonic exposure of zebrafish (Daniorerio) to methylmercury (MeHg). Aquatic Toxicology 51(4):369–376. Elsevier.

Sandheinrich, M. B., and G. J. Atchison. 1990. Sublethal toxicant effects on fish foraging behavior: Empirical vs. mechanistic approaches. Environmental Toxicology and Chemistry 9(1):107–119.

Sandheinrich, M., and J. Wiener. 2011. Methylmercury in freshwater fish: recent advances in assessing toxicity of environmentally relevant exposures. Environmental contaminants in biota: interpreting tissue concentrations 2:169–190.

Sastry, K. V., and K. Sharma. 1980. Mercury induced haematological and biochemical anomalies in Ophiocephalus (Channa) punctatus. Toxicology Letters 5(3–4):245–249.

Scott, G. R., and K. A. Sloman. 2004. The effects of environmental pollutants on complex fish behaviour: integrating behavioural and physiological indicators of toxicity. Aquatic Toxicology 68(4):369–392.

Seegal, R. F., K. O. Brosch, and R. J. Okoniewski. 2005. Coplanar PCB Congeners Increase Uterine Weight and Frontal Cortical Dopamine in the Developing Rat: Implications for Developmental Neurotoxicity. Toxicological Sciences 86(1):125–131.

Seim, R. F., D. A. Glinski, C. M. Lavelle, J. A. Awkerman, B. L. Hemmer, P. Harris, S. Raimondo, M. N. Snyder, B. W. Acrey, S. T. Purucker, D. K. MacMillan, A. A. Brennan, and W. M. Henderson. 2022. Using metabolomic profiling to inform use of surrogate species in ecological risk assessment practices. Comparative Biochemistry and Physiology Part D: Genomics and Proteomics 41:100947.

Selderslaghs, I. W. T., R. Blust, and H. E. Witters. 2012. Feasibility study of the zebrafish assay as an alternative method to screen for developmental toxicity and embryotoxicity using a training set of 27 compounds. Reproductive Toxicology 33(2):142–154.

Severi, K. E., U. L. Böhm, and C. Wyart. 2018. Investigation of hindbrain activity during active locomotion reveals inhibitory neurons involved in sensorimotor processing. Scientific Reports 8(1):13615.

Shankar, P., S. Dasgupta, M. E. Hahn, and R. L. Tanguay. 2020. A Review of the Functional Roles of the Zebrafish Aryl Hydrocarbon Receptors. Toxicological Sciences 178(2):215–238.

Sharp, J. R., and J. M. Neff. 1982. The toxicity of mercuric chloride and methylmercuric chloride to Fundulus heteroclitus embryos in relation to exposure conditions. Environmental Biology of Fishes 7(3):277–284.

Smith, G. M., and J. S. Weis. 1997. Predator-prey relationships in mummichogs (Fundulus heteroclitus): effects of living in a polluted environment. J. Exp. Mar. Biol. Ecol. 209:75–87.

Smith, K. J., G. L. Taghon, and K. W. Able. 2002. Trophic Linkages in Marshes: Ontogenetic Changes in Diet for Young-of-the-Year Mummichog, Fundulus Heteroclitus. Pages 121–237 in M. P. Weinstein and D. A. Kreeger, editors. Concepts and Controversies in Tidal Marsh Ecology. Kluwer Academic Publishers, Dordrecht.

Soneson, C., M. I. Love, and M. D. Robinson. 2015. Differential analyses for RNA-seq: transcript-level estimates improve gene-level inferences. F1000Research 4:1521.

Spitsbergen, J. M., J. M. Kleeman, and R. E. Peterson. 1988. 2,3,7,8-Tetrachlorodibenzo- p - dioxin toxicity in yellow perch (Perca flavescens). Journal of Toxicology and Environmental Health 23(3):359–383.

Stewart, D. R., Z. E. Underwood, F. J. Rahel, and A. W. Walters. 2018. The effectiveness of surrogate taxa to conserve freshwater biodiversity. Conservation Biology 32(1):183–194.

Stinckens, E., L. Vergauwen, G. T. Ankley, R. Blust, V. M. Darras, D. L. Villeneuve, H. Witters, D. C. Volz, and D. Knapen. 2018. An AOP-based alternative testing strategy to predict the impact of thyroid hormone disruption on swim bladder inflation in zebrafish. Aquatic Toxicology 200:1–12.

Sturtz, S., U. Ligges, and A. Gelman. 2005. R2WinBUGS : A Package for Running WinBUGS from R. Journal of Statistical Software 12(3).

Toomey, B. H., S. Bello, M. E. Hahn, S. Cantrell, P. Wright, D. E. Tillit, and R. T. Di Giulio. 2001. 2,3,7,8-Tetrachlorodibenzodibenzo-p-dioxin induces apoptotic cell death and cytochrome P4501A expression in developing Fundulus heteroclitus embryos. Aquatic Toxicology 53:127–138.

Valiela, I., J. E. Wright, J. M. Teal, and S. B. Volkmann. 1977. Growth, production and energy transformations in the salt-marsh killifish Fundulus heteroclitus. Marine Biology 40(2):135–144.

Vargas, R., I. þ. Jóhannesdóttir, B. Sigurgeirsson, H. Þorsteinsson, and K. Æ. Karlsson. 2011. The zebrafish brain in research and teaching: a simple in vivo and in vitro model for the study of spontaneous neural activity. Advances in Physiology Education 35(2):188–196.

Van Veld, P. A., and D. E. Nacci. 2008. Toxicity resistance. Pages 597–644 The Toxicology of Fishes. Taylor and Francis, Boca Raton, FL.

Vélez-Espino, L. A., M. G. Fox, and R. L. McLaughlin. 2006. Characterization of elasticity patterns of North American freshwater fishes. Canadian Journal of Fisheries and Aquatic Sciences 63(9):2050–2066.

Venables, W. N., and B. D. Ripley. 2002. Modern Applied Statistics with SFourth. Springer New York.

Villeneuve, D. L., K. Coady, B. I. Escher, E. Mihaich, C. A. Murphy, T. Schlekat, and N. Garcia-Reyero. 2018. High-throughput screening and Environmental Risk Assessment: State of the science and emerging applications. Environmental Toxicology and Chemistry.

Villeneuve, D. L., D. Crump, N. Garcia-Reyero, M. Hecker, T. H. Hutchinson, C. A. LaLone, B. Landesmann, T. Lettieri, S. Munn, M. Nepelska, M. A. Ottinger, L. Vergauwen, and M. Whelan. 2014a. Adverse Outcome Pathway Development II: Best Practices. Toxicological Sciences 142(2):321–330. Oxford University Press.

Villeneuve, D. L., D. Crump, N. Garcia-Reyero, M. Hecker, T. H. Hutchinson, C. A. LaLone, B. Landesmann, T. Lettieri, S. Munn, M. Nepelska, M. A. Ottinger, L. Vergauwen, and M. Whelan. 2014b. Adverse Outcome Pathway (AOP) Development I: Strategies and Principles. Toxicological Sciences 142(2):312–320. Oxford University Press.

Villeneuve, D. L., and N. Garcia-Reyero. 2010. Vision & strategy: Predictive ecotoxicology in the 21st century. Environmental Toxicology and Chemistry 30(1):1–8. Wiley-Blackwell.

Visha, A., N. Gandhi, S. P. Bhavsar, and G. B. Arhonditsis. 2018. Assessing mercury

contamination patterns of fish communities in the Laurentian Great Lakes: A Bayesian perspective. Environmental Pollution 243:777–789.

Vitalone, A., A. Catalani, V. Chiodi, C. Cinque, V. Fattori, M. Goldoni, P. Matteucci, D. Poli, A. R. Zuena, and L. G. Costa. 2008. Neurobehavioral assessment of rats exposed to low doses of PCB126 and methyl mercury during development. Environmental Toxicology and Pharmacology 25(1):103–113.

Vitalone, A., A. Catalani, C. Cinque, V. Fattori, P. Matteucci, A. R. Zuena, and L. G. Costa. 2010. Long-term effects of developmental exposure to low doses of PCB 126 and methylmercury. Toxicology Letters 197(1):38–45.

Walton, A., M. J. Sheehan, and A. L. Toth. 2020. Going wild for functional genomics: RNA interference as a tool to study gene-behavior associations in diverse species and ecological contexts. Hormones and Behavior 124:104774.

Wang, Z., M. Snyder, J. E. Kenison, K. Yang, B. Lara, E. Lydell, K. Bennani, O. Novikov, A. Federico, S. Monti, and D. H. Sherr. 2020. How the AHR Became Important in Cancer: The Role of Chronically Active AHR in Cancer Aggression. International Journal of Molecular Sciences 22(1):387.

Weber, D. N., R. H. Klingler, and M. J. Carvan. 2012. Zebrafish as a Model for Methylmercury Neurotoxicity. Pages 335–355 in S. Ceccatelli and M. Aschner, editors. Methylmercury and Neurotoxicity. Springer US, Boston, MA.

Weir, P. A., and C. H. Hine. 1970. Effects of Various Metals on Behavior of Conditioned Goldfish. Archives of Environmental Health: An International Journal 20(1):45–51.

Weis, J. 2014. Delayed Behavioral Effects of Early Life Toxicant Exposures in Aquatic Biota. Toxics 2(2):165–187.

Weis, J. S., and A. Candelmo. 2012. Pollutants and fish predator/prey behavior: A review of laboratory and field approaches. Current Zoology 58(1):9–20.

Weis, J. S., and P. Weis. 1995a. Effects of embryonic exposure to methylmercury on larval prey-capture ability in the mummichog, fundulus heteroclitus. Environmental Toxicology and Chemistry 14(1):153–156.

Weis, J. S., and P. Weis. 1995b. Swimming performance and predator avoidance by mummichog (Fundulus heteroclitus) larvae after embryonic or larval exposure to methylmercury. Canadian Journal of Fisheries and Aquatic Sciences 52(10):2168–2173. NRC Research Press.

Weis, J. S., P. Weis, M. Heber, and S. Vaidya. 1981. Methylmercury tolerance of killifish (Fundulus heteroclitus) embryos from a polluted vs non-polluted environment. Marine Biology 65(3):283–287.

Weiss, B., S. Stern, E. Cernichiari, and R. Gelein. 2005. Methylmercury Contamination of Laboratory Animal Diets. Environmental Health Perspectives 113(9):1120–1122.

Wentz, D. A., M. E. Brigham, L. C. Chasar, M. A. Lutz, and D. P. Krabbenhoft. 2014. Mercury in the Nation's streams - levels, trends and implications.

Westerlund, L., K. Billsson, P. L. Andersson, M. Tysklind, and P.-E. Olsson. 2000. Early life-stage mortality in zebrafish (Danio rerio) following maternal exposure to polychlorinated biphenyls and estrogen. Environmental Toxicology and Chemistry 19(6):1582–1588.

Whitehead, A., W. Pilcher, D. Champlin, and D. Nacci. 2012. Common mechanism underlies repeated evolution of extreme pollution tolerance. Proceedings of the Royal Society B: Biological Sciences 279(1728):427–433.

Whitehead, A., D. A. Triant, D. Champlin, and D. Nacci. 2010. Comparative transcriptomics implicates mechanisms of evolved pollution tolerance in a killifish population. Molecular Ecology 19(23):5186–5203.

Wiener, J. G., M. B. Sandheinrich, S. P. Bhavsar, J. R. Bohr, D. C. Evers, B. A. Monson, and C. S. Schrank. 2012. Toxicological significance of mercury in yellow perch in the Laurentian Great Lakes region. Environmental Pollution 161:350–357.

Xu, H., C. Li, Y. Li, G. H. B. Ng, C. Liu, X. Zhang, and Z. Gong. 2015. Generation of Tg(cyp1a:gfp) Transgenic Zebrafish for Development of a Convenient and Sensitive In Vivo Assay for Aryl Hydrocarbon Receptor Activity. Marine Biotechnology 17(6):831–840.

Xu, X., D. Weber, M. J. Carvan, R. Coppens, C. Lamb, S. Goetz, and L. A. Schaefer. 2012. Comparison of neurobehavioral effects of methylmercury exposure in older and younger adult zebrafish (Danio rerio). NeuroToxicology 33(5):1212–1218.

Yang, L., Y. Zhang, F. Wang, Z. Luo, S. Guo, and U. Strähle. 2020. Toxicity of mercury: Molecular evidence. Chemosphere 245:125586.

Ye, X., and N. S. Fisher. 2020. Minor effects of dietary methylmercury on growth and reproduction of the sheepshead minnow Cyprinodon variegatus and toxicity to their offspring. Environmental Pollution 266:115226.

Zhang, W., R. M. Sargis, P. A. Volden, C. M. Carmean, X. J. Sun, and M. J. Brady. 2012. PCB 126 and Other Dioxin-Like PCBs Specifically Suppress Hepatic PEPCK Expression via the Aryl Hydrocarbon Receptor. PLoS ONE 7(5):e37103.

Zhang, X. J., H. W. Qin, L. M. Su, W. C. Qin, M. Y. Zou, L. X. Sheng, Y. H. Zhao, and M. H. Abraham. 2010. Interspecies correlations of toxicity to eight aquatic organisms: Theoretical considerations. Science of The Total Environment 408(20):4549–4555.

Zhou, R. Scali, J. S. Weis, T. 2001. Effects of Methylmercury on Ontogeny of Prey Capture Ability and Growth in Three Populations of Larval Fundulus heteroclitus. Archives of Environmental Contamination and Toxicology 41(1):47–54.

Zhou, T., and J. . Weis. 1998. Swimming behavior and predator avoidance in three populations of Fundulus heteroclitus larvae after embryonic and/or larval exposure to methylmercury. Aquatic Toxicology 43(2–3):131–148.

Zolkos, S., A. V. Zhulidov, T. Y. Gurtovaya, V. V. Gordeev, S. Berdnikov, N. Pavlova, E. A. Kalko, Y. A. Kuklina, D. A. Zhulidov, L. S. Kosmenko, A. I. Shiklomanov, A. Suslova, B. M. Geyman, C. P. Thackray, E. M. Sunderland, S. E. Tank, J. W. McClelland, R. G. M. Spencer, D. P. Krabbenhoft, R. Robarts, and R. M. Holmes. 2022. Multidecadal declines in

particulate mercury and sediment export from Russian rivers in the pan-Arctic basin. Proceedings of the National Academy of Sciences 119(14).

Zucchini, W., I. L. MacDonald, and R. Langrock. 2017. Hidden Markov Models for Time Series. Page Journal of Time Series Analysis. Chapman and Hall/CRC, Second edition / Walter Zucchini, Iain L. MacDonald, and Roland Langrock. | Boca Raton : Taylor & Francis, 2016. | Series: Monographs on statistics and applied probability ; 150 | "A CRC title."

APPENDIX I

Chapter 2 Supplementary Materials

Table S2.1. List of included research studies and values collected from them used in the analysis.

Submitted table as a sheet in an Excel file.

APPENDIX II

Chapter 3 Supplementary Materials

Fish Husbandry

To improve survival, egg masses were transferred into 9-L flow though fish tanks and secured to polyethylene mesh (which was wedged diagonally into the tank) using 2" zip ties. Tanks were supplied with continuous flow-through dechlorinated water using adjustable flow misting hoses (Orbit Drip Master Adjustable Flow Flex-Mist Sprayer #66190). Egg masses from each parent and treatment group were randomly assigned into three replicate tanks for the remainder of the experiment. As described by Mora-Zamorano et al. (2017), embryos started at 10°C with a 14 hour light period and water temperature was increased by 1°C every second day until 20°C was reached. At 12 dpf, hatching was assisted by vigorously pipetting eggs using a 50 mL pipette and chorion debris and dead embryos were removed from each tank. Following hatch, larvae were fed 3-4 times daily with a variety of live rotifers supplemented with Golden Pearl 50-100μm Reef and Larval Diet (Brine Shrimp Direct) and 24-h hatched *Artemia*. At 25dph, larvae were transferred to 3-L static tanks to allow easier access to fish for behavior studies. Tanks were maintained at 20°C with daily water changes and fed as described for the remainder of the experiment. A separate set of fish were used for each behavior assay, so no residual effects would occur between assays.

Bayesian Treatment Testing

Model Description

For each behavioral endpoint we conducted a series of preliminary and final tests to determine whether there were differences between chemical dose treatments. The model used for all behavior endpoints contained two main effect factors, chemical dose treatment and year, and the interaction of these. The model also contained a random effect of batch due to the nested

structure of data collection where assays were conducted in batches of 10 larvae per petri dish. The Bayesian model used in this study was

$$Behavior\ Endpoint_{ijkl}$$

$$= \alpha + \beta_j * year_j + \delta_k * treatment_k + \gamma_{jk} * year:treatment_{jk}$$

$$+ \omega_{jl} * batch_{jl(i)} + \varepsilon_{ijkl}$$

where $Behavior\ Endpoint_{ijkl}$ is the behavioral response metric on the ith individual, jth year, kth treatment and lth batch; α is the intercept, β_j is the year coefficient with a $Normal(0, \sigma_\beta^2)$ distribution, δ_k is the treatment coefficient with a $Normal(0, \sigma_\delta^2)$ distribution, ω_{jl} is the year specific batch coefficient, and ε_{ijkl} is the residual error with a $Normal(0, \sigma_\varepsilon^2)$ distribution. Treatment, year:treatment and batch are indicator variables containing 1 if the observation belongs to the corresponding factor category and 0 otherwise. The assumption of constant variance between the main effects was rarely satisfied, so a non-constant variance model was used for all tests. We assumed the $Behavior\ Endpoint_{ijkl}$ could be distributed using one of two distributions. The normal distribution model (Table S3.6) assumes the overall behavior response is distributed as a $Normal(0, \sigma_\beta^2)$ distribution, with variance $\sigma_\beta^2 \sim power(\sigma_\beta, -2)$; where the standard deviation $\sigma_\beta \sim uniform(a_j, b_j)$. In addition the year specific batch effect is distributed as a $Normal(0, \sigma_\omega^2)$ distribution, where $\sigma_\omega^2 \sim uniform(a_{jl}, b_{jl})$. The Student's t distribution model (Table S3.7) assumes the overall behavior response is disturbed as a $t(0, \tau_j, df)$ distribution, with variance $\tau_j \sim I - Gamma(c_j, d_j)$ and degrees of freedom $df \sim uniform(e, f)$. In addition the year specific batch effect is distributed as a $t(0, \tau_{jl}, df_l)$ distribution, where $\tau_{jl} \sim I - Gamma(c_{jl}, d_{jl})$ and degrees of freedom $df_l \sim uniform(e_l, f_l)$.

The use of two possible distributions was necessary due to the behavior endpoints such as total distance traveled or fish length that were so highly right skewed that even Box Cox transformations were not successful in normalizing the data (see Table S3.5 for final transformation and model used for each behavior endpoint).

Priors were needed for the α, year, treatment, year:treatment and batch effects. For the both models, we used vague, flat priors for α, year, treatment and year:treatment effects and assumed a normal distribution with a mean of 0 and standard deviation of 1.0×10^6 (i.e. precision of 1.0×10^{-6}). For the normal distribution model, the prior for σ^2 was flat and vague as well, assuming a uniform distribution with a minimum of 0.01 (a_j or a_{jl}) and maximum (b_j or b_{jl}) of 100. For the Student's t distribution model we again used vague flat priors, where τ_j assumed an inverse scaled chi-squared distribution (i.e. I-gamma) with mean $c_j = 0.0001$ and standard deviation $d_j = 10,000$ (i.e. precision of 1.0×10^{-4}); τ_{jl} assumed an inverse scaled chi-squared distribution (i.e. I-gamma) with mean $c_j = 0.01$ and standard deviation $d_j = 100$ (i.e. precision of 1.0×10^{-2}). The degrees of freedom assumed a uniform distribution with a minimum of 3 degrees of freedom (e or e_l) and maximum of 30 (f or f_l).

Model Fitting and Convergence Diagnostics

Bayesian models were constructed using OpenBUGS version 3.2.3 rev 1012 (Lunn et al. 2009), R version 3.6.0 (R Core Team 2019) and packages R2OpenBUGS version 3.2 (Sturtz et al. 2005) and coda version 0.19-2 (Plummer et al. 2005). We also applied the boxcox function in the R MASS package to attempt to transform the behavioral endpoints (Table S3.5; Venables and Ripley 2002). Using the basic model described above, behavior endpoints were normalized using the boxcox function in the R MASS package (Table S3.5; Venables and Ripley 2002). We ran the basic model using three chains, each with a minimum of 10000 iterations, 1000 burn in,

and 1 thin, and monitored a subsample of variables: main year and treatment effects and interaction, overall mean, residuals, variance, tau and df. Then we performed preliminary multiple MCMC chain convergence diagnostics using Trace plots. If model did not converge, we increased either the number of iterations, burn in, or thin (maximum tested was 100000, 75000, or 30, respectively). Once the preliminary model trace plots were not showing any obvious convergence problems, further MCMC diagnostics were applied using a suite of tools to determine adequate run length, model convergence and fit. 1) Autocorrelation plots indicated the level of thinning required to remove any autocorrelation. 2) Gelman-Rubin-Brooks shrink factor plots indicated the adequate number of iterations needed for burn in. 3) Raftery and Lewis's diagnostic tables were used to determine the number of additional iterations needed for accurate parameter estimation (default values of $q = 0.025$, $r = \pm 0.005$ and $s = 0.95$). 4) Finally, model fit was evaluated residual diagnostics.

Once a good fitting model had been determined, we reran the model with the appropriate settings and monitored a slightly different suite of parameters: overall mean; population level treatment, year and their interaction effects; variance and tau for both levels; all probabilities of difference; df; individual level predicted means. With the model output and iteration levels we also determined effective sample size (effectiveSize function in coda R package), posterior distributions of parameters, and calculated a one-sided P-value from the two sided difference probabilities.

Examples of Model Fitting issues encountered

Skewed response variables are not uncommon in biological data collection. For this study, most of the response variables had a non-normal distribution and thus did not meet the assumption for normally distributed residuals. Traditionally, response data distribution is

normalized using a transformation but it can also be modified by using a different assumed

distribution in the model. For example, the total distance a larva traveled during an assay varied

between 0 and 4252 mms (Figure S3.1A) with most fish swimming less than 1000 mm. This

resulted in a right skewed distribution that was difficult to normalize with a transformation.

Consequently, we assumed the overall response for the model was best described using a

Student's t distribution with a mean, tau and degrees of freedom. This resulted in the model

residuals to have a more normal density distribution (Figure S3.1B). We also applied the boxcox

function in the R MASS package to attempt to transform the behavioral endpoints (Table S3.5;

Venables and Ripley 2002). For example, the average swimming bout speed for yellow perch

larvae in the PCB126 treatments ranged from 0 when they did not swim to 33 mm/s, where most

larvae swam less than 10 mm/s (Figure S3.2A). Using the suggested Box-Cox transformation

and scalar (see below), the density distribution was more normal (Figure S3.2C) as well as the

residuals (Figure S3.2D).

Model convergence can be difficult if the scale of your response variable is low. For

example, many of the behavior response variables examined in this study ranged from 1 to 2,

especially after a Box-Cox transformation (Figure S3.2B). Due to the number of parameters in

the model, the model convergence is poor due the limited range of the response variable. To

solve this problem we multiplied the response variable by 10 or 100 to increase the

variability/scale so as to allow the model to converge.

A second model assumption that we did not always pass was that the variance remain

constant over the different effects. In this study there were large differences between years for

some behavioral responses (e.g. average total distance traveled in 2017 MeHg control group was

1060 mm whereas in 2016 control traveled and average of 141 mm; Table S3.8). Reasons for

this may be due to the quality (e.g. size, fitness) of the hatch from year to year in the hatchery. Even though some larvae speeds from this study were slower, while others larger, than a previous study using the same laboratory techniques (Mora-Zamorano et al. 2017), the range did overlap with the only two previous studies (Houde 1969; Mora-Zamorano et al. 2017). To remedy this problem, we constructed a model that estimated the variance separately for each year and used that year specific variance to predict the overall treatment effect means. This allowed for variability between years without violating any assumptions.

A third main assumption in the model used in this study is independence of observations, i.e. individual larvae. This assumption usually is only considered during the experimental design process, but also needs to be addressed when constructing the model. We added another continuous variable in the model to estimate the variability due to collecting data in batches. Each assay, the level of replication, contained 10 larvae. It could be argued that these larvae are not independent from one another even if the larvae were randomly selected when put in the assay. For example, one fish in one assay might be very active, thus impacting the activity levels in others. Consequently, the lack of independence can be modeled using the batch effect and thus moving the variability due to batches from the other parameters into the batch effect. Allowing the treatment effects to be more accurately represented and tested; also making the independence violation less so.

For some of the HMM behavior response tests, batch tau (tau.a) was very small with occasional spikes in the traceplots. This suggested that batch tau was very close to zero. To test this we reran the model with a smaller batch standard deviation (sdev.a) prior with a uniform distribution (minimum of 0.1 and maximum of 100) and examined whether the main factor 2.5 and 97.5th percentiles changed. If they were different, this would indicate the model is over

parameterized and the main effect estimates may be inaccurate. This check was conducted on a subset of models, one in each behavior endpoint group, since the design was the same in each test and the only difference was the number of fish that had a slow, medium, or fast state identified. No major changes in main effects were found, with 2.5 and 97.5th percentiles estimates varying less than 1. Consequently, the final model contained a batch standard deviation prior (sdev.a) with a minimum of 0.01.

Table S3.1. Whole 24 hours post fertilization embryo tissue concentrations of PCB126 and mercury after 20 hour exposure found in this study. Dose levels were mixed using MeHgCl and 100% ethanol for mercury treatments and PCB126 and 100% DMSO for the PCB126 treatments. Total mercury and PCB126 levels were detected and reported. In 2016, three replicate tissue samples were collected from each treatment. NA, not applicable; ND, not detected.

	Concentration in Solvent (ppm)	Dose (μM)	Dry Weight Tissue Concentration (n=3) mean	SD	Wet Weight Tissue Concentration (n=3) mean	SD	units
MeHgCl Treatments							
Control	0	0	5.26	1.16	0.39	0.08	ppb
Middle	0.00021	0.001	40.35	5.76	3.34	0.64	ppb
High	0.02156	0.1	5251.49	1187.30	420.62	88.02	ppb
PCB126 Treatments							
Control	0	NA	NA	NA	ND	NA	ppm
Middle	0.01	NA	NA	NA	ND	NA	ppm
High	1	NA	NA	NA	0.006367	0.005	ppm

Table S3.2. Summary of the number of assays and yellow perch larvae (*Perca flavescens*) that were used in this study.

Chemical	Treatment Level	Year	Locomotion Assay					HMMs		
			Number of Assays	Number of Larvae	Total Length (mm ± SD)	Total Number of Larvae		Number of Larvae attempted Model Fitting	Number of Larvae with Fitted Model	Total Number of Larvae
MeHg	Control	2016	15	150	6.59 ± 1.45	621		147	141	592
	Control	2017	5	50	6.93 ± 0.88			50	49	
	Middle	2016	2	20	4.67 ± 0.72			20	16	
	Middle	2017	18	181	6.64 ± 0.89			179	179	
	Upper	2016	18	180	6.51 ± 1.16			176	169	
	Upper	2017	4	40	6.65 ± 0.69			39	38	
PCB126	Control	2016	11	110	6.68 ± 1.51	599		110	106	559
	Control	2017	9	90	6.71 ± 0.94			90	85	
	Middle	2016	9	90	6.36 ± 1.36			89	85	
	Middle	2017	11	110	6.75 ± 0.84			109	104	
	Upper	2016	4	40	7.74 ± 1.14			39	39	
	Upper	2017	16	159	6.66 ± 0.76			159	140	

Table S3.3. Description of behavior endpoints examined in this study.

Behavior Endpoint	Definition
Swimming Bouts (per sec)	The number of active swimming bouts per second. A swimming bout was defined as movement at least 1 mm/s for more than 5 frames (0.166 sec).
Extreme Swimming Bouts (per sec)	The number of extreme swimming bouts per second. An extreme swimming bout was defined as movement at least 30 mm/s for more than 5 frames (0.166 sec).
Swimming Bout Duration (sec)	Duration of all swimming bouts averaged over the 5 min period.
Swimming Bout Speed (mm/s)	Per frame swimming speed averaged during a swimming bout; average bout speed averaged over the 5 min period.
Swimming Bout Turning Angle	Per frame absolute turning angle averaged during a swimming bout; average absolute turning angle averaged over the 5 min period. Range from 0 to 3.14, where 0 is straight ahead and 3.14 is straight behind.
Total Distance Traveled (mm)	Total distanced traveled during swimming bouts for the entire 5 min assay.
Total Time Swimming (sec)	Total time larvae were swimming during 5 min test.
Fish Lengths	The total distance traveled (mm) divided by fish length (mm).
Overall Step Length (mm)	Per frame distance traveled during a 0.033 sec period (one frame to the next) averaged over the entire 5 min test [i.e. includes zeros when fish moved less than 1 mm/s for more than 5 frames (0.166 sec)].
Overall Step Length Variation	Standard deviation of distance traveled during 0.033 sec period (one frame to the next).
Overall Turning Angle	Turning angle during 0.033 sec period (one frame to the next) averaged over frames when fish were swimming. Ranges from -3.14 to 3.14, where negative values indicate right turns and positive values indicate left turns.
Overall Turning Angle Variation	Standard deviation of per frame turning angle during 0.033 sec period (one frame to the next).
HMM Model Parameters	
Step Length (mm)	Per frame distance traveled during a 0.033 sec period (one frame to the next); averaged over entire 5 min test while the larvae was in a behavior state.
Step Length Variation	Standard deviation of the per frame distance traveled during 0.033 sec period (one frame to the next) while in a behavior state.
Turning Angle	Per frame turning angle; averaged over entire 5 min test while the larvae was in a behavior state. Ranges from -3.14 to 3.14, where negative values indicate right turns and positive values indicate left turns.
Turning Angle Variation	Angle concentration, i.e. kappa parameter in the von Mises distribution while in a behavior state.

Table S3.3 (cont'd)

Count	Number of frames a behavior was performed.
Slow -> Slow, Medium -> Slow, Slow -> Medium, Medium -> Medium, Fast -> Slow, Fast -> Medium, Slow -> Fast, Medium -> Fast, Fast -> Fast	Transition probability from state to state (e.g. Medium -> Slow is the probability of a fish transitioning from a medium speed swimming state to a slow swimming state).

Table S3.4. List of all hidden Markov models examined for each larva in this study. Data groupings or settings used to calculate initial parameter values for the hidden Markov models. SD = standard deviation. s1 HMMs contained one behavior state, s2 HMMs contained two behavior states, and s3 HMMs contained three behavior states.

Model abbreviation	Number of behavior states	Initial behavior states values		
		First Behavior State	Second Behavior State	Third Behavior State
s1_slow	1	0.1 mm, SD = 0.01	NA	NA
s1_25	1	SDs and angle mean from all data, 25th percentile of all step lengths for step length mean	NA	NA
s1_50	1	SDs and angle mean from all data, 50th percentile of all step lengths for step length mean	NA	NA
s1_75	1	SDs and angle mean from all data, 75th percentile of all step lengths for step length mean	NA	NA
s2_25	2	0.1 mm, SD = 0.01	SDs and angle mean from step lengths > 0.15 mm; 25th step length percentile for step length mean from step lengths > 0.15 mm;	NA
s2_50	2	0.1 mm, SD = 0.01	SDs and angle mean from step lengths > 0.15 mm; 50th step length percentile for step length mean from step lengths > 0.15 mm;	NA
s2_75	2	0.1 mm, SD = 0.01	SDs and angle mean from step lengths > 0.15 mm; 75th step length percentile for step length mean from step lengths > 0.15 mm;	NA
s3_25	3	0.1 mm, SD = 0.01	from step lengths > 0.15 mm and < 25th step length percentile	from step lengths > 0.15 mm and > 25th step length percentile

Table S3.4 (cont'd)

s3_50	3	0.1 mm, SD = 0.01	from step lengths > 0.15 mm and < 50th step length percentile	from step lengths > 0.15 mm and > 50th step length percentile
s3_75	3	0.1 mm, SD = 0.01	from step lengths > 0.15 mm and < 75th step length percentile	from step lengths > 0.15 mm and > 75th step length percentile

Table S3.5. Linear Discriminant Models (LDA) cross validation results for different Hidden Markov Chain Model (HMM) behavioral states. N = 50 iterations, SD = standard deviation, s3 = three behavior state HMM, s2 = two behavior state HMM, s1 = one behavior state HMM.

Group	Num. of larvae with s3 models	Num. of larvae with s2 models	Num. of larvae with s1 models	Num. of obs./behavior states in s3 LDA	Total num. of obs./behavior states in s1 and s2	Num. of renamed behavior states in s1 and s2	Slow State Accuracy of s3 LDA Mean	SD	Medium State Accuracy of s3 LDA Mean	SD	Fast State Accuracy of s3 LDA Mean	SD	Total Accuracy of s3 LDA Mean	SD
MeHg														
Control Dose - Year 2016	31	108	2	93	218	50	0.71	0.20	0.51	0.23	0.72	0.17	0.64	0.11
Control Dose - Year 2017	29	16	4	87	36	8	0.63	0.27	0.39	0.22	0.66	0.20	0.56	0.10
Middle Dose - Year 2016	1	15	0	3	30	0								
Middle Dose - Year 2017	82	90	7	246	187	56	0.64	0.18	0.54	0.16	0.70	0.13	0.63	0.09
Upper Dose - Year 2016	22	140	7	66	287	141	0.44	0.30	0.72	0.24	0.68	0.24	0.61	0.14
Upper Dose - Year 2017	23	11	4	69	26	8	0.69	0.30	0.06	0.15	0.73	0.20	0.49	0.11
PCB 126														
Control Dose - Year 2016	18	84	4	54	172	62	0.71	0.23	0.50	0.29	0.71	0.22	0.64	0.13
Control Dose - Year 2017	46	34	5	138	73	25	0.32	0.27	0.64	0.25	0.49	0.25	0.49	0.13
Middle Dose - Year 2016	16	66	3	48	135	28	0.73	0.27	0.39	0.30	0.79	0.23	0.64	0.13
Middle Dose - Year 2017	47	52	5	141	109	18	0.42	0.22	0.76	0.14	0.62	0.18	0.60	0.09
Upper Dose - Year 2016	10	26	3	30	55	20	0.53	0.29	0.31	0.32	0.84	0.28	0.56	0.15
Upper Dose - Year 2017	76	59	5	228	123	31	0.34	0.13	0.93	0.07	0.65	0.13	0.64	0.06

Table S3.6. Model summary for each behavioral endpoint.

Chemical	Parameter	BoxCox Transformation	Distribution	Larvae	Chains	Iterations	Burnin	Thin	Sample
						Number of			
MeHg	Swimming Bouts (per sec)	(y+1)^-4.5, y*100	Normal	621	3	70000	50000	30	60000
	Extreme Swimming Bouts (per sec)	(y+1)^-30.8, y*100	Normal	621	3	95000	70000	30	75000
	Swimming Bout Duration (sec)	(y+1)^-0.6, y*100	Normal	621	3	80000	60000	30	60000
	Swimming Bout Speed (mm/s)	(y+1)^-0.5, y*100	Normal	621	3	95000	60000	30	105000
	Swimming Bout Turning Angle	(y+1)^0.75, y*100	Normal	611	3	145000	60000	30	255000
	Total Distance Traveled (mm)	NA	Student's T	621	3	105000	50000	30	165000
	Total Time Swimming (sec)	NA	Student's T	621	3	125000	80000	30	135000
	Fish Lengths	NA	Student's T	621	3	100000	70000	30	90000
	Overall Step Length (mm)	(y+1)^-12.4, y*10	Normal	592	3	110000	80000	30	90000
	Overall Step Length Variation	(y+1)^-3.35, y*10	Normal	592	3	100000	80000	30	60000
	Overall Turning Angle	(y+1)^-0.65, y*100	Normal	592	3	110000	80000	30	90000
	Overall Turning Angle Variation	(y+1)^1.13, y*10	Normal	592	3	100000	30000	30	210000
	HMM Model Parameters								
	Slow State								
	Step Length (mm)	(y+1)^-11.5, y*100	Normal	490	3	111000	50000	30	183000
	Step Length Variation	(y+1)^-3.3, y*100	Normal	485	3	103000	40000	30	189000
	Turning Angle	NA	Normal	490	3	90000	60000	30	90000
	Turning Angle Variation	(y+1)^-0.8, y*100	Normal	490	3	110000	50000	30	180000
	Count	(y+1)^1.8, y/100000	Normal	490	3	95000	60000	20	105000
	Medium State								
	Step Length (mm)	(y+1)^-3.5, y*10	Normal	530	3	130000	80000	30	150000
	Step Length Variation	(y+1)^-3.7, y*10	Normal	530	3	125000	70000	30	165000
	Turning Angle	NA	Normal	530	3	130000	80000	30	150000
	Turning Angle Variation	(y+1)^-0.75, y*10	Normal	529	3	95000	50000	30	135000
	Count	(y+1)^0.13, y*100	Normal	530	3	105000	50000	20	165000

Table S3.6 (cont'd)

	Fast State								
	Step Length (mm)	$(y+1)^{-1.7}$, $y*10$	Normal	328	3	75000	40000	30	105000
	Step Length Variation	$(y+1)^{-1.57}$, $y*10$	Normal	322	3	100000	70000	30	90000
	Turning Angle	NA	Normal	328	3	190000	150000	30	120000
	Turning Angle Variation	$(y+1)^{-0.51}$, $y*10$	Normal	328	3	150000	90000	30	180000
	Count	$(y+1)^{0.15}$, $y*100$	Normal	328	3	315000	50000	30	795000
	State Transition Probabilities								
	Slow -> Slow	asin(sqrt(y)), $y*100$	Normal	482	3	117000	50000	30	201000
	Medium -> Slow	$(y+1)^{-15.75}$, $y*100$	Normal	428	3	115000	50000	30	195000
	Slow -> Medium	$(y+1)^{-34.5}$, $y*100$	Normal	428	3	120000	50000	30	210000
	Medium -> Medium	$(y+1)^{23}$, $y/100000$	Normal	514	3	95000	40000	30	165000
	Fast -> Slow	$(y+1)^{-22}$, $y*100$	Normal	242	3	110000	40000	30	210000
	Fast -> Medium	$(y+1)^{-12.3}$, $y*100$	Normal	274	3	130000	40000	30	270000
	Slow -> Fast	$(y+1)^{-71}$, $y*100$	Normal	242	3	120000	40000	30	240000
	Medium -> Fast	$(y+1)^{-19}$, $y*100$	Normal	274	3	105000	30000	30	225000
	Fast -> Fast	$(y+1)^{21}$, $y/100000$	Normal	328	3	115000	40000	30	225000
PCB 126	Swimming Bouts (per sec)	$(y+1)^{-6.2}$, $y*100$	Normal	599	3	85000	60000	30	75000
	Extreme Swimming Bouts (per sec)	$(y+1)^{-22.6}$, $y*100$	Normal	599	3	80000	60000	30	60000
	Swimming Bout Duration (sec)	$(y+1)^{-1}$, $y*100$	Normal	599	3	100000	80000	30	60000
	Swimming Bout Speed (mm/s)	$(y+1)^{0.05}$, $y*100$	Normal	599	3	95000	70000	30	75000
	Swimming Bout Turning Angle	$(y+1)^{-0.6}$, $y*100$	Normal	596	3	140000	60000	30	240000
	Total Distance Traveled (mm)	NA	Student's T	599	3	884000	50000	30	2502000
	Total Time Swimming (sec)	NA	Student's T	599	3	102000	70000	30	96000
	Fish Lengths	NA	Student's T	599	3	120000	80000	30	120000
	Overall Step Length (mm)	$(y+1)^{-13.1}$, $y*10$	Normal	559	3	100000	90000	30	30000
	Overall Step Length Variation	$(y+1)^{-2.6}$, $y*10$	Normal	559	3	70000	50000	30	60000
	Overall Turning Angle	$(y+1)^{2.65}$, $y*10$	Normal	559	3	120000	100000	30	60000
	Overall Turning Angle Variation	$(y+1)^{-0.015}$, $y*1000$	Normal	559	3	100000	60000	30	120000
	HMM Model Parameters								

Table S3.6 (cont'd)

Slow State

Step Length (mm)	(y+1)^-14.5, y*100	Normal	471	3	104000	50000	30	162000
Step Length Variation	(y+1)^-2.5, y*100	Normal	460	3	108000	40000	30	204000
Turning Angle	NA	Normal	471	3	150000	80000	30	210000
Turning Angle Variation	(y+1)^-0.7, y*100	Normal	471	3	120000	50000	30	210000
Count	(y+1)^1.58, y/10000	Normal	471	3	65000	40000	20	75000

Medium State

Step Length (mm)	(y+1)^-2.8, y*100	Normal	517	3	115000	50000	30	195000
Step Length Variation	(y+1)^-2.8, y*100	Normal	517	3	120000	40000	30	240000
Turning Angle	NA	Normal	517	3	90000	60000	30	90000
Turning Angle Variation	(y+1)^-0.87, y*10	Normal	515	3	100000	70000	30	90000
Count	(y+1)^0.07, y*100	Normal	517	3	75000	50000	20	75000

Fast State

Step Length (mm)	(y+1)^-1.52, y*10	Normal	318	3	90000	60000	30	90000
Step Length Variation	(y+1)^-1.43, y*10	Normal	317	3	110000	60000	30	150000
Turning Angle	NA	Normal	318	3	120000	90000	30	90000
Turning Angle Variation	(y+1)^-0.31, y*10	Normal	318	3	85000	50000	30	105000
Count	(y+1)^0.16, y*100	Normal	318	3	105000	40000	20	195000

State Transition Probabilities

Slow -> Slow	asin(sqrt(y)), y*100	Normal	466	3	105000	40000	30	195000
Medium -> Slow	(y+1)^-20, y*100	Normal	434	3	95000	50000	30	135000
Slow -> Medium	(y+1)^-63.5, y*100	Normal	434	3	70000	50000	30	60000
Medium -> Medium	(y+1)^27, y/10000000	Normal	502	3	100000	60000	30	120000
Fast -> Slow	(y+1)^-35, y*100	Normal	245	3	110000	50000	30	180000
Fast -> Medium	(y+1)^-8.5, y*10	Normal	281	3	80000	40000	30	120000
Slow -> Fast	(y+1)^-94, y*10	Normal	245	3	115000	50000	30	195000
Medium -> Fast	(y+1)^-13.7, y*10	Normal	281	3	120000	60000	30	180000
Fast -> Fast	(y+1)^-13.3, y*100	Normal	313	3	120000	40000	30	240000

Table S3.7. Normal distribution OpenBUGS model containing treatment and year main effects and a random batch effect.

```
#inits<-function(){
#  list(sdev=runif(2,0.01,100),sdev.a=runif#(2,0.01,100),batch.eff=runif(N2,-1000,1000))}
#inits()

model;
{
        for(i in 1:N){
        y[i]~dnorm(mu[i],tau[year[i]])
        mu[i]<-mean+trt.eff[trt[i]]+year.eff[year[i]]+inter.eff[year[i],trt[i]]+batch.eff[batchid[i]]
        }
        mean~dnorm(0,1.0E-6)
#make fixed main effect priors
        trt.eff[1]<-0
        for (i in 2:3){
        trt.eff[i]~dnorm(0,1.0E-6)
        }
        year.eff[1]<-0
        year.eff[2]~dnorm(0,1.0E-6)
#make random effect of batch priors
        for (i in 1:N2){
        batch.eff[i]~dnorm(0,tau.a[year_of_batch[i]])
        }
#year_of_batch is a data vector length of N2, where 1 is first year, 2 is second.
#make fixed main effect interaction priors
        inter.eff[1,1]<-0
        inter.eff[1,2]<-0
        inter.eff[1,3]<-0
        inter.eff[2,1]<-0
        for (i in 2:2){
        for(j in 2:3){
        inter.eff[i,j] ~dnorm(0,1.0E-6)
        }
        }
#predict estimates using cell means model
        for (i in 1:2){
        for(j in 1:3){
        Trt.by.yr.mean[i,j]<-mean+trt.eff[j]+year.eff[i]+inter.eff[i,j]
        }
        }
#initial values
        sdev[1]~dunif(0.01,100)
```

Table S3.7 (cont'd)
```
        sdev[2]~dunif(0.01,100)
        sdev.a[1]~dunif(0.01,100)
        sdev.a[2]~dunif(0.01,100)

        var[1]<-pow(sdev[1],2)
        var[2]<-pow(sdev[2],2)
        var.a[1]<-pow(sdev.a[1],2)
        var.a[2]<-pow(sdev.a[2],2)

        tau[1]<-pow(sdev[1],-2)
        tau[2]<-pow(sdev[2],-2)
        tau.a[1]<-pow(sdev.a[1],-2)
        tau.a[2]<-pow(sdev.a[2],-2)
#difference calculations
        difyear<-year.eff[2]-year.eff[1]
        pvalyear<-step(difyear)

        trt1<-(Trt.by.yr.mean[1,1]+Trt.by.yr.mean[2,1])/2
        trt2<-(Trt.by.yr.mean[1,2]+Trt.by.yr.mean[2,2])/2
        trt3<-(Trt.by.yr.mean[1,3]+Trt.by.yr.mean[2,3])/2

        diftrt2<-trt2-trt1
        pvaltrt2_1<-step(diftrt2)
        diftrt3<-trt3-trt1
        pvaltrt3_1<-step(diftrt3)
        diftrt3_2<-trt3-trt2
        pvaltrt3_2<-step(diftrt3_2)

        difinter1_1vs1_2<-inter.eff[1,1]-inter.eff[1,2]
        pvalinter1_1vs1_2<-step(difinter1_1vs1_2)
        difinter1_1vs1_3<-inter.eff[1,1]-inter.eff[1,3]
        pvalinter1_1vs1_3<-step(difinter1_1vs1_3)
        difinter1_2vs1_3<-inter.eff[1,2]-inter.eff[1,3]
        pvalinter1_2vs1_3<-step(difinter1_2vs1_3)
        difinter2_1vs2_2<-inter.eff[2,1]-inter.eff[2,2]
        pvalinter2_1vs2_2<-step(difinter2_1vs2_2)
        difinter2_1vs2_3<-inter.eff[2,1]-inter.eff[2,3]
        pvalinter2_1vs2_3<-step(difinter2_1vs2_3)
        difinter2_2vs2_3<-inter.eff[2,2]-inter.eff[2,3]
        pvalinter2_2vs2_3<-step(difinter2_2vs2_3)
#ratio calculations
        ratiotrt2_1<-trt2/trt1
        ratiotrt3_1<-trt3/trt1
```

Table S3.7 (cont'd)

```
        ratiotrt3_2<-trt3/trt2
#posterior model checking, generate new obs based on model params mu, tau. assume normal
dist
  for( i in 1 : N ) {
    ypred[i] ~ dnorm(mu[i],tau[year[i]])
  }
#generate individual level predictions
    #indiv at the year level
        ypred_1_y1 ~ dnorm(Trt.by.yr.mean[1,1],tau[1])
        ypred_2_y1 ~ dnorm(Trt.by.yr.mean[1,2],tau[1])
        ypred_3_y1 ~ dnorm(Trt.by.yr.mean[1,3],tau[1])
        ypred_1_y2 ~ dnorm(Trt.by.yr.mean[2,1],tau[2])
        ypred_2_y2 ~ dnorm(Trt.by.yr.mean[2,2],tau[2])
        ypred_3_y2 ~ dnorm(Trt.by.yr.mean[2,3],tau[2])
#ypred using averages
        ypred_1<-(ypred_1_y1+ypred_1_y2)/2
        ypred_2<-(ypred_2_y1+ypred_2_y2)/2
        ypred_3<-(ypred_3_y1+ypred_3_y2)/2
#compute residuals using the kurtosis formula for both orig data (e) and rep data
  for( i in 1 : N ) {
    e[i]<-y[i]-mu[i]
  }
  SSE<-inprod(e[],e[])#sum of squares which is e squared
  ku<-sum(e[]) #sum up all values, there is one for each data point
  kpred<-sum(ypred[])
difs<-kpred-ku #find difference
difpval<-step(difs) #count how many times the rep data is larger than orig data
}
```

Table S3.8. Student's t distribution OpenBUGS model containing treatment and year main effects and a random batch effect.

```
#inits<-function(){
#  list(tau=runif(2,0,10),tau.a=runif(2,0,10),batch.eff=runif(N2,-1000,1000), df=runif(1,3,30),
df.a=runif(1,3,30))}
#inits()

model;
{
        for(i in 1:N){
        y[i]~dt(mu[i],tau[year[i]],df)
        mu[i]<-mean+trt.eff[trt[i]]+year.eff[year[i]]+inter.eff[year[i],trt[i]]+batch.eff[batchid[i]]
        }
        mean~dnorm(0,1.0E-6)
#make fixed main effect priors
        trt.eff[1]<-0
        for (i in 2:3){
        trt.eff[i]~dnorm(0,1.0E-6)
        }
        year.eff[1]<-0
        year.eff[2]~dnorm(0,1.0E-6)
#make random effect of batch priors
        for (i in 1:N2){
        batch.eff[i]~dt(0,tau.a[year_of_batch[i]],df.a)
        }
#year_of_batch is a data vector length of N2, where 1 is first year, 2 is second.
#make fixed main effect interaction priors
        inter.eff[1,1]<-0
        inter.eff[1,2]<-0
        inter.eff[1,3]<-0
        inter.eff[2,1]<-0
        for (i in 2:2){
        for(j in 2:3){
        inter.eff[i,j] ~dnorm(0,1.0E-6)
        }
        }
#predict estimates using cell means model
        for (i in 1:2){
        for(j in 1:3){
        Trt.by.yr.mean[i,j]<-mean+trt.eff[j]+year.eff[i]+inter.eff[i,j]
        }
        }
#initial values
```

Table S3.8 (cont'd)

```
df~dunif(3,30)
df.a~dunif(3,30)

tau.a[1]~dgamma(0.01,0.01)
tau.a[2]~dgamma(0.01,0.01)
tau[1]~dgamma(0.0001,0.0001)
tau[2]~dgamma(0.0001,0.0001)

var[1]<-1/tau[1]
var[2]<-1/tau[2]
var.a[1]<-1/tau.a[1]
var.a[2]<-1/tau.a[2]
```
#difference calculations
```
difyear<-year.eff[2]-year.eff[1]
pvalyear<-step(difyear)

trt1<-(Trt.by.yr.mean[1,1]+Trt.by.yr.mean[2,1])/2
trt2<-(Trt.by.yr.mean[1,2]+Trt.by.yr.mean[2,2])/2
trt3<-(Trt.by.yr.mean[1,3]+Trt.by.yr.mean[2,3])/2

diftrt2<-trt2-trt1
pvaltrt2_1<-step(diftrt2)
diftrt3<-trt3-trt1
pvaltrt3_1<-step(diftrt3)
diftrt3_2<-trt3-trt2
pvaltrt3_2<-step(diftrt3_2)

difinter1_1vs1_2<-inter.eff[1,1]-inter.eff[1,2]
pvalinter1_1vs1_2<-step(difinter1_1vs1_2)
difinter1_1vs1_3<-inter.eff[1,1]-inter.eff[1,3]
pvalinter1_1vs1_3<-step(difinter1_1vs1_3)
difinter1_2vs1_3<-inter.eff[1,2]-inter.eff[1,3]
pvalinter1_2vs1_3<-step(difinter1_2vs1_3)
difinter2_1vs2_2<-inter.eff[2,1]-inter.eff[2,2]
pvalinter2_1vs2_2<-step(difinter2_1vs2_2)
difinter2_1vs2_3<-inter.eff[2,1]-inter.eff[2,3]
pvalinter2_1vs2_3<-step(difinter2_1vs2_3)
difinter2_2vs2_3<-inter.eff[2,2]-inter.eff[2,3]
pvalinter2_2vs2_3<-step(difinter2_2vs2_3)
```
#ratio calculations
```
ratiotrt2_1<-trt2/trt1
ratiotrt3_1<-trt3/trt1
ratiotrt3_2<-trt3/trt2
```

Table S3.8 (cont'd)

```
#posterior model checking, generate new obs based on model params mu, tau. assume t dist
  for( i in 1 : N ) {
    ypred[i] ~ dt(mu[i],tau[year[i]],df)
    }
#generate individual level predictions
    #indiv at the year level
        ypred_1_y1 ~ dt(Trt.by.yr.mean[1,1],tau[1],df)
        ypred_2_y1 ~ dt(Trt.by.yr.mean[1,2],tau[1],df)
        ypred_3_y1 ~ dt(Trt.by.yr.mean[1,3],tau[1],df)
        ypred_1_y2 ~ dt(Trt.by.yr.mean[2,1],tau[2],df)
        ypred_2_y2 ~ dt(Trt.by.yr.mean[2,2],tau[2],df)
        ypred_3_y2 ~ dt(Trt.by.yr.mean[2,3],tau[2],df)
#ypred using averages
        ypred_1<-(ypred_1_y1+ypred_1_y2)/2
        ypred_2<-(ypred_2_y1+ypred_2_y2)/2
        ypred_3<-(ypred_3_y1+ypred_3_y2)/2
#compute residuals using the kurtosis formula for both orig data (e) and rep data
  for( i in 1 : N ) {
    e[i]<-y[i]-mu[i]
    }
  SSE<-inprod(e[],e[])#sum of squares which is e squared
  ku<-sum(e[]) #sum up all values, there is one for each data point
  kpred<-sum(ypred[])
difs<-kpred-ku #find difference
difpval<-step(difs) #count how many times the rep data is larger than orig data
}
```

Table S3.9. Posterior distributions for all model parameters and each yellow perch *Perca flavescens* behavioral endpoint.

Submitted table as a sheet in an Excel file.
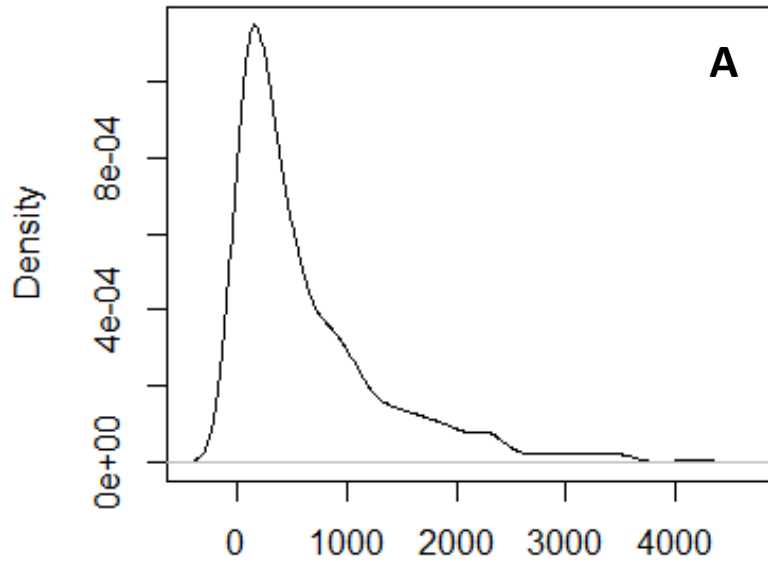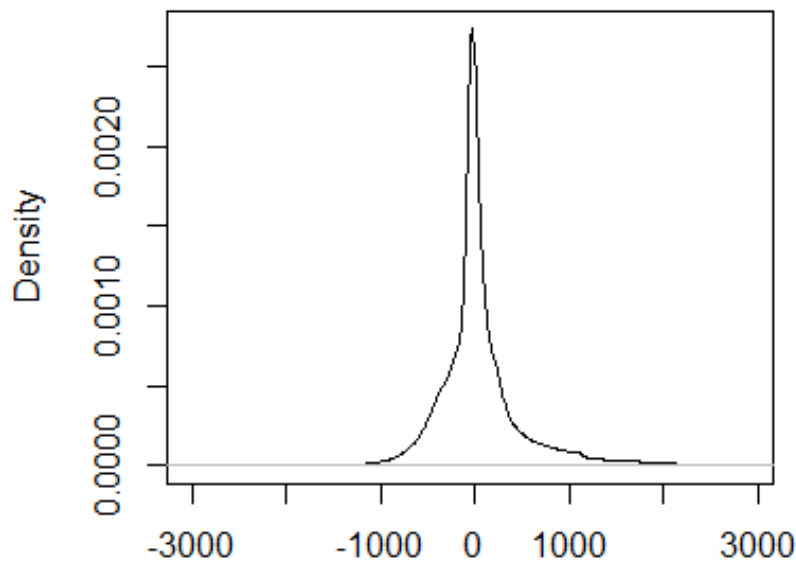
Figure S3.1. Density plots of total distance traveled (mm) for yellow perch during a 5-minute assay from the PCB126 treatments. A) Density plot of original data, B) Density plot of the model residuals using a Student's t distribution.
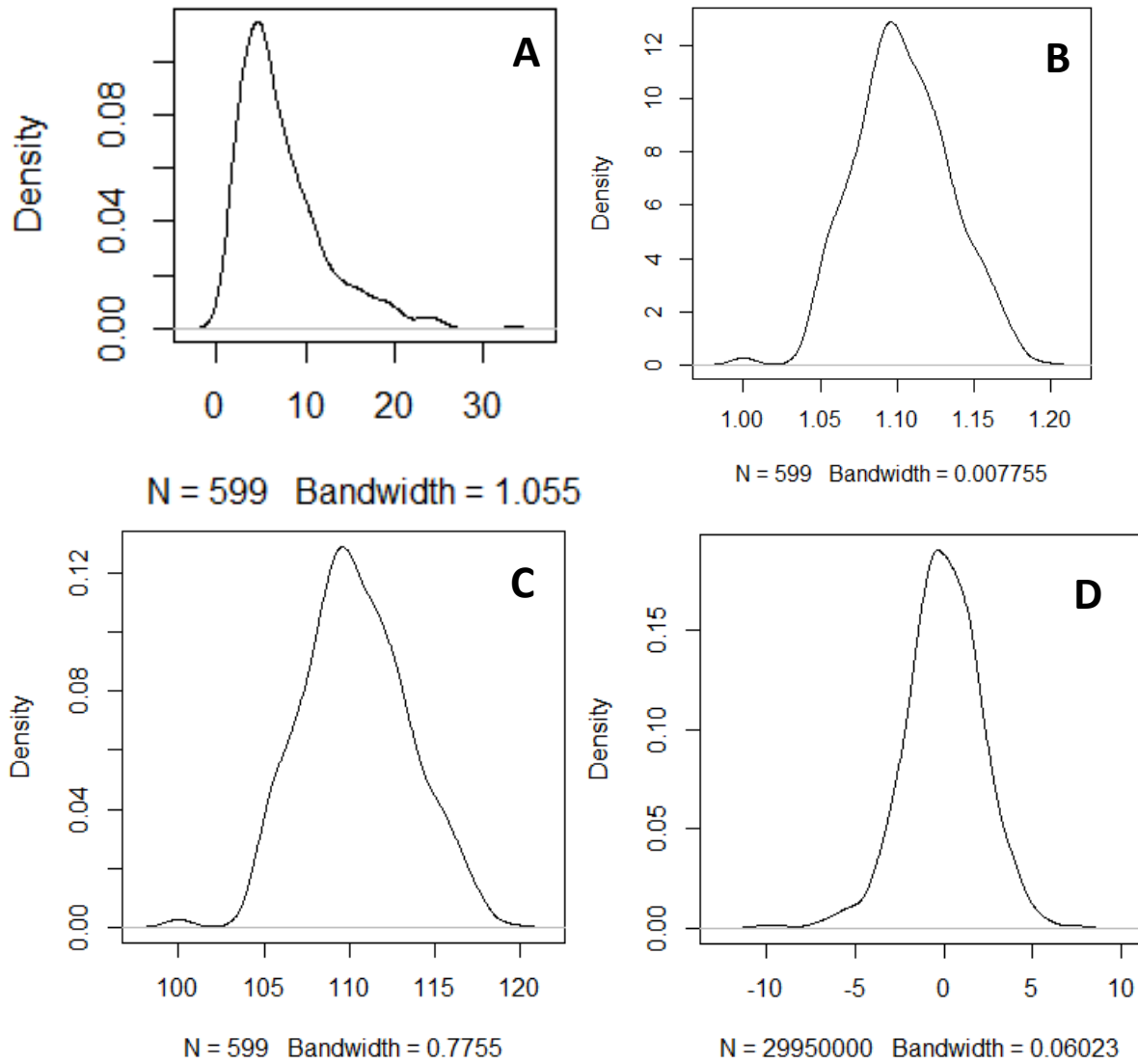
Figure S3.2. Density plots of the average swimming bout speed (mm/sec) for yellow perch larvae in the PCB126 treatments. A) Density plot of original data, B) Density plot of transformed data after applying a Box Cox transformation, C) Density plot of the transformed data after applying a scalar, D) model residuals.
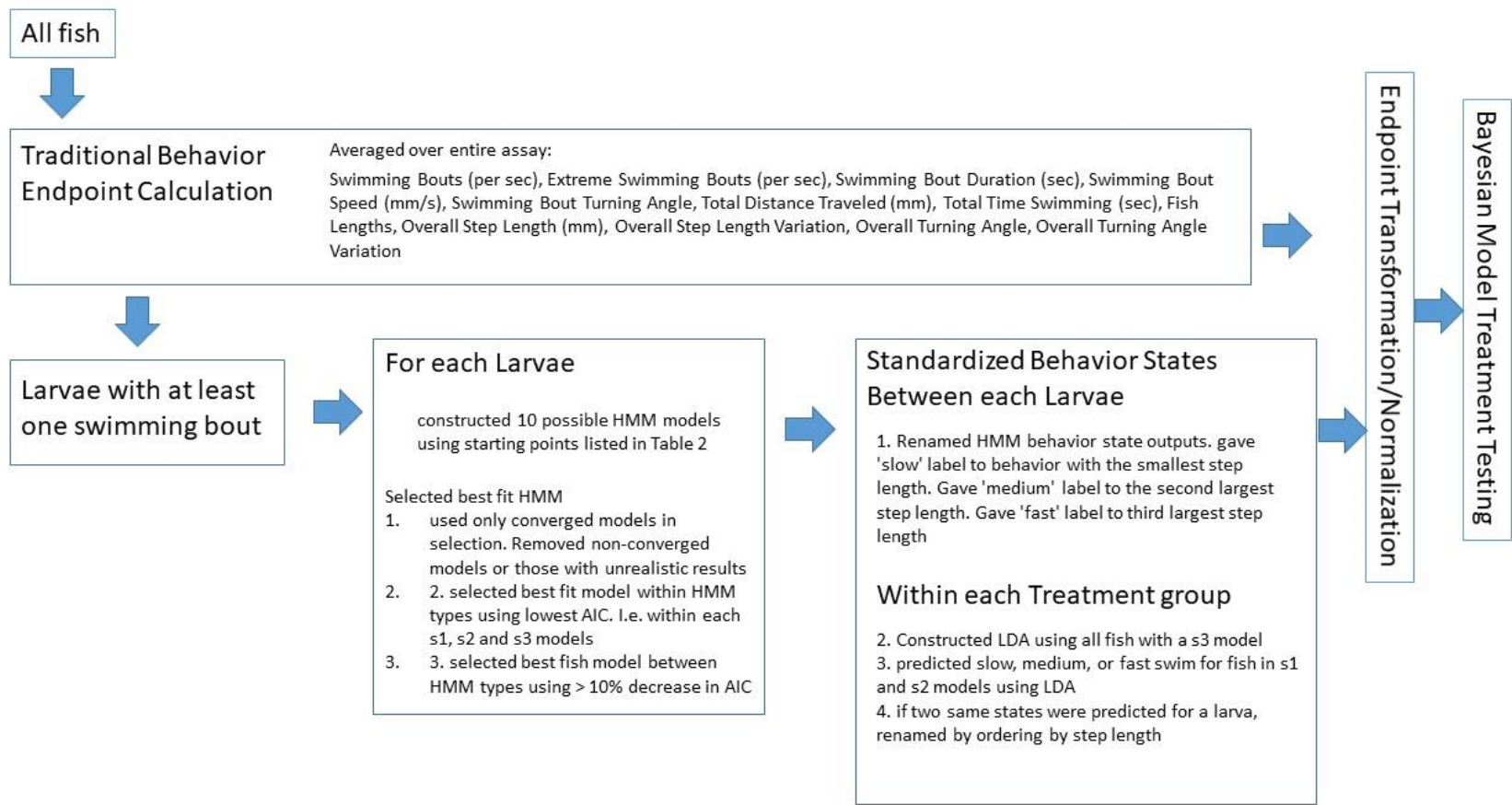
Figure S3.3. Analytical steps taken in this study showing the traditional route and the new method using Hidden Markov Chain Models.

APPENDIX III:

Chapter 4 Supplementary Materials

Behavior Assay Methods

After exposure, 7dpf embryos were rinsed in fresh seawater and transferred into 50-ml conical centrifuge tubes full of fresh seawater (< 50 embryos per tube) and shipped overnight to UWM, where they were placed in 12-well plates and maintained at 23° C (1-2 embryos per well with 1ml artificial seawater; Falcon® Corning, NY 12 well plate 85 x 128 mm, 22 mm diameter well). At 10 dpf, embryos were phenotyped microscopically when abnormalities in developmental stage and features were noted (Clark et al. 2010; Whitehead et al. 2010). At 14 dpf, plates were rocked gently (~120rpm) and seawater added to each well to initiate hatching. Individual larvae were maintained in single wells for all assessments containing 3 mL seawater, incubated at 23° C, fed 24-h hatched *Artemia* ad lib daily, and renewed with seawater on alternate days. Individuals were assessed daily for survival until 23-24 dpf.

During larvae development, multiple behavior assays were conducted to determine if chemical exposure altered important behavioral milestones. Logistical constraints required two separate batches of fish to be produced (fertilized on August-8-2017 from parents on diets for 103 days and August-21-2017 from parents on diets for 115 days) and for some fish to be included in multiple assays. KF were exposed to MeHg as embryos via parental transfer and a portion of these were dosed with PCB126 1-7 dpf. Embryos hatched at 14 dpf, assessed with the Visual Motor Response (VMR) assay at 16 dpf (n=144), a random subset contributed brain samples using lethal methods for gene expression at 16 dpf (n=69, 36 of whom had been through the VMR assay), assessed with Locomotion Behavior assay at 17 dpf (n=256, 108 of whom had been through the VMR assay), and feeding abilities were assessed at 23 or 24 dpf (n=192, 84 of whom had been through the VMR and Locomotion assay and 192 had been through the Locomotion assay; see Table S4.1 for the total number of fish in each assay and treatment).

Visual Motor Response (VMR) assays are a common test of fish neurological system function by startling the fish and evaluating their response (Emran et al. 2008). VMRs were conducted using the same methodology as (Mora-Zamorano et al. 2017), where 16 dpf larvae were tested in a special behavior chamber while in the transparent 12-well microliter plates. The testing chamber isolated the larvae from light and sound, as described in three previous studies (Mora-Zamorano et al. 2016b, 2016a, 2017) and provided adequate light and video surveillance to view all individual movement. VMR assays were conducted between the hours of 1200 and 1800 to minimize within day variability (MacPhail et al. 2009). KF larvae were positioned in a dark behavior chamber and acclimated in the dark for 10 minutes (did not use data during this period), after which they underwent two cycles of alternating 10 min light and dark periods for a total of 50 min. This resulted in larvae used in the VMR analysis experiencing two startles each from dark to light and from light to dark and 4-10 minute periods differing light conditions: two dark and two light. Light levels during the light periods were set to 69 lx based on the work by MacPhail et al. (2009; Fisher Scientific Traceable Dual-Range Light Meter, Pittsburgh, PA).

Spontaneous movement of larvae was constantly recorded at a rate of 30 frames per sec and tracked using DanioVision© system version 8.0 (Noldus Information Technology, Leesburg, VA). Settings for tracking did not include smoothing of track. The minimal distance before movement was recorded was set to 0.2 mm, at which time the direct distance between the two points was calculated. Tracking errors were corrected by plotting all x, y coordinates and locating and correcting occurrences where the track indicated movement but the fish did not move or track was outside the boundary of the dish. Occasionally when Ethovision lost a fish for 1 to 3 frames (4-

SCO-MeHg, 3-NBH-Ctrl, 3-NBH-PCB), the equidistant point/s between the previous and next location were calculated and used as locations.

Similar to Albers et al. (2022), this study used the censored fish locations to define individual larvae activity at each frame within each period. Speed at each frame was calculated as mm per sec and distance traveled in mm. Swimming was defined as larval movement that was at least 6 mm/sec or 0.2 mm per frame (i.e. magnitude of velocity at larvae center) and lasted longer than 5 frames (0.166 sec). Whereas the resting behavior occurred during frames where movement was less than 1 mm/sec or if greater than 1 mm/sec, lasted less than 5 frames. Where resting behavior was defined, speed and distance for those frames were changed to zero. In addition, the turning angle associated with each frame of swimming was calculated using the difference between the four-quadrant inverse tangent of the two trajectories. Where the first trajectory was constructed from the first two locations in the sequence, and the second trajectory from the second two locations in the sequence. This results in a turning angle that ranges from -3.14 to 3.14, where zero is straight ahead movement, negative values indicate right turns and positive values indicate left turns. Swimming bout characteristics (i.e. time between rest periods) were summarized using multiple metrics: number of bouts per second; the mean duration, speed and turning angle (See Table S4.2 for definitions). The overall larval behavior during each period in the assay was also summarized using multiple overall summary metrics: total distance traveled, total time swimming, overall average step length and variation, overall turning angle and variation.

The fish larvae responded to the visual startle from the light change as is typical of previous startle responses (Emran et al. 2008). Consequently, two behavior endpoints were calculated specifically to determine how larvae responding to the visual startle of the light turning off and on. To determine the magnitude of the response to the visual startle, we determined the frame

where the maximum speed was traveled within 5 seconds after the startle. Then the difference

between this maximum speed and the speed at the time of the startle was calculated to define the

magnitude of the startle response. Startle response time was calculated as the difference in time

between the startle and the frame where the maximum speed was traveled.

Locomotion Assay

Typically, KF larvae initiate swimming soon after hatching (Weis and Weis 1995b). The

focus of this study was to assess larvae behavior at the point that larvae were independent and

actively swimming. Consequently, the locomotion assay was conducted when KF larvae were 17

dpf (3 dph, 6.8 ± 0.67 mm in length, n=180), where each 12-well plate was transferred to the

behavior testing chamber. Since previous locomotion assays indicated some neurotoxicants

impact larvae only during light periods (Mora-Zamorano et al. 2017), light levels were constant

during the entire assay and set to 69 lx (MacPhail et al. 2009). Assays were conducted during the

afternoon between 1200 and 1730 hr After an acclimation period of 5 min, spontaneous movement

of larvae were tracked every 30th of a second using DanioVision© software 8.0 with the same

settings described for the VMR assay. Additionally, DanioVision© lost track of one fish for more

than 300 frames, so this fish was not included in the analysis (treatment SCO-PCB).

Using the censored fish locations, the same activity endpoints used the VMR assay were

calculated: average swimming bout speed, duration, frequency, turning angle (Table S4.2).

Additional behavior metrics that summarized other behaviors over the entire assay were also

calculated: total distance traveled and swimming time, average step length and turning angle with

their respective variations.

Using the same methods as Albers et al. (2022), a Hidden Markov Chain Model (HMM) was constructed for each fish in the locomotion assay (all fish swam at least once) to describe the different behavioral states and used them as additional behavior endpoints to determine effects from chemical exposure. A brief description of the method follows. For each larva and video frame, the step length and turning angle during the assay were used to construct multiple larval specific HMMs using the R package moveHMM (Michelot et al. 2016; R Core Team 2019). Multiple behavior state models were examined that contained three possible swimming states: slow, medium, and fast swimming states where s1 HMMs contained only one behavior state, s2 HMMs contained any two behavior states, and s3 HMMs contained all three behavior states. The best fit HMM for each larvae was determined from a suite of ten potential HMM models, differing in the number of behavior states and initial starting values for each state (see Albers et al. 2022 Table S4.2 for model description and initial values).

Once all 10 of the possible HMMs were completed, a hierarchical selection for the best fitting model was conducted, essentially using successfully converged models with the lowest AIC. Even though the initial state values were set up in increasing step length means, the resulting best fit HMM state parameter estimates did not always have increasing step length for each additional behavior. This is probably due to the final HMM behavior state being defined by not only the step length but also turning angle characteristics. To make sure the behavior state comparisons were comparing similar states with the same name, the states were reordered and renamed in order to compare between larvae. First, states were reordered using the mean step length to describe them as slow, medium and faster swimming behavior states (i.e. changed the state name). Next a Linear Discriminant Model was constructed using the lda function in the MASS package (Venables and Ripley 2002) and cross validation to compare between models using the s3 models as a reference.

LDA prediction accuracy for all models (s1, s2 and s3) was measured using cross validation where a random draw of 80% of the data was used to construct a model and then calculated prediction accuracy of the remaining 20% of the data. This was done 50 times for each treatment group of data to determine overall accuracy (98 ± 0.02 %) and within state accuracy (slow state = 99 ± 0.01 %, medium state = 99 ± 0.01 % and fast state = 95 ± 0.05 %; Table S4.3).

When treatment level tests were conducted on slow, medium and fast states, this comparison was only conducted with fish that performed those states making the number of larvae used for the model (see Treatment Testing section below) different for each comparison (Table S4.1).

Feeding Assay

Typically, KF larvae initiate feeding at 17 dpf (Weis and Weis 1995a). This study focused on assessing larvae behavior at the point that larvae were independent and feeding. Consequently, feeding ability in KF was assessed when they were 23 or 24 dpf (9 or 10 dph; 10.6 ± 0.82 mm). Larva were transferred from the 22 mm diameter wells to 54 mm diameter petri dishes at 22 dpf (60 mm petri dish). Feeding of *Artemia* continued morning and evening until ~24hr prior to the assay, so fish would be in a hungry state for the test. Similar to locomotion assays, feeding assays were conducted over a two-day period between 1300 and 1920 hr at a light level of 69 lx. Feeding assays were conducted in the same behavior chamber as the locomotion assay, when after 5 minutes of acclimation, recording started and ~15 (range 13-19) live *Artemia* were added to the dish. The test ended when 5 minutes had elapsed from when the *Artemia* were added to the dish.

Feeding bouts consisted of multiple presentations; the characteristic curved body posture, continuously swimming straight or at rest by just opening their mouths. For each of these presentations, the distance between the middle of the larva's mouth and *Artemia* was measured at

168

the time the larva orientated toward the *Artemia*, with their either eyes or body. This distance was termed reactive distance and was measured using ImageJ (version 1.51j8). For each capture attempt toward an *Artemia*, we recorded whether the larva successfully captured the *Artemia* and the time it took the larva to handle and consume the *Artemia*. Typically after a catching an *Artemia*, the larva sat or drifted momentarily and did not swim while it was consuming the prey. Handling time was defined as the time between prey capture and when the larva resumed normal swimming activity. Additionally, three consumption metrics were calculated: capture proportion defined as the number of captures divided by the total number of *Artemia* added to the dish, miss proportion defined as the number of feeding capture attempts that missed the *Artemia* divided by the total number of successful and unsuccessful capture attempts, and capture attempt ratio defined as the total number of feeding capture attempts (successful and unsuccessful) divided by the total number of *Artemia* added to the dish. When two *Artemia* were consumed during one feeding capture attempt, the consumption of both *Artemia* were assigned the same measurements.

Bayesian Model Analysis

For each behavioral endpoint (Table S4.2), we conducted a series of preliminary and final tests to determine whether there were differences between chemical dose treatments. The three different behavior assays and the number of behavior responses we measured were Feeding-5, Visual Motor Response (VMR) - 58, Locomotion - 30. Behavior responses that were not already normally distributed, we attempted to normalize using the boxcox function in the R MASS package (Table S4.4; Venables and Ripley 2002). Using a basic model containing only the treatment factor, behavior endpoints were transformed using the maximum lambda parameter for the exponential transformation suggested by the boxcox function in the R MASS package.

169

Below we describe the five different models that were used on the 93 behavior responses to determine differences between treatments, (see Table S4.4 for final transformation and model used for each behavior endpoint). Fitting multiple model types was necessary due to the various behavior endpoints having distinctively different distributions such as a proportional, normal, or a skewed response that even Box Cox transformations were not successful in normalizing.

Model Description

The Bayesian models used in locomotion and VMR behavior response models consisted of one main effect (treatment with 5 levels), covariate variable time of assay and a random batch effect because assays were ran in batches of 24-well dishes. The Bayesian model used for a locomotion and VMR behavior responses was

$$Locomotion\ or\ VMR\ Behavior\ Endpoint_{ijkl}$$
$$= \alpha + \beta_j * treatment_j + \delta_k * assay\ time_{k(i)} + \omega_l * batch_{l(i)} + \varepsilon_{ijkl}$$

where $Locomotion\ or\ VMR\ Behavior\ Endpoint_{ijkl}$ is the behavioral response metric on the ith individual, jth treatment, kth assay time and lth batch; α is the intercept, β_j is the treatment coefficient with a $Normal(0, \sigma_\beta^2)$ distribution, δ is the assay time coefficient with a $Normal(0, \sigma_\delta^2)$ distribution, ω_l is the batch coefficient, and ε_{ijkl} is the residual error. Treatment and batch are indicator variables containing 1 if the observation belongs to the corresponding factor category and 0 otherwise. Prior distributions for these two components are described in Table S4.5. Additionally, priors were needed for the α, treatment and assay time effects. In all models, we used non-informative, flat priors. For α, treatment and assay time we assumed a

normal distribution with a mean of 0 and standard deviation of at least 1.0×10^4 (i.e. precision of 1.0×10^{-4}). OpenBUGS model code for these models is shown in Tables S4.6, S4.7 and S4.8.

Two other Bayesian models were used to model the five feeding behavior responses that did not contain a batch effect since feeding assays were conducted one fish at a time. Additionally, days post fertilization (dpf) was included as a covariate since larvae were either 23 or 24 dpf. Lastly, these models did include intercept, treatment and assay time as described for the locomotion and VMR behavior models.

1) Normal response model

$$Feeding\ Behavior\ Endpoint_{ijkl}$$
$$= \alpha + \beta_j * treatment_j + \delta * assay\ time_{k(i)} + \omega * dpf_{l(i)} + \varepsilon_{ijkl}$$

where $Feeding\ Behavior\ Endpoint_{ijkl}$ is the prey handling time, lunge ratio or reaction distance (Table S4.4) on the ith individual, j^{th} treatment, k^{th} assay time and l^{th} dpf; α, β_j and, δ and their priors where described before, and ω is the dpf coefficient also with a non-informative normal prior assuming a normal distribution with a mean of 0 and standard deviation of at least 1.0×10^4 (i.e. precision of 1.0×10^{-4}). Lastly, the residual error followed a normal distribution $\varepsilon \sim Normal(0, \sigma_\varepsilon^2)$ with variance $\frac{1}{\sigma_\varepsilon^2} = \tau_j \sim I - Gamma(0.0001,\ 0.0001)$.

OpenBUGS code is presented in Table S4.9.

2) Binomial response model

$$Feeding\ Behavior\ Endpoint_{ijkl} \sim Binomial(p_{ijkl}, N_{ijkl})$$
$$logit(p_{ijkl}) = \beta_j * treatment_{j(i)} + \delta * assay\ time_{k(i)} + \omega * dpf_{l(i)} + \varepsilon_{ijkl}$$

where $Feeding\ Behavior\ Endpoint_{ijkl}$ is the prey capture probability or prey miss proportion (Table S4.7) on the ith individual, jth treatment, kth assay time and lth dpf and N_{ijkl} is the number of trials and p_{ijkl} is the probability of success distributed on a logit scale. The priors for β_j, δ and ω where described before. Lastly, the residual error followed a normal distribution $\varepsilon \sim Normal(0, \sigma_\varepsilon^2)$ with variance $\frac{1}{\sigma_\varepsilon^2} = \tau_j \sim I - Gamma(0.01,\ 0.01)$. OpenBUGS code is presented in Table S4.10.

Model Fitting and Convergence Diagnostics

Bayesian models were constructed using OpenBUGS version 3.2.3 rev 1012 (Lunn et al. 2009), R version 3.6.0 (R Core Team 2019) and packages R2OpenBUGS version 3.2 (Sturtz et al. 2005) and coda version 0.19-2 (Plummer et al. 2005). We fit the basic model using three chains, each with a minimum of 10000 iterations, 1000 burn in, and 1 thin, and monitored a subsample of parameters for convergence: treatment effects, overall mean, residuals, variance(s), precision parameter(s) and degree of freedom parameter(s). Then we performed preliminary multiple MCMC chain convergence diagnostics using Trace plots. If model did not converge, we increased either the number of iterations, burn in, or thin. Once the preliminary model trace plots were not showing any obvious convergence problems, further MCMC diagnostics were applied using a suite of tools to determine adequate MCMC chain length, model convergence and fit. 1) Autocorrelation plots indicated the level of thinning required to remove any autocorrelation. 2) Gelman-Rubin-Brooks shrink factor plots indicated the adequate number of iterations needed for burn in. 3) Raftery and Lewis's diagnostic tables were used to determine the number of additional iterations needed for accurate parameter estimation (default values of q

= 0.025, r = ± 0.005 and s = 0.95). 4) Finally, model goodness-of-fit was evaluated using residual diagnostics. When alternative models were to be compared, the model with the best posterior predictive distributions of residuals and replicated observations was retained.

Once a best-fitted model had been determined, we re-fit the model with the appropriate settings and monitored a slightly different suite of parameters: overall mean; population level treatment effects; variance and precision parameters; tail area probabilities of observing a difference; degrees of freedom; individual level predicted means, etc. With the model output and iteration levels we also determined effective sample size (effectiveSize function in coda R package), posterior distributions of parameters, and calculated a one-sided tail area probabilities (Bayesian P-values) from the two sided difference of parameter distributions. The summary output of this last model fit is presented in the results section of the paper and all relevant parameter posterior distributions can be found in Table S4.12.

Results

All larvae within each chemical/year/treatment group were successfully fitted with a HMM (Table S4.1). The number of larvae that consisted of one, two, or three behavior states exhibited a consistent pattern within each treatment, where a one state behavior model was never the best, three fish exhibited a two state model, and the rest of the fish were best fit using a three state behavior model (253 fish; Figure S4.1).

Genetics

Behavior Gene

This study focused on finding behaviors that reacted in a similar pattern to either MeHg or PCB126 treatments. In addition, we also tested individual genes and whether they responded in a similar pattern as any of the behavior endpoints. These results are reported in Tables S4.16 to S4.21.

Table S4.1. Summary of the number of assays and Atlantic killifish larvae (*Fundulus heteroclitus*) used in this study

Groups	SCO-Ctrl	SCO-Hg	SCO-PCB	NBH-Ctrl	NBH-PCB
VMRs					
Number of Assays-Larvae	30	29	28	29	28
Locomotion Assays					
Number of Assays-Larvae	56	68	31	66	35
HMMs					
Number of Larvae Attempted and Fitted a Model	56	68	31	66	35
Feeding Assays					
Number of Assays-Larvae	47	44	23	50	28
Total Length (mm ± SD)	10.78 (0.77)	10.63 (0.60)	9.80 (0.98)	10.81 (0.77)	10.35 (0.80)
Number of Larvae that did not consume Artemia	0	1	0	0	0

Table S4.2. Description of behavior endpoints examined in this study.

Behavior Endpoint	Definition
Feeding Assay	
Prey Capture Probability	The number of artemia captures divided by the total number of artemia added to the assay
Prey Handling Time (sec)	The number of seconds between the prey capture attempt and resuming normal activity, averaged over all feeding capture attempts during the 5 min assay
Capture Attempt Ratio	The total number of prey capture attempts divided by the total number of artemia added to the assay.
Prey Miss Proportion	The number of prey capture attempts that missed the artemia divided by the total number of prey capture attempts during the assay.
Reaction Distance (proportion of body length)	The distance (mm) between the artemia and larva when the larvae first orientates (notices) the artemia divided by the larva total length (mm), averaged over all the feeding capture attempts during the 5 minute assay.
Visual Motor Response Assay	
Startle Magnitude (mm)	Per frame maximum speed within 5 seconds after the startle minus the speed at the time of the startle.
Startle Response time (sec)	Difference in time between the startle and the maximum speed traveled within 5 seconds after the startle
Locomotion and VMR Assay	
Swimming Bouts (per sec)	The number of active swimming bouts per second. Swimming was defined as movement at least 1 mm/s for more than 5 frames (0.166 sec).
Swimming Bout Duration (sec)	Duration of all swimming bouts averaged over the 5 minute period.
Swimming Bout Speed (mm/s)	Per frame swimming speed averaged during a swimming bout; average bout speed averaged over the 5 minute period.
Swimming Bout Turning Angle	Per frame turning angle averaged during a swimming bout; individual average bout turning angle averaged over the 5 minute period. Ranges from -3.14 to 3.14, where negative values indicate right turns and positive values indicate left turns.
Total Distance Traveled (mm)	Total distanced traveled during swimming bouts for the entire 5 minute assay.
Total Time Swimming (sec)	Total time larvae were swimming during 5 minute test.
Overall Step Length (mm)	Per frame distance traveled during a 0.033 second period (one frame to the next) averaged over the entire 5 minute test [i.e. includes zeros when fish moved less than 1 mm/s for more than 5 frames (0.166 sec)].

Table S4.2 (cont'd)

Overall Step Length Variation	Standard deviation of distance traveled during 0.033 second period (one frame to the next).
Overall Turning Angle	Per frame turning angle averaged over frames when fish were swimming. Ranges from -3.14 to 3.14, where negative values indicate right turns and positive values indicate left turns.
Overall Turning Angle Variation	Standard deviation of per frame turning angle during 0.033 second period (one frame to the next).

HMM Model Parameters	
Step Length (mm)	Per frame distance traveled during a 0.033 sec period (one frame to the next) while the larvae was in each behavior state.
Step Length Variation	Standard deviation of the per frame distance traveled during 0.033 second period (one frame to the next) while in each behavior state.
Turning Angle	Per frame turning angle while in each behavior state. Ranges from -3.14 to 3.14, where negative values indicate right turns and positive values indicate left turns.
Turning Angle Variation	Angle concentration, i.e. kappa parameter in the von Mises distribution while in each behavior state.
Count	Number of frames a behavior state was performed.
Slow -> Slow, Medium -> Slow, Slow -> Medium, Medium -> Medium, Fast -> Slow, Fast -> Medium, Slow -> Fast, Medium -> Fast, Fast -> Fast	Per frame transition probability from state to state (e.g. Medium -> Slow is the probability of a fish transitioning from a medium speed swimming state to a slow swimming state).

Table S4.3. LDA cross validation results for different HMM behavioral states. N = 50 iterations. SD = standard deviation

Group	Overall Accuracy s3		Slow State		Medium State		Fast State		Num. of obs. in s3 LDA	Total num. of behavior states in s1 and s2	Num. of renamed state ID in s1 and s2	Num. of larvae with s3	Num. of larvae with s2	Num. of larvae with s1
	Mean	SD	Mean	SD	Mean	SD	Mean	SD						
NBH-Ctrl	1.00	0.01	1.00	0.00	1.00	0.00	0.98	0.03	198	0	0	66	0	0
NBH-PCB	1.00	0.00	1.00	0.00	1.00	0.00	1.00	0.00	108	4	1	36	2	0
SCO-Ctrl	1.00	0.10	1.00	0.01	1.00	0.01	0.99	0.02	168	0	0	56	0	0
SCO-Hg	0.96	0.03	0.98	0.03	1.00	0.00	0.90	0.07	204	0	0	68	0	0
SCO-PCB	0.99	0.02	1.00	0.00	0.98	0.05	0.97	0.06	90	2	0	30	1	0

Table S4.4. Model summary for each yellow perch *Perca flavescens* behavioral endpoint.

Submitted table as a sheet in an Excel file.

Table S4.5. Distributions and priors for parameters in models used to determine differences in treatments for locomotion behavior responses.

Model Table	Residual	Residual Variance	Batch Effect	Batch Effect Variance
S4.6	$\varepsilon \sim Normal(0, \sigma_\varepsilon^2)$	$\frac{1}{\sigma_\varepsilon^2} = \tau_j \sim I - Gamma(0.0001, 0.0001)$	$\varepsilon \sim Normal(0, \sigma_\varepsilon^2)$	$\frac{1}{\sigma_\varepsilon^2} = \tau_j \sim I - Gamma(0.01, 0.01)$
S4.7	$\varepsilon \sim Normal(0, \sigma_\varepsilon^2)$	$\sqrt{\sigma_\varepsilon^2} = \sigma_\varepsilon \sim U(0,01, 1000)$	$\varepsilon \sim Normal(0, \sigma_\varepsilon^2)$	$\sqrt{\sigma_\varepsilon^2} = \sigma_\varepsilon \sim U(0,01, 1000)$
S4.8	$\varepsilon \sim Student's\ T(0, \sigma_\varepsilon^2, df)$	$\frac{1}{\sigma_\varepsilon^2} = \tau_j \sim I - Gamma(0.0001, 0.0001)$	$\varepsilon \sim Student's\ T(0, \sigma_\varepsilon^2, df)$	$\frac{1}{\sigma_\varepsilon^2} = \tau_j \sim I - Gamma(0.01, 0.01)$

Table S4.6. Normal distribution OpenBUGS model containing treatment and time of assay effects and a random batch effect used to analyze locomotion behavior endpoints.

```
#inits<-function(){
#   list(batch.eff=runif(N2,-1000,1000),tau=runif(1,0,10),tau.a=runif(1,0,10))}
#inits()
model;
{
        for(i in 1:N){
        y[i]~dnorm(mu[i],tau)
        mu[i]<-mean+trt.eff[trt[i]]+time[i]*betta_mfn+batch.eff[batchid[i]]
        }
        mean~dnorm(0,1.0E-6)
#make covariate effect priors
        #time
        betta_mfn~dnorm(0,0.0001)
#make fixed main effect priors
        trt.eff[1]<-0
        for (i in 2:5){
        trt.eff[i]~dnorm(0,1.0E-6)
        }
#make random effect of batch priors
        for (i in 1:N2){
        batch.eff[i]~dnorm(0,tau.a)
        }
#predict estimates
#cell means models
        for(j in 1:5){
        Trt.mean[j]<-mean+trt.eff[j]
        }
#initial values
        var<-1/tau
        var.a<-1/tau.a
        tau~dgamma(0.0001,0.0001)
        tau.a~dgamma(0.01,0.01)
#difference calculations
        trt1<-Trt.mean[1]#sco salmon-fed ctl
        trt2<-Trt.mean[2]#sco tuna/hg fed
        trt3<-Trt.mean[3]#sco salmon-fed pcb40
        trt4<-Trt.mean[4]#nbh salmon-fed ctl
        trt5<-Trt.mean[5]#nbh salmon-fed pcb40
        diftrt2_1<-trt2-trt1
        pvaltrt2_1<-step(diftrt2_1)
        diftrt3_1<-trt3-trt1
        pvaltrt3_1<-step(diftrt3_1)
        diftrt3_2<-trt3-trt2
```

Table S4.6 (cont'd)

```
        pvaltrt3_2<-step(diftrt3_2)
        diftrt4_1<-trt4-trt1
        pvaltrt4_1<-step(diftrt4_1)
        diftrt5_4<-trt5-trt4
        pvaltrt5_4<-step(diftrt5_4)
        diftrt3_5<-trt3-trt5
        pvaltrt3_5<-step(diftrt3_5)
#ratio calculations
        ratiotrt2_1<-trt2/trt1
        ratiotrt3_1<-trt3/trt1
        ratiotrt3_2<-trt3/trt2
        ratiotrt4_1<-trt4/trt1
        ratiotrt5_4<-trt5/trt4
        ratiotrt3_5<-trt3/trt5
#posterior model checking, generate new obs based on model params mu, tau. assume normal dist
  for( i in 1 : N ) {
    ypred[i] ~ dnorm(mu[i],tau)
  }
#generate individual level predictions
    ypred_1 ~ dnorm(trt1,tau)#approximation of the individual observation, using average for other factors in the model.
    ypred_2 ~ dnorm(trt2,tau)#randomly selected individual
    ypred_3 ~ dnorm(trt3,tau)
    ypred_4 ~ dnorm(trt4,tau)
    ypred_5 ~ dnorm(trt5,tau)
#compute residuals using the kurtosis formula for both orig data (e) and rep data
  for( i in 1 : N ) {
    e[i]<-y[i]-mu[i]
  }
 SSE<-inprod(e[],e[])#sum of squares which is e squared
 ku<-sum(e[]) #sum up all values, there is one for each data point
 kpred<-sum(ypred[])
difs<-kpred-ku #find difference
difpval<-step(difs) #count how many times the rep data is larger than orig data
}
```

Table S4.7. Normal distribution OpenBUGS model containing treatment and time of assay effects and a random batch effect using uniform tau prior used to analyze locomotion behavior endpoints.

```
#inits<-function(){
#  list(batch.eff=runif(N2,-1000,1000),sdev=runif(1,0.01,1000),sdev.a=runif(1,0.01,1000))}
#inits()
model;
{
        for(i in 1:N){
        y[i]~dnorm(mu[i],tau)
        mu[i]<-mean+trt.eff[trt[i]]+time[i]*betta_mfn+batch.eff[batchid[i]]
        }
        mean~dnorm(0,1.0E-6)
#make covariate effect priors
        #time
        betta_mfn~dnorm(0,0.0001)
#make fixed main effect priors
        trt.eff[1]<-0
        for (i in 2:5){
        trt.eff[i]~dnorm(0,1.0E-6)
        }
#make random effect of batch priors
        for (i in 1:N2){
        batch.eff[i]~dnorm(0,tau.a)
        }
#predict estimates
#cell means models
        for(j in 1:5){
        Trt.mean[j]<-mean+trt.eff[j]
        }
#initial values
        sdev~dunif(0.01,1000)
        sdev.a~dunif(0.01,1000)
        var<-pow(sdev,2)
        var.a<-pow(sdev.a,2)
        tau<-pow(sdev,-2)
        tau.a<-pow(sdev.a,-2)
#difference calculations
        trt1<-Trt.mean[1]#sco salmon-fed ctl
        trt2<-Trt.mean[2]#sco tuna/hg fed
        trt3<-Trt.mean[3]#sco salmon-fed pcb40
        trt4<-Trt.mean[4]#nbh salmon-fed ctl
        trt5<-Trt.mean[5]#nbh salmon-fed pcb40
        diftrt2_1<-trt2-trt1
        pvaltrt2_1<-step(diftrt2_1)
```

Table S4.7 (cont'd)
```
        diftrt3_1<-trt3-trt1
        pvaltrt3_1<-step(diftrt3_1)
        diftrt3_2<-trt3-trt2
        pvaltrt3_2<-step(diftrt3_2)
        diftrt4_1<-trt4-trt1
        pvaltrt4_1<-step(diftrt4_1)
        diftrt5_4<-trt5-trt4
        pvaltrt5_4<-step(diftrt5_4)
        diftrt3_5<-trt3-trt5
        pvaltrt3_5<-step(diftrt3_5)
#ratio calculations
        ratiotrt2_1<-trt2/trt1
        ratiotrt3_1<-trt3/trt1
        ratiotrt3_2<-trt3/trt2
        ratiotrt4_1<-trt4/trt1
        ratiotrt5_4<-trt5/trt4
        ratiotrt3_5<-trt3/trt5
#posterior model checking, generate new obs based on model params mu, tau. assume normal
dist
  for( i in 1 : N ) {
    ypred[i] ~ dnorm(mu[i],tau)
    }
#generate individual level predictions
    ypred_1 ~ dnorm(trt1,tau)#approximation of the individual observation
    ypred_2 ~ dnorm(trt2,tau)#randomly selected individual
    ypred_3 ~ dnorm(trt3,tau)
    ypred_4 ~ dnorm(trt4,tau)
    ypred_5 ~ dnorm(trt5,tau)

#compute residuals using the kurtosis formula for both orig data (e) and rep data
  for( i in 1 : N ) {
    e[i]<-y[i]-mu[i]
    }
  SSE<-inprod(e[],e[])#sum of squares which is e squared
  ku<-sum(e[]) #sum up all values, there is one for each data point
  kpred<-sum(ypred[])
difs<-kpred-ku #find difference
difpval<-step(difs) #count how many times the rep data is larger than orig data
}
```

Table S4.8. Student's t distribution OpenBUGS model containing treatment and time of assay main effects and a random batch effect used to analyze locomotion behavior endpoints.

```
#inits<-function(){
#  list(batch.eff=runif(N2,-
1000,1000),df=runif(1,3,30),df.a=runif(1,3,30),tau=runif(1,0,10),tau.a=runif(1,0,10))}
#inits()
model;
{
        for(i in 1:N){
        y[i]~dt(mu[i],tau,df)
        mu[i]<-mean+trt.eff[trt[i]]+time[i]*betta_mfn+batch.eff[batchid[i]]
        }
        mean~dnorm(0,1.0E-6)
#make covariate effect priors
        #time
        betta_mfn~dnorm(0,0.0001)
#make fixed main effect priors
        trt.eff[1]<-0
        for (i in 2:5){
        trt.eff[i]~dnorm(0,1.0E-6)
        }
#make random effect of batch priors
        for (i in 1:N2){
        batch.eff[i]~dt(0,tau.a,df.a)
        }
#predict estimates
#cell means models
        for(j in 1:5){
        Trt.mean[j]<-mean+trt.eff[j]
        }
#initial values
        df~dunif(3,30)
        df.a~dunif(3,30)
        var<-1/tau
        var.a<-1/tau.a
        tau~dgamma(0.0001,0.0001)
        tau.a~dgamma(0.01,0.01)
#difference calculations
        trt1<-Trt.mean[1]#sco salmon-fed ctl
        trt2<-Trt.mean[2]#sco tuna/hg fed
        trt3<-Trt.mean[3]#sco salmon-fed pcb40
        trt4<-Trt.mean[4]#nbh salmon-fed ctl
        trt5<-Trt.mean[5]#nbh salmon-fed pcb40
        diftrt2_1<-trt2-trt1
```

Table S4.8 (cont'd)
```
        pvaltrt2_1<-step(diftrt2_1)
        diftrt3_1<-trt3-trt1
        pvaltrt3_1<-step(diftrt3_1)
        diftrt3_2<-trt3-trt2
        pvaltrt3_2<-step(diftrt3_2)
        diftrt4_1<-trt4-trt1
        pvaltrt4_1<-step(diftrt4_1)
        diftrt5_4<-trt5-trt4
        pvaltrt5_4<-step(diftrt5_4)
        diftrt3_5<-trt3-trt5
        pvaltrt3_5<-step(diftrt3_5)
#ratio calculations
        ratiotrt2_1<-trt2/trt1
        ratiotrt3_1<-trt3/trt1
        ratiotrt3_2<-trt3/trt2
        ratiotrt4_1<-trt4/trt1
        ratiotrt5_4<-trt5/trt4
        ratiotrt3_5<-trt3/trt5
#posterior model checking, generate new obs based on model params mu, tau. assume normal
dist
  for( i in 1 : N ) {
    ypred[i] ~ dt(mu[i],tau,df)
  }
#generate individual level predictions
    ypred_1 ~ dt(trt1,tau,df)#approximation of the individual observation, using average for other
factors in the model.
    ypred_2 ~ dt(trt2,tau,df)#randomly selected individual
    ypred_3 ~ dt(trt3,tau,df)
    ypred_4 ~ dt(trt4,tau,df)
    ypred_5 ~ dt(trt5,tau,df)
#compute residuals using the kurtosis formula for both orig data (e) and rep data
  for( i in 1 : N ) {
    e[i]<-y[i]-mu[i]
  }
  SSE<-inprod(e[],e[])#sum of squares which is e squared
  ku<-sum(e[]) #sum up all values, there is one for each data point
  kpred<-sum(ypred[])
difs<-kpred-ku #find difference
difpval<-step(difs) #count how many times the rep data is larger than orig data
}
```

Table S4.9. Normal distribution OpenBUGS model containing treatment, time of assay and days post hatch (dpf) effects used to analyze feeding behavior endpoints.

```
#inits<-function(){
#  list(tau=runif(1,0,10))
#}
model;
{
        for(i in 1:N){
        y[i]~dnorm(mu[i],tau)
        mu[i]<-mean+trt.eff[trt[i]]+time[i]*betta_mfn+dpf[i]*betta_dpf
        }
        mean~dnorm(0,1.0E-6)
#make covariate effect priors
        #time
        betta_mfn~dnorm(0,0.0001)
        #dpf
        #independent gaussian priors for the linear covariate
        betta_dpf~dnorm(0,0.0001)
#make fixed main effect priors
        trt.eff[1]<-0
        for (i in 2:5){
        trt.eff[i]~dnorm(0,1.0E-6)
        }
#back transform the outputs
#cell means models
        for(j in 1:5){
        Trt.mean[j]<-mean+trt.eff[j]
        }
#initial values
        tau~dgamma(0.0001,0.0001)
        var<-1/tau
        trt1<-Trt.mean[1]#sco salmon-fed ctl
        trt2<-Trt.mean[2]#sco tuna/hg fed
        trt3<-Trt.mean[3]#sco salmon-fed pcb40
        trt4<-Trt.mean[4]#nbh salmon-fed ctl
        trt5<-Trt.mean[5]#nbh salmon-fed pcb40
        diftrt2_1<-trt2-trt1
        pvaltrt2_1<-step(diftrt2_1)
        diftrt3_1<-trt3-trt1
        pvaltrt3_1<-step(diftrt3_1)
        diftrt3_2<-trt3-trt2
        pvaltrt3_2<-step(diftrt3_2)
        diftrt4_1<-trt4-trt1
        pvaltrt4_1<-step(diftrt4_1)
```

Table S4.9 (cont'd)

```
        diftrt5_4<-trt5-trt4
        pvaltrt5_4<-step(diftrt5_4)
        #diftrt6_4<-trt6-trt4
        #pvaltrt6_4<-step(diftrt6_4)
        #diftrt6_5<-trt6-trt5
        #pvaltrt6_5<-step(diftrt6_5)
        diftrt3_5<-trt3-trt5
        pvaltrt3_5<-step(diftrt3_5)
#ratio calculations
        ratiotrt2_1<-trt2/trt1
        ratiotrt3_1<-trt3/trt1
        ratiotrt3_2<-trt3/trt2
        ratiotrt4_1<-trt4/trt1
        ratiotrt5_4<-trt5/trt4
        #ratiotrt6_4<-trt6/trt4
        #ratiotrt6_5<-trt6/trt5
        ratiotrt3_5<-trt3/trt5
#posterior model checking, generate new obs based on model params mu, tau. assume normal
dist
  for( i in 1 : N ) {
    ypred[i] ~ dnorm(mu[i],tau)
  }
#generate individual level predictions
    ypred_1 ~ dnorm(trt1,tau)#approximation of the individual observation, using average for
other factors in the model.
    ypred_2 ~ dnorm(trt2,tau)#randomly selected individual
    ypred_3 ~ dnorm(trt3,tau)
    ypred_4 ~ dnorm(trt4,tau)
    ypred_5 ~ dnorm(trt5,tau)
    #ypred_6 ~ dnorm(trt6,tau)
#compute residuals using the kurtosis formula for both orig data (e) and rep data
  for( i in 1 : N ) {
    e[i]<-y[i]-mu[i]
  }
  SSE<-inprod(e[],e[])#sum of squares which is e squared
  ku<-sum(e[]) #sum up all values, there is one for each data point
  kpred<-sum(ypred[])
difs<-kpred-ku #find difference
difpval<-step(difs) #count how many times the rep data is larger than orig data
}
```

Table S4.10. Binomial distribution OpenBUGS model containing treatment, time of assay and days post hatch (dpf) effects used to analyze feeding endpoints.

```
#inits<-function(){
#  list(betta_mfn=runif(1,0,5),Trt.mean=runif(5,0,5),tau=runif#(1,0,10),betta_dpf=runif(1,0,5))
#}
#inits()
model
{
        for( i in 1 : N ) {
        y[i] ~ dbin(p[i],bs[i])
        e[i]~dnorm(0,tau)
        logit(p[i]) <-time[i]*betta_mfn+dpf[i]*betta_dpf+Trt.mean[trt[i]]+e[i]
        }
#set priors
        tau ~ dgamma(0.01,0.01)
        var<-1/tau
#make covariate effect priors
        #time
        betta_mfn~dnorm(0,0.0001)
        #dpf
        #independent gaussian priors for the linear covariate
        betta_dpf~dnorm(0,0.0001)
#make fixed main effect priors
        for (i in 1:5){
        Trt.mean[i]~dnorm(0,1.0E-6)
        }
#back transform the outputs
#cell means models
        for(j in 1:5){
        trt.eff[j]<-Trt.mean[j]-Trt.mean[1]
        }
#other values
        trt1<-1/(1+exp(-Trt.mean[1]))#sco salmon-fed ctl, back transformed trt mean, in the scale
of the binomial prob. the probability of being attacked by the average population. do not back
transformed
        trt2<-1/(1+exp(-Trt.mean[2]))#sco tuna/hg fed
        trt3<-1/(1+exp(-Trt.mean[3]))#sco salmon-fed pcb40
        trt4<-1/(1+exp(-Trt.mean[4]))#nbh salmon-fed ctl
        trt5<-1/(1+exp(-Trt.mean[5]))#nbh salmon-fed pcb40

        diftrt2_1<-Trt.mean[2]-Trt.mean[1]#compare on linear scale logit
        pvaltrt2_1<-step(diftrt2_1)
        diftrt3_1<-Trt.mean[3]-Trt.mean[1]
        pvaltrt3_1<-step(diftrt3_1)
        diftrt3_2<-Trt.mean[3]-Trt.mean[2]
```

Table S4.10 (cont'd)

```
        pvaltrt3_2<-step(diftrt3_2)
        diftrt4_1<-Trt.mean[4]-Trt.mean[1]
        pvaltrt4_1<-step(diftrt4_1)
        diftrt5_4<-Trt.mean[5]-Trt.mean[4]
        pvaltrt5_4<-step(diftrt5_4)
        diftrt3_5<-Trt.mean[3]-Trt.mean[5]
        pvaltrt3_5<-step(diftrt3_5)
#ratio calculations
        ratiotrt2_1<-trt2/trt1 #use the back transformed scale
        ratiotrt3_1<-trt3/trt1
        ratiotrt3_2<-trt3/trt2
        ratiotrt4_1<-trt4/trt1
        ratiotrt5_4<-trt5/trt4
        ratiotrt3_5<-trt3/trt5
#posterior model checking, generate new obs based on model params
        for( i in 1 : N ) {
                ypred[i] ~ dbin(p[i],bs[i])
        }
#generate individual level predictions
        #need to estimate error for each group
        for(j in 1:5){
        ee[j]~dnorm(0,tau)
        }
        ypred_1 <- 1/(1+exp(-(Trt.mean[1]+ee[1]))) #probability of bs capture by a random
individual in trt1
        ypred_2 <- 1/(1+exp(-(Trt.mean[2]+ee[2])))
        ypred_3 <- 1/(1+exp(-(Trt.mean[3]+ee[3])))
        ypred_4 <- 1/(1+exp(-(Trt.mean[4]+ee[4])))
        ypred_5 <- 1/(1+exp(-(Trt.mean[5]+ee[5])))

}
```

Table S4.11. A list of all parameters included in the individual-based model, units, equation reference and references (mm = millimeter, m = meter, d = day, g = gram, °C = celcius, J = joule, # = count, s = sec, hr = hour, µg = microgram, O_2 = oxygen, W = weight, L = length, SD = standard deviation, ml = milliliter).

Variable	Value	Units	Explanation	Reference
Initialize larva				
Number of fish	2500	#	Number of larva	Smith et al. 2002
Mean Length	5.96	mm	Mean length	Marteinsdottir and Able 1992
Mean SD of Length	0.4	mm	Standard deviation of length	Marteinsdottir and Able 1992
Length max	8	mm	Maximum length	Estimated
Length min	5	mm	Minimum length	Estimated
Length at which fish exists model	24	mm	Size at Exit	Abraham 1985
Time & physical				
Initial day of model	100	day	Julian Date	
Number of days model runs	100	day		
Volume	1000	m³	Volume of the lake modeled	
Yolk-sac growth				
Yolk-sac growth	0.40	mm/d	growth of yolk-sac larvae	Marteinsdottir and Able 1992
Length exogenous feeding begins	4	days	Days until switch to feeding	Estimated
W_L A parameter	0.0000015	g dry	Length-weight intercept	Kneib and Parker 1991
W-L b parameter	3.25	g dry	Length-weight slope	Kneib and Parker 1991
Bioenergetics (from Deslauriers et al. 2017 unless otherwise noted)				
CA	0.2	g/g	Intercept of the mass dependence function for consumption	
CB	-0.25	g/g/d	Slope of mass dependence function for consumption	
CQ	2.22	g/g/d	Temperature-dependent coefficient of consumption (approximates Q10)	
CTO	27	°C	Optimal temperature for consumption	

Table S4.11 (cont'd)

CTM	34	°C	Maximum consumption temperature	
RA	0.02	gO_2/g	Intercept of the mass dependence function for respiration	
RB	-0.17	$gO_2/g/d$	Slope of mass dependence function for respiration	
RQ	2	$gO_2/g/d$	Temperature-dependent coefficient of respiration (approximates Q10)	
RTO	29	°C	Optimal temperature for respiration	
RTM	36	°C	Maximum respiration temperature	
Act	1.25	NA	Activity multiplier on respiration	
SDA	0.1	NA	Specific dynamic action coefficient	
FA	0.1	NA	Egestion coefficient	
UA	0.06	NA	Excretion coefficient	
ED	3000	J/g wet	Energy density of larvae	
percent dry	0.2	%	Dry to wet conversion	Estimated
Starvation	75	%	Probability of starvation	Letcher et al. 1996
			Prey	
Small prey density	0.0175	#/ml	Copepods	Fleeger et al. 2008
Large prey density	0.008	#/ml	Amphipods	Estimated but based on ostracods in Fleeger et al. 2008
Small prey length	0.485	ml	Copepods	Fulford et al. 2006
Large prey length	0.6	ml	Amphipods	Fulford et al. 2006
Small Prey mass	1.215	µg dry	Copepods	Fulford et al. 2006
Large prey mass	3.8	µg dry	Amphipods	Fulford et al. 2006
Large prey energy density	2301.2	J/g wet	Copepods	Hartman and Brandt 1995
Small prey energy density	4125.424	J/g wet	Amphipods	Hartman and Brandt 1995

Table S4.11 (cont'd)

			Foraging	
Ssa	0.776	mm/s	Swimming speed intercept	Letcher et al. 1996
SSb	1.07	mm/s/mm	Swimming speed slope	Letcher et al. 1996
Handling Time a	0.264	s	Handling time intercept	Letcher et al. 1996
Handling Time a	7.0151	s	Handling time slope	Letcher et al. 1996
Light	12	hr	Active time during the day	Letcher et al. 1996
			Killifish Predators (Adults)	
Number of predators	200	#	Number of predators	Calibrated
Mean predator length	45	mm	Mean predator length	Assigned (Age 1 size)
SD predator length	2.5	mm	Standard deviation of length	Estimated
Min predator length	25.5	mm	Minimum length	Estimated
Max predator length	96	mm	Maximum length	Valiela et al. 1977
Predator CTM	34	∘C	Maximum temperature for consumption	Madon et al. 2001
Predator CTO	27	∘C	Optimum temperature for consumption	Madon et al. 2001
Predator CQ	2.22	g/g/d	Temperature-dependent coefficient of consumption (approximates Q10)	Madon et al. 2001
Predator swimming speed	3	Body Lengths	Multiplier on body lengths for distance swum in a second	Cowan et al. 1996
Predator reactive distance	0.8	mm	Reactive distance multiplier	Cowan et al. 1996
			Calibration	
Growth	0.31	mm/d		Nacci unpublished data

Table S4.12. A list of all behavior parameter distributions and resulting multipliers used to assess treatment impacts in the individual based model. Posterior distributions are from the individual level predicted responses and multipliers were generated from back transformed values. N indicates this behavior was significantly lower than the control, P indicates this behavior was significantly higher than the control.

Killifish Group	Chemical	Variable	Individual Level Distribution					Multipliers			
			Mean	SD	Min.	Max.		Mean	SD	Min.	Max.
SCO	Control	Prey Handling Time	27.89	8.186	11.88	43.67		1.000	0.287	0.547	1.986
SCO	Control	Prey Miss Proportion	-2.674	1.308	-5.255	-0.1185		1.000	0.110	0.589	1.105
SCO	Control	Reaction Distance (mm)	167.3	19.05	129.4	204.9		1.000	0.232	0.464	1.510
SCO	Control	Swimming Bout Speed (mm/s)	137.1	27.9	82.41	191.7		1.000	0.221	0.644	1.698
SCO	Control	Total Time Swimming (sec)	58.94	16.72	26.14	91.75		0.547	0.168	0.194	0.943
SCO	MeHg	Prey Handling Time	28.51	8.2	12.4	44.64		0.972	0.281	0.530	1.924
SCO	MeHg	Prey Miss Proportion	-3.305	1.328	-5.952	-0.7121		1.047	0.070	0.746	1.108
SCO	MeHg	Reaction Distance (mm)	177.7	19.1	139.9	215.3	p	1.151	0.226	0.619	1.643
SCO	MeHg	Swimming Bout Speed (mm/s)	144.4	27.91	89.75	199.1		0.936	0.194	0.614	1.547
SCO	MeHg	Total Time Swimming (sec)	53.25	16.69	20.48	85.98		0.481	0.163	0.142	0.869
SCO	PCB126	Prey Handling Time	17.94	8.278	1.574	34.12	p	1.662	0.827	0.756	7.003
SCO	PCB126	Prey Miss Proportion	-1.346	1.327	-3.963	1.251	p	0.826	0.211	0.247	1.090
SCO	PCB126	Reaction Distance (mm)	172.3	19.32	134.6	209.9		1.078	0.230	0.540	1.575
SCO	PCB126	Swimming Bout Speed (mm/s)	142.8	28.13	87.5	197.8		0.951	0.203	0.619	1.591
SCO	PCB126	Total Time Swimming (sec)	48	16.85	14.91	81.09	n	0.425	0.161	0.094	0.808
NBH	Control	Prey Handling Time	27.89	8.162	11.74	43.84		1.000	0.287	0.545	2.004
NBH	Control	Prey Miss Proportion	-3.003	1.308	-5.589	-0.4375		1.000	0.083	0.657	1.076

Table S4.12 (cont'd)

NBH	Control	Reaction Distance (mm)	179.9	18.97	142.5	216.9		1.000	0.190	0.557	1.414
NBH	Control	Swimming Bout Speed (mm/s)	141.5	27.87	86.93	196		1.000	0.212	0.654	1.670
NBH	Control	Total Time Swimming (sec)	51.82	16.7	19.06	84.56		0.466	0.163	0.130	0.851
NBH	PCB126	Prey Handling Time	23.22	8.243	6.883	39.16	p	1.238	0.424	0.637	2.917
NBH	PCB126	Prey Miss Proportion	-2.261	1.323	-4.893	0.314		0.933	0.135	0.457	1.072
NBH	PCB126	Reaction Distance (mm)	172	19.27	133.6	210		0.907	0.198	0.446	1.339
NBH	PCB126	Swimming Bout Speed (mm/s)	134.3	28.12	79.02	189.3		1.073	0.243	0.682	1.856
NBH	PCB126	Total Time Swimming (sec)	49.88	16.81	16.94	82.89		0.443	0.161	0.111	0.830

Table S4.13. Posterior distributions for all model parameters and each behavioral endpoint.

Submitted table as a sheet in an Excel file.

Table S4.14. Significant results of the treatment effects on Atlantic killifish larvae behavior after exposure to sublethal levels of MeHg and PCB126. Presented for each behavior endpoint and treatment is the mean (original or back-transformed), transformed mean, P-value in parentheses, and pattern of significant trends. Trends are based on original mean trends. P-values and trends are reported in the following order: SCO-Ctrl vs SCO-Hg, SCO-Ctrl vs SCO-PCB, SCO-Ctrl vs NBH-Ctrl, SCO-PCB vs NBH-PCB, NBH-Ctrl vs NBH-PCB (Neg = significant negative trend, Pos = significant positive trend, ⚊ = no significant trend, HMM = Hidden Markov Chain model endpoint).

Submitted table as a sheet in an Excel file.

Table S4.15. Total number of significantly differentially expressed genes (alpha = 0.05) found in the brains of Atlantic killifish *Fundulus heteroclitus* in this study.

Treatment Comparison	Number of Differentially Expressed Genes
SCO-Ctrl vs SCO-Hg	22
SCO-Ctrl vs SCO-PCB 40 ng/L	383
SCO-Ctrl vs NBH-Ctrl	3220
SCO-PCB 40 ng/L vs NBH-Ctrl	602
SCO-PCB 40 ng/L vs NBH-PCB 40 ng/L	210
SCO-PCB 40 ng/L vs NBH-PCB 400 ng/L	1348
NBH-Ctrl vs NBH-PCB 40 ng/L	8
NBH-Ctrl vs NBH-PCB 400 ng/L	830
NBH-PCB 40 ng/L vs NBH-PCB 400 ng/L	896

Table S4.16. Significantly differentially expressed genes (alpha = 0.05) found in the brains of Atlantic killifish *Fundulus heteroclitus* in this study. Significant trends and FDR value are reported (Neg = significant negative trend, Pos = significant positive trend). Blanks indicate comparison was tested but did not result in a significant difference.

Submitted table as a sheet in an Excel file.

Table S4.17. Significantly altered gene pathways (alpha = 0.05) found in the brains of Atlantic killifish *Fundulus heteroclitus* in this study. Significant trends and FDR value are reported (Neg = significant negative trend, Pos = significant positive trend). Blanks indicate comparison was tested but did not result in a significant difference.

Submitted table as a sheet in an Excel file.

Table S4.18. Significant treatment patterns from MeHg and PCB126 exposure shared by genes and behavior endpoints in Scorton Creek (SCO) and New Bedford Harbor (NBH) Atlantic killifish Fundulus heteroclitus found in this study. Both the original and opposite behavior endpoint trends are listed. Significant trends are reported in the following order: SCO-Low Hg vs SCO-High Hg, SCO-Low Hg vs SCO-Low Hg – Low PCB, SCO-Low Hg vs NBH-Low Hg, SCO-Low Hg – Low PCB vs NBH-Low Hg – Low PCB, NBH-Low Hg vs NBH-Low Hg – Low PCB (neg = significant negative trend, pos = significant positive trend, - = no significant trend, HMM = Hidden Markov Chain model endpoint).

| Reference Number | Significant Treatment Pattern | | | | | Altered Gene | Significant Treatment Pattern in a Behavior Endpoint | |
	SCO-Ctrl vs SCO-Hg	SCO-Ctrl vs SCO-PCB	SCO-Ctrl vs NBH-Ctrl	SCO-PCB vs NBH-PCB	NBH-Ctrl vs NBH-PCB		Original Treatment Pattern	Opposite Treatment Pattern
1						LOC105917295, LOC105934237		Swimming Bout Duration Period 3 (sec)
2						LOC105924291	Capture Attempt Ratio	
3						scamp1		Capture Attempt Ratio

Table S4.19. Significant MeHg treatment patterns shared by differentially expressed genes and behavior endpoints in Atlantic killifish *Fundulus heteroclitus* found in this study. Both the original and opposite behavior endpoint trends are listed (Neg = significant negative trend, Pos = significant positive trend, - = no significant trend, HMM = Hidden Markov Chain model endpoint).

Significant Treatment Pattern	Gene Expression	Behavior Endpoint
	LOC105915521, LOC105916522, LOC105917295, LOC105918273, LOC105922825, LOC105924291, LOC105934237, LOC105936060, LOC110366363, LOC110366373, LOC118559084, LOC118560703, LOC118560704, LOC118562969, LOC118563898, si:ch211-186j3.6	HMM Fast -> Fast TP, Capture Attempt Ratio, HMM Medium -> Medium TP, Prey Capture Probability, Reaction Distance (mm)
	klhl6, LOC105915433, LOC105933875, LOC118566104, scamp1, si:dkey-21c1.4	HMM Medium State Turning Angle Variation, HMM Medium -> Fast TP, Overall Step Length Period 4 (mm), Overall Step Length Variation Period 4, Swimming Bout Duration Period 3 (sec), Total Distance Traveled Period 4 (mm), Total Time Swimming Period 3 (sec)

Table S4.20. Significant PCB126 treatment patterns shared by differentially expressed genes and behavior endpoints in Atlantic killifish *Fundulus heteroclitus* found in this study. Both the original and opposite behavior endpoint trends are listed. Significant trends are reported in the following order: SCO-Ctrl vs SCO-PCB, SCO-Ctrl vs NBH-Ctrl, SCO-PCB vs NBH-PCB, NBH-Ctrl vs NBH-PCB (Neg = significant negative trend, Pos = significant positive trend, ⊢ = no significant trend, HMM = Hidden Markov Chain model endpoint, TP = Transition Probability).

Submitted table as a sheet in an Excel file.

Table S4.21. Significant mercury treatment patterns shared by gene pathways and behavior endpoints in Scorton Creek (SCO) Atlantic killifish found in this study. Both the original and opposite behavior endpoint trends are listed. Significant trends are reported in the following order: SCO-Ctrl vs SCO-MeHg (Tan = significant negative trend compared to control, Blue = significant positive trend compared to control, Black = no significant trend compared to control, HMM = Hidden Markov Chain model endpoint, TP = Transition Probability).

Submitted table as a sheet in an Excel file.

Table S4.22. Individual based model results showing treatment means for individual larva survival and growth of Atlantic killifish *Fundulus heteroclitus* found in this study.

Scenario	IBM Output Mean	
	Survival (%)	Growth (mm/d)
Spring		
SCO-Ctrl	1.512	0.29871
SCO-MeHg	1.648	0.29782
SCO-PCB	0.044	0.12975
NBH-Ctrl	1.084	0.29197
NBH-PCB	0.416	0.29251
Summer		
SCO-Ctrl	1.068	0.30167
SCO-MeHg	1.244	0.30697
SCO-PCB	0.288	0.25546
NBH-Ctrl	0.788	0.28597
NBH-PCB	0.42	0.28322
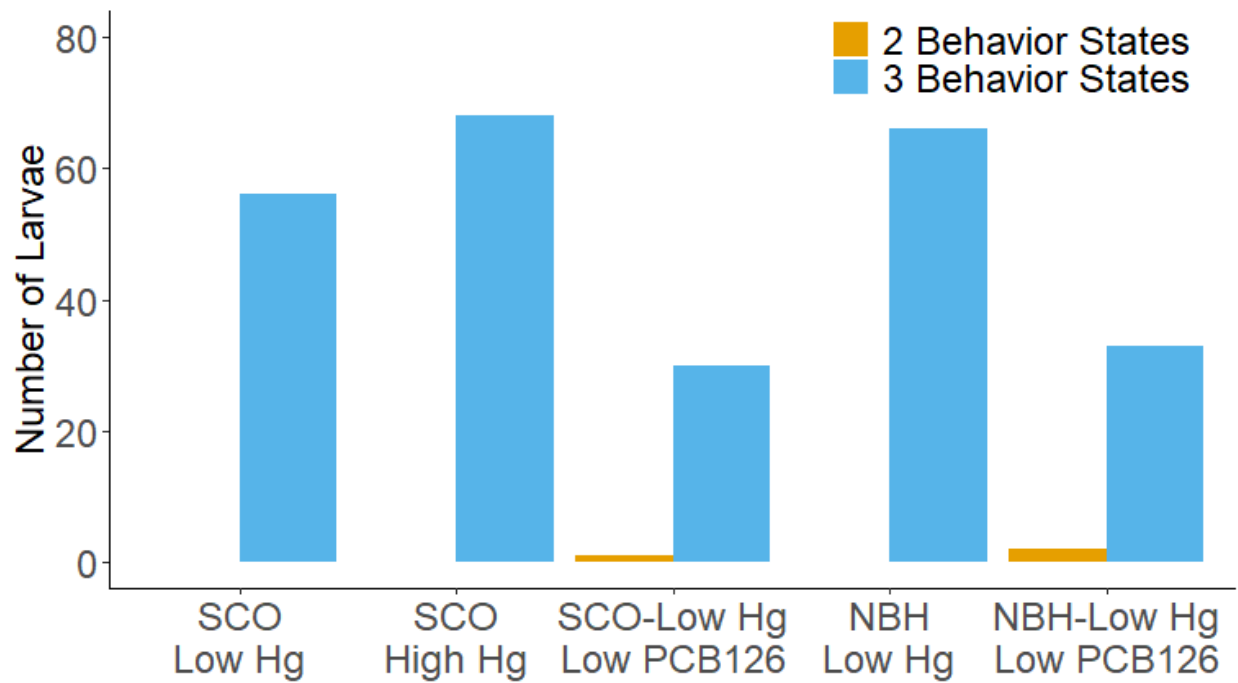
Figure S4.1. Number of best fit hidden Markov models for Atlantic killifish larvae in the locomotion assay that contained two or three different behavior states.
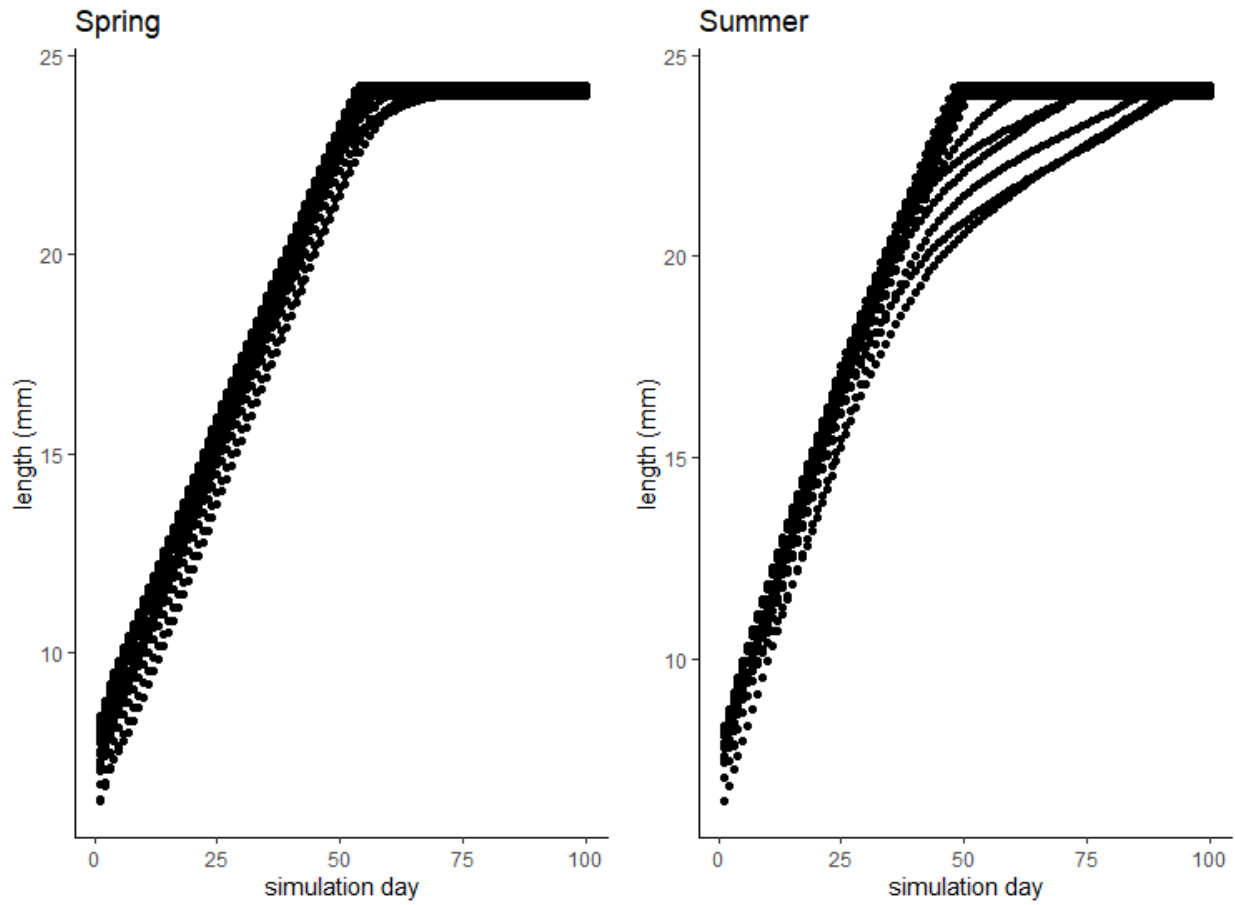
Figure S4.2. An example of the length (mm) verses simulation day for individual Scorton Creek control fish that were alive at the end of one run of a spring and summer scenario.

Adverse Outcome Pathway
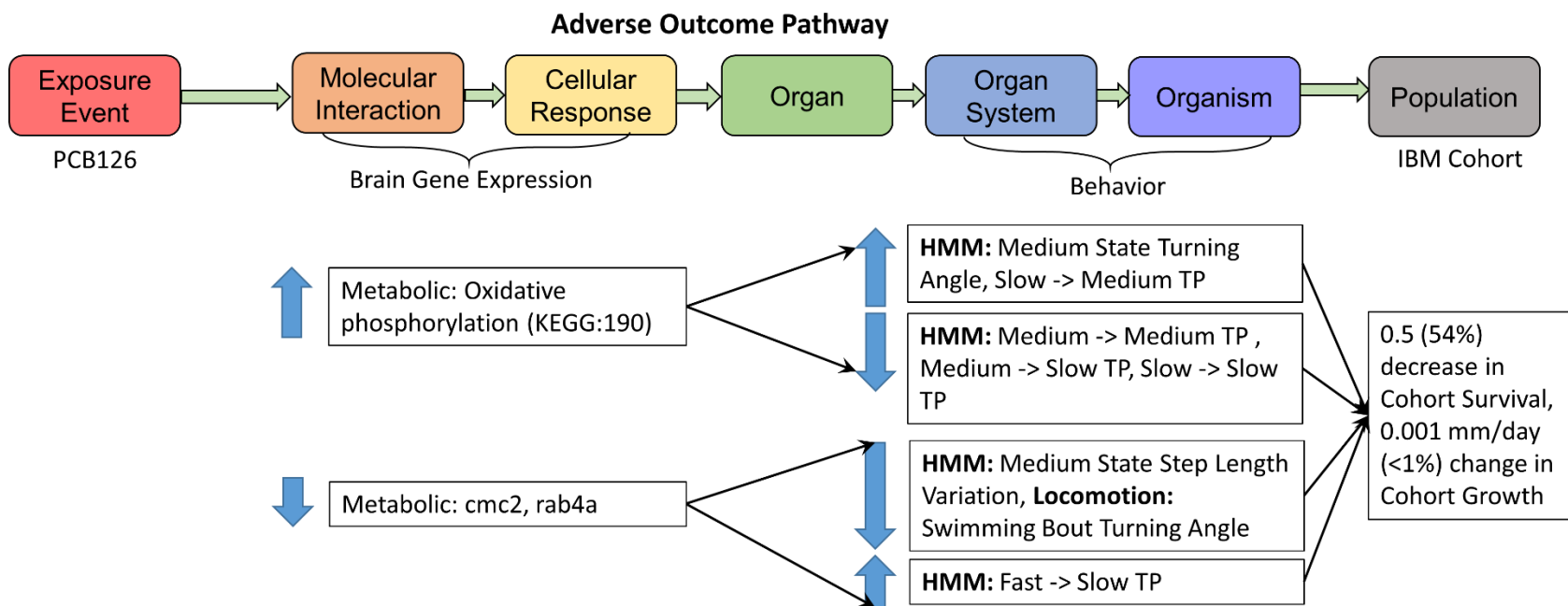
Figure S4.3. Significant PCB126 treatment patterns shared by gene expression and behavior endpoints in the New Bedford Harbor (NBH) Atlantic killifish found in this study. Both the original and opposite behavior endpoint trends are listed. (HMM = Hidden Markov Chain model endpoint, TP = Transition Probability).

APPENDIX IV:

Chapter 5 Supplementary Materials

Methods used with zebrafish *Danio rerio* (ZF) and yellow perch *Perca flavescens* (YP) data collection are the same as those reported in (Albers et al. 2022a, 2022d), specific details follow.

All Species Brain Gene Expression

Brain collection

Brain collection was performed essentially as described by Vargas et al. (2011) on a random subset of 25 dpf YP (n=36) and 6 dpf ZF (n=36), before any behavior assays. The exception was for Atlantic killifish *Fundulus heteroclitus* (KF), where a random subset of 16 dpf larvae were removed after the VMR assay to contribute brain samples for gene expression (n=69), about half had been through the VMR assay (n=36) and half had not been through the VMR assay (n=33). Larvae were gently transferred to a 60 mm petri dish and 4°C embryo medium was quickly added to provide anesthesia. Larvae were transferred to a new petri dish, water was removed, and individuals were immobilized in a drop of 2% low melting point agarose made with artificial cerebral spinal fluid (aCSF; 131 mM NaCl, 2 mM KCl, 1.25 mM KH$_2$PO$_4$, 2 mM MgSO$_4$, 10 mM glucose, 2.5 mM CaCl$_2$, 20 mM NaHCO$_3$). A dissection pin was used to mount the larvae in dorsal/ventral recumbency, just under the surface of the agarose. aCSF was added and dishes were placed on ice. Intact brains were removed using dissection pins, transferred individually in 5µl aCSF to 1.5 ml microcentrifuge tubes, then frozen in liquid nitrogen prior to storage at -80°C.

<u>Brain Gene Analysis</u>

Total RNA was isolated from 6 embryos brains per treatment using the Qiagen RNeasy®
Micro Kit (Germantown, MD, USA) following the Purification of Total RNA from Animal and
Human Tissues protocol in the RNeasy® Micro Handbook with slight modifications. The
modification included homogenization of brain tissue in 350 µL of RLT buffer using a pellet
pestle and elution of Total RNA using 15 µL of RNase-free water. RNA quality was assayed
using the Agilent High Sensitivity RNA ScreenTape System (Waldbronn, Germany) for the
Agilent 2200 TapeStation (Palo Alto, CA, USA), and RNA was quantified using the NanoDrop
2000 (ThermoFisher Scientific, Waltham, MA).

The raw reads from (6 larvae from each treatment) were mapped and quantified using
salmon (Patro et al. 2017) (v1.3.0) against the reference transcriptome (see below). tximport
(Soneson et al. 2015) (v1.16.1) was used to import transcript-level estimates from salmon
summarize the data to the gene level. These genes were filtered such that only genes with an
average log Counts per Million > 1 across all samples were retained for differential expression.
edgeR (v3.30.3) was used to determine differentially expressed genes (DEGs). OrthoFinder
(v2.5.4) was used to find orthologous genes in *D. rerio.* The GAGE R package (Luo et al. 2009)
(v2.40.0) was used to perform gene-set enrichment analysis using *D. rerio* GO gene-sets, KEGG
gene-sets and the *D. rerio* orthologs of genes that passed the filter. Significant pathway trends
were determined using a false discovery rate (FDR) of 0.05.

Behavior/Gene expression comparisons

Each endpoint response, either gene or behavior, were summarized over all treatments by
first determining whether there was a significant difference found while testing the treatment

comparisons (alpha = 0.05). When a significant difference was found, a positive (Pos) or negative (Neg) trend was indicated using the relative amount of the first treatment to the second treatment. The endpoint value used to determine the trend direction were the back-transformed treatment means. The resulting summary pattern was used to group behavior and gene expression endpoints that responded the same together. This approach is more robust than other data mining methods (e.g. PCA) because it 1) takes into account the treatment design of the experiment and the comparisons and 2) limits comparisons to only those endpoints that were determined to be statistically different from one another, which limits the excess of comparing all endpoints.

Zebrafish Dosimetry and Husbandry

Zebrafish embryo procurement and husbandry protocols from Carvan et al. (2017) and exposure protocols from Albers et al. (2022) were followed. A general description and noted exceptions follow. All methods were approved by the University of Wisconsin at Milwaukee Institutional Animal Care and Use Committee (IACUC, #18-19#04). Adult EK strain zebrafish were housed at a maximum density of 10 fish/L (~20 females + 10 males per 3L tank), in a flow-through dechlorinated water system maintained at 26–29°C on a 14:10 hour light: dark photoperiod at the UWM School of Freshwater Sciences. The evening before spawning, each tank of adult fish was transferred to its own static spawning tanks according to standard methods and allowed to spawn the following morning for approximately one hour. For this study, tanks containing roughly 20 females and 10 males were spawned and eggs were collected ≤1 hpf and placed into metal-free, plastic culture dishes (100 mm diameter × 25 mm depth) in E2 medium

(pH 7.2; 1 L of E2 medium contained: 0.875 g NaCl, 0.038 g KCl, 0.120 g MgSO₄, 0.021 g KH2PO₄ and 0.006 g Na₂HPO₄).

This study chose exposure levels and timing that either mimicked parental transfer of MeHg or water transfer for PCB126 (Westerlund et al. 2000; Alvarez et al. 2006; Mora-Zamorano et al. 2016a; Bridges et al. 2016a, 2016b; Carvan et al. 2017). Since behavior effects are a focus of this study, we used dose levels of these chemicals that did not create any observable physical deformities [e.g. Early Life-Stage Toxicity score; (Heiden et al. 2005)] which would alter behavioral endpoints like swimming or eating. To that end, a preliminary dosimetry/sensitivity study was used in addition to previous research results [e.g. (Mora-Zamorano et al. 2016a)] to determine dosing levels that met these criteria and all larvae exhibiting deformities or died with 24 hr after assay were removed from analysis. Embryos in this study were collected ≤1 hpf and placed into plastic Petri dishes (100 mm diameter × 25 mm depth) in E2 medium. The newly fertilized eggs were then counted into new dishes at a density of 200 eggs per plate and exposed to 40ml E2 medium containing MeHg or PCB126 (0.2mL media per embryo). Embryos were exposed immediately following plating until ~24 hours post-fertilization (~2-24 hpf, starting at 2-4 cell stage] with either 0, 0.00021 and 0.02156 ppm MeHg (based on 0, 0.001 and 0.1 µM of MeHg; MeHgCl in a 100% ethanol solvent), or 0, 0.1 and 10ppm PCB126 (PCB126 in a 100% DMSO) [each 0 concentration treatment (i.e. control) contained water and the appropriate solvent resulting in all treatments containing either 33.33ppm ethanol or 500ppm DMSO]. At 24 hpf, zebrafish eggs were rinsed 4 times with clean embryo medium to stop chemical exposure. Embryos were maintained in culture plates and incubated at 26-28°C for 5 days (until 6dpf) and given fresh E2 medium daily. At 6dpf, healthy larvae were transferred into 1L static tanks at a density of 60 larvae per tank where they were

maintained until all behavior assays were conducted. Starting on day 6 post fertilization, larvae were fed 5–100 micron Golden Pearl Reef & Larval Fish Diet (Brine Shrimp Direct, Ogden, UT), as previously described (Carvan et al. 2017). Platinum grade *Artemia nauplii* (Argent Laboratories, Redmond, WA) were added to the larval diet starting at 9 dpf. A separate group of ZF were used for each assay so no larva was used twice.

Directly after exposure and rinsing, embryos were collected from 3 different clutches of eggs (biological replicates) and were removed from their petri dish and stored at -80°C until chemical analysis in glass vials with Teflon coated tops for PCB126 treatments. PCB126 treated samples were analyzed with GC/ECD using EPA method 8082 with a minimum detection limit of 0.5 pg of PCB126 in the 0.5 mL sample. Estimates of MeHg in ZF larva were assumed to be the same as those found in (Carvan et al. 2017) table S5.2 f0 generation.

Movement Data collection

Spontaneous movement of larvae was tracked using Ctrax software (version 0.5.18 (Branson et al. 2009)) or DanioVision© system version 8.0 (Noldus Information Technology, Leesburg, VA). After reviewing the video in both assays, one major tracking error type was identified where artificial movement was added when the track bounced back and forth between two parts of the same fish. The error occurred most frequently when the fish ceased movement but the track did not (this occurred from a mismatch between the precise tracking software and the pixelated video of small larvae and it presents as a type of sudden movement between two separate parts of the fish's body, i.e. the track "jitters" rapidly back and forth). This error type as well as incorrect fish identities were corrected using a combination of manual correction using the Ctrax Fixerrors GUI (version 0.2.24) and automatic corrections using a set of error

identifying criteria. Manual correction was used to correct all types of tracking errors, where any track deviation greater than 1 pixel or 0.15 mm, was manually corrected to accurately represent the middle point of each larvae. In addition, automated error correction first identified and flagged fish locations containing errors using the following criteria: turning angle between previous and future location was > 150 degrees and distance between previous and future location was < 0.2 mm. During periods with high error occurrence, movement less than 0.2 mm was ignored. Additionally, locations large erratic jumps were flagged using the following criteria: turning angle between previous and future location was > 160 degrees and distance between previous and future location was <= 0.7 mm and the distance traveled between the location and each of the previous and future locations was >= 2 mm and <= 30% difference in length. Once locations of errors were identified as well as the occasional missing locations, the x, y coordinates were replaced using equidistance locations between the nearest two non-error locations.

Locomotion Assay

Typically, ZF larvae initiate swimming at 5 dpf and by 6 dpf ZF were independent and actively swimming. Consequently, the locomotion assay was conducted on 6 dpf ZF larvae, where 10 larvae were placed in a square slanted side petri-dish (outside dimensions of 72.5 x 72.5 mm, swimming area dimensions of 56 x 56 mm) with 25 ml of water (~8 mm water depth; see Table S5.1 for the number of assays and fish). Since previous locomotion assays indicated some neurotoxicants impact larvae only during light periods (Mora-Zamorano et al. 2017), light levels were constant during the entire assay and set to 69 lux (MacPhail et al. 2009). Similar to previous studies(Mora-Zamorano et al. 2017), light was generated using an LCD computer

monitor placed below the petri dish and set to illuminate the dish using pure white light (Red

255, Green 255, Blue 255). Since LCD screens do no generate much heat, temperature in the

petri dish was assumed to be similar to the room and water temperature (19-21 °C). Assays were

conducted during the afternoon between 1200 and 1730 hr to minimize within day variability

(MacPhail et al. 2009). The swimming assay was performed within a testing chamber that

isolated the 10 larvae in the petri dish from light and sound, has been described in three previous

studies (Mora-Zamorano et al. 2016b, 2016a, 2017), and provided adequate light and video

surveillance to view all individual movement. Similar to previous studies (Mora-Zamorano et al.

2016b, 2016a, 2017; Carvan et al. 2017), the larvae were allowed to acclimate for 5 min, then

spontaneous larval movement was constantly recorded at a rate of 30 frames per sec for 5 more

minutes (8987 total frames after processing), resolution of 640 x 640 pixels/mm with a final

mean visual resolution of 7.38 pixels/mm (SD = 0.28, n=127). Spontaneous movement data was

collected (movement not initiated by some external stimuli but by the fish's inner impulse or

inclination) in contrast to other common toxicological assays that use external stimuli to instigate

fish movement. Videos were saved in avi format using a Logitech C920 camera and MATLAB

Image Acquisition Toolbox (R2012b).

Similar to Ingebretson and Masino (2013), the corrected centroid locations defined the

individual larvae location and activity at each frame, where swimming was defined as movement

that was at least 1 mm/sec or 0.03333 mm per frame (i.e. magnitude of velocity at larvae center)

and lasted longer than 5 frames (0.166 sec). Whereas the resting behavior occurred during

frames where movement was less than 1 mm/sec or if greater than 1 mm/sec, lasted less than 5

frames. Where resting behavior occurred, speed and distance for those frames were changed to

zero. In addition, starting at frame three, we calculated the turning angle using the same method

as Ctrax, as the difference between the four-quadrant inverse tangent of the two trajectories where the first trajectory was constructed from the first two locations in the sequence, and the second trajectory from the second two locations in the sequence. This calculation results in a turning angle that ranges from -3.14 to 3.14, where zero is straight ahead movement, a negative value indicates a right turn and a positive value indicates a left turn. Larval orientation was assumed to be in the direction of movement. Twelve overall average behavioral endpoints were assessed from the swimming assay to determine effects from exposure (Table S5.2): number of swimming and extreme swimming bouts; swimming bout duration, speed and turning angle; total distance traveled and time swimming; number of fish lengths swam during entire assay; overall average step length and variability, turning angle and variability.

Using the same methods as Albers et al. (2022), a hidden Markov chain model (HMM) was constructed for each ZF larva in the locomotion assay (all fish swam at least once) to describe the different behavioral states and used them as additional behavior endpoints to determine effects from chemical exposure. A brief description of the method follows. For each larva and video frame, the step length and turning angle during the assay were used to construct multiple larval specific HMMs using the R package moveHMM (Michelot et al. 2016; R Core Team 2019). Multiple behavior state models were examined that contained three possible swimming states: slow, medium and fast swimming states where s1 HMMs contained only one behavior state, s2 HMMs contained any two behavior states, and s3 HMMs contained all three behavior states. The best fit HMM for each larvae was determined from a suite of ten potential HMM models, differing in the number of behavior states and initial starting values for each state (see Albers et al. 2022 Table S.2 for model description and initial values).

Once all 10 of the possible HMMs were completed, a hierarchical selection for the best fitting model was conducted, essentially using successfully converged models with the lowest AIC. Even though the initial state values were set up in increasing step length means, the resulting best fit HMM state parameter estimates did not always have increasing step length for each additional behavior, probably from the final HMM behavior state being defined by not only the step length but also turning angle characteristics. To make sure the behavior state comparisons were comparing similar states with the same name, the states were reordered and renamed in order to compare between larvae. First, states were reordered using the mean step length to describe them as slow, medium and faster swimming behavior states (i.e. changed the state name). Next a Linear Discriminant Model was constructed using the lda function in the MASS package (Venables and Ripley 2002) and cross validation to compare between models using the s3 models as a reference. LDA prediction accuracy for all models (s1, s2 and s3) was measured using cross validation where a random draw of 80% of the data was used to construct a model and then calculated prediction accuracy of the remaining 20% of the data. The LDA prediction was repeated 50 times for each treatment group of data to determine overall accuracy (75 ± 0.07 %) and within state accuracy (slow state = 95 ± 0.03 %, medium state = 69 ± 0.09 % and fast state = 60 ± 0.07 %; Table S5.3).

When treatment level tests were conducted on slow, medium and fast states, they were only conducted with fish that performed those states making the number of larvae used for the model (see Bayesian Model Analysis section below) different for each comparison (Table S5.3).

Visual Motor Response Assay

Visual Motor Response (VMR) assays are a common test of fish neurological system function by startling the fish and evaluating their response (Emran et al. 2008). VMRs were conducted using the same methodology as (Mora-Zamorano et al. 2017), where 6 dpf ZF larvae were tested in a special behavior chamber while in the transparent 12-well microliter plates. The testing chamber isolated the larvae from light and sound, as described in three previous studies (Mora-Zamorano et al. 2016b, 2016a, 2017) and provided adequate light and video surveillance to view all individual movement. VMR assays were conducted between the hours of 1200 and 1800 to minimize within day variability (MacPhail et al. 2009). ZF larvae were positioned in a dark behavior chamber and acclimated in the dark for 10 minutes (did not use data during this period), after which they underwent two cycles of alternating 10 min light and dark periods for a total of 50 min. This procedure resulted in larvae used in the VMR analysis experiencing two startles each from dark to light and from light to dark and 4-10 minute periods differing light conditions: two dark and two light. Light levels during the light periods were set to 69 lux based on the work by MacPhail et al. (2009; Fisher Scientific Traceable Dual-Range Light Meter, Pittsburgh, PA). VMRs were not conducted on YP larvae since they did not survive the individual well plates.

Spontaneous movement of larvae was constantly recorded at a rate of 30 frames per sec and tracked using DanioVision© system version 8.0 (Noldus Information Technology, Leesburg, VA). Settings for tracking did not include smoothing of track. The minimal distance before movement was recorded was set to 0.2 mm, at which time the direct distance between the two points was calculated. The same automated error correcting procedure described for the locomotion assay was also applied to VMR fish locations. The corrected and censored fish

locations were used to define individual larvae activity at each frame within each period. Speed

at each frame was calculated as mm per sec and distance traveled in mm. Swimming was

defined as larval movement that was at least 6 mm/sec or 0.2 mm per frame (i.e. magnitude of

velocity at larvae center) and lasted longer than 5 frames (0.166 sec). Whereas the resting

behavior occurred during frames where movement was less than 1 mm/sec or if greater than 1

mm/sec, lasted less than 5 frames. Where resting behavior was defined, speed and distance for

those frames were changed to zero. In addition, the turning angle associated with each frame of

swimming was calculated using the difference between the four-quadrant inverse tangent of the

two trajectories. Where the first trajectory was constructed from the first two locations in the

sequence, and the second trajectory from the second two locations in the sequence. This

calculation results in a turning angle that ranges from -3.14 to 3.14, where zero is straight ahead

movement, negative values indicate right turns and positive values indicate left turns.

Using the censored fish locations, swimming bout characteristics (i.e. time between rest

periods) within each VMR period were summarized using multiple metrics: number of bouts per

second; the mean duration, speed and turning angle (See Table S4.2 for definitions). The overall

larval behavior during each period in the assay was also summarized using multiple overall

summary metrics: total distance traveled, total time swimming, overall average step length and

variation, overall turning angle and variation. In addition, fish larvae responded to the visual

startle from the light change as is typical of previous startle responses (Emran et al. 2008).

Consequently, two behavior endpoints were calculated specifically to determine how larvae

responding to the visual startle of the light turning off and on. To determine the magnitude of

the response to the visual startle, we determined the frame where the maximum speed was

traveled within 5 seconds after the startle. Then the difference between the maximum speed and

212

the speed at the time of the startle was calculated to define the magnitude of the startle response. Startle response time was calculated as the difference in time between the startle and the frame where the maximum speed was traveled.

Feeding Assay

In this study, YP and ZF larvae initiate feeding at 13 and 6 dpf, respectively. This study focused on assessing larvae behavior at the point that larvae were independent and actively feeding. Consequently, feeding ability in YP and ZF was assessed when they were 30-38 and 16 dpf, respectively (Table S5.1). Larva were transferred from the rearing containers to 54 mm diameter round petri dishes (60 mm petri dish). Feeding of *Artemia* to larvae continued morning and evening until ~24hr prior to the assay, so fish would be in a hungry state for the test. The exception was with YP larvae that were feed 5 *Artemia* the morning of the feeding assay in order to not starve. Similar to locomotion assays, feeding assays were conducted between 1130 and 2130 hr at a light level of 69 lux. Feeding assays were conducted in the same behavior chamber as the locomotion assay, when after 5 minutes of acclimation, recording started and ~15 (range 11-17) live *Artemia* were added to the dish. The test ended when 5 minutes had elapsed from when the *Artemia* were added to the dish.

Feeding bouts consisted of multiple presentations; the characteristic curved body posture, continuously swimming straight or at rest by just opening their mouths. For each of these presentations, the distance between the middle of the larva's mouth and *Artemia* was measured at the time the larva orientated toward the *Artemia*, with their either eyes or body. This distance was termed reactive distance and was measured using ImageJ© (version 1.51j8). For each capture attempt toward an *Artemia*, we recorded whether the larva successfully captured the

213

Artemia and the time it took the larva to handle and consume the *Artemia*. Typically after a

catching an *Artemia*, the larva sat or drifted momentarily and did not swim while it was

consuming the prey. Handling time was defined as the time between prey capture and when the

larva resumed normal swimming activity. Additionally, three consumption metrics were

calculated: capture proportion defined as the number of captures divided by the total number of

Artemia added to the dish, miss proportion defined as the number of feeding capture attempts

that missed the *Artemia* divided by the total number of successful and unsuccessful capture

attempts, and capture attempt ratio defined as the total number of feeding capture attempts

(successful and unsuccessful) divided by the total number of *Artemia* added to the dish. When

two *Artemia* were consumed during one feeding capture attempt, the consumption of both

Artemia were assigned the same measurements.

Bayesian Model Analysis

For each behavioral endpoint (Table S4.2), we conducted a series of preliminary and final

tests to determine whether there were differences between chemical dose treatments. The three

different behavior assays and the number of behavior responses we measured were Feeding-5,

Visual Motor Response (VMR) - 58, Locomotion - 30. Behavior responses that were not already

normally distributed, we attempted to normalize using the boxcox function in the R MASS

package (Venables and Ripley 2002). Using a basic model containing only the treatment factor,

behavior endpoints were transformed using the maximum lambda parameter for the exponential

transformation suggested by the boxcox function in the R MASS package. Below we describe

the five different models that were used on the behavior responses to determine differences

between treatments, (see Table S5.4 for final transformation and model used for each behavior

214

endpoint). Fitting multiple model types was necessary because of the various behavior endpoints having distinctively different distributions such as a proportional, normal, or a skewed response that even Box Cox transformations were not successful in normalizing.

Model Description

The Bayesian models used in locomotion and VMR behavior response models consisted of one main effect (treatment with 3 levels), covariate variable time of assay and a random batch effect because assays were ran in batches of 24-well dishes for the VMR or 10 fish in a petri dish for the locomotion assay. The Bayesian model used for a locomotion and VMR behavior responses was

$$Locomotion\ or\ VMR\ Behavior\ Endpoint_{ijkl}$$
$$= \alpha + \beta_j * treatment_j + \delta_k * assay\ time_{k(i)} + \omega_l * batch_{l(i)} + \varepsilon_{ijkl}$$

where $Locomotion\ or\ VMR\ Behavior\ Endpoint_{ijkl}$ is the behavioral response metric on the ith individual, jth treatment, kth assay time and lth batch; α is the intercept, β_j is the treatment coefficient with a $Normal(0, \sigma_\beta^2)$ distribution, δ is the assay time coefficient with a $Normal(0, \sigma_\delta^2)$ distribution, ω_l is the batch coefficient, and ε_{ijkl} is the residual error. Treatment and batch are indicator variables containing 1 if the observation belongs to the corresponding factor category and 0 otherwise. Prior distributions for these two components can be found in Albers et al. (2022; Table S5.5). Additionally, priors were needed for the α, treatment and assay time effects. In all models, we used non-informative, flat priors. For α, treatment and assay time we assumed a normal distribution with a mean of 0 and standard deviation of at least 1.0×10^4

(i.e. precision of 1.0 x 10^{-4}). OpenBUGS model code for these models was presented in Albers et al. (2022) Tables S5.6, S5.7 and S5.8.

Two other Bayesian models were used to model the five feeding behavior responses that did not contain a batch effect since feeding assays were conducted one fish at a time. Additionally, days post fertilization (dpf) was included as a covariate in YP feeding assay endpoints larvae age ranged from 30-38 dpf (the dpf covariate was not included in ZF models since all ZF larvae were 6 or 16 dpf for locomotion and feeding assays, respectively). Lastly, these models did include intercept, treatment and assay time as described for the locomotion and VMR behavior models.

3) Normal response model

$Feeding\ Behavior\ Endpoint_{ijkl}$

$$= \alpha + \beta_j * treatment_j + \delta * assay\ time_{k(i)} + \omega * dpf_{l(i)} + \varepsilon_{ijkl}$$

where $Feeding\ Behavior\ Endpoint_{ijkl}$ is the prey handling time, lunge ratio or reaction distance (Albers et al. 2022; Table S5.4) on the ith individual, j[th] treatment, k[th] assay time and l[th] dpf; α, β_j and, δ and their priors where described before, and ω is the dpf coefficient also with a non-informative normal prior assuming a normal distribution with a mean of 0 and standard deviation of at least 1.0 x 10^4 (i.e. precision of 1.0 x 10^{-4}). Lastly, the residual error followed a normal distribution $\varepsilon \sim Normal(0, \sigma_\varepsilon^2)$ with variance $\frac{1}{\sigma_\varepsilon^2} = \tau_j \sim I - Gamma(0.0001,$ 0.0001). OpenBUGS code can be found in Albers et al. (2022) Table S5.9.

4) Binomial response model

$$Feeding\ Behavior\ Endpoint_{ijkl} \sim Binomial(p_{ijkl}, N_{ijkl})$$
$$logit(p_{ijkl}) = \beta_j * treatment_{j(i)} + \delta * assay\ time_{k(i)} + \omega * dpf_{l(i)} + \varepsilon_{ijkl}$$

where $Feeding\ Behavior\ Endpoint_{ijkl}$ is the prey capture probability or prey miss

proportion (Albers et al. 2022; Table S5.7) on the ith individual, j^{th} treatment, k^{th} assay time and

l^{th} dpf and N_{ijkl} is the number of trials and p_{ijkl} is the probability of success distributed on a

logit scale. The priors for β_j, δ and ω where described before. Lastly, the residual error

followed a normal distribution $\varepsilon \sim Normal(0, \sigma_\varepsilon^2)$ with variance $\frac{1}{\sigma_\varepsilon^2} = \tau_j \sim I - Gamma(0.01,$

$0.01)$.

Model Fitting and Convergence Diagnostics

Bayesian models were constructed using OpenBUGS version 3.2.3 rev 1012 (Lunn et al.

2009), R version 3.6.0 (R Core Team 2019) and packages R2OpenBUGS version 3.2 (Sturtz et

al. 2005) and coda version 0.19-2 (Plummer et al. 2005). We fit the basic model using three

chains, each with a minimum of 10000 iterations, 1000 burn in, and 1 thin, and monitored a

subsample of parameters for convergence: treatment effects, overall mean, residuals, variance(s),

precision parameter(s) and degree of freedom parameter(s). Then we performed preliminary

multiple MCMC chain convergence diagnostics using Trace plots. If model did not converge,

we increased either the number of iterations, burn in, or thin. Once the preliminary model trace

plots were not showing any obvious convergence problems, further MCMC diagnostics were

applied using a suite of tools to determine adequate MCMC chain length, model convergence

and fit. 1) Autocorrelation plots indicated the level of thinning required to remove any

autocorrelation. 2) Gelman-Rubin-Brooks shrink factor plots indicated the adequate number of

iterations needed for burn in. 3) Raftery and Lewis's diagnostic tables were used to determine

the number of additional iterations needed for accurate parameter estimation (default values of q = 0.025, r = ± 0.005 and s = 0.95). 4) Finally, model goodness-of-fit was evaluated using residual diagnostics. When alternative models were to be compared, the model with the best posterior predictive distributions of residuals and replicated observations was retained.

Once a best-fitted model had been determined, we re-fit the model with the appropriate settings and monitored a slightly different suite of parameters: overall mean; population level treatment effects; variance and precision parameters; tail area probabilities of observing a difference; degrees of freedom; individual level predicted means, etc. With the model output and iteration levels we also determined effective sample size (effectiveSize function in coda R package), posterior distributions of parameters, and calculated a one-sided tail area probabilities (Bayesian P-values) from the two sided difference of parameter distributions. The summary output of this last model fit is presented in the results section of the paper and all relevant parameter posterior distributions can be found in Table S5.5.

Table S5.1. Summary of the number of larval zebrafish larvae *Danio rerio* and yellow perch *Perca flavescens* that were used in this study (MeHg = methylmercury, PCB126 = 3,3',4,4',5-pentachlorobiphenyl, SD = standard deviation).

Species	Groups	MeHg Control Treatment	MeHg Low Treatment	MeHg High Treatment	PCB126 Control Treatment	PCB126 Low Treatment	PCB126 High Treatment
Yellow Perch	Feeding Assays						
	Number of Larvae	57	51	52	44	44	44
	Total Length (mm ± SD)	11.69 (1.25)	11.42 (1.31)	11.67 (1.31)	11.88 (1.39)	11.61 (1.40)	12.03 (1.36)
	Number of Larvae that did not consume *Artemia*	1	1	2	1	2	0
Zebrafish	Visual Motor Response Assays						
	Number of Larvae	124	127	126	129	126	127
	Locomotion Assays						
	Number of Larvae	170	180	140	270	260	250
	Total Length (mm ± SD)	4.76 (0.66)	4.66 (0.72)	4.60 (0.74)	4.58 (0.70)	4.49 (0.69)	4.47 (0.61)
	Hidden Markov Chain Models						
	Number of Larvae Attempted to Fit a Model	162	172	131	252	255	234
	Number of Larvae with a Fitted Model	162	172	131	252	255	234
	Feeding Assays						
	Number of Larvae	35	41	39	41	43	21
	Total Length (mm ± SD)	5.83 (0.69)	6.05 (0.64)	6.28 (0.73)	5.91 (0.69)	6.08 (0.78)	5.27 (0.78)
	Number of Larvae that did not consume *Artemia*	5	5	3	9	6	13

Table S5.2. Description of behavior endpoints examined in this study

Submitted table as a sheet in an Excel file.

Table S5.3. Linear Discriminant Models (LDA) cross validation results for different Hidden Markov Chain Model (HMM) behavioral states (N = 50 iterations, MeHg = methylmercury, PCB126 = 3,3',4,4',5-pentachlorobiphenyl, SD = standard deviation, s3 = three behavior state HMM, s2 = two behavior state HMM, s1 = one behavior state HMM).

Group	Num. of larvae with s3 models	Num. of larvae with s2 models	Num. of larvae with s1 models	Num. of obs./behavior states in s3 LDA	Total num. of obs./behavior states in s1 and s2	Num. of renamed behavior states in s1 and s2	Slow State Accuracy of s3 LDA Mean	SD	Medium State Accuracy of s3 LDA Mean	SD	Fast State Accuracy of s3 LDA Mean	SD	Total Accuracy of s3 LDA Mean	SD
MeHg														
Control Dose	89	71	2	267	144	65	0.93	0.05	0.70	0.09	0.84	0.07	0.82	0.04
Middle Dose	88	83	1	264	167	36	0.91	0.06	0.78	0.09	0.60	0.12	0.75	0.05
Upper Dose	71	58	2	213	118	56	0.96	0.04	0.78	0.12	0.77	0.14	0.83	0.07
PCB 126														
Control Dose	131	115	6	393	236	47	0.96	0.04	0.62	0.09	0.49	0.11	0.69	0.04
Middle Dose	151	103	1	453	207	23	0.98	0.03	0.57	0.07	0.48	0.10	0.67	0.04
Upper Dose	140	91	3	420	185	28	0.99	0.03	0.55	0.10	0.40	0.09	0.64	0.04

Table S5.4. Bayesian model summary for each behavioral response endpoint (MeHg = methylmercury, PCB126 = 3,3',4,4',5-pentachlorobiphenyl).

Submitted table as a sheet in an Excel file.

Table S5.5. Posterior distributions for all model parameters and each behavioral endpoint (MeHg = methylmercury, PCB126 = 3,3',4,4',5-pentachlorobiphenyl, Trt = treatment, vs = versus, sec = second, mm = millimeter).

Submitted table as a sheet in an Excel file.

Table S5.6. Total number of significantly differentially expressed genes (alpha = 0.05) found in the brains of zebrafish *Danio rerio* in this study (MeHg = methylmercury, PCB126 = 3,3',4,4',5-pentachlorobiphenyl, vs = versus).

Treatment Comparison	Number of Differentially Expressed Genes
MeHg-Control vs MeHg-Low	3
MeHg-Low vs MeHg-High	1349
MeHg -Control vs MeHg-High	1455
PCB126-Control vs PCB126-Low	162
PCB126-Low vs PCB126-High	1418
PCB126-Control vs PCB126-High	218

Table S5.7. Significantly differentially expressed genes (alpha = 0.05) found in the brains of zebrafish *Danio rerio* in this study. Significant trends and FDR are reported (MeHg = methylmercury, PCB126 = 3,3',4,4',5-pentachlorobiphenyl, vs = versus, neg = significant negative trend, pos = significant positive trend). Blanks indicate comparison was tested but did not result in a significant difference.

Submitted table as a sheet in an Excel file.

Table S5.8. Significantly altered gene sets and pathways (alpha = 0.05) found in the brains of zebrafish *Danio rerio* in this study. Significant trends and FDR are reported (MeHg = methylmercury, PCB126 = 3,3',4,4',5-pentachlorobiphenyl, vs = versus, neg = significant negative trend, pos = significant positive trend). Blanks indicate comparison was tested but did not result in a significant difference.

Submitted table as a sheet in an Excel file.

Table S5.9. Significant methylmercury treatment patterns by behavior endpoints in zebrafish *Danio rerio* found in this study. Significant trends are reported in the following order: first level is the trend between control and middle treatment, second is middle verses upper treatment and third is control vs upper treatment (neg = significant negative trend, pos = significant positive trend, - = no significant trend, HMM = hidden Markov chain model, TP = transition probability, sec = second, mm = millimeter).

Significant Treatment Pattern	Behavior Endpoint
- - neg	Prey Handling Time, Swimming Bout Speed Period 3 (mm/sec)
- - pos	HMM Fast State Step Length Variation
- neg -	Startle Magnitude Period 1, Startle Time Period 1, Startle Time Period 2, Startle Time Period 3
- neg neg	Overall Step Length Period 3 (mm), Overall Step Length Variation Period 3, Startle Magnitude Period 3, Swimming Bout Duration Period 3 (sec), Swimming Bouts Period 3 (per sec), Swimming Bouts Period 4 (per sec), Total Distance Traveled Period 3 (mm), Total Time Swimming Period 3 (sec)
- pos -	HMM Slow State Count
- pos pos	Swimming Bout Duration Period 2 (sec)
neg - -	HMM Fast -> Fast TP, HMM Medium State Turning Angle Variation
neg - neg	Prey Miss Proportion
neg pos -	HMM Medium -> Slow TP
pos - -	Fish Lengths, HMM Medium -> Medium TP, HMM Medium State Count, Overall Step Length (mm), Overall Step Length Variation Period 2, Overall Step Length Variation, Swimming Bout Duration (sec), Total Distance Traveled (mm)
pos - pos	Prey Capture Probability, Swimming Bout Speed Period 2 (mm/sec), Swimming Bout Speed Period 4 (mm/sec)
pos neg -	HMM Medium -> Fast TP, HMM Medium State Step Length Variation, HMM Slow -> Medium TP, Overall Step Length Period 2 (mm), Overall Step Length Period 4 (mm), Overall Step Length Variation Period 4, Swimming Bouts (per sec), Total Distance Traveled Period 2 (mm), Total Distance Traveled Period 4 (mm), Total Time Swimming (sec), Total Time Swimming Period 2 (sec)
pos neg neg	Swimming Bouts Period 2 (per sec), Total Time Swimming Period 4 (sec)
pos pos pos	Swimming Bout Duration Period 4 (sec)

Table S5.10. Significant 3,3',4,4',5-pentachlorobiphenyl treatment patterns by behavior endpoints in zebrafish *Danio rerio* found in this study. Significant trends are reported in the following order: first level is the trend between control and middle treatment, second is middle verses upper treatment and third is control vs upper treatment (neg = significant negative trend, pos = significant positive trend, - = no significant trend, HMM = hidden Markov chain model, TP = transition probability, sec = second, mm = millimeter).

Significant Treatment Pattern	Behavior Endpoint
- - neg	Overall Step Length Variation Period 2, Overall Step Length Variation Period 4, Startle Magnitude Period 1, Swimming Bout Speed Period 2 (mm/sec), Swimming Bout Speed Period 4 (mm/sec)
- - pos	HMM Fast State Step Length Variation, HMM Medium State Step Length Variation
- neg -	Overall Step Length Period 3 (mm), Overall Step Length Variation Period 3, Startle Magnitude Period 4, Swimming Bout Duration Period 3 (sec), Total Distance Traveled Period 3 (mm), Total Time Swimming Period 3 (sec)
- neg neg	Capture Attempt Ratio, Prey Capture Probability, Startle Magnitude Period 3, Startle Time Period 1, Swimming Bout Speed Period 3 (mm/sec)
- pos -	HMM Fast State Step Length (mm), Startle Time Period 2
- pos pos	Prey Miss Proportion
neg - -	HMM Fast -> Fast TP
neg - neg	HMM Slow State Turning Angle Variation, Overall Turning Angle Variation, Swimming Bout Turning Angle
pos - -	Fish Lengths, Overall Step Length (mm), Total Distance Traveled (mm)
pos - pos	HMM Medium State Turning Angle Variation, Overall Step Length Variation
pos neg -	Swimming Bouts (per sec), Total Time Swimming (sec)
pos pos pos	HMM Medium State Step Length (mm), Swimming Bout Speed (mm/sec)

Table S5.11. Significant treatment patterns from methylmercury (MeHg) and 3,3',4,4',5-pentachlorobiphenyl (PCB126) exposure by behavior endpoints in zebrafish *Danio rerio* found in this study. Significant trends are reported in the following order: first level is the trend between MeHg control and middle MeHg treatment, second is middle MeHg verses upper MeHg treatment, third is MeHg control vs upper MeHg treatment, forth level is the trend between PCB126 control and middle PCB126 treatment, fifth is middle PCB126 verses upper PCB126 treatment and sixth is PCB126 control vs upper PCB126 treatment (neg = significant negative trend, pos = significant positive trend, - = no significant trend, HMM = hidden Markov chain model, TP = transition probability, sec = second, mm = millimeter).

Submitted table as a sheet in an Excel file.

Table S5.12. Significant methylmercury treatment patterns shared by differentially expressed genes and behavior endpoints in zebrafish *Danio rerio* found in this study. Both the original and opposite behavior endpoint trends are listed. Significant trends are reported in the following order: first level is the trend between control and middle treatment, second is middle verses upper treatment and third is control vs upper treatment (neg = significant negative trend, pos = significant positive trend, - = no significant trend, HMM = hidden Markov chain model, TP = transition probability, sec = second, mm = millimeter).

Submitted table as a sheet in an Excel file.

Table S5.13. Significant 3,3',4,4',5-pentachlorobiphenyl treatment patterns shared by differentially expressed genes and behavior endpoints in zebrafish *Danio rerio* found in this study. Both the original and opposite behavior endpoint trends are listed. Significant trends are reported in the following order: first level is the trend between control and middle treatment, second is middle verses upper treatment and third is control vs upper treatment (neg = significant negative trend, pos = significant positive trend, - = no significant trend, HMM = hidden Markov chain model, TP = transition probability, sec = second, mm = millimeter).

Submitted table as a sheet in an Excel file.

Table S5.14. Significant treatment patterns from methylmercury (MeHg) and 3,3',4,4',5-pentachlorobiphenyl (PCB126) exposure shared by differentially expressed genes and behavior endpoints in zebrafish *Danio rerio* found in this study. Both the original and opposite behavior endpoint trends are listed. Significant trends are reported in the following order: first level is the trend between MeHg control and middle MeHg treatment, second is middle MeHg verses upper MeHg treatment, third is MeHg control vs upper MeHg treatment, forth level is the trend between PCB126 control and middle PCB126 treatment, fifth is middle PCB126 verses upper PCB126 treatment and sixth is PCB126 control vs upper PCB126 treatment (neg = significant negative trend, pos = significant positive trend, - = no significant trend, HMM = hidden Markov chain model, TP = transition probability, sec = second, mm = millimeter).

Submitted table as a sheet in an Excel file.

Table S5.15. Significant methylmercury treatment patterns shared by gene sets and behavior endpoints in zebrafish *Danio rerio* found in this study. Both the original and opposite behavior endpoint trends are listed. Significant trends are reported in the following order: first level is the trend between control and middle treatment, second is middle verses upper treatment and third is control vs upper treatment (neg = significant negative trend, pos = significant positive trend, - = no significant trend, HMM = hidden Markov chain model, TP = transition probability, sec = second, mm = millimeter).

Submitted table as a sheet in an Excel file.

Table S5.16. Significant 3,3',4,4',5-pentachlorobiphenyl treatment patterns shared by gene sets and behavior endpoints in zebrafish *Danio rerio* found in this study. Both the original and opposite behavior endpoint trends are listed. Significant trends are reported in the following order: first level is the trend between control and middle treatment, second is middle verses upper treatment and third is control vs upper treatment (neg = significant negative trend, pos = significant positive trend, - = no significant trend, HMM = hidden Markov chain model, TP = transition probability, sec = second, mm = millimeter).

Submitted table as a sheet in an Excel file.

Table S5.17. Significant treatment patterns from methylmercury (MeHg) and 3,3',4,4',5-pentachlorobiphenyl (PCB126) exposure shared by gene sets and behavior endpoints in zebrafish *Danio rerio* found in this study. Both the original and opposite behavior endpoint trends are listed. Significant trends are reported in the following order: first level is the trend between MeHg control and middle MeHg treatment, second is middle MeHg verses upper MeHg treatment, third is MeHg control vs upper MeHg treatment, forth level is the trend between PCB126 control and middle PCB126 treatment, fifth is middle PCB126 verses upper PCB126 treatment and sixth is PCB126 control vs upper PCB126 treatment (neg = significant negative trend, pos = significant positive trend, - = no significant trend, HMM = hidden Markov chain model, TP = transition probability, sec = second, mm = millimeter).

Submitted table as a sheet in an Excel file.

Table S5.18. Total number of significantly differentially expressed genes (alpha = 0.05) found in the brains of yellow perch *Perca flavescens* in this study (MeHg = methylmercury, PCB126 = 3,3',4,4',5-pentachlorobiphenyl, vs = versus).

Treatment Comparison	Number of Differentially Expressed Genes
MeHg-Control vs MeHg-Low	8
MeHg-Low vs MeHg-High	1
MeHg -Control vs MeHg-High	44
PCB126-Control vs PCB126-Low	19
PCB126-Low vs PCB126-High	7
PCB126-Control vs PCB126-High	11

Table S5.19. Significantly differentially expressed genes (alpha = 0.05) found in the brains of yellow perch *Perca flavescens* in this study. Significant trends and FDR are reported (MeHg = methylmercury, PCB126 = 3,3',4,4',5-pentachlorobiphenyl, vs = versus, neg = significant negative trend, pos = significant positive trend). Blanks indicate comparison was tested but did not result in a significant difference.

Submitted table as a sheet in an Excel file.

Table S5.20. Significantly altered gene sets and pathways (alpha = 0.05) found in the brains of yellow perch *Perca flavescens* in this study. Significant trends and FDR are reported (MeHg = methylmercury, PCB126 = 3,3',4,4',5-pentachlorobiphenyl, vs = versus, neg = significant negative trend, pos = significant positive trend). Blanks indicate comparison was tested but did not result in a significant difference.

Submitted table as a sheet in an Excel file.

Table S5.21. Significant methylmercury treatment patterns shared by differentially expressed genes and behavior endpoints in yellow perch *Perca flavescens* found in this study. Both the original and opposite behavior endpoint trends are listed. Significant trends are reported in the following order: first level is the trend between control and middle treatment, second is middle

verses upper treatment and third is control vs upper treatment (neg = significant negative trend, pos = significant positive trend, - = no significant trend, HMM = hidden Markov chain model, TP = transition probability, sec = second, mm = millimeter).

Submitted table as a sheet in an Excel file.

Table S5.22. Significant 3,3',4,4',5-pentachlorobiphenyl treatment patterns shared by differentially expressed genes and behavior endpoints in yellow perch *Perca flavescens* found in this study. Both the original and opposite behavior endpoint trends are listed. Significant trends are reported in the following order: first level is the trend between control and middle treatment, second is middle verses upper treatment and third is control vs upper treatment (neg = significant negative trend, pos = significant positive trend, - = no significant trend, HMM = hidden Markov chain model, TP = transition probability, sec = second, mm = millimeter).

Submitted table as a sheet in an Excel file.

Table S23. Significant methylmercury treatment patterns shared by gene sets and behavior endpoints in yellow perch *Perca flavescens* found in this study. Both the original and opposite behavior endpoint trends are listed. Significant trends are reported in the following order: first level is the trend between control and middle treatment, second is middle verses upper treatment, and third is control vs upper treatment (neg = significant negative trend, pos = significant positive trend, - = no significant trend, HMM = hidden Markov chain model, TP = transition probability, sec = second, mm = millimeter).

Submitted table as a sheet in an Excel file.

Table S5.24. Significant biological endpoints found in this study (KF = Atlantic killifish *Fundulus heteroclitus*, YP = yellow perch *Perca flavescens*, ZF = zebrafish *Danio rerio*, HMM = hidden Markov chain model, TP = transition probability, sec = second, mm = millimeter). Note that KEGG 2D pathways are noted in this table as positive, but both positive and negative KEGG 2D trends were used to find similarities with other endpoints.

Submitted table as a sheet in an Excel file.